

DYNAMIC EFFECTS OF MOVING TRAFFIC
ON
RAILWAY BRIDGES

A THESIS SUBMITTED TO
THE GRADUATE SCHOOL OF NATURAL AND APPLIED SCIENCES
OF
MIDDLE EAST TECHNICAL UNIVERSITY

BY

FATİH ÇİNEK

IN PARTIAL FULFILLMENT OF THE REQUIREMENTS
FOR
THE DEGREE OF MASTER OF SCIENCE
IN
CIVIL ENGINEERING

MAY 2010

Approval of the thesis:

**DYNAMIC EFFECTS OF MOVING TRAFFIC
ON
RAILWAY BRIDGES**

submitted by **FATİH CİNEK** in partial fulfillment of the requirements for the degree of **Master of Science in Civil Engineering Department, Middle East Technical University** by,

Prof. Dr. Canan ÖZGEN _____
Dean, Graduate School of **Natural and Applied Sciences**

Prof. Dr. Güney ÖZCEBE _____
Head of Department, **Civil Engineering**

Prof. Dr. Çetin YILMAZ _____
Supervisor, **Civil Engineering Dept., METU**

Examining Committee Members:

Assoc. Prof. Dr. Uğur POLAT _____
Civil Engineering Dept., METU

Prof. Dr. Çetin YILMAZ _____
Civil Engineering Dept., METU

Assoc. Prof. Dr. Ahmet TÜRER _____
Civil Engineering Dept., METU

Asst. Prof. Dr. Alp CANER _____
Civil Engineering Dept., METU

Civil Engineer, M.S. Deniz HANHAN _____
DEHA Proje

Date: _____ 05.05.2010 _____

I hereby declare that all information in this document has been obtained and presented in accordance with academic rules and ethical conduct. I also declare that, as required by these rules and conduct, I have fully cited and referenced all material and results that are not original to this work.

Name, Last name: Fatih CİNEK

Signature :

ABSTRACT

DYNAMIC EFFECTS OF MOVING TRAFFIC ON RAILWAY BRIDGES

Cinek, Fatih

M. Sc., Department of Civil Engineering

Supervisor: Prof. Dr. Çetin Yılmaz

May 2010, 215 pages

In this study, dynamic effects on high speed railway bridges under moving traffic are investigated. Within this context, the clear definition of the possible dynamic effects is provided and the related studies that exist in literature are investigated. In the light of those studies, analytical procedures that are defined to find the critical dynamic responses such as deflections, accelerations and resonance conditions are examined and a MatLab programming language is written to obtain the responses for different train loading and velocity values. The reliability of the written program is conformed by comparing the results with the related studies in literature. In addition to the analytical procedures, the approaches in the European standards concerning the dynamic effects of railway traffic are defined. A case study is investigated for a bridge that is in the scope of the Ankara-Sivas High Speed Railway Project. The related bridge is modeled by using finite element program, SAP2000 according to the definitions that are stated in European standards. The related high speed railway bridge is analysed with a real train which is French TGV together with the HSLM trains that are defined in Eurocode and the results obtained are compared with each other. This study also includes the analysis

of the bridges performed for 7 different stiffness and 3 different mass values to determine the parameters affecting dynamic behaviour.

Keywords: Dynamic analysis, resonance, acceleration, high speed.

ÖZ

DEMİRYOLU KÖPRÜLERİNDE TREN YÜKLERİNİN DİNAMİK ETKİSİ

Cinek, Fatih

Yüksek Lisans, İnşaat Mühendisliği Bölümü

Tez Yöneticisi: Prof. Dr. Çetin Yılmaz

Mayıs 2010, 215 sayfa

Bu çalışmada, yüksek hızlı demiryolu köprülerinde trafik etkisi altında oluşabilecek dinamik etkiler incelenmiştir. Bu bağlamda, demiryolu köprüleri dinamik etkilerinin tanımı yapılmış ve literatürde konuyla ilgili yer alan yaklaşımlar incelenmiştir. Bu çalışmaların ışığında, demiryolu trafiği altında köprülerin deplasman ve ivme tepkileri, rezonans durumu gibi kritik dinamik etkilerini belirlemek amacıyla geliştirilen analitik yöntemler tanımlanmış, çeşitli tren yüklemesi ve hızında oluşacak etkilerin, bu yöntemlere göre bulunabilmesi için MatLab kullanılarak programlama dili oluşturulmuştur. Elde edilen analitik sonuçlar literatürde yer alan çalışmalarla karşılaştırılarak sonuçların güvenilirliğinin doğrulaması yapılmıştır. Analitik yöntemlere ilave olarak, demiryolu trafiği dinamik etkilerine Avrupa şartnamelerinde yer alan yaklaşımlar tanımlanmış ve şartnamelerde belirlenen tanımlara uygun olarak, Ankara-Sivas Hızlı Tren Projesi kapsamında yer alan bir demiryolu köprüsünün, SAP2000 sonlu elemanlar programı kullanılarak analiz modeli oluşturulmuştur. Avrupa şartnamelerinde belirtilen kritik tren yüklemesi ve kritik hız değerlerine göre elde edilen sonuçların, analitik yaklaşım yöntemleri kullanılarak elde edilen değerlerle karşılaştırılmasında bu çalışmanın kapsamında yer almaktadır. Bahse konu demiryolu köprüsü Avrupa şartnamelerinde tanımlanan trenlere ilave olarak, Fransız TGV treni için de analiz edilmiş ve elde edilen sonuçların karşılaştırılması yapılmıştır. Ayrıca demiryolu trafiği altında oluşabilecek etkilerin incelenmesi

açısından 7 farklı atalet ve 3 farklı kütle değeri için analizlerin yapılması ve elde edilen sonuçların değerlendirilmesi bu çalışma kapsamında yer almaktadır.

Anahtar Kelimeler: Dinamik analiz, rezonans, ivme, yüksek hızlı.

To My Family

ACKNOWLEDGMENTS

This study was conducted under the supervision of Prof.Dr. Çetin Yılmaz I would like to express sincere appreciation to Prof.Dr. Çetin Yılmaz for his support, guidance, advice, encouragement and insight throughout the study.

I also would like to express my thanks to Asst.Prof.Dr. Alp Caner for his precious helps during my study.

Tamer Fenercioğlu deserves special thanks for his valuable suggestions during this study.

I would also express my thanks to my friend Gizem Sevgili for her support during my thesis study.

I am also gratefull to Emrah Yenier for his frendship and encouragment during my thesis study.

I am grateful to my family for their encouragement, confidence in me, support and love.

TABLE OF CONTENTS

ABSTRACT	iv
ÖZ	vi
ACKNOWLEDGMENTS.....	ix
TABLE OF CONTENTS.....	x
LIST OF TABLES	xiii
LIST OF FIGURES.....	xiv
CHAPTERS	
1. INTRODUCTION.....	1
1.1 General	1
1.2 Literature Survey.....	2
1.3 Object and Scope.....	6
2. ANALYTICAL PROCEDURE FOR THE SIMPLE BEAM SUBJECTED TO SERIES OF MOVING LOADS.....	8
2.1 General	8
2.2 Method of Solution for the Beam Subjected to Series of Moving Loads (Vehicle Bridge Interaction Dynamics, 2004)	8
2.3 Resonance Condition.....	14
2.4 Cancellation Condition.....	16
2.5 Limitations in Analytical Approach.....	17
2.6 DER Method	18
2.7 Validation of the Program.....	24
2.7.1 Study of J.M. Goicolea et al., (2002)	24
2.7.2 Study of C.C. Lin et al., (2005).....	26
3. EUROCODE PROCEDURE FOR THE DYNAMIC ANALYSIS OF THE RAILWAY BRIDGES.....	32
3.1 General	32
3.2 Requirement for Dynamic Analysis.....	34

3.3 Dynamic Analysis Train Models.....	38
3.4 Speeds to be Considered	40
3.5 Damping of the Structure	40
3.6 Mass of the Bridge	41
3.7 Stiffness of the Bridge.....	42
3.8 Determination of Critical HSLM Train for Dynamic Analysis	42
3.8.1 Determination of Maximum Design Speed Wavelength of Exication... 43	
3.8.2 Determination of Critical Wavelength of Exication	43
4. CASE STUDY	50
4.1 General	50
4.2 Case Study for L = 30 m Railway Bridge	50
4.2.1 Properties for Composite Bridge Section.....	51
4.2.2 Project Speed.....	51
4.2.3 Type of Structure.....	52
4.2.4 Span Length.....	52
4.2.5 Damping Ratio of the Structure	52
4.2.6 Definition of Model for SAP2000.....	52
4.2.7 Eigenvalue Analysis for the Bridge	54
4.2.8 Determination of Critical Wavelength of Exication	55
4.2.9 Determination of Critical Train Loading	56
4.2.10 Determination of Critical Train Speed	56
4.2.11 Determination of Load Case and Analysis Case in SAP2000	56
4.2.12 Analysis Results	58
4.2.13 Analytical Approach to the Problem.....	61
4.2.14 Comparison of the Results	69
5. PARAMETRIC STUDY	75
5.1 General	75
5.2 Stiffness Values for Parametric Study	75
5.3 Mass Values for Parametric Study	76
5.4 Speeds Considered in Parametric Study.....	76
5.5 Train Model Considered for Parametric Study	77

5.6 Summary of the Parameters	77
5.7 Analysis Results	78
5.7.1 Results and Discussion on Results for Critical Speed.....	78
5.7.2 Results and Discussion on Results for Displacement and Acceleration	85
5.7.3 Comparison of Results with Initial Estimations by DER Method	88
5.7.4 Comparison of Results with a Real Train, French TGV	89
6. CONCLUSIONS	91
6.1 Summary	91
6.2 Mass of the Bridge	93
6.3 Stiffness of the Bridge.....	93
6.4 Aggressivity from the Bridge and Train Properties	94
6.5 Critical Speed	95
REFERENCES.....	96
APPENDICES	
A. CRITICAL WAVELENGTH V.S. DYNAMIC SIGNATURE OF TRAIN	
GRAPHS	99
B. DISPLACEMENT V.S. TIME AND ACCELERATION V.S. TIME GRAPHS	
FOR CASE STUDY	111
C. DISPLACEMENT V.S. TIME AND ACCELERATION V.S. TIME GRAPHS	
FOR PARAMETRIC STUDY	131
C1. GRAPHS FOR HSLM TRAIN	131
C2. GRAPHS FOR TGV TRAIN	172
D. FREQUENCY V.S. MODE SHAPE GRAPHS FOR PARAMETRIC STUDY	
.....	186
E. MATLAB CODE FOR ANALYTICAL APPROACH.....	189

LIST OF TABLES

TABLES

Table 2.1 Comparison of Results from (C.C. Lin et al., (2005)) and Thesis	30
Table 3.1 Maximum value of $(v/n_0)_{lim}$ for a simply supported beam or slab and a maximum permitted acceleration of $a_{max} < 3.50 \text{ m/s}^2$. (from EN 1991-2 : 2003)	37
Table 3.2 Maximum value of $(v/n_0)_{lim}$ for a simply supported beam or slab and a maximum permitted acceleration of $a_{max} < 5.0 \text{ m/s}^2$. (from EN 1991-2 : 2003)	37
Table 3.3 HSLM-A train model definitions (from EN 1991-2 : 2003).....	39
Table 3.4 Application of HSLM-A and HSLM-B (from EN 1991-2 : 2003)	39
Table 3.5 Values of damping to be assumed for design purposes (from EN 1991-2 : 2003)	41
Table 4.1 Tabular presentation of the obtained results from SAP2000 and analytical approach	71
Table 4.2 Comparison of Results with DER method	73
Table 4.3 Critical trains for different maximum design speeds	74
Table 5.1 Analysis Parameters	77
Table 5.2 Analysis results for different speed values, $EI=5047800$, $m= 25 \text{ t/m}$	80
Table 5.3 Analysis results for different speed values, $EI=5047800$, $m= 35 \text{ t/m}$	80
Table 5.4 Analysis results for different speed values, $EI=5047800$, $m= 45 \text{ t/m}$	80
Table 5.5 Analysis results for different speed values, $EI=25239000$, $m= 25 \text{ t/m}$...	82
Table 5.6 Analysis results for different speed values, $EI=25239000$, $m= 35 \text{ t/m}$...	83
Table 5.7 Analysis results for different speed values, $EI=25239000$, $m= 45 \text{ t/m}$...	83
Table 5.8 Summary of results for peak responses.....	85
Table 5.9 Aggressivity values for the analysis.....	87
Table 5.10 Comparison of analysis results with DER method	88
Table 5.11 Comparison of analysis results HSLM and TGV trains.....	89

LIST OF FIGURES

FIGURES

Figure 1.1 Simple beam subjected to a moving force P.....	3
Figure 2.1 The simple beam subjected to train loading (Vehicle Bridge Interaction Dynamics, 2004)	9
Figure 2.2 The most critical loading for the beam	15
(from Vehicle Bridge Interaction Dynamics, 2004).....	15
Figure 2.3 HSLM trains spectras for L=30 m and 1% damping.....	21
Figure 2.4 HSLM trains spectras for L=40 m and 1% damping.....	21
Figure 2.5 TGV train spectra for L=30 m and 1% damping.....	22
Figure 2.6 TGV train spectras for L=40 m and 1% damping	22
Figure 2.7 Influence Line of a simply supported beam expressed as a function of span length over wavelength (from ERRI D214/RP6).....	23
Figure 2.8 Maximum displacement results for speeds of 288 km/h and 360 km/h (from J.M. Goicolea et al., (2002))	25
Figure 2.9 Maximum displacement results for speed of 288 km/h from MathLab	25
Figure 2.10 Maximum displacement results for speed of 360 km/h from MathLab	26
Figure 2.11 Properties of Taiwan High Speed Railway Bridge (from C.C. Lin et al., (2005)).....	27
Figure 2.12 Axle arrangement of French TGV train (from C.C. Lin et al., (2005))	27
Figure 2.13 Axle arrangement of German ICE train (from C.C. Lin et al., (2005))	27
Figure 2.14 Axle arrangement of Japanese SKS train (from C.C. Lin et al., (2005))	28
Figure 2.15 Properties of TGV, ICE, and SKS trains (from C.C. Lin et al., (2005))	28

Figure 2.16 Displacement v.s. time graph obtained in paper for French TGV (from C.C. Lin et al., (2005))	29
Figure 2.17 Acceleration v.s. time graph obtained in paper for French TGV (from C.C. Lin et al., (2005))	29
Figure 2.18 Displacement v.s. time graph obtained in MatLab for French TGV ...	30
Figure 2.19 Acceleration v.s. time graph obtained in MatLab for French TGV....	30
Figure 3.1 LM71 loading scheme (from EN 1991-2 : 2003).....	32
Figure 3.2 SW0 and SW2 loading scheme (from EN 1991-2 : 2003).....	33
Figure 3.3 Flow Chart for the requirement of dynamic analysis (EN 1991-2 : 2003)	35
Figure 3.5 HSLM-A train model (from EN 1991-2 : 2003)	38
Figure 3.6 HSLM-B train model (from EN 1991-2 : 2003).....	39
Figure 3.7 Additional damping as a function of span length (from EN 1991-2 : 2003)	41
Figure 3.8 Aggressivity $A_{(L/\lambda)}G_{(\lambda)}$ as a function of excitation wavelength λ for a simply supported span of $L = 7.5 m$ and damping ratio $\varepsilon = 0.01$ (EN 1991-2:2003)	43
Figure 3.9 Aggressivity $A_{(L/\lambda)}G_{(\lambda)}$ as a function of excitation wavelength λ for a simply supported span of $L = 10.0 m$ and damping ratio $\varepsilon = 0.01$ (EN 1991-2:2003)	44
Figure 3.10 Aggressivity $A_{(L/\lambda)}G_{(\lambda)}$ as a function of excitation wavelength λ for a simply supported span of $L = 12.5 m$ and damping ratio $\varepsilon = 0.01$ (EN 1991-2:2003)	44
Figure 3.11 Aggressivity $A_{(L/\lambda)}G_{(\lambda)}$ as a function of excitation wavelength λ for a simply supported span of $L = 15.0 m$ and damping ratio $\varepsilon = 0.01$ (EN 1991-2:2003)	44
Figure 3.12 Aggressivity $A_{(L/\lambda)}G_{(\lambda)}$ as a function of excitation wavelength λ for a simply supported span of $L = 17.5 m$ and damping ratio $\varepsilon = 0.01$ (EN 1991-2:2003)	45

Figure 3.13 Aggressivity $A_{(L/\lambda)}G_{(\lambda)}$ as a function of excitation wavelength λ for a simply supported span of $L = 20.0$ m and damping ratio $\varepsilon = 0.01$ (EN 1991-2:2003)	45
Figure 3.14 Aggressivity $A_{(L/\lambda)}G_{(\lambda)}$ as a function of excitation wavelength λ for a simply supported span of $L = 22.5$ m and damping ratio $\varepsilon = 0.01$ (EN 1991-2:2003)	45
Figure 3.15 Aggressivity $A_{(L/\lambda)}G_{(\lambda)}$ as a function of excitation wavelength λ for a simply supported span of $L = 25.0$ m and damping ratio $\varepsilon = 0.01$ (EN 1991-2:2003)	46
Figure 3.16 Aggressivity $A_{(L/\lambda)}G_{(\lambda)}$ as a function of excitation wavelength λ for a simply supported span of $L = 27.5$ m and damping ratio $\varepsilon = 0.01$ (EN 1991-2:2003)	46
Figure 3.17 Aggressivity $A_{(L/\lambda)}G_{(\lambda)}$ as a function of excitation wavelength λ for a simply supported span of $L = 30.0$ m and damping ratio $\varepsilon = 0.01$ (EN 1991-2:2003)	46
Figure 3.18 Aggressivity $A_{(L/\lambda)}G_{(\lambda)}$ as a function of excitation wavelength λ for a simply supported span of $L = 32.5$ m and damping ratio $\varepsilon = 0.01$ (EN 1991-2:2003)	47
Figure 3.19 Aggressivity $A_{(L/\lambda)}G_{(\lambda)}$ as a function of excitation wavelength λ for a simply supported span of $L = 35.0$ m and damping ratio $\varepsilon = 0.01$ (EN 1991-2:2003)	47
Figure 3.20 Aggressivity $A_{(L/\lambda)}G_{(\lambda)}$ as a function of excitation wavelength λ for a simply supported span of $L = 37.5$ m and damping ratio $\varepsilon = 0.01$ (EN 1991-2:2003)	47
Figure 3.21 Aggressivity $A_{(L/\lambda)}G_{(\lambda)}$ as a function of excitation wavelength λ for a simply supported span of $L = 40.0$ m and damping ratio $\varepsilon = 0.01$ (EN 1991-2:2003)	48
Figure 3.22 Parameters defining critical Universal Train in HSLM-A as a function of critical wavelength of excitation λ_c (EN 1991-2:2003)	49
Figure 4.1 Composite section for $L=30$ m	51

Figure 4.2 Analysis model of the bridge structure	53
Figure 4.3 Section View of Analysis Model	53
Figure 4.4 Marking of members in the analysis model	54
Figure 4.5 First bending mode shape	54
Figure 4.6 First torsional mode shape	55
Figure 4.7 Vehicle Definition in SAP2000	57
Figure 4.8 Moving Load Definition in SAP2000	57
Figure 4.9 Linear Modal History Analysis Definition in SAP2000	58
Figure 4.10 Displacement v.s. Time for HSLMA6 (from SAP2000)	59
Figure 4.11 Acceleration v.s. Time for HSLMA6 (from SAP2000)	59
Figure 4.12 Displacement v.s. Time for French TGV (from SAP2000)	60
Figure 4.13 Acceleration v.s. Time for French TGV (from SAP2000)	60
Figure 4.14 Displacement v.s. Speed for HSLMA1	61
Figure 4.15 Acceleration v.s. Speed for HSLMA1	61
Figure 4.16 Displacement v.s. Speed for HSLMA2	62
Figure 4.17 Acceleration v.s. Speed for HSLMA2	62
Figure 4.18 Displacement v.s. Speed for HSLMA3	62
Figure 4.19 Acceleration v.s. Speed for HSLMA3	63
Figure 4.20 Displacement v.s. Speed for HSLMA4	63
Figure 4.21 Acceleration v.s. Speed for HSLMA4	63
Figure 4.22 Displacement v.s. Speed for HSLMA5	64
Figure 4.23 Acceleration v.s. Speed for HSLMA5	64
Figure 4.24 Displacement v.s. Speed for HSLMA6	64
Figure 4.25 Acceleration v.s. Speed for HSLMA6	65
Figure 4.26 Displacement v.s. Speed for HSLMA7	65
Figure 4.27 Acceleration v.s. Speed for HSLMA7	65
Figure 4.28 Displacement v.s. Speed for HSLMA8	66
Figure 4.29 Acceleration v.s. Speed for HSLMA8	66
Figure 4.30 Displacement v.s. Speed for HSLMA9	66
Figure 4.31 Acceleration v.s. Speed for HSLMA9	67
Figure 4.32 Displacement v.s. Speed for HSLMA10	67

Figure 4.33 Acceleration v.s. Speed for HSLMA10	67
Figure 4.34 Displacement v.s. Time Graph for HSLMA6 (Analytical Approach)	68
Figure 4.35 Acceleration v.s. Time Graph for HSLMA6 (Analytical Approach) ..	68
Figure 4.36 Displacement v.s. Time Graph for TGV (Analytical Approach)	68
Figure 4.37 Acceleration v.s. Time Graph for TGV (Analytical Approach)	69
Figure 4.38 Comparison of Displacement responses of SAP2000 and Analytical Solution for HSLM A6 train	69
Figure 4.39 Comparison of Acceleration responses of SAP2000 and Analytical Solution for HSLM A6 train	70
Figure 4.40 Comparison of Displacement responses of SAP2000 and Analytical Solution for TGV train	70
Figure 4.41 Comparison of Acceleration responses of SAP2000 and Analytical Solution for TGV train	71
Figure 4.42 Comparison of Displacement responses of SAP2000 With and Without Torsion for HSLM A6 train	72
Figure 4.43 Comparison of Acceleration responses of SAP2000 With and Without Torsion for HSLM A6 train	72
Figure 5.1 Displacement v.s. Time graph for $EI = 5047800 \text{ kNm}^2$, $m=25 \text{ t/m}$ and $V=79.40 \text{ m/s}$	79
Figure 5.2 Acceleration v.s. Time graph for $EI = 5047800 \text{ kNm}^2$, $m=25 \text{ t/m}$ and $V=79.40 \text{ m/s}$	79
Figure 5.3 Frequency v.s. Mode Shapes for $EI = 5047800 \text{ kNm}^2$, $m=25 \text{ t/m}$	81
Figure 5.4 Modal Shape in Design Frequency Range for $EI = 5047800 \text{ kNm}^2$, $m=25 \text{ t/m}$	81
Figure 5.5 Displacement v.s. Time graph for $EI = 25239000 \text{ kNm}^2$, $m=25 \text{ t/m}$ and $V=88.78 \text{ m/s}$	82
Figure 5.6 Acceleration v.s. Time graph for $EI = 25239000 \text{ kNm}^2$, $m=25 \text{ t/m}$ and $V=88.78 \text{ m/s}$	82
Figure 5.7 Frequency v.s. Mode Shape for $EI = 25239000 \text{ kNm}^2$, $m=25 \text{ t/m}$	84
Figure 6.1 Stiffness v.s. Acceleration Graph	93
Figure 6.2 Stiffness v.s. Displacement Graph	94

Figure A.1 Wavelength v.s. Dynamic Signature L=30 m, $\varepsilon=0.01$ (HSLM A1)	99
Figure A.2 Wavelength v.s. Dynamic Signature L=30 m, $\varepsilon=0.01$ (HSLM A2)	99
Figure A.3 Wavelength v.s. Dynamic Signature L=30 m, $\varepsilon=0.01$ (HSLM A3) ...	100
Figure A.4 Wavelength v.s. Dynamic Signature L=30 m, $\varepsilon=0.01$ (HSLM A4) ...	100
Figure A.5 Wavelength v.s. Dynamic Signature L=30 m, $\varepsilon=0.01$ (HSLM A5) ...	100
Figure A.6 Wavelength v.s. Dynamic Signature L=30 m, $\varepsilon=0.01$ (HSLM A6) ...	101
Figure A.7 Wavelength v.s. Dynamic Signature L=30 m, $\varepsilon=0.01$ (HSLM A7) ...	101
Figure A.8 Wavelength v.s. Dynamic Signature L=30 m, $\varepsilon=0.01$ (HSLM A8) ...	101
Figure A.9 Wavelength v.s. Dynamic Signature L=30 m, $\varepsilon=0.01$ (HSLM A9) ...	102
Figure A.10 Wavelength v.s. Dynamic Signature L=30 m, $\varepsilon=0.01$ (HSLM A10)	102
Figure A.11 Wavelength v.s. Dynamic Signature L=30 m, $\varepsilon=0.01$ (TGV)	102
Figure A.12 Wavelength v.s. Dynamic Signature L=40 m, $\varepsilon=0.01$ (HSLM A1) .	103
Figure A.13 Wavelength v.s. Dynamic Signature L=40 m, $\varepsilon=0.01$ (HSLM A2) .	103
Figure A.14 Wavelength v.s. Dynamic Signature L=40 m, $\varepsilon=0.01$ (HSLM A3) .	103
Figure A.15 Wavelength v.s. Dynamic Signature L=40 m, $\varepsilon=0.01$ (HSLM A4) .	104
Figure A.16 Wavelength v.s. Dynamic Signature L=40 m, $\varepsilon=0.01$ (HSLM A5) .	104
Figure A.17 Wavelength v.s. Dynamic Signature L=40 m, $\varepsilon=0.01$ (HSLM A6) .	104
Figure A.18 Wavelength v.s. Dynamic Signature L=40 m, $\varepsilon=0.01$ (HSLM A7) .	105
Figure A.19 Wavelength v.s. Dynamic Signature L=40 m, $\varepsilon=0.01$ (HSLM A8) .	105
Figure A.20 Wavelength v.s. Dynamic Signature L=40 m, $\varepsilon=0.01$ (HSLM A9) .	105
Figure A.21 Wavelength v.s. Dynamic Signature L=40 m, $\varepsilon=0.01$ (HSLM A10)	106
Figure A.22 Wavelength v.s. Dynamic Signature L=40 m, $\varepsilon=0.01$ (TGV)	106
Figure A.23 Wavelength v.s. Dynamic Signature L=40 m, $\varepsilon=0.025$ (HSLM A1)	106
Figure A.24 Wavelength v.s. Dynamic Signature L=40 m, $\varepsilon=0.025$ (HSLM A2)	107
Figure A.25 Wavelength v.s. Dynamic Signature L=40 m, $\varepsilon=0.025$ (HSLM A3)	107
Figure A.26 Wavelength v.s. Dynamic Signature L=40 m, $\varepsilon=0.025$ (HSLM A4)	107
Figure A.27 Wavelength v.s. Dynamic Signature L=40 m, $\varepsilon=0.025$ (HSLM A5)	108
Figure A.28 Wavelength v.s. Dynamic Signature L=40 m, $\varepsilon=0.025$ (HSLM A6)	108
Figure A.29 Wavelength v.s. Dynamic Signature L=40 m, $\varepsilon=0.025$ (HSLM A7)	108

Figure A.30 Wavelength v.s. Dynamic Signature $L=40$ m, $\varepsilon=0.025$ (HSLM A8)	109
Figure A.31 Wavelength v.s. Dynamic Signature $L=40$ m, $\varepsilon=0.025$ (HSLM A9)	109
Figure A.32 Wavelength v.s. Dynamic Signature $L=40$ m, $\varepsilon=0.025$ (HSLM A10)	109
.....	109
Figure A.33 Wavelength v.s. Dynamic Signature $L=40$ m, $\varepsilon=0.025$ (TGV)	110
Figure B.1 Displacement v.s. Time graph $V = 40$ m/s, for HSLM A1	111
Figure B.2 Acceleration v.s. Time graph $V = 40$ m/s, for HSLM A1	111
Figure B.3 Displacement v.s. Time graph $V = 64.26$ m/s, for HSLM A1	112
Figure B.4 Acceleration v.s. Time graph $V = 64.26$ m/s, for HSLM A1	112
Figure B.5 Displacement v.s. Time graph $V = 83.33$ m/s, for HSLM A1	112
Figure B.6 Acceleration v.s. Time graph $V = 83.33$ m/s, for HSLM A1	113
Figure B.7 Displacement v.s. Time graph $V = 40$ m/s, for HSLM A2	113
Figure B.8 Acceleration v.s. Time graph $V = 40$ m/s, for HSLM A2	113
Figure B.9 Displacement v.s. Time graph $V = 67.83$ m/s, for HSLM A2	114
Figure B.10 Acceleration v.s. Time graph $V = 67.83$ m/s, for HSLM A2	114
Figure B.11 Displacement v.s. Time graph $V = 83.33$ m/s, for HSLM A2	114
Figure B.12 Acceleration v.s. Time graph $V = 83.33$ m/s, for HSLM A2	115
Figure B.13 Displacement v.s. Time graph $V = 40$ m/s, for HSLM A3	115
Figure B.14 Acceleration v.s. Time graph $V = 40$ m/s, for HSLM A3	115
Figure B.15 Displacement v.s. Time graph $V = 71.40$ m/s, for HSLM A3	116
Figure B.16 Acceleration v.s. Time graph $V = 71.40$ m/s, for HSLM A3	116
Figure B.17 Displacement v.s. Time graph $V = 83.33$ m/s, for HSLM A3	116
Figure B.18 Acceleration v.s. Time graph $V = 83.33$ m/s, for HSLM A3	117
Figure B.19 Displacement v.s. Time graph $V = 40$ m/s, for HSLM A4	117
Figure B.20 Acceleration v.s. Time graph $V = 40$ m/s, for HSLM A4	117
Figure B.21 Displacement v.s. Time graph $V = 74.97$ m/s, for HSLM A4	118
Figure B.22 Acceleration v.s. Time graph $V = 74.97$ m/s, for HSLM A4	118
Figure B.23 Displacement v.s. Time graph $V = 83.33$ m/s, for HSLM A4	118
Figure B.24 Acceleration v.s. Time graph $V = 83.33$ m/s, for HSLM A4	119
Figure B.25 Displacement v.s. Time graph $V = 40$ m/s, for HSLM A5	119
Figure B.26 Acceleration v.s. Time graph $V = 40$ m/s, for HSLM A5	119

Figure B.27 Displacement v.s. Time graph $V = 78.54$ m/s, for HSLM A5	120
Figure B.28 Acceleration v.s. Time graph $V = 78.54$ m/s, for HSLM A5.....	120
Figure B.29 Displacement v.s. Time graph $V = 83.33$ m/s, for HSLM A5	120
Figure B.30 Acceleration v.s. Time graph $V = 83.33$ m/s, for HSLM A5.....	121
Figure B.31 Displacement v.s. Time graph $V = 40$ m/s, for HSLM A6	121
Figure B.32 Acceleration v.s. Time graph $V = 40$ m/s, for HSLM A6.....	121
Figure B.33 Displacement v.s. Time graph $V = 83.33$ m/s, for HSLM A6	122
Figure B.34 Acceleration v.s. Time graph $V = 83.33$ m/s, for HSLM A6.....	122
Figure B.35 Displacement v.s. Time graph $V = 40$ m/s, for HSLM A7	122
Figure B.36 Acceleration v.s. Time graph $V = 40$ m/s, for HSLM A7.....	123
Figure B.37 Displacement v.s. Time graph $V = 42.84$ m/s, for HSLM A7	123
Figure B.38 Acceleration v.s. Time graph $V = 42.84$ m/s, for HSLM A7.....	123
Figure B.39 Displacement v.s. Time graph $V = 83.33$ m/s, for HSLM A7	124
Figure B.40 Acceleration v.s. Time graph $V = 83.33$ m/s, for HSLM A7.....	124
Figure B.41 Displacement v.s. Time graph $V = 40$ m/s, for HSLM A8	124
Figure B.42 Acceleration v.s. Time graph $V = 40$ m/s, for HSLM A8.....	125
Figure B.43 Displacement v.s. Time graph $V = 44.625$ m/s, for HSLM A8	125
Figure B.44 Acceleration v.s. Time graph $V = 44.625$ m/s, for HSLM A8.....	125
Figure B.45 Displacement v.s. Time graph $V = 83.33$ m/s, for HSLM A8	126
Figure B.46 Acceleration v.s. Time graph $V = 83.33$ m/s, for HSLM A8.....	126
Figure B.47 Displacement v.s. Time graph $V = 40$ m/s, for HSLM A9	126
Figure B.48 Acceleration v.s. Time graph $V = 40$ m/s, for HSLM A9.....	127
Figure B.49 Displacement v.s. Time graph $V = 46.41$ m/s, for HSLM A9	127
Figure B.50 Acceleration v.s. Time graph $V = 46.41$ m/s, for HSLM A9.....	127
Figure B.51 Displacement v.s. Time graph $V = 83.33$ m/s, for HSLM A9	128
Figure B.52 Acceleration v.s. Time graph $V = 83.33$ m/s, for HSLM A9.....	128
Figure B.53 Displacement v.s. Time graph $V = 40$ m/s, for HSLM A10	128
Figure B.53 Acceleration v.s. Time graph $V = 40$ m/s, for HSLM A10.....	129
Figure B.54 Displacement v.s. Time graph $V = 48.195$ m/s, for HSLM A10	129
Figure B.54 Acceleration v.s. Time graph $V = 48.195$ m/s, for HSLM A10.....	129
Figure B.55 Displacement v.s. Time graph $V = 83.33$ m/s, for HSLM A10	130

Figure B.56 Acceleration v.s. Time graph $V = 83.33$ m/s, for HSLM A10.....	130
Figure C.1 Displacement v.s. Time graph, (Analysis 1, $V = 40$ m/s).....	131
Figure C.2 Acceleration v.s. Time graph, (Analysis 1, $V = 40$ m/s).....	131
Figure C.3 Displacement v.s. Time graph, (Analysis 1, $V = 97.22$ m/s).....	132
Figure C.4 Acceleration v.s. Time graph, (Analysis 1, $V = 97.22$ m/s).....	132
Figure C.5 Displacement v.s. Time graph, (Analysis 2, $V = 40$ m/s).....	132
Figure C.6 Acceleration v.s. Time graph, (Analysis 2, $V = 40$ m/s).....	133
Figure C.7 Displacement v.s. Time graph, (Analysis 2, $V = 67.10$ m/s).....	133
Figure C.8 Acceleration v.s. Time graph, (Analysis 2, $V = 67.10$ m/s).....	133
Figure C.9 Displacement v.s. Time graph, (Analysis 2, $V = 97.22$ m/s).....	134
Figure C.10 Acceleration v.s. Time graph, (Analysis 2, $V = 97.22$ m/s).....	134
Figure C.11 Displacement v.s. Time graph, (Analysis 3, $V = 40$ m/s).....	134
Figure C.12 Acceleration v.s. Time graph, (Analysis 3, $V = 40$ m/s).....	135
Figure C.13 Displacement v.s. Time graph, (Analysis 3, $V = 59.18$ m/s).....	135
Figure C.14 Acceleration v.s. Time graph, (Analysis 3, $V = 59.18$ m/s).....	135
Figure C.15 Displacement v.s. Time graph, (Analysis 3, $V = 97.22$ m/s).....	136
Figure C.16 Acceleration v.s. Time graph, (Analysis 3, $V = 97.22$ m/s).....	136
Figure C.17 Displacement v.s. Time graph, (Analysis 4, $V = 40$ m/s).....	136
Figure C.18 Acceleration v.s. Time graph, (Analysis 4, $V = 40$ m/s).....	137
Figure C.19 Displacement v.s. Time graph, (Analysis 4, $V = 97.22$ m/s).....	137
Figure C.20 Acceleration v.s. Time graph, (Analysis 4, $V = 97.22$ m/s).....	137
Figure C.21 Displacement v.s. Time graph, (Analysis 5, $V = 40$ m/s).....	138
Figure C.22 Acceleration v.s. Time graph, (Analysis 5, $V = 40$ m/s).....	138
Figure C.23 Displacement v.s. Time graph, (Analysis 5, $V = 75$ m/s).....	138
Figure C.24 Acceleration v.s. Time graph, (Analysis 5, $V = 75$ m/s).....	139
Figure C.25 Displacement v.s. Time graph, (Analysis 5, $V = 97.22$ m/s).....	139
Figure C.26 Acceleration v.s. Time graph, (Analysis 5, $V = 97.22$ m/s).....	139
Figure C.27 Displacement v.s. Time graph, (Analysis 6, $V = 40$ m/s).....	140
Figure C.28 Acceleration v.s. Time graph, (Analysis 6, $V = 40$ m/s).....	140
Figure C.29 Displacement v.s. Time graph, (Analysis 6, $V = 66.17$ m/s).....	140
Figure C.30 Acceleration v.s. Time graph, (Analysis 6, $V = 66.17$ m/s).....	141

Figure C.31 Displacement v.s. Time graph, (Analysis 6, $V = 97.22$ m/s).....	141
Figure C.32 Acceleration v.s. Time graph, (Analysis 6, $V = 97.22$ m/s).....	141
Figure C.33 Displacement v.s. Time graph, (Analysis7, $V = 40$ m/s).....	142
Figure C.34 Acceleration v.s. Time graph, (Analysis 7, $V = 40$ m/s).....	142
Figure C.35 Displacement v.s. Time graph, (Analysis7, $V = 78.91$ m/s).....	142
Figure C.36 Acceleration v.s. Time graph, (Analysis 7, $V = 78.91$ m/s).....	143
Figure C.37 Displacement v.s. Time graph, (Analysis7, $V = 97.22$ m/s).....	143
Figure C.38 Acceleration v.s. Time graph, (Analysis 7, $V = 97.22$ m/s).....	143
Figure C.39 Displacement v.s. Time graph, (Analysis 8, $V = 40$ m/s).....	144
Figure C.40 Acceleration v.s. Time graph, (Analysis 8, $V = 40$ m/s).....	144
Figure C.41 Displacement v.s. Time graph, (Analysis 8, $V = 66.695$ m/s).....	144
Figure C.42 Acceleration v.s. Time graph, (Analysis 8, $V = 66.695$ m/s).....	145
Figure C.43 Displacement v.s. Time graph, (Analysis 8, $V = 97.22$ m/s).....	145
Figure C.44 Acceleration v.s. Time graph, (Analysis 8, $V = 97.22$ m/s).....	145
Figure C.45 Displacement v.s. Time graph, (Analysis 9, $V = 40$ m/s).....	146
Figure C.46 Acceleration v.s. Time graph, (Analysis 9, $V = 40$ m/s).....	146
Figure C.47 Displacement v.s. Time graph, (Analysis 9, $V = 88.23$ m/s).....	146
Figure C.48 Acceleration v.s. Time graph, (Analysis 9, $V = 88.23$ m/s).....	147
Figure C.49 Displacement v.s. Time graph, (Analysis 9, $V = 97.22$ m/s).....	147
Figure C.50 Acceleration v.s. Time graph, (Analysis 9, $V = 97.22$ m/s).....	147
Figure C.51 Displacement v.s. Time graph, (Analysis 10, $V = 40$ m/s).....	148
Figure C.52 Acceleration v.s. Time graph, (Analysis 10, $V = 40$ m/s).....	148
Figure C.53 Displacement v.s. Time graph, (Analysis 10, $V = 88.22$ m/s).....	148
Figure C.54 Acceleration v.s. Time graph, (Analysis 10, $V = 88.22$ m/s).....	149
Figure C.55 Displacement v.s. Time graph, (Analysis 10, $V = 97.22$ m/s).....	149
Figure C.56 Acceleration v.s. Time graph, (Analysis 10, $V = 97.22$ m/s).....	149
Figure C.57 Displacement v.s. Time graph, (Analysis 11, $V = 40$ m/s).....	150
Figure C.58 Acceleration v.s. Time graph, (Analysis 11, $V = 40$ m/s).....	150
Figure C.59 Displacement v.s. Time graph, (Analysis 11, $V = 74.56$ m/s).....	150
Figure C.60 Acceleration v.s. Time graph, (Analysis 11, $V = 74.56$ m/s).....	151
Figure C.61 Displacement v.s. Time graph, (Analysis 11, $V = 97.22$ m/s).....	151

Figure C.62 Acceleration v.s. Time graph, (Analysis 11, $V = 97.22$ m/s).....	151
Figure C.63 Displacement v.s. Time graph, (Analysis 12, $V = 40$ m/s)	152
Figure C.64 Acceleration v.s. Time graph, (Analysis 12, $V = 40$ m/s).....	152
Figure C.65 Displacement v.s. Time graph, (Analysis 12, $V = 65.80$ m/s)	152
Figure C.66 Acceleration v.s. Time graph, (Analysis 12, $V = 65.80$ m/s).....	153
Figure C.67 Displacement v.s. Time graph, (Analysis 12, $V = 97.22$ m/s)	153
Figure C.68 Acceleration v.s. Time graph, (Analysis 12, $V = 97.22$ m/s).....	153
Figure C.69 Displacement v.s. Time graph, (Analysis 13, $V = 40$ m/s)	154
Figure C.70 Acceleration v.s. Time graph, (Analysis 13, $V = 40$ m/s).....	154
Figure C.71 Displacement v.s. Time graph, (Analysis 13, $V = 94.16$ m/s)	154
Figure C.72 Acceleration v.s. Time graph, (Analysis 13, $V = 94.16$ m/s).....	155
Figure C.73 Displacement v.s. Time graph, (Analysis 13, $V = 97.22$ m/s)	155
Figure C.74 Acceleration v.s. Time graph, (Analysis 13, $V = 97.22$ m/s).....	155
Figure C.75 Displacement v.s. Time graph, (Analysis 14, $V = 40$ m/s)	156
Figure C.76 Acceleration v.s. Time graph, (Analysis 14, $V = 40$ m/s).....	156
Figure C.77 Displacement v.s. Time graph, (Analysis 14, $V = 79.58$ m/s)	156
Figure C.78 Acceleration v.s. Time graph, (Analysis 14, $V = 79.58$ m/s).....	157
Figure C.79 Displacement v.s. Time graph, (Analysis 14, $V = 97.22$ m/s)	157
Figure C.80 Acceleration v.s. Time graph, (Analysis 14, $V = 97.22$ m/s).....	157
Figure C.81 Displacement v.s. Time graph, (Analysis 15, $V = 40$ m/s)	158
Figure C.82 Acceleration v.s. Time graph, (Analysis 15, $V = 40$ m/s).....	158
Figure C.83 Displacement v.s. Time graph, (Analysis 15, $V = 49.39$ m/s)	158
Figure C.84 Acceleration v.s. Time graph, (Analysis 15, $V = 49.39$ m/s).....	159
Figure C.85 Displacement v.s. Time graph, (Analysis 15, $V = 97.22$ m/s)	159
Figure C.86 Acceleration v.s. Time graph, (Analysis 15, $V = 97.22$ m/s).....	159
Figure C.87 Displacement v.s. Time graph, (Analysis 16, $V = 40$ m/s)	160
Figure C.88 Acceleration v.s. Time graph, (Analysis 16, $V = 40$ m/s).....	160
Figure C.89 Displacement v.s. Time graph, (Analysis 16, $V = 65.89$ m/s)	160
Figure C.90 Acceleration v.s. Time graph, (Analysis 16, $V = 65.89$ m/s).....	161
Figure C.91 Displacement v.s. Time graph, (Analysis 16, $V = 97.22$ m/s)	161
Figure C.92 Acceleration v.s. Time graph, (Analysis 16, $V = 97.22$ m/s).....	161

Figure C.93 Displacement v.s. Time graph, (Analysis 17, $V = 40$ m/s).....	162
Figure C.94 Acceleration v.s. Time graph, (Analysis 17, $V = 40$ m/s).....	162
Figure C.95 Displacement v.s. Time graph, (Analysis 17, $V = 86.74$ m/s).....	162
Figure C.96 Acceleration v.s. Time graph, (Analysis 17, $V = 86.74$ m/s).....	163
Figure C.97 Displacement v.s. Time graph, (Analysis 17, $V = 97.22$ m/s).....	163
Figure C.98 Acceleration v.s. Time graph, (Analysis 17, $V = 97.22$ m/s).....	163
Figure C.99 Displacement v.s. Time graph, (Analysis 18, $V = 40$ m/s).....	164
Figure C.100 Acceleration v.s. Time graph, (Analysis 18, $V = 40$ m/s).....	164
Figure C.101 Displacement v.s. Time graph, (Analysis 18, $V = 76.55$ m/s).....	164
Figure C.102 Acceleration v.s. Time graph, (Analysis 18, $V = 76.55$ m/s).....	165
Figure C.103 Displacement v.s. Time graph, (Analysis 18, $V = 97.22$ m/s).....	165
Figure C.103 Acceleration v.s. Time graph, (Analysis 18, $V = 97.22$ m/s).....	165
Figure C.104 Displacement v.s. Time graph, (Analysis 19, $V = 40$ m/s).....	166
Figure C.105 Acceleration v.s. Time graph, (Analysis 19, $V = 40$ m/s).....	166
Figure C.106 Displacement v.s. Time graph, (Analysis 19, $V = 89.76$ m/s).....	166
Figure C.107 Acceleration v.s. Time graph, (Analysis 19, $V = 89.76$ m/s).....	167
Figure C.108 Displacement v.s. Time graph, (Analysis 19, $V = 97.22$ m/s).....	167
Figure C.109 Acceleration v.s. Time graph, (Analysis 19, $V = 97.22$ m/s).....	167
Figure C.110 Displacement v.s. Time graph, (Analysis 20, $V = 40$ m/s).....	168
Figure C.111 Acceleration v.s. Time graph, (Analysis 20, $V = 40$ m/s).....	168
Figure C.112 Displacement v.s. Time graph, (Analysis 20, $V = 65.75$ m/s).....	168
Figure C.113 Acceleration v.s. Time graph, (Analysis 20, $V = 65.75$ m/s).....	169
Figure C.114 Displacement v.s. Time graph, (Analysis 20, $V = 97.22$ m/s).....	169
Figure C.115 Acceleration v.s. Time graph, (Analysis 20, $V = 97.22$ m/s).....	169
Figure C.116 Displacement v.s. Time graph, (Analysis 21, $V = 40$ m/s).....	170
Figure C.117 Acceleration v.s. Time graph, (Analysis 21, $V = 40$ m/s).....	170
Figure C.118 Displacement v.s. Time graph, (Analysis 21, $V = 90.32$ m/s).....	170
Figure C.119 Acceleration v.s. Time graph, (Analysis 21, $V = 90.32$ m/s).....	171
Figure C.120 Displacement v.s. Time graph, (Analysis 21, $V = 97.22$ m/s).....	171
Figure C.121 Acceleration v.s. Time graph, (Analysis 21, $V = 97.22$ m/s).....	171
Figure C.122 Displacement v.s. Time graph, (Analysis 1, $V = 74.24$ m/s, TGV)	172

Figure C.123 Acceleration v.s. Time graph, (Analysis 1, $V = 74.24$ m/s, TGV) .	172
Figure C.124 Displacement v.s. Time graph, (Analysis 2, $V = 62.74$ m/s, TGV)	172
Figure C.125 Acceleration v.s. Time graph, (Analysis 2, $V = 62.74$ m/s, TGV) .	173
Figure C.126 Displacement v.s. Time graph, (Analysis 3, $V = 55.33$ m/s, TGV) .	173
Figure C.127 Acceleration v.s. Time graph, (Analysis 3, $V = 55.33$ m/s, TGV) .	173
Figure C.128 Displacement v.s. Time graph, (Analysis 4, $V = 73.78$ m/s, TGV) .	174
Figure C.129 Acceleration v.s. Time graph, (Analysis 4, $V = 73.78$ m/s, TGV) .	174
Figure C.130 Displacement v.s. Time graph, (Analysis 5, $V = 62.36$ m/s, TGV) .	174
Figure C.131 Acceleration v.s. Time graph, (Analysis 5, $V = 62.36$ m/s, TGV) .	175
Figure C.132 Displacement v.s. Time graph, (Analysis 6, $V = 97.22$ m/s, TGV) .	175
Figure C.133 Acceleration v.s. Time graph, (Analysis 6, $V = 97.22$ m/s, TGV) .	175
Figure C.134 Displacement v.s. Time graph, (Analysis 7, $V = 97.22$ m/s, TGV) .	176
Figure C.135 Acceleration v.s. Time graph, (Analysis 7, $V = 97.22$ m/s, TGV) .	176
Figure C.136 Displacement v.s. Time graph, (Analysis 8, $V = 93.54$ m/s, TGV) .	176
Figure C.137 Acceleration v.s. Time graph, (Analysis 8, $V = 93.54$ m/s, TGV) .	177
Figure C.138 Displacement v.s. Time graph, (Analysis 9, $V = 97.22$ m/s, TGV) .	177
Figure C.139 Acceleration v.s. Time graph, (Analysis 9, $V = 97.22$ m/s, TGV) .	177
Figure C.140 Displacement v.s. Time graph, (Analysis 10, $V = 82.49$ m/s, TGV)	178
Figure C.141 Acceleration v.s. Time graph, (Analysis 10, $V = 82.49$ m/s, TGV)	178
Figure C.142 Displacement v.s. Time graph, (Analysis 11, $V = 69.72$ m/s, TGV)	178
Figure C.143 Acceleration v.s. Time graph, (Analysis 11, $V = 69.72$ m/s, TGV)	179
Figure C.144 Displacement v.s. Time graph, (Analysis 12, $V = 61.50$ m/s, TGV)	179
Figure C.145 Acceleration v.s. Time graph, (Analysis 12, $V = 61.50$ m/s, TGV)	179
Figure C.146 Displacement v.s. Time graph, (Analysis 13, $V = 65.22$ m/s, TGV)	180
Figure C.147 Acceleration v.s. Time graph, (Analysis 13, $V = 65.22$ m/s, TGV)	180
Figure C.148 Displacement v.s. Time graph, (Analysis 14, $V = 55.12$ m/s, TGV)	180
Figure C.149 Acceleration v.s. Time graph, (Analysis 14, $V = 55.12$ m/s, TGV)	181
Figure C.150 Displacement v.s. Time graph, (Analysis 15, $V = 97.22$ m/s, TGV)	181
Figure C.151 Acceleration v.s. Time graph, (Analysis 15, $V = 97.22$ m/s, TGV)	181
Figure C.152 Displacement v.s. Time graph, (Analysis 16, $V = 71.10$ m/s, TGV)	182
Figure C.153 Acceleration v.s. Time graph, (Analysis 16, $V = 71.10$ m/s, TGV)	182

Figure C.154 Displacement v.s. Time graph, (Analysis 17, V =60.10 m/s, TGV)	182
Figure C.155 Acceleration v.s. Time graph, (Analysis 17, V = 60.10 m/s, TGV)	183
Figure C.156 Displacement v.s. Time graph, (Analysis 18, V =97.22 m/s, TGV)	183
Figure C.157 Acceleration v.s. Time graph, (Analysis 18, V = 97.22 m/s, TGV)	183
Figure C.158 Displacement v.s. Time graph, (Analysis 19, V =83.93 m/s, TGV)	184
Figure C.159 Acceleration v.s. Time graph, (Analysis 19, V = 83.93 m/s, TGV)	184
Figure C.160 Displacement v.s. Time graph, (Analysis 20, V =70.93 m/s, TGV)	184
Figure C.161 Acceleration v.s. Time graph, (Analysis 20, V = 70.93 m/s, TGV)	185
Figure C.162 Displacement v.s. Time graph, (Analysis 21, V =62.55 m/s, TGV)	185
Figure C.163 Acceleration v.s. Time graph, (Analysis 21, V = 62.55 m/s, TGV)	185
Figure D.1 Frequency v.s. Mode Shape, (Analysis 2)	186
Figure D.3 Frequency v.s. Mode Shape, (Analysis 5)	187
Figure D.4 Frequency v.s. Mode Shape, (Analysis 6)	187
Figure D.6 Frequency v.s. Mode Shape, (Analysis 8)	188
Figure D.7 Frequency v.s. Mode Shape, (Analysis 9)	188

CHAPTER 1

INTRODUCTION

1.1 General

High-speed railway network has showed remarkable development in the countries especially where transportation became the major concern for the human life and economy. The sense of providing large capacity transportation, higher safety and using the energy in the most economical way leads countries to develop solutions.

During the early years of the development of high-speed networks, the term “high-speed” was used for the speeds above 200 km/h. Japan is the first country that introduced the high-speed term to the world with the Tokaido Shinkansen railway line for which the operating speed was 210 km/h. In Europe, France is the first country that has constructed the first high-speed railway line with 270 km/h operating speed. Germany, Belgium, Italy, Netherlands, Spain and Turkey followed France and European high-speed railway network reached great levels during the recent years. In Asia, China has also constructed high-speed railway networks and has considerable share in the development of the high-speed railway technology. Development of high-speed railway networks brought the race of the countries in the manner of the maximum speeds together with the comfort requirements. The train speed that has started with 210 km/h has reached 581 km/h with the MLX-01 train in Japan which is the current world record holder.

From the structural point of view, the differences between the conventional railway lines and the high-speed railway lines lead changes in the design process. Dynamic effects are the major concerns that have to be considered in the design of the high-speed railway structures. Besides, human comfort criteria has also gained importance with the introduction of the high operating speeds.

The most important effect on the high-speed railway bridges is the -resonance- which is the coincidence of the natural frequency of vibration of the structure, with the exciting frequency by the train. In order to avoid from the resonance effects, the structural design engineer should ensure that the response of the bridge is in the acceptable limits to provide its safety. The analysis procedures and acceptable limits were included in the scope of the European standards and some procedures for dynamic analyses were defined.

1.2 Literature Survey

Y.S. Cheng, F.T.K. Au and Y.K. Cheung (2001), studied the effect of train properties together with the track structure and bridge. The train is modelled as mass spring damper in their study at axle locations. They modelled the rails as upper beam elements and deck as lower beam element. And spring and dampers are used as link elements between rail beam and deck beam to account for rail pad. The results showed that the effect of track structure on the responses of bridge structure is negligible, whereas the effect of bridge structure on the response of track is considerable.

Clough, R., Penzien, J. (2003), presented wide range of information about dynamic behaviour of structures in their book of "Dynamic of Structures". The response of single degree of freedom systems to harmonic, periodic and impulsive loading was described. Analysis for the dynamic response of multi degree of freedom systems were also presented by using different methods such as

superposition and step by step methods. Supporting examples which let reader to understand the subject clearly were also provided in the book .

Delgado, R.M. Cruz, S (1997), studied the dynamic behaviour of the bridge under high-speed traffic action in two ways. First, the train is considered as set of moving forces and masses of each axle of train are induced on the bridge. As second, structural behaviour of train together with the interaction effects with the bridge were considered. Different parameters such as train and bridge stiffness, bridge mass, track irregularities were studied in order to define the effect of each parameter on the dynamic response of the bridge.

Ladislav Fryba (1999), considered the subject in a broad way in his book “Vibration of Solids and Structures Under Moving Loads”. He studied the one, two and three dimensional solids with different loading conditions such as moving constant force, moving harmonic force, moving force arbitrarily varying in time. He also studied the effects of boundary conditions on dynamic responses of the bridges. He also presented the effects of the moving speed and track irregularities on bridge responses (Fryba, 1996). He worked on the phenemonon of resonance and the critical speeds that lead to resonance conditions. He stated that the high operating speeds and repeated action of the train loads on the structure can lead to the resonance condition to occur and respectively increase in the vertical acceleration responses of the bridge (Fryba, 2001).

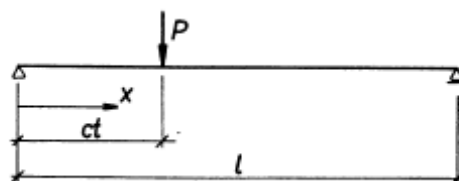


Figure 1.1 Simple beam subjected to a moving force P

K. Liu, G. De Roeck, and G. Lombaert, (2009) determined the conditions for which the train-bridge interaction should be considered to determine the dynamic response of the bridge. Different parameters such as train mass, train speed, the natural frequency ratio of the train and bridge and damping ratio were studied in that paper to determine the effects of these items on the dynamic response of the bridge.

M., K., Song et. all. (2003), studied a new finite element method to determine the dynamic effects on railway bridges. Shell elements with six degree of freedoms per node were used for modelling deck and it was provided that the inplane and out of plane deformations are coupled. Shell elements with variable nodes were used for modelling the connection regions between the rail, sleepers and deck. Track irregularities were also considered in the analysis. A simply supported steel concrete composite bridge together with the two span PC box girder bridge were analysed and results are compared with the experimental and previous researches. It was found at the end of the study that the obtained results are well matched with the experimentally obtained results.

P. Museros and E. Alarcon (2005), studied the influence of second bending mode on the dynamic response of high speed railway bridges. They determined the equation of motion for simply supported bridge and presented the parameters that are affecting the dynamic behaviour. With the light of the presented information, they studied a real case and found that there may be some cases for which the consideration of only the first natural bending mode is not enough to determine the dynamic response of high speed bridges. It was also concluded in their study that the maximum response is not needed to be obtained at midspan and the maximum response may be obtained at the quarter orr three quarter of the span lenght.

He Xia et. all. (2003), studied a practical case such that he presented a report that contains the comparison of the finite element dynamic analysis results of Antoing Bridge with the results obtained from experimental measurements. He analysed the

bridge under the effect of Thalys train composed of one locomotive followed by one transition carriage, six normal articulated cars, one transition carriage and one locomotive. He regarded the articulated train group as a series of articulated vehicle elements composed of car bodies, bogies and wheel sets. There were some assumptions in the analysis of Antoin Bridge such that the track bridge interaction effects are neglected. Accordingly, inertial effects of the connecting elements such as fasteners, rail pads and ballast were not considered. Another assumption was that the cross section deformation of the girder was considered in the modal analysis. He Xia et. all. (2003), stated that the analytical model of the bridge was acceptable in the manner of reflecting the bridge behaviour, The obtained results are considered as matched with the measured data obtained from site, the dynamic characteristics of Antoin Bridge are in the limits of the current safety and comfort standards, the articulated trains have positive effect on the bridge structures such that they reduce the impact effect on trains on the structures.

In the paper of H. Xia et al. (2006), theoretical derivations were used to obtain the effects of the resonance condition. The condition was investigated in three parts. First, the periodical actions of moving loads with vertical weights, centrifugal forces and wind forces were investigated. Secondly, loading rates of moving loads were investigated. And finally, swing forces of the train excited by track irregularities and wheel hunting movements were investigated. The comparisons were provided between estimated resonant speeds and results of dynamic simulations together with the field measurements.

Y.B. Yang, J.D. Yau, Y.S. Wu (2004), had great contribution to the problem of dynamic effects on railway bridges by presenting a book named "Vehicle Bridge Interaction Dynamics" in which all kinds of problems that had previously been worked were clearly stated and user friendly solutions were defined. They defined the method of solutions by emphasizing them with the illustrative examples. Moving load problems were presented by defining the impact responses of simply supported beams, simply supported bridges with elastic bearings, response of the

curved beams. They worked on vehicle-bridge interaction for different conditions such that the method of contact forces, pitching effect, stability of the trains under earthquake conditions.

1.3 Object and Scope

The major objective of this study is to determine the analytical procedure to obtain the dynamic behaviour of a simply supported bridge structure and perform the related comparisons with other methods such as finite element method. After the comparison of the finite element method and the analytical approaches to the problem, the assumptions that are stated in the relevant standards will be investigated and the reliability of them will be checked. And finally, different stiffness and mass properties will be checked and effect of them will be presented.

This study starts with the determination of the analytical procedures in Chapter 2. Fryba's analytical solution is used to obtain the results. However, the simplified method determined by Y.B. Yang, J.D. Yau and Y.S. Wu is followed since they presented the procedure in a more clear way. Also in the book of Y.B. Yang, J.D. Yau and Y.S. Wu, analytical procedure was modified for the current train loadings for high speed railway lines. The effect of the vehicle body mass on the response of the structure was neglected and an assumption was made such that the mass of the structure is higher than the vehicle mass. The resonance and cancellation phenomena are explained.. In addition to Fryba's solution, the DER method which is used by Eurocodes to define the critical train loading is also explained in Section 2.6. The validation of the written MatLab program is checked with two examples presented by J.M. Goicolea et. al. (2002), and C. C. Lin et. al. (2005) at Section 2.7.

In Chapter 3, the approach of EN 1991-2 to the problem is explained and the related procedure defined by the standard is presented.

In Chapter 4, a simply supported 30 m span bridge from the Ankara-Sivas High Speed Railway project is modeled by using the finite element program, SAP2000. The modeling properties are clearly defined and emphasized with the related figures presented. The dynamic analysis of the related bridge is performed. Analytical procedure is applied for the same bridge and the results obtained from the finite element dynamic analysis are compared with the analytically obtained results.

In Chapter 5, analyses for different mass and stiffness values are performed for different speeds and also for the critical trains chosen according to the procedure defined in Eurocode.

Chapter 6 includes the related summary and conclusions for the analyses performed in the scope of the study.

CHAPTER 2

ANALYTICAL PROCEDURE FOR THE SIMPLE BEAM SUBJECTED TO SERIES OF MOVING LOADS

2.1 General

This chapter describes the problem of a simple beam subjected to a series of moving loads determined by Fryba and presented in a clear way and updated for the current loading diagram of trains by Y.B. Yang, J.D. Yau, Y.S. Wu in the book of Vehicle Bridge Interaction Dynamics, 2004. In addition, DER method based on the decomposition of excitation at resonance is explained in Section 2.6.

2.2 Method of Solution for the Beam Subjected to Series of Moving Loads (Vehicle Bridge Interaction Dynamics, 2004)

For the analytical solution, train is modeled as the identical cars each of which contains two axles with constant intervals (Vehicle Bridge Interaction Dynamics, 2004).

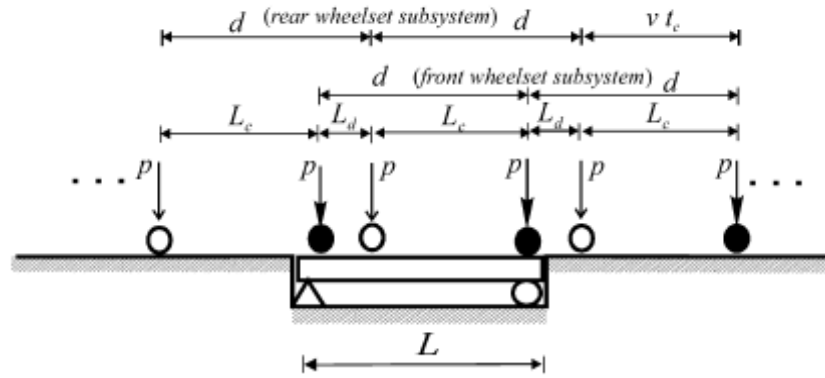


Figure 2.1 The simple beam subjected to train loading (Vehicle Bridge Interaction Dynamics, 2004)

The train is assumed to have N identical cars each of which is supported by two boggies. Each car length is determined as d while the distance between the two wheel of the car is L_c and the distance between the rear wheels is L_d . The load p is assumed to be constant which is in accordance with the train models described by EN 1991-2 that will be explained in Chapter 3. Considering the each car as the combination of two wheel sets leads to a time lag of $t_c = L_c / v$. The load function for the train can be determined as (Vehicle Bridge Interaction Dynamics, 2004);

$$F(t) = \sum_{j=1}^N p \cdot [U_j(t, v, L) + U_j(t - t_c, v, L)] \quad (2.1)$$

$$U_j(t, v, L) = \delta[x - v(t - t_j)] [H(t - t_j) - H(t - t_j - L/v)] \quad (2.2)$$

The meanings of the parameters stated in the formulas above are determined below (Vehicle Bridge Interaction Dynamics, 2004);

- p = Series of Lumped Train Loads
- $U_j(t, v, L)$ = Function to model the effect and position of wheel load on the bridge.
- t = Time
- v = Travelling Speed of Train

L	= Span Length of Bridge
δ	= Direct delta function
x	= Coordinate of the beam
t_j	= Arriving time of j^{th} load at the beam = $(j-1) \times d/v$
$H(t-t_j)$	= Unit step function that turns on the effect of j^{th} moving load when it enters the beam.
$H(t-t_j-L/v)$	= Unit step function that turns off the effect of j^{th} moving load when it leaves the beam.

The values for unit step function are determined below;

$$H(t) = 0 \quad \text{if } t < 0 \quad (2.3)$$

$$H(t) = 1 \quad \text{if } t \geq 0 \quad (2.4)$$

The equation (2.1) presented above neglects the effect of inertia of the moving masses and the interaction between the train cars and the beam. (Vehicle Bridge Interaction Dynamics, 2004). In order to consider those effects the function above is modified to the function determined below (Bolotin, 1964);

$$F(p, M, v) = p - M(\ddot{u} + 2v\dot{u}' + v^2u'') \quad (2.5)$$

M is the lumped mass for the each load, u is the vertical deflection of the beam. Dots denotes for the differentiation with respect to time while primes denotes the derivative with respect to coordinate (Vehicle Bridge Interaction Dynamics, 2004).

The equation of motion for the beam under moving load can be written by using the load function in equation (2.5) as (Vehicle Bridge Interaction Dynamics, 2004);

$$m\ddot{u} + c_e\dot{u} + c_i I \dot{u}'''' + EIu'''' = \sum_{j=1}^N F(p, M, v) [U_j(t, v, L) + U_j(t-t_c, v, L)] \quad (2.6)$$

m is the mass of the bridge per unit length, E is the elastic modulus, I is the moment of inertia, t_c is the time lag as defined in Section 2.1, c_e and c_i are the external and internal damping coefficients respectively (Vehicle Bridge Interaction Dynamics, 2004).

Defining the related boundary conditions for the simply supported case;

$$\begin{aligned} u(0,t) &= 0, \\ u(L,t) &= 0, \\ u(x,0) &= 0, \\ \dot{u}(x,0) &= 0, \\ E I u''(0,t) &= 0, \\ E I u''(L,t) &= 0, \end{aligned}$$

By using the related boundary conditions, the vertical deflection of the beam can be presented in a series form as shown below (Vehicle Bridge Interaction Dynamics, 2004);

$$u(x,t) = \sum_{n=1}^{\infty} q_n(t) \sin\left(\frac{n\pi x}{L}\right) \quad (2.7)$$

$q_n(t)$ is the generalized coordinate for the n^{th} mode. The equation of the motion in terms of the generalized coordinates, q_n is obtained by substituting the equation (2.4) in equation (2.3), multiplying both sides with $\sin\left(\frac{n\pi x}{L}\right)$ and integrating with respect to length L of the beam (Vehicle Bridge Interaction Dynamics, 2004).

$$(1 + \varepsilon_{m,n}) \ddot{q}_n + (2\varepsilon_n \omega_n + \varepsilon_{c,n}) \dot{q}_n + (\omega_n^2 + \varepsilon_{s,n}) q_n = F_n(t) \quad (2.8)$$

ε_n is damping coefficient and w_n is the angular frequency of the vibration of the n^{th} mode defined as (Vehicle Bridge Interaction Dynamics, 2004);

$$w_n = n^2 \pi^2 \sqrt{\frac{EI}{mL^4}}$$

$\varepsilon_{m,n}$ is the coefficient to account for the effect of the mass of moving loads, $\varepsilon_{c,n}$ represents the Coriolis force as a result of the coupling interaction between the speed of the moving mass and the angular velocity of the beam. $\varepsilon_{s,n}$ is the coefficient to take the centrifugal force into account. Those effects mentioned may lead the beam to lose its stability. However, the high speed railway bridges designed are commonly too rigid such that those effects can be neglected. $F_n(t)$ in the equation (2.8) is the forcing function for the n^{th} generalized coordinate and determined below (Vehicle Bridge Interaction Dynamics, 2004).

$$F_n(t) = -\frac{2p}{mL} \sum_{j=1}^N [f_n(t, v, L) + f_n(t - t_c, v, L)] \quad (2.9)$$

$f_n(t, v, L)$ = Part of forcing function for the front wheel of an identical car.

$f_n(t - t_c, v, L)$ = Part of forcing function for the rear wheel of an identical car.

The function f_n is defined as shown below (Vehicle Bridge Interaction Dynamics, 2004);

$$f_n(t, v, L) = \sin\left(\frac{n\pi v(t - t_j)}{L}\right)H(t - t_j) + (-1)^{n+1} \sin\left(\frac{n\pi v(t - t_j - L/v)}{L}\right)H\left(t - t_j - \frac{L}{v}\right) \quad (2.10)$$

By neglecting the coefficients $\varepsilon_{m,n}$, $\varepsilon_{c,n}$, $\varepsilon_{s,n}$ in equation (2.8), generalized coordinate $q_n(t)$ is obtained as (Vehicle Bridge Interaction Dynamics, 2004);

$$\begin{aligned}
q_n(t) &= \frac{1}{m\omega_{dn}} \int_0^t F_n(\tau) e^{-\varepsilon_n \omega_n (t-\tau)} \sin(\omega_{dn}(t-\tau)) d\tau \\
&= \frac{2pL^3}{EI\pi^4} [P_n(v,t) + P_n(v,t-t_c)] \quad (2.11)
\end{aligned}$$

ω_{dn} is the damped circular frequency of the beam and defined as $\omega_{dn} = \omega_n \sqrt{1 - \varepsilon_n^2}$ and the functions $P_n(v,t)$ and $P_n(v,t-t_c)$ are defined as (Vehicle Bridge Interaction Dynamics, 2004);

$P_n(v,t)$ = Dynamic response from the front wheel of an identical car.

$P_n(v,t-t_c)$ = Dynamic response from the rear wheel of an identical car.

$$P_n(v,t) = \frac{1}{n^4} \sum_{j=1}^N \frac{1}{(1 - S_n^2)^2 + 4(\varepsilon_n S_n)^2} x \left[A.H(t-t_j) + (-1)^{n+1}.B.H(t-t_j - \frac{L}{v}) \right] \quad (2.12)$$

The coefficients A and B are determined as follows (Vehicle Bridge Interaction Dynamics, 2004);

$$\begin{aligned}
A &= (1 - S_n^2) \sin(\Omega_n(t-t_j)) - 2\varepsilon_n S_n \cos(\Omega_n(t-t_j)) + \\
&e^{-\varepsilon_n \omega_n (t-t_j)} \left[2\varepsilon_n S_n \cos(\omega_{dn}(t-t_j)) + \frac{S_n}{\sqrt{1 - \varepsilon_n^2}} (2\varepsilon_n^2 + S_n^2 - 1) \sin(\omega_{dn}(t-t_j)) \right] \quad (2.13)
\end{aligned}$$

$$\begin{aligned}
B = & (1 - S_n^2) \sin(\Omega_n (t - t_j - \frac{L}{v})) - 2\varepsilon_n S_n \cos(\Omega_n (t - t_j - \frac{L}{v})) + \\
& e^{-\varepsilon_n w_n (t - t_j - \frac{L}{v})} \left[2\varepsilon_n S_n \cos(w_{dn} (t - t_j - \frac{L}{v})) + \frac{S_n}{\sqrt{1 - \varepsilon_n^2}} (2\varepsilon_n^2 + S_n^2 - 1) \sin(w_{dn} (t - t_j - \frac{L}{v})) \right]
\end{aligned} \tag{2.14}$$

Ω_n is the frequency due to the moving loads, and S_n is the speed parameter and the values are determined as shown below (Vehicle Bridge Interaction Dynamics, 2004);

$$\Omega_n = \frac{n\pi v}{L} \tag{2.15}$$

$$S_n = \frac{n\pi v}{w_n L} \tag{2.16}$$

2.3 Resonance Condition

Resonance condition occurs when the excitation frequency by the moving load and the natural frequency of the structure are the same. If the damping is neglected and only the first mode is considered in the equation (2.12) reduces to (Vehicle Bridge Interaction Dynamics, 2004);

$$\begin{aligned}
P_1(v, t) = & \sum_{j=1}^N [\sin \Omega_1 (t - t_j) - S_1 \sin w_1 (t - t_j)] H(t - t_j) + \\
& \left[\sin \Omega_1 (t - t_j - \frac{L}{v}) + S_1 \sin w_1 (t - t_j - \frac{L}{v}) \right] H(t - t_j - \frac{L}{v})
\end{aligned} \tag{2.17}$$

The most critical case for the displacement occurs when the rear wheel of (N-1)th identical car and the front wheel of the Nth car acts on the beam simultaneously (Vehicle Bridge Interaction Dynamics, 2004).

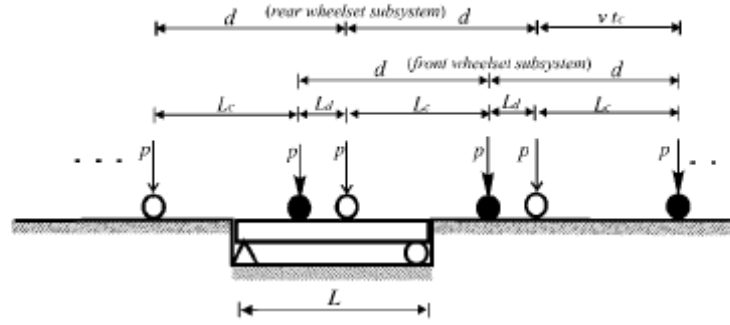


Figure 2.2 The most critical loading for the beam
(from Vehicle Bridge Interaction Dynamics, 2004)

Therefore if the equation (2.17) is rewritten according to the critical displacement condition, it reduces to (Vehicle Bridge Interaction Dynamics, 2004);

$$P_1(v, t) = [\sin \Omega_1(t - t_N) - S_1 \sin w_1(t - t_N)]H(t - t_N) -$$

$$2S_1 \cos \frac{w_1 L}{2v} \left[\sin w_1 \left(t - \frac{L}{2v} \right) + \sin w_1 \left(t - \frac{L}{2v} - \frac{t_N}{2} \right) \frac{\sin w_1 \left(\frac{t_N}{2} - \frac{d}{2v} \right)}{\sin \frac{w_1 d}{2v}} \right] H \left(t - t_{N-1} - \frac{L}{v} \right)$$

(2.18)

The displacement goes to infinity therotically in the case of resonance. However, the displacement will be damped practically. In order to obtain the infinite displacement in the equation (2.18) (Vehicle Bridge Interaction Dynamics, 2004);

$$\sin \frac{w_1 d}{2v} = 0 \quad \text{and} \quad \frac{w_1 d}{2v} = i\pi$$

If the equation (2.16) is arranged according to the condition above (Vehicle Bridge Interaction Dynamics, 2004);

$$S_1 = \frac{d}{2iL} \text{ and } i = 1,2,3,4,\dots$$

The resonance speeds for the structure can be found according to the formula stated above. i is the resonance number which means n th mode completes i number of oscillations between the passage of two consecutive loads.

2.4 Cancellation Condition

Cancellation is the situation in which the resonance effects are suppressed. In the case of cancellation, the resonance effects will be at very low level. The physical meaning of cancellation can be defined as the prevention of accumulation of effects by the loads that leave the bridge. As can be seen from equation (2.18), the effects of axle loads except from the last one are cancelled for the condition shown below (Vehicle Bridge Interaction Dynamics,2004);

$$\text{Cos}(w_1 L / 2v) = 0$$

In case of that the equation above is satisfied the term that is related to $N-1$ axles in the equation (2.18) becomes 0. Then, only the last axle of the train has the effect on the dynamic behaviour of the bridge. Besides, since the speed parameter S_1 is defined as $S_1 = \pi v / w_1 L$, the speed parameter for the cancellation case can be found as (Vehicle Bridge Interaction Dynamics,2004);

$$S_1 = \frac{1}{2i-1} \text{ for } i = 1, 2, 3, \dots$$

If we equate the two speed parameter equations for resonance and cancellation phenomena, we can obtain another determination for cancellation such that;

$$\frac{L}{d} = \frac{2j-1}{2i}$$

As can be seen from the equation above, for $\frac{L}{d} = 1.5$ which can be obtained with $i = 1$ and $j = 2$, cancellation occurs for the bridges. From that point, bridge parameters can be selected such that the probability of cancellation will be high according to the properties of the operating train.

2.5 Limitations in Analytical Approach

There are some limitations in the analytical approach for which the obtained results may not reflect the real behaviour of the structure such that;

- Vehicle-structure interaction including mass of vehicle and inertial effects of bogies is neglected.
- Load distribution by the ballast and sleepers is neglected
- Effect of torsional mode is neglected since the analytical approach is based on a Euler-Bernoulli beam and only the bending modes are considered.
- Excitation due to the track irregularities is neglected.

Vehicle-structure interaction and load distribution according to the ballast and sleepers leads lower dynamic responses. However, influence of torsional mode and track irregularities increase the dynamic response of the bridge. Eurocode proposes that the dynamic analysis can be performed by moving loads and effects of the vehicle-structure interaction, ballast and sleepers may be taken into account if desired.

2.6 DER Method

DER method is the decomposition of excitation at resonance and is developed to provide initial prediction for the dynamic behaviour of the bridges at resonant speeds. In this method, the equation of motion for Euler-Bernoulli beam is used as basis and the dynamic behaviour is decomposed into Fourier series. There are two solutions for the dynamic behaviour of the bridge named as complementary and particular solution. The total response is obtained from the combination of both solutions. Complementary part is the response according to the system free vibrations while the particular one is obtained from the forced vibration of the system. The passage of the train with N axles, with constant or varying axle distances is used for the particular solution and the excitation from the passage of the train is considered as a periodic function. From the required solutions for the problem the following equation for the acceleration is obtained. (ERRI D214/RP6);

$$\ddot{y}(t) \leq \left(\frac{8\pi f_0^2}{K} \right) \left| \frac{\cos(\pi L / \lambda)}{(2L/\lambda)^2 - 1} \right| \cdot \frac{L}{\varepsilon(L + X_N)} \left(\sqrt{\left(\sum_{n=1}^N F_n \cos\left(\frac{2\pi x_n}{\lambda}\right) \right)^2 + \left(\sum_{n=1}^N F_n \sin\left(\frac{2\pi x_n}{\lambda}\right) \right)^2} \right) \left(1 - e^{\left(-\varepsilon v_0 \frac{(x_N + L)}{\lambda}\right)} \right) \quad (2.22)$$

Where the parameters are as defined below;

- f_0 = First natural frequency of the bridge
- K = Stiffness of the bridge
- L = Span length of the bridge
- F_n = Load of n^{th} axle
- X_N = Total length of the train that consists of N axles
- x_n = Distance of n^{th} axle load from the first axle load.
- ε = Damping ratio
- λ = Wavelength

The equation can be defined in three parts as shown below;

$$\ddot{y} \leq C_t \cdot A(L/\lambda) \cdot G(\lambda) \quad (2.23)$$

Where;

$$C_t = \text{A constant term} = \frac{8\pi f_0^2}{K} = \frac{4}{mL\pi}$$

$A(L/\lambda)$ = Bridge influence line

$G(\lambda)$ = Excitation due to train

By assuming that the contribution of span length in train spectrum can be ignored when compared to the contribution of X_N , the L value can be removed from excitation and can be placed into the constant term. Then;

$$C_t = \frac{4}{m\pi}$$

$$A(L/\lambda) = \frac{\left| \cos\left(\frac{\pi L}{\lambda}\right) \right|}{\left| \left(\frac{2L}{\lambda}\right)^2 - 1 \right|} \quad (2.24)$$

$$G(\lambda) = \frac{1}{\varepsilon X_N} \left(\sqrt{\left(\sum_{n=1}^N F_n \cos\left(\frac{2\pi x_n}{\lambda}\right) \right)^2 + \left(\sum_{n=1}^N F_n \sin\left(\frac{2\pi x_n}{\lambda}\right) \right)^2} \right) \left(1 - e^{-2\pi \frac{X_N}{\lambda}} \right) \quad (2.25)$$

are obtained.

The term C_t and $A(L/\lambda)$ is depended on the bridge characteristics and the term $G(\lambda)$ is depended on the train characteristics. The multiplication of the two terms, $G(\lambda) \times A(L/\lambda)$ is defined as aggressivity in EN 1991-2:2003 and ERRI D214/RP6.

The excitation due to train found above considers that the maximum response is obtained after the last axle of the train leaves the bridge. However, there is possibility of that the maximum response is obtained when any axle combination of the train is located on the bridge. Therefore, all the combinations of the axle loads on the bridge should be considered and the envelope of these combinations should be taken as the maximum response. This phenomenon is called as subtrain concept and the value of $G(\lambda)$ obtained above becomes (ERRI D214/RP6);

$$G(\lambda) = \underset{i=1}{\overset{N}{\text{Max}}} \frac{1}{\varepsilon x_i} \left(\sqrt{\left(\sum_{n=1}^i F_n \cos\left(\frac{2\pi x_n}{\lambda}\right)\right)^2 + \left(\sum_{n=1}^i F_n \sin\left(\frac{2\pi x_n}{\lambda}\right)\right)^2} \right) \left(1 - e^{\left(-2\pi \varepsilon \frac{x_i}{\lambda}\right)} \right) \quad (2.26)$$

The graph of aggressivities for the HSLM trains presented in Eurocode and French TGV train for dynamic analysis in accordance with DER method are presented below;

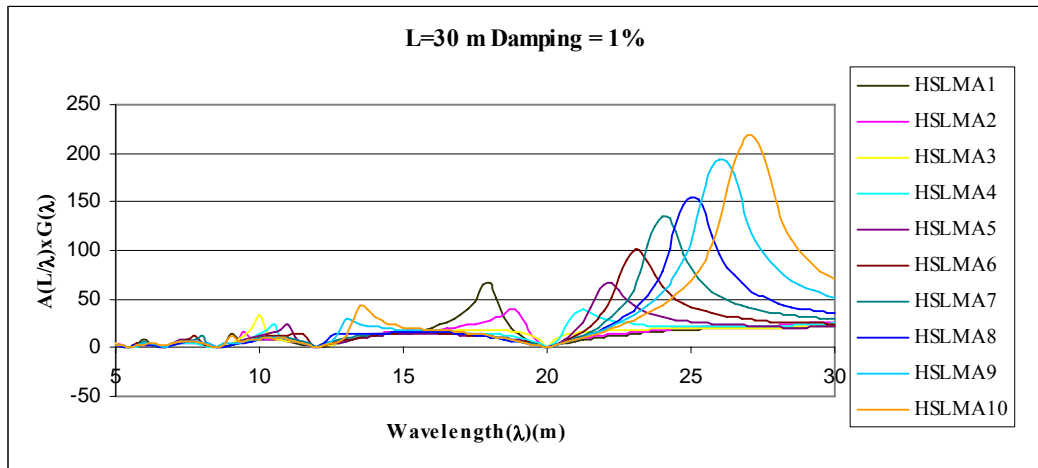


Figure 2.3 HSLM trains spectras for L=30 m and 1% damping

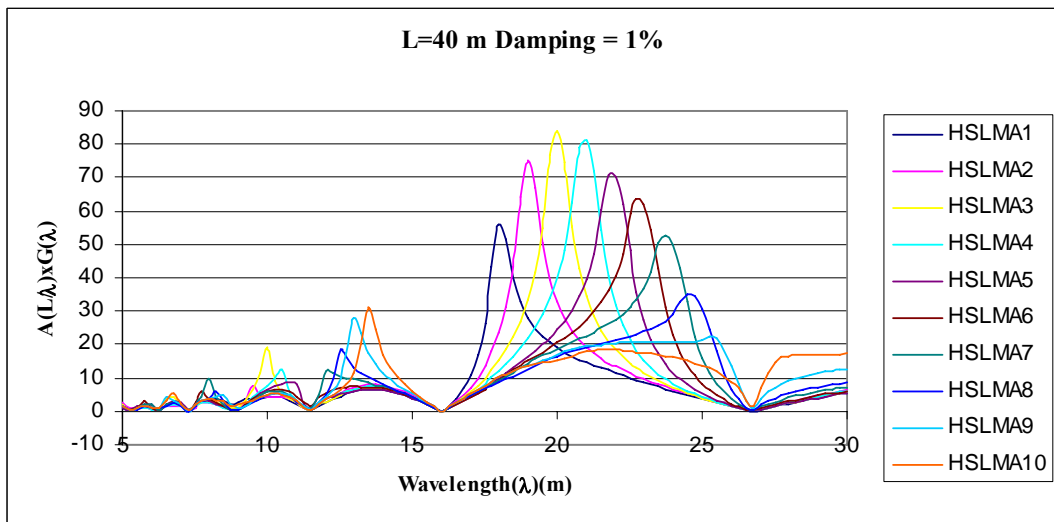


Figure 2.4 HSLM trains spectras for L=40 m and 1% damping

Wavelength v.s. $G(\lambda)$ (dynamic signature of train) graphs for each train is presented in Appendix A of this study. The graphs are given for 30 m span length and 1% damping ratio and 40 m span length with 1% and 2.5% damping ratio which are the cases studied in this thesis study.

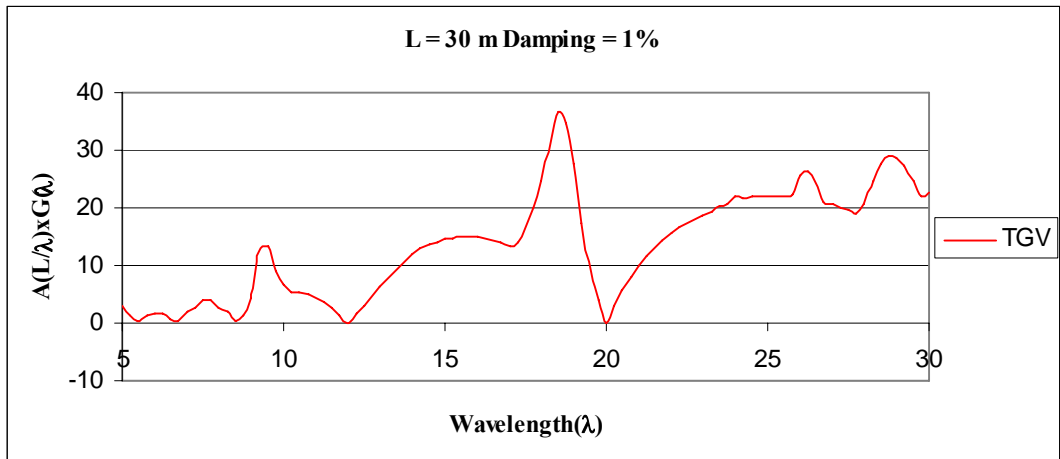


Figure 2.5 TGV train spectra for L=30 m and 1% damping

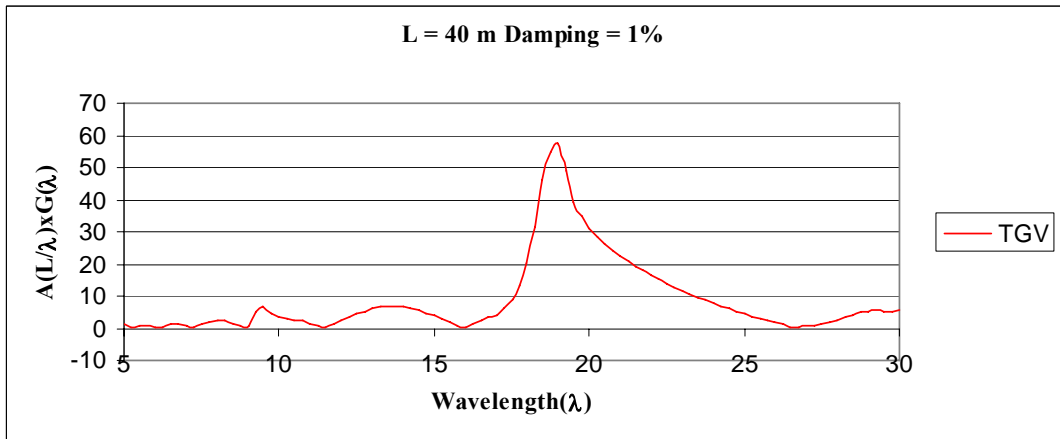


Figure 2.6 TGV train spectras for L=40 m and 1% damping

The displacement can also be found by DER method according to the formula shown below (ERRI D214/RP6);

$$y = y_{res} + \frac{\ddot{y}}{w_0^2} \quad (2.27)$$

Given the aggressivities of the trains by DER method, it is possible to predict the dynamic responses of the bridges before performing detailed dynamic analysis.

However, there are limitations in DER method which are defined in ERRI D214/RP6;

- For the speeds out of resonant speeds, the method is not suitable for determining the acceleration responses.
- It was defined in ERRI D214/RP6 that the the maximum responses for some real trains such that the axle loads of locomotives and coaches are significantly different from eachother, the responses are overestimated. This situation is explained with the example of ICE2 train in ERRI D214/RP6.
- The term $A(L/\lambda)$ which is defined as influence line tends to be zero for some L/λ values. It is stated in ERRI D214/RP6 that the response can not be found correctly at those points. A chart that shows the change of influence line according to different L/λ ratios is presented below;

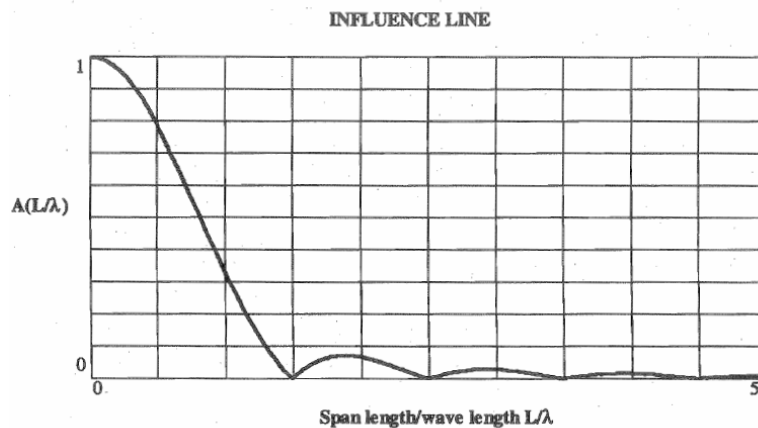


Figure 2.7 Influence Line of a simply supported beam expressed as a function of span length over wavelength (from ERRI D214/RP6)

2.7 Validation of the Program

As explained before, a MatLab program was prepared to perform analytical approach for the high speed railway bridges. In this part, the program will be compared with two studies in literature in which the same analytical approach was used before. In addition to that, validation of the procedure will be checked with the results obtained from SAP2000 finite element model in Chapter 5.

2.7.1 Study of J.M. Goicolea et al., (2002)

The bridge parameters worked in that study are summarized below;

Span Length = 15 m
m = 15 t/m
EI = 7694081 kN/m²
Damping, ϵ = 2%

The train model used is the 10 axle train with equal axle distance of 16 m. The analysis is performed for two different speeds of 288 km/h and 360 km/h which are equal to 80 m/s and 100 m/s respectively.

The results obtained in the report of J.M. Goicolea et. al., 2002 and the results from the MatLab program used in this thesis study are presented in figures in the following pages. Since there is only displacement graphs presented in the study of Spanish group, comparisons will be based on displacement responses.

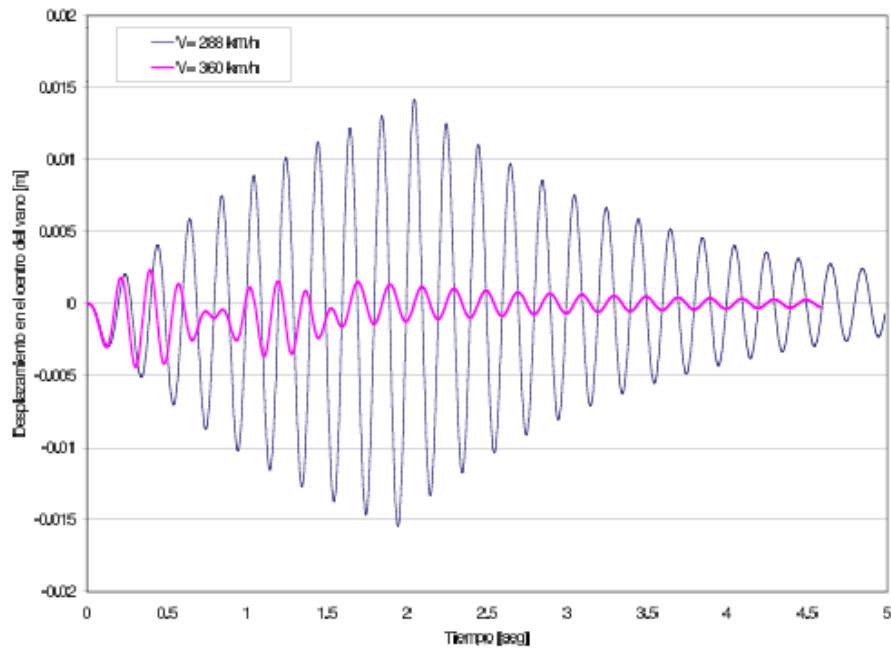


Figure 2.8 Maximum displacement results for speeds of 288 km/h and 360 km/h (from J.M. Goicolea et al., (2002))

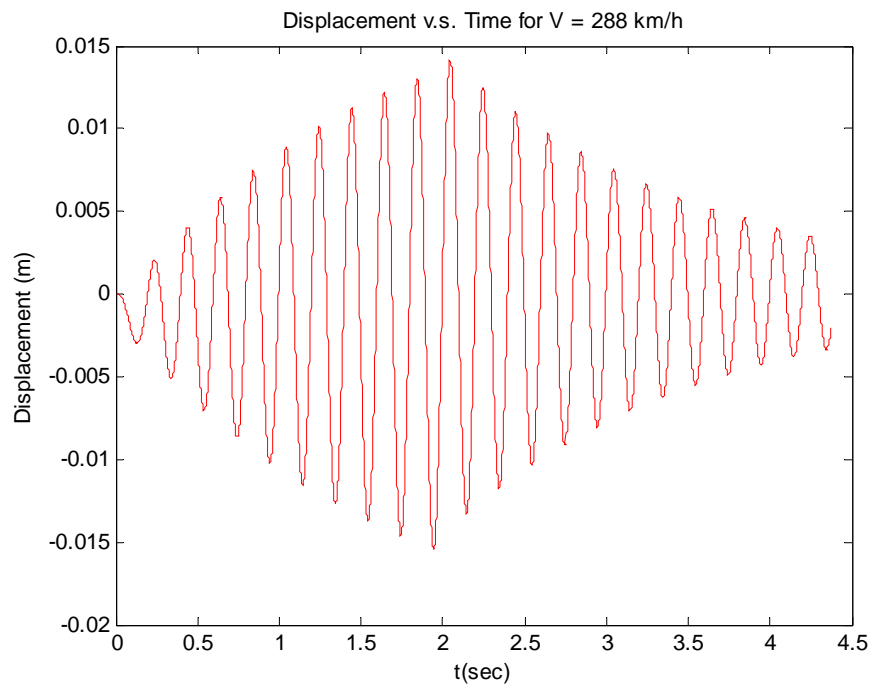


Figure 2.9 Maximum displacement results for speed of 288 km/h from MathLab

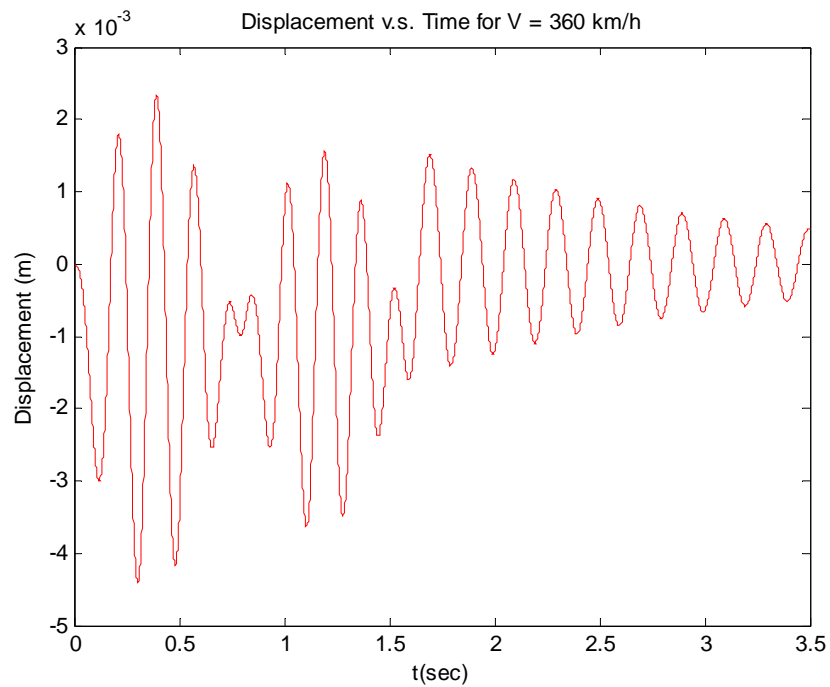


Figure 2.10 Maximum displacement results for speed of 360 km/h from MathLab

2.7.2 Study of C.C. Lin et al., (2005)

In this study, a high-speed railway bridge in Taiwan is analysed both with and without tuned mass dampers. Analytical approach is used in that study to obtain the dynamic response of the bridge under French TGV train. The mass of the train is also considered in this study. The Taiwan high speed bridge will be analysed and the results obtained will be compared with the results obtained in the related study.

The parameters of the bridge worked on this study can be summarized as shown below;

Parameter	Value
Physical parameters	
Mass per unit length, \bar{m}	38,240 N·s ² /m ²
Young's modulus, E	2.82×10^{10} N/m ²
Bending moments of inertia, I	17.9 m ⁴
Area, A	8.85 m ²
Mass polar moments of inertia, \bar{J}_m	464,500 N·s ²
Shear modulus, G	1.18×10^{10} N/m ²
Torsional moments of inertia, J_T	35.0 m ⁴
Radius of gyration, r	3.5 m
Eccentricity of rails, e_e	2.35 m
Modal parameters	
Damping ratio for each vibration mode	2.5%
First flexural frequency, ω_{f1}	3.56 Hz
First torsional frequency, $\omega_{\theta1}$	11.79 Hz
Dimensionless parameters	
Eccentricity ratio of rails, λ_e	0.67
Torsion-to-flexure frequency ratio, λ_ω	3.3

Figure 2.11 Properties of Taiwan High Speed Railway Bridge (from C.C. Lin et al., (2005))

The analyses are performed under the passage of French TGV, German ICE and Japanese SKS train of which the properties are shown below;

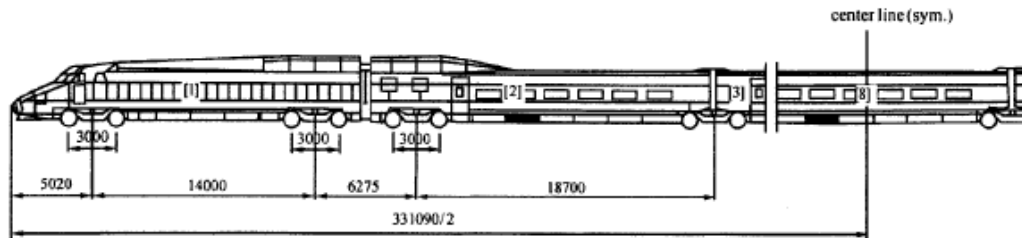


Figure 2.12 Axle arrangement of French TGV train (from C.C. Lin et al., (2005))

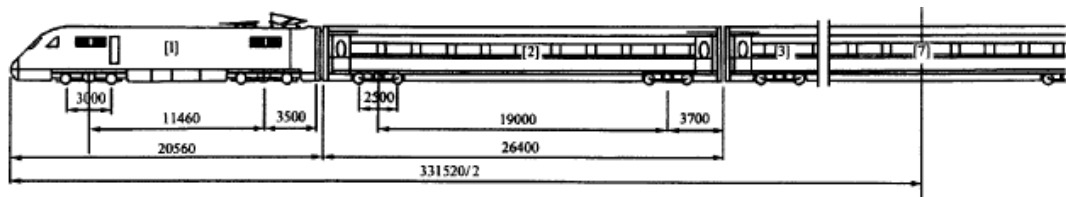


Figure 2.13 Axle arrangement of German ICE train (from C.C. Lin et al., (2005))

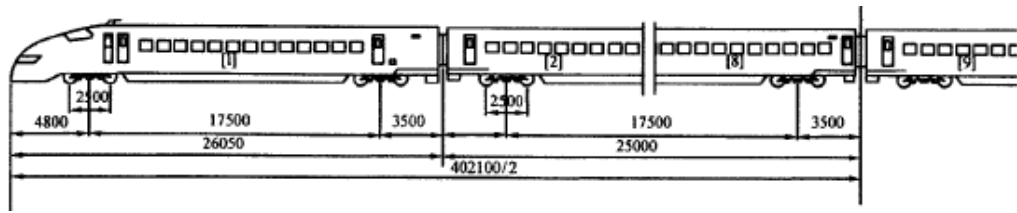


Figure 2.14 Axle arrangement of Japanese SKS train (from C.C. Lin et al., (2005))

Train properties	ICE	SKS	TGV
Number of bogie	52	64	52
Car spacing, d (m)	26.4	25.0	18.7
$(v_c)_{n-1}$ (km/h)	338	320	240
$(v_c)_{n-2}$ (km/h)	169	160	120
m_v (kg)	27,000	20,875	27,000
c_v (N s/m)	22,700	90,200	96,700
k_v (N/m)	660,000	530,000	664,000
m_b (kg)	3,000	3,040	3,000
I_b (kg-m ²)	4,000	3,930	4,000
c_b (N s/m)	78,400	78,400	78,400
k_b (N/m)	2,360,000	2,360,000	2,360,000
m_w (kg)	1,800	1,780	1,800
I_w (m)	1.5	1.25	1.5

Figure 2.15 Properties of TGV, ICE, and SKS trains (from C.C. Lin et al., (2005))

The analysis for comparison of this thesis study with the the related paper will be performed under French TGV train and at speed of 240 km/h. The span length of the bridge is 40 m. The results obtained in that study and by the MatLab program written for this thesis study are compared below;

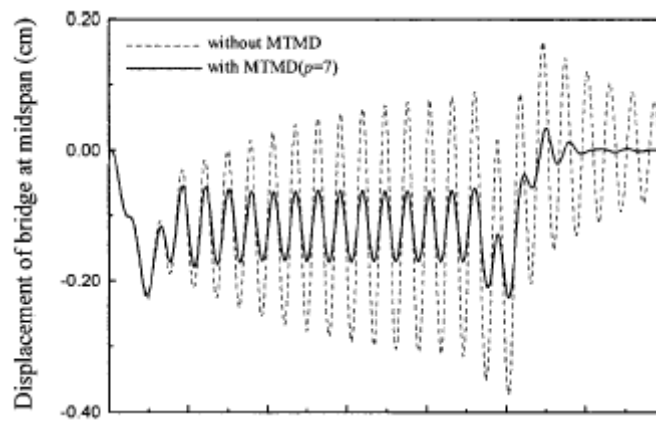


Figure 2.16 Displacement v.s. time graph obtained in paper for French TGV (from C.C. Lin et al., (2005))

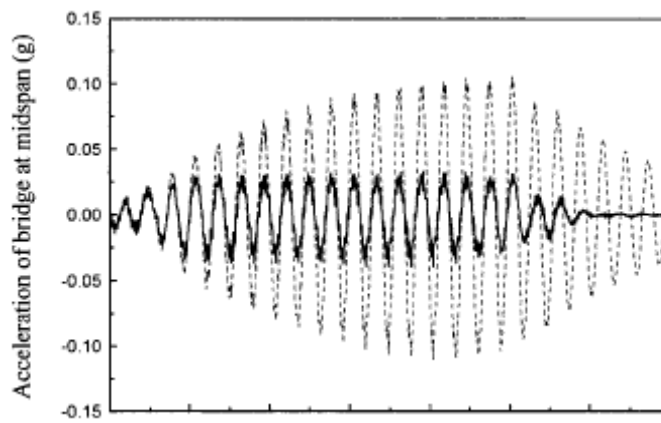


Figure 2.17 Acceleration v.s. time graph obtained in paper for French TGV (from C.C. Lin et al., (2005))

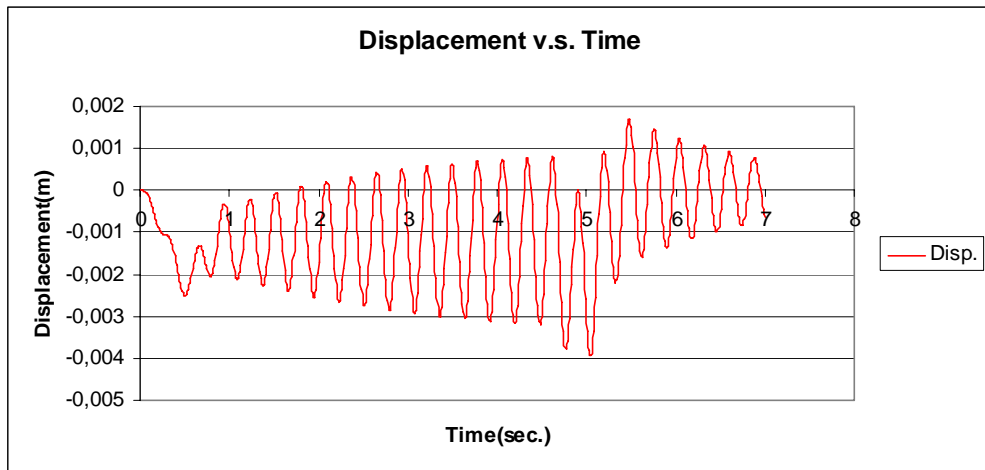


Figure 2.18 Displacement v.s. time graph obtained in MatLab for French TGV

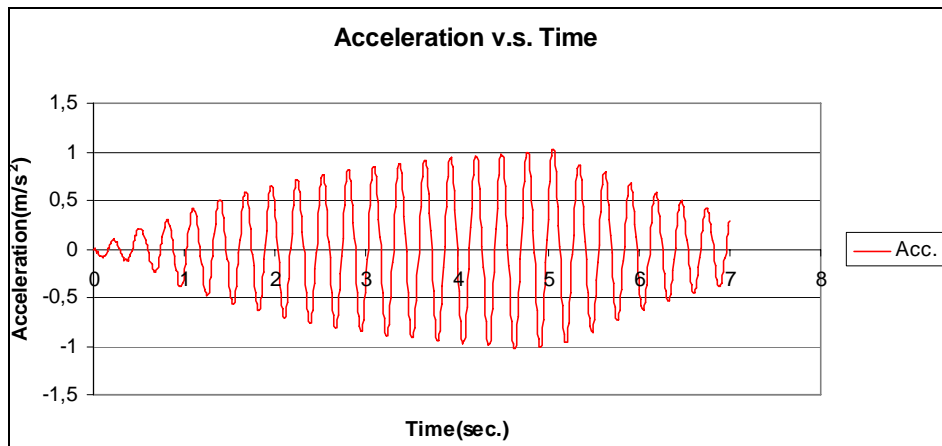


Figure 2.19 Acceleration v.s. time graph obtained in MatLab for French TGV

Table 2.1 Comparison of Results from (C.C. Lin et al., (2005)) and Thesis

Analysis	Responses	
	u(mm)	a(m/s ²)
C.C. Lin et al., (2005)	3,73	1,03
Thesis	3,94	1,03

As can be observed from the figures obtained from MatLab programming and from Table 2.1, the responses are totally same with the results obtained in papers. Therefore, it can be concluded that there is no error in the written language of the analytical procedure. And, also it can be understood that the analytical approaches are used to define the effects of different parameters on the dynamic response of high-speed railway bridges in literature.

CHAPTER 3

EUROCODE PROCEDURE FOR THE DYNAMIC ANALYSIS OF THE RAILWAY BRIDGES

3.1 General

In this chapter, the procedure that is defined in Eurocodes for the dynamic analysis of the railway bridges is explained. The dynamic analysis procedure that is defined in EN 1991-2 is followed by all European countries for the design of railway bridges. There are train models defined in EN 1991-2 for the static analysis of the structure named LM71, SW0, SW2.

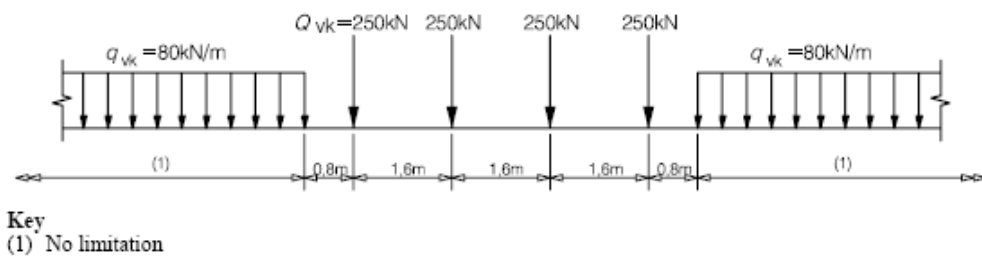


Figure 3.1 LM71 loading scheme (from EN 1991-2 : 2003)

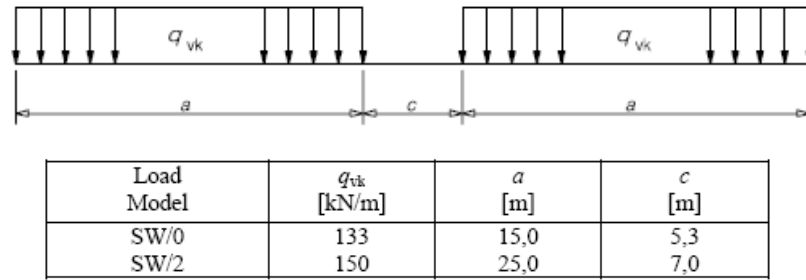


Figure 3.2 SW0 and SW2 loading scheme (from EN 1991-2 : 2003)

EN 1991-2 defines that the static analysis can be performed by using LM71 train model and SW trains when required by using the suitable impact factors defined as shown below;

$$\phi_2 = \frac{1.44}{\sqrt{L_\phi} - 0.2} + 0.82 \quad \text{for carefully maintained tracks}$$

$$1.0 < \phi_2 < 1.67$$

$$\phi_3 = \frac{2.16}{\sqrt{L_\phi} - 0.2} + 0.73 \quad \text{for standard maintenance}$$

$$1.0 < \phi_3 < 2.00$$

L_ϕ = Determined Length for the Bridge, m (EN 1991-2 : 2003)

The different values are defined for determined length in EN 1991-2:2003 and it is stated that L_ϕ is equal to span length for simply supported bridges.

Those impact factors are determined in order to take the effect of the moving speed of the train into account. However, they can't guarantee that the structure will not exposed worse conditions during its operating life. Therefore, the procedure for

additional dynamic analysis is required in order to check whether the structure is in the limits of serviceability or not.

3.2 Requirement for Dynamic Analysis

EN 1991-2 presents a flow chart to define whether there is a need for dynamic analysis or not. The factors that affect the dynamic behaviour of the structure are;

- The speed of traffic across the bridge.
- The span L of the element and the influence line length for deflection of the element being considered.
- The mass of the structure.
- The natural frequencies of the whole structure and relevant elements of the structure and the associated mode shapes along the line of the track.
- The number of axles, axle loads and the spacing of axles.
- The damping of the structure.
- Vertical irregularities in the track
- The unsprung/sprung mass and suspension characteristics such that the inertial effects of bogies of the vehicle.

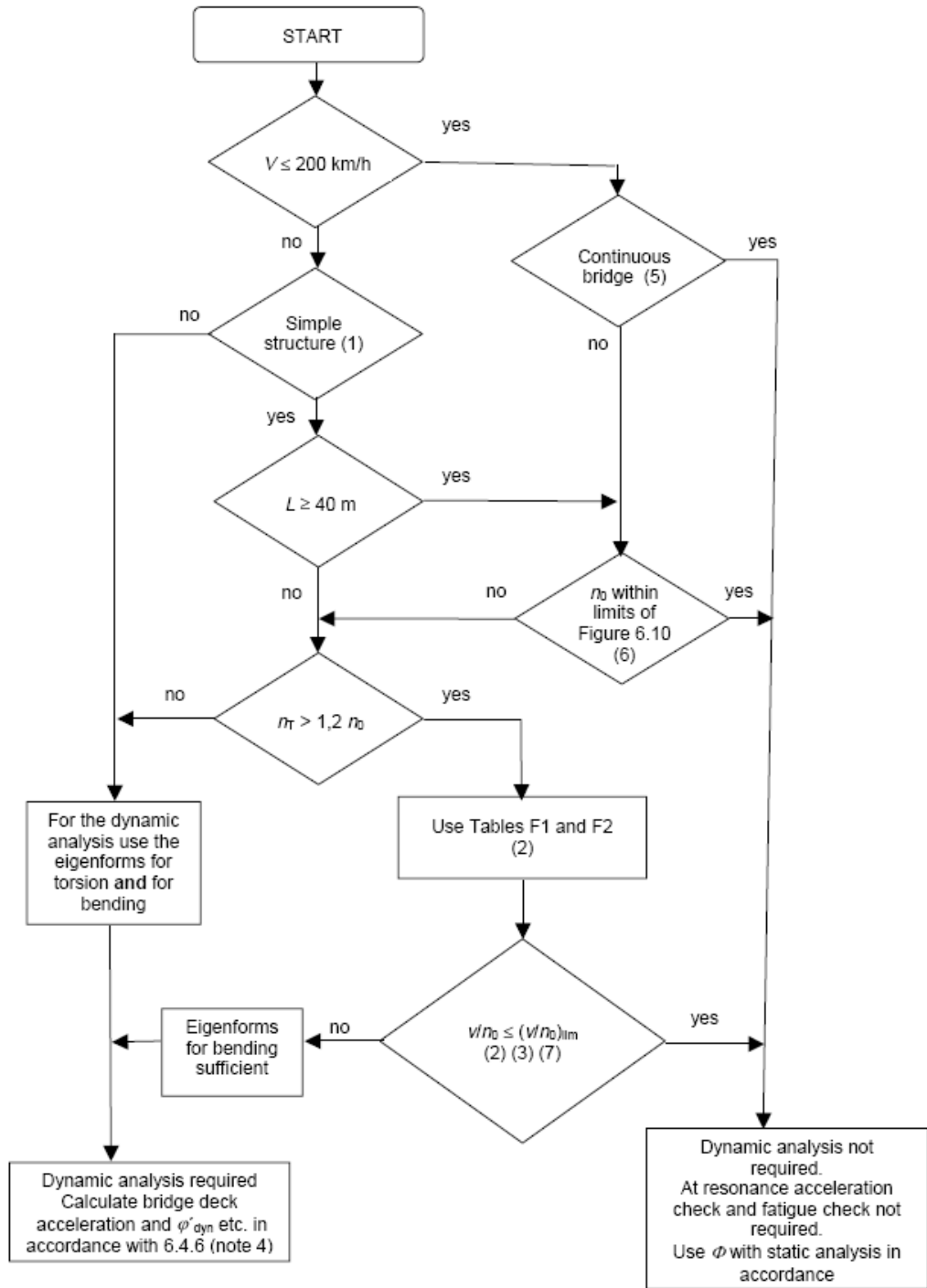


Figure 3.3 Flow Chart for the requirement of dynamic analysis (EN 1991-2 : 2003)

As can be seen from the flow chart first control is about the speed of the project. If the maximum design speed is less than 200 km/h then the type of the bridge is

checked. If the bridge is continuous, there is no need for dynamic analysis. However, in case of that the bridge is not a continuous bridge, Eurocode flow chart shows that there is a need to check bending frequency of the structure whether it is in the limits of the Figure 3.4 shown below;

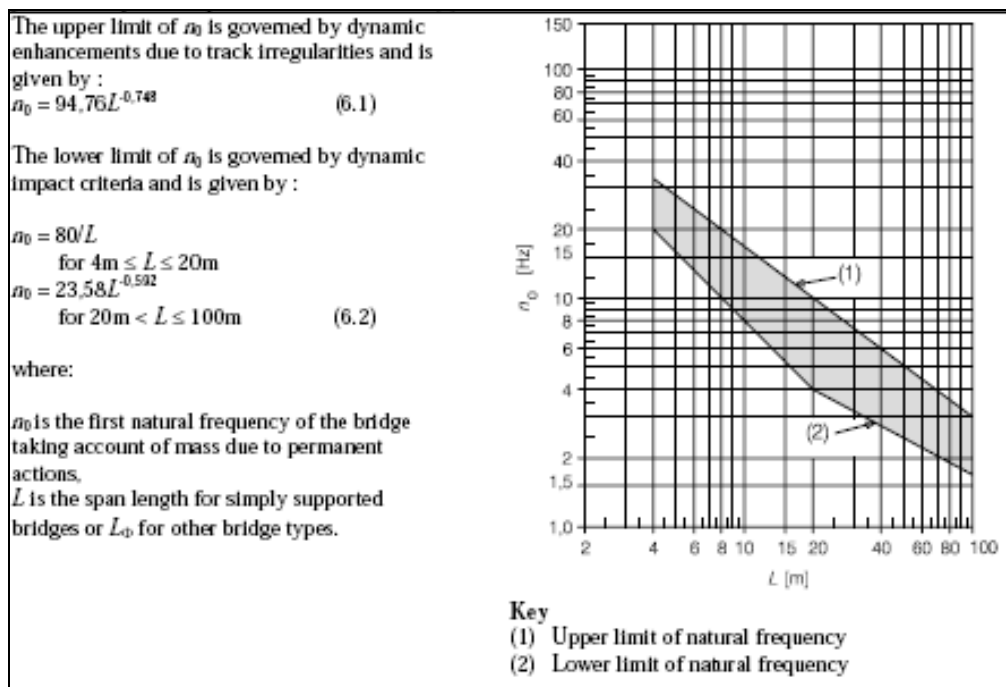


Figure 3.4 Limits of bridge natural frequency n_0 as a function of L (EN 1991-2 : 2003)

If the first natural bending frequency satisfies the limits defined in the Figure 3.4, then there is no need for dynamic analysis. If the natural bending frequency is out of the limits, then the ratio of torsional frequency to bending frequency is checked. If the ratio is larger than 1.2, following tables are used to determine the necessity for dynamic analyses;

Table 3.1 Maximum value of $(v/n_0)_{lim}$ for a simply supported beam or slab and a maximum permitted acceleration of $a_{max} < 3.50 \text{ m/s}^2$. (from EN 1991-2 : 2003)

Mass m 10^3 kg/m	Span $L \in$ m^*	ζ %	$\geq 5,0$	$\geq 7,0$	$\geq 9,0$	$\geq 10,0$	$\geq 13,0$	$\geq 15,0$	$\geq 18,0$	$\geq 20,0$	$\geq 25,0$	$\geq 30,0$	$\geq 40,0$	$\geq 50,0$
			$< 7,0$	$< 9,0$	$< 10,0$	$< 13,0$	$< 15,0$	$< 18,0$	$< 20,0$	$< 25,0$	$< 30,0$	$< 40,0$	$< 50,0$	-
			v/n_0 m	v/n_0 m	v/n_0 m	v/n_0 m	v/n_0 m	v/n_0 m	v/n_0 m	v/n_0 m	v/n_0 m	v/n_0 m	v/n_0 m	v/n_0 m
[5,00,7,50)	2		1,71	1,78	1,88	1,88	1,93	1,93	2,13	2,13	3,08	3,08	3,54	3,59
	4		1,71	1,83	1,93	1,93	2,13	2,24	3,03	3,08	3,38	3,54	4,31	4,31
[7,50,10,0)	2		1,94	2,08	2,64	2,64	2,77	2,77	3,06	5,00	5,14	5,20	5,35	5,42
	4		2,15	2,64	2,77	2,98	4,93	5,00	5,14	5,21	5,35	5,62	6,39	6,53
[10,0,12,5)	1		2,40	2,50	2,50	2,50	2,71	6,15	6,25	6,36	6,36	6,45	6,45	6,57
	2		2,50	2,71	2,71	5,83	6,15	6,25	6,36	6,36	6,45	6,45	7,19	7,29
[12,5,15,0)	1		2,50	2,50	3,58	3,58	5,24	5,24	5,36	5,36	7,86	9,14	9,14	9,14
	2		3,45	5,12	5,24	5,24	5,36	5,36	7,86	8,22	9,53	9,76	10,36	10,48
[15,0,17,5)	1		3,00	5,33	5,33	5,33	6,33	6,33	6,50	6,50	6,50	7,80	7,80	7,80
	2		5,33	5,33	6,33	6,33	6,50	6,50	10,17	10,33	10,33	10,50	10,67	12,40
[17,5,20,0)	1		3,50	6,33	6,33	6,33	6,50	6,50	7,17	7,17	10,67	12,80	12,80	12,80
	1		5,21	5,21	5,42	7,08	7,50	7,50	13,54	13,54	13,96	14,17	14,38	14,38
[25,0,30,0)	1		6,25	6,46	6,46	10,21	10,21	10,21	10,63	10,63	12,75	12,75	12,75	12,75
[30,0,40,0)	1					10,56	18,33	18,33	18,61	18,61	18,89	19,17	19,17	19,17
$\geq 40,0$	1					14,73	15,00	15,56	15,56	15,83	18,33	18,33	18,33	18,33

* $L \in [a,b)$ means $a \leq L < b$

NOTE 1 Table F.1 includes a safety factor of 1.2 on $(v/n_0)_{lim}$ for acceleration, deflection and strength criteria and a safety factor of 1.0 on the $(v/n_0)_{lim}$ for fatigue.

NOTE 2 Table F.1 includes an allowance of $(1+\phi^2/2)$ for track irregularities.

Table 3.2 Maximum value of $(v/n_0)_{lim}$ for a simply supported beam or slab and a maximum permitted acceleration of $a_{max} < 5.0 \text{ m/s}^2$. (from EN 1991-2 : 2003)

Mass m 10^3 kg/m	Span $L \in$ m^*	ζ %	$\geq 5,0$	$\geq 7,0$	$\geq 9,0$	$\geq 10,0$	$\geq 13,0$	$\geq 15,0$	$\geq 18,0$	$\geq 20,0$	$\geq 25,0$	$\geq 30,0$	$\geq 40,0$	$\geq 50,0$
			$< 7,0$	$< 9,0$	$< 10,0$	$< 13,0$	$< 15,0$	$< 18,0$	$< 20,0$	$< 25,0$	$< 30,0$	$< 40,0$	$< 50,0$	-
			v/n_0 m	v/n_0 m	v/n_0 m	v/n_0 m	v/n_0 m	v/n_0 m	v/n_0 m	v/n_0 m	v/n_0 m	v/n_0 m	v/n_0 m	v/n_0 m
[5,00,7,50)	2		1,78	1,88	1,93	1,93	2,13	2,13	3,08	3,08	3,44	3,54	3,59	4,13
	4		1,88	1,93	2,13	2,13	3,08	3,13	3,44	3,54	3,59	4,31	4,31	4,31
[7,50,10,0)	2		2,08	2,64	2,78	2,78	3,06	5,07	5,21	5,21	5,28	5,35	6,33	6,33
	4		2,64	2,98	4,86	4,93	5,14	5,21	5,35	5,42	6,32	6,46	6,67	6,67
[10,0,12,5)	1		2,50	2,50	2,71	6,15	6,25	6,36	6,36	6,46	6,46	6,46	7,19	7,19
	2		2,71	5,83	6,15	6,15	6,36	6,46	6,46	6,46	7,19	7,19	7,75	7,75
[12,5,15,0)	1		2,50	3,58	5,24	5,24	5,36	5,36	7,86	8,33	9,14	9,14	9,14	9,14
	2		5,12	5,24	5,36	5,36	7,86	8,22	9,53	9,64	10,36	10,36	10,48	10,48
[15,0,17,5)	1		5,33	5,33	6,33	6,33	6,50	6,50	6,50	7,80	7,80	7,80	7,80	7,80
	2		5,33	6,33	6,50	6,50	10,33	10,33	10,50	10,50	10,67	10,67	12,40	12,40
[17,5,20,0)	1		6,33	6,33	6,50	6,50	7,17	10,67	10,67	12,80	12,80	12,80	12,80	12,80
	1		5,21	7,08	7,50	7,50	13,54	13,75	13,96	14,17	14,38	14,38	14,38	14,38
[25,0,30,0)	1		6,46	10,20	10,42	10,42	10,63	10,63	12,75	12,75	12,75	12,75	12,75	12,75
[30,0,40,0)	1					18,33	18,61	18,89	18,89	19,17	19,17	19,17	19,17	19,17
$\geq 40,0$	1					15,00	15,56	15,83	18,33	18,33	18,33	18,33	18,33	18,33

* $L \in [a,b)$ means $a \leq L < b$

NOTE 1 Table F.2 includes a safety factor of 1.2 on $(v/n_0)_{lim}$ for acceleration, deflection and strength criteria and a safety factor of 1.0 on the $(v/n_0)_{lim}$ for fatigue.

NOTE 2 Table F.2 include an allowance of $(1+\phi^2/2)$ for track irregularities.

In the Tables 3.1 and 3.2, the limit for the ratio of maximum design speed and natural bending frequency is checked. If the ratio satisfies the limits shown on tables, the dynamic analysis is not required. Otherwise, the dynamic analysis will be performed using bending modes.

If the ratio of torsional frequency and bending frequency is less than 1.2, then dynamic analysis is performed by using eigenforms for bending and torsion together.

3.3 Dynamic Analysis Train Models

In case of that there is a need for dynamic analysis; EN 1991-2 defines 10 each train loading models names as HSLM-A trains and one HSLM-B train to be used for loading. The HSLM-A and HSLM-B train models and the conditions to choose which one to use are presented in the figures and tables below;

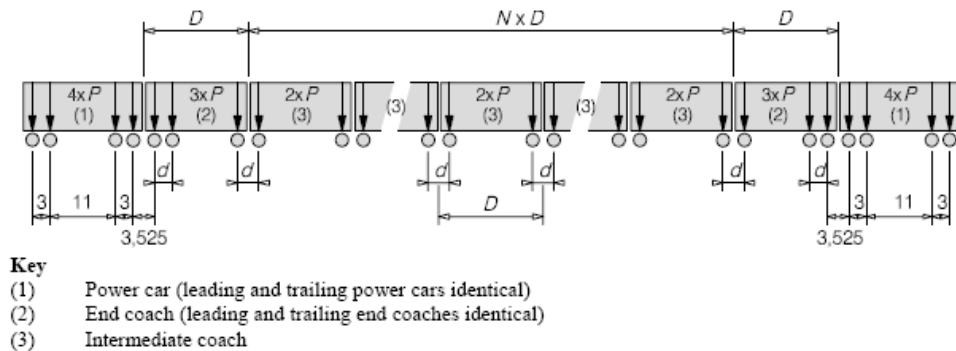


Figure 3.5 HSLM-A train model (from EN 1991-2 : 2003)

Table 3.3 HSLM-A train model definitions (from EN 1991-2 : 2003)

Universal Train	Number of intermediate coaches N	Coach length D [m]	Bogie axle spacing d [m]	Point force P [kN]
A1	18	18	2,0	170
A2	17	19	3,5	200
A3	16	20	2,0	180
A4	15	21	3,0	190
A5	14	22	2,0	170
A6	13	23	2,0	180
A7	13	24	2,0	190
A8	12	25	2,5	190
A9	11	26	2,0	210
A10	11	27	2,0	210

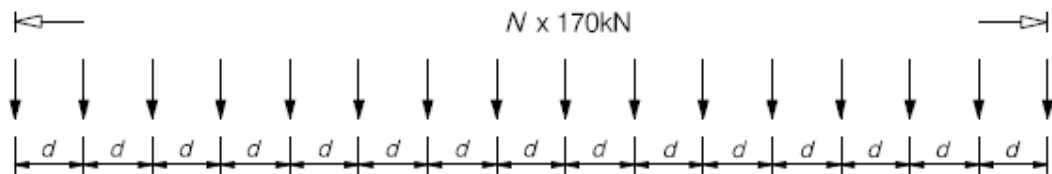


Figure 3.6 HSLM-B train model (from EN 1991-2 : 2003)

Table 3.4 Application of HSLM-A and HSLM-B (from EN 1991-2 : 2003)

Structural configuration	Span	
	$L < 7\text{m}$	$L \geq 7\text{m}$
Simply supported span ^a	HSLM-B ^b	HSLM-A ^c
Continuous structure ^a or Complex structure ^e	HSLM-A Trains A1 to A10 inclusive ^d	HSLM-A Trains A1 to A10 inclusive ^d

^a Valid for bridges with only longitudinal line beam or simple plate behaviour with negligible skew effects on rigid supports.
^b For simply supported spans with a span of up to 7 m a single critical Universal Train from HSLM-B may be used for the analysis in accordance with 6.4.6.1.1(5).
^c For simply supported spans with a span of 7 m or greater a single critical Universal Train from HSLM-A may be used for the dynamic analysis in accordance with annex E (Alternatively Universal trains A1 to A10 inclusive may be used).
^d All Trains A1 to A10 inclusive should be used in the design.
^e Any structure that does not comply with Note a above. For example a skew structure, bridge with significant torsional behaviour, half through structure with significant floor and main girder vibration modes etc. In addition, for complex structures with significant floor vibration modes (e.g. half through or through bridges with shallow floors) HSLM-B should also be applied.

NOTE The National Annex or the individual project may specify additional requirements relating to the application of HSLM-A and HSLM-B to continuous and complex structures.

3.4 Speeds to be Considered

It is stated in EN 1991-2 that the dynamic analysis should be performed for different speed values within the range of 40 m/s and maximum design speed. Maximum design speed is determined as the 1.2 times the maximum operating speed. The speed values in that range are determined according to the equation below;

$$v_i = n_0 \lambda_i \quad (3.1)$$

$$40 \text{ m/s} < v_i < \text{Maximum design speed}$$

where;

- v_i = Resonant speed
- n_0 = First natural frequency of the unloaded structure
- λ_i = The principle wavelength of frequency = d / i
- d = Regular spacing of group of axles
- i = 1,2,3,4

3.5 Damping of the Structure

It is defined in EN 1991-2 that the peak response of the structure at resonance conditions is highly dependent on damping. Therefore, it is emphasized that the lower bounds of damping shall be used for the dynamic analysis calculations. The conditions that are defined in EN 1991-2 to choose the damping to be used in analysis are summarized in the table below;

Table 3.5 Values of damping to be assumed for design purposes (from EN 1991-2 : 2003)

Bridge Type	ζ Lower limit of percentage of critical damping [%]	
	Span $L < 20\text{m}$	Span $L \geq 20\text{m}$
Steel and composite	$\zeta = 0,5 + 0,125 (20 - L)$	$\zeta = 0,5$
Prestressed concrete	$\zeta = 1,0 + 0,07 (20 - L)$	$\zeta = 1,0$
Filler beam and reinforced concrete	$\zeta = 1,5 + 0,07 (20 - L)$	$\zeta = 1,5$

According to EN 1991-2, damping ratios found from the formulas above can be increased due to span length values according to the figure presented below;

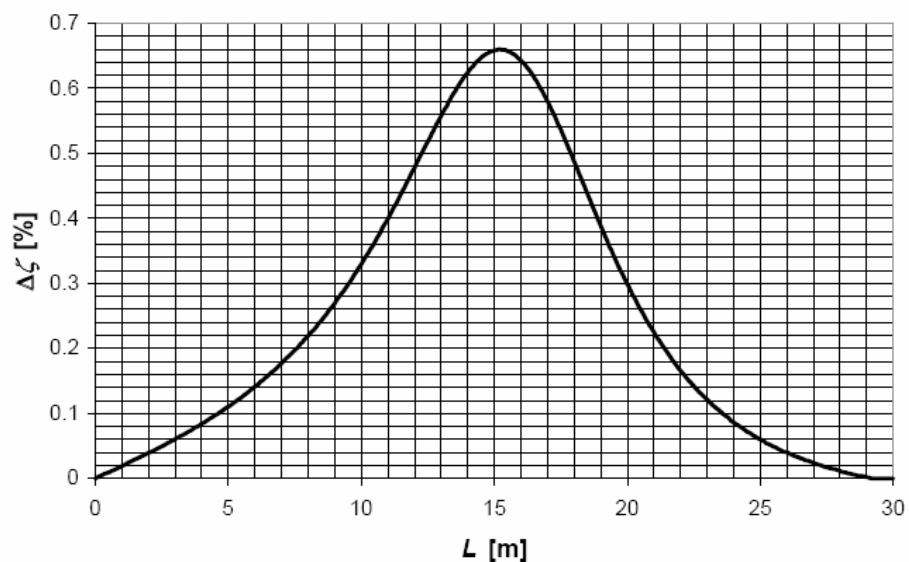


Figure 3.7 Additional damping as a function of span length (from EN 1991-2 : 2003)

3.6 Mass of the Bridge

Mass parameter is important since any underestimation or overestimation in mass determinations leads to obtain results far from the real case. However, there can be

different probabilities such that the structure may be exposed to different mass conditions during its operating life.

Any underestimation in mass calculations results in higher natural frequency values, thus higher resonant speeds. However, overestimating the mass leads to obtain lower resonant speeds.

EN 1991-2 determines two conditions to calculate the mass of the structure such that;

- Using minimum likely dry clean density and minimum thickness of ballast to obtain maximum deck accelerations at high resonant speeds.
- Using maximum saturated density of dirty ballast to allow the future track lifts to obtain the maximum deck accelerations at lower resonant speeds.

3.7 Stiffness of the Bridge

Any overestimation of the stiffness property of the bridge gives maximum deck accelerations at high resonant speeds, whereas underestimating the stiffness shows high acceleration responses at lower speeds. However, it is not possible to obtain the exact Young's modulus values that completely reflect the real situations. This is mainly because of that, there are a lot of parameters that affect modulus which prevents the designer to obtain sufficient accuracy for the dynamic analysis. Therefore, EN 1991-2 emphasizes that the modulus values should be determined by tests performed, and the values used shall be conformed with relevant authority for the project.

3.8 Determination of Critical HSLM Train for Dynamic Analysis

EN 1991-2 determines a procedure to choose the critical HSLM train loading to perform dynamic analysis. The number of axles, axle loads, and distances between axles are the main parameters that are related to train properties. All these

parameters are effective for determination of the wavelength of excitation of the train loading. Therefore, the procedure of choosing the critical train model for dynamic analysis is based on wavelength values.

3.8.1 Determination of Maximum Design Speed Wavelength of Exication

The maximum design speed wavelength is determined in EN 1991-2 Annex E part E2 as shown below;

$$\lambda_v = V_{ds} / n_0 \quad (3.2)$$

V_{ds} = Maximum design speed = 1.2 x maximum operating speed

n_0 = First natural frequency of the unloaded structure

λ_v = Maximum design speed wavelength of excitation

3.8.2 Determination of Critical Wavelength of Exication

After the determination of maximum design speed wavelength of excitation, the critical wavelength of excitation is determined according to the figures presented for different span lengths in EN 1991-2 Annex E part E2.

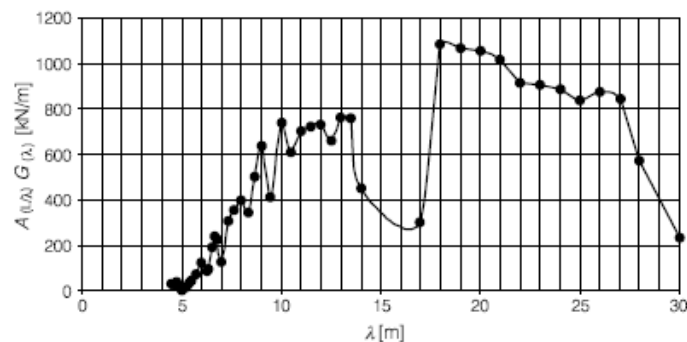


Figure 3.8 Aggressivity $A_{(L/\lambda)}G_{(\lambda)}$ as a function of excitation wavelength λ for a simply supported span of $L = 7.5 \text{ m}$ and damping ratio $\varepsilon = 0.01$ (EN 1991-2:2003)

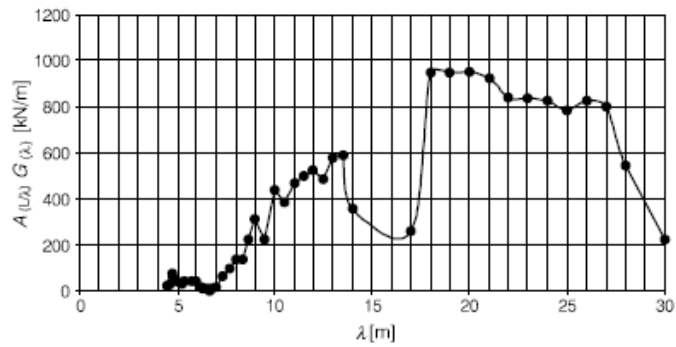


Figure 3.9 Aggressivity $A_{(L/\lambda)}G_{(\lambda)}$ as a function of excitation wavelength λ for a simply supported span of $L = 10.0 \text{ m}$ and damping ratio $\varepsilon = 0.01$ (EN 1991-2:2003)

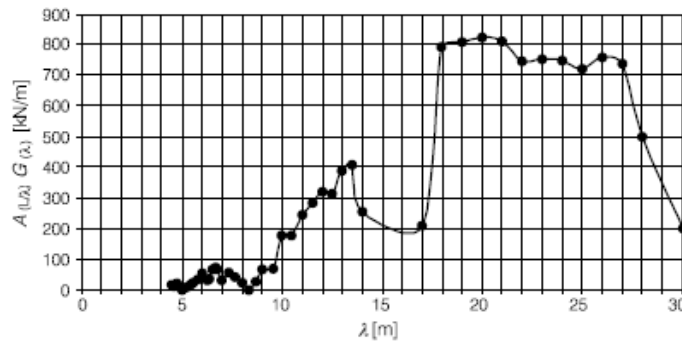


Figure 3.10 Aggressivity $A_{(L/\lambda)}G_{(\lambda)}$ as a function of excitation wavelength λ for a simply supported span of $L = 12.5 \text{ m}$ and damping ratio $\varepsilon = 0.01$ (EN 1991-2:2003)

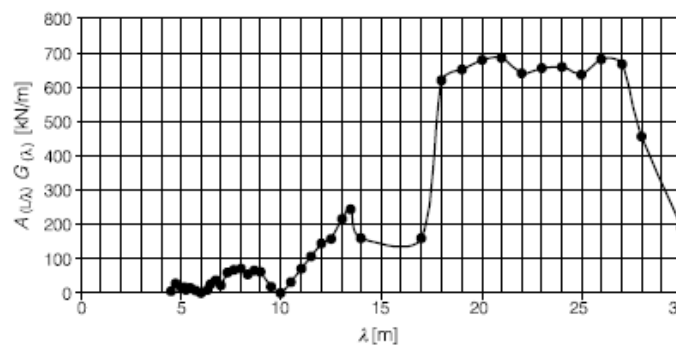


Figure 3.11 Aggressivity $A_{(L/\lambda)}G_{(\lambda)}$ as a function of excitation wavelength λ for a simply supported span of $L = 15.0 \text{ m}$ and damping ratio $\varepsilon = 0.01$ (EN 1991-2:2003)

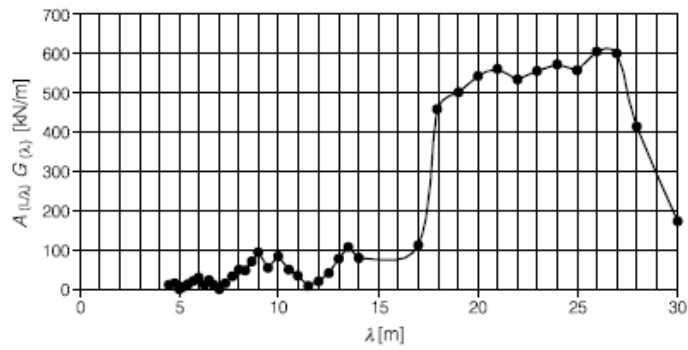


Figure 3.12 Aggressivity $A_{(L/\lambda)}G_{(\lambda)}$ as a function of excitation wavelength λ for a simply supported span of $L = 17.5 \text{ m}$ and damping ratio $\varepsilon = 0.01$ (EN 1991-2:2003)

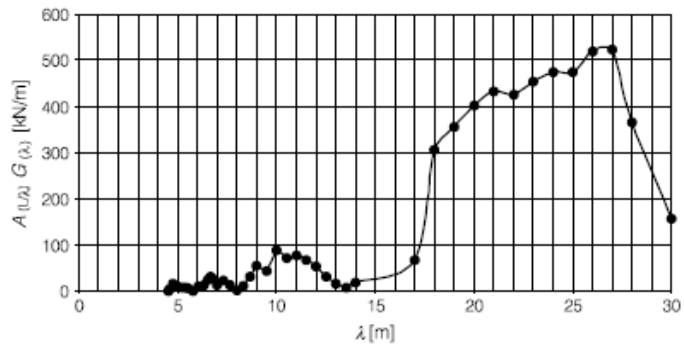


Figure 3.13 Aggressivity $A_{(L/\lambda)}G_{(\lambda)}$ as a function of excitation wavelength λ for a simply supported span of $L = 20.0 \text{ m}$ and damping ratio $\varepsilon = 0.01$ (EN 1991-2:2003)

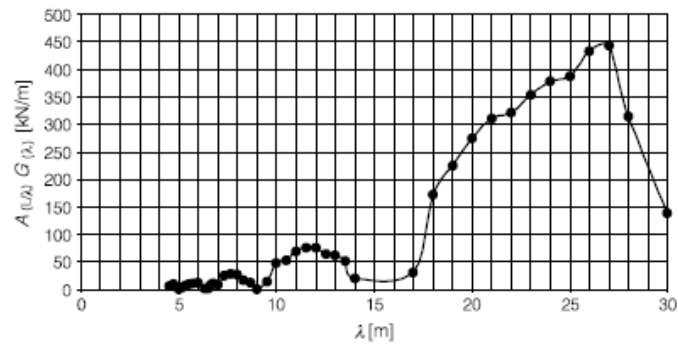


Figure 3.14 Aggressivity $A_{(L/\lambda)}G_{(\lambda)}$ as a function of excitation wavelength λ for a simply supported span of $L = 22.5 \text{ m}$ and damping ratio $\varepsilon = 0.01$ (EN 1991-2:2003)

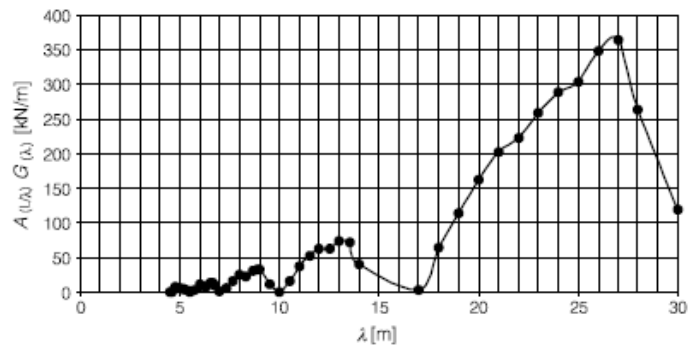


Figure 3.15 Aggressivity $A_{(L/\lambda)}G_{(\lambda)}$ as a function of excitation wavelength λ for a simply supported span of $L = 25.0$ m and damping ratio $\varepsilon = 0.01$ (EN 1991-2:2003)

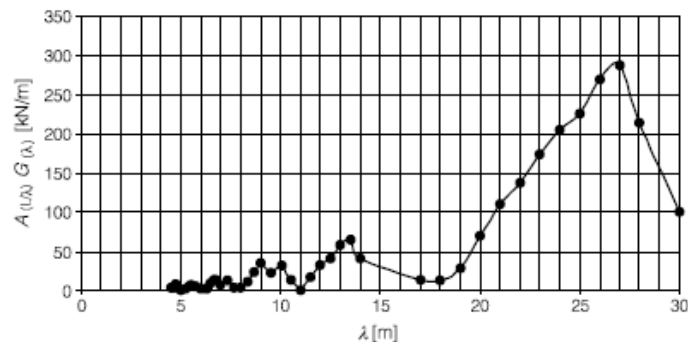


Figure 3.16 Aggressivity $A_{(L/\lambda)}G_{(\lambda)}$ as a function of excitation wavelength λ for a simply supported span of $L = 27.5$ m and damping ratio $\varepsilon = 0.01$ (EN 1991-2:2003)

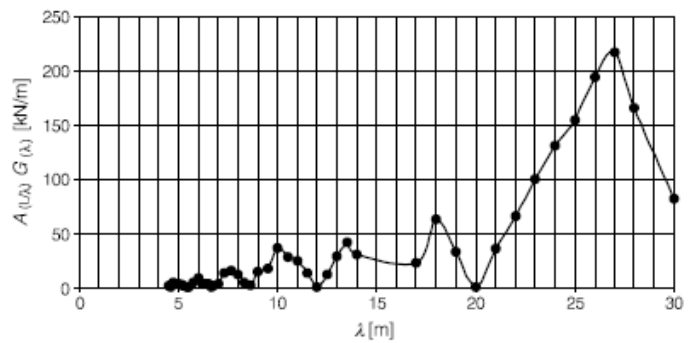


Figure 3.17 Aggressivity $A_{(L/\lambda)}G_{(\lambda)}$ as a function of excitation wavelength λ for a simply supported span of $L = 30.0$ m and damping ratio $\varepsilon = 0.01$ (EN 1991-2:2003)

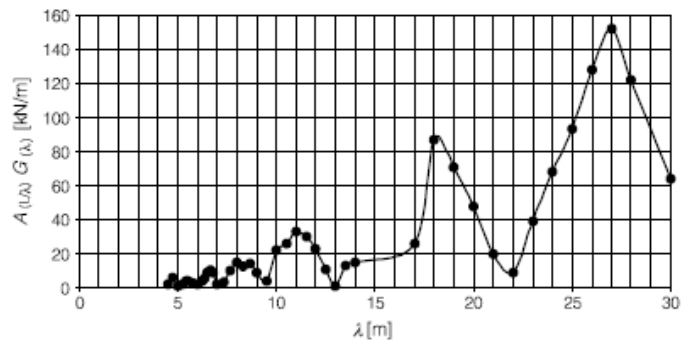


Figure 3.18 Aggressivity $A_{(L/\lambda)}G_{(\lambda)}$ as a function of excitation wavelength λ for a simply supported span of $L = 32.5 \text{ m}$ and damping ratio $\epsilon = 0.01$ (EN 1991-2:2003)

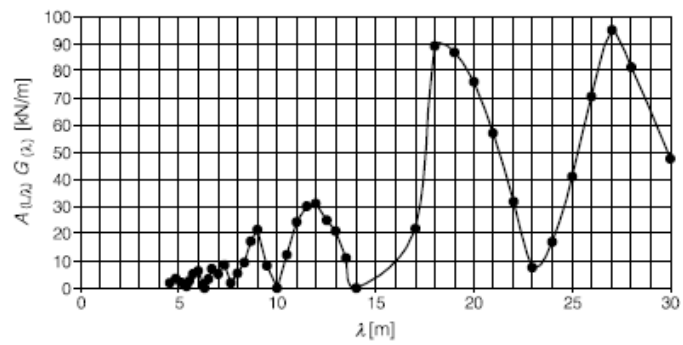


Figure 3.19 Aggressivity $A_{(L/\lambda)}G_{(\lambda)}$ as a function of excitation wavelength λ for a simply supported span of $L = 35.0 \text{ m}$ and damping ratio $\epsilon = 0.01$ (EN 1991-2:2003)

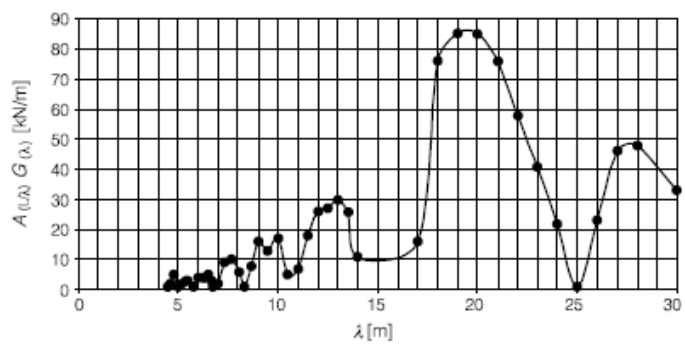


Figure 3.20 Aggressivity $A_{(L/\lambda)}G_{(\lambda)}$ as a function of excitation wavelength λ for a simply supported span of $L = 37.5 \text{ m}$ and damping ratio $\epsilon = 0.01$ (EN 1991-2:2003)

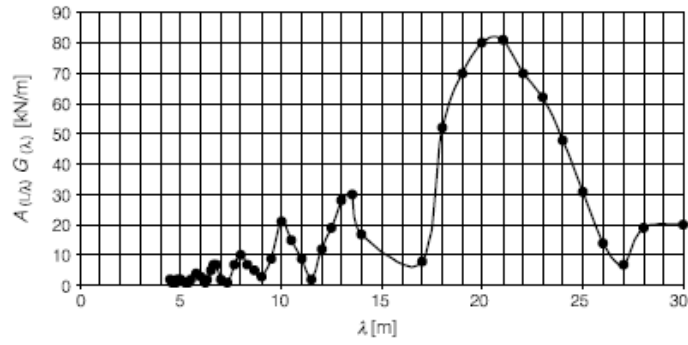


Figure 3.21 Aggressivity $A_{(L/\lambda)}G_{(\lambda)}$ as a function of excitation wavelength λ for a simply supported span of $L = 40.0$ m and damping ratio $\varepsilon = 0.01$ (EN 1991-2:2003)

As a special note in EN 1991-2, if higher values of aggressivity is obtained for $\lambda < \lambda_v$, λ_c is taken equal to λ . If the analysis to be performed for span lengths and damping ratios different from the values of figures shown above, the formulation for the aggressivity functions shown below can be used (EN 1991-2:2003);

$$A\left(\frac{L}{\lambda}\right) = \left| \frac{\cos\left(\frac{\pi L}{\lambda}\right)}{\left(\frac{2L}{\lambda}\right)^2 - 1} \right|$$

$$G(\lambda) = \frac{E n v}{\varepsilon x_i} \frac{1}{\sqrt{\left(\sum_{n=1}^i F_n \cos\left(\frac{2\pi x_n}{\lambda}\right)\right)^2 + \left(\sum_{n=1}^i F_n \sin\left(\frac{2\pi x_n}{\lambda}\right)\right)^2}} \left(1 - e^{-2\pi \varepsilon \frac{x_i}{\lambda}}\right)$$

As can be seen from the formulas presented by Eurocode, DER method is used for the determination of critical HSLM train. (See Chapter 2)

After the determination of the critical wavelength according to the figures or formula presented, critical HSLM train is selected from the figure in EN 1991-2 Annex E as shown below;

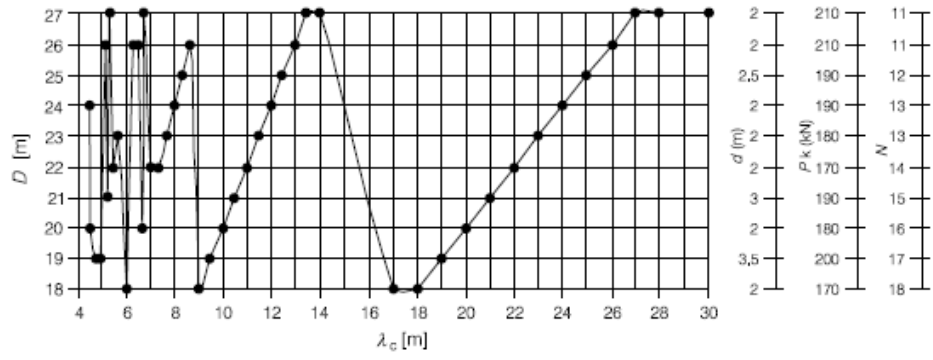


Figure 3.22 Parameters defining critical Universal Train in HSLM-A as a function of critical wavelength of excitation λ_c (EN 1991-2:2003)

CHAPTER 4

CASE STUDY

4.1 General

This chapter contains a case study work for a 30 m span railway bridge which is in the scope of Ankara-Sivas High Speed Railway Project. The bridges in Ankara-Sivas High Speed Railway Project are designed as prestressed concrete bridges. Four different span lengths are used for the project such as 15m, 20m, 25m and 30m. Since 30 m span length is the commonly chosen length for the prestressed concrete bridges that are designed in Turkey, a 30 m bridge is chosen as case study.

SAP2000 finite element analysis program is used to model the bridge, and the dynamic analysis results obtained from the finite element program are compared with the results found from analytical approaches. The procedures that are defined in EN 1991-2 are followed to choose the critical loading train and critical speed values. And, analysis will be performed for all HSLM trains and various speeds in analytical approach.

4.2 Case Study for L = 30 m Railway Bridge

Bridge properties that are basis for the analysis are determined in following parts.

4.2.1 Properties for Composite Bridge Section

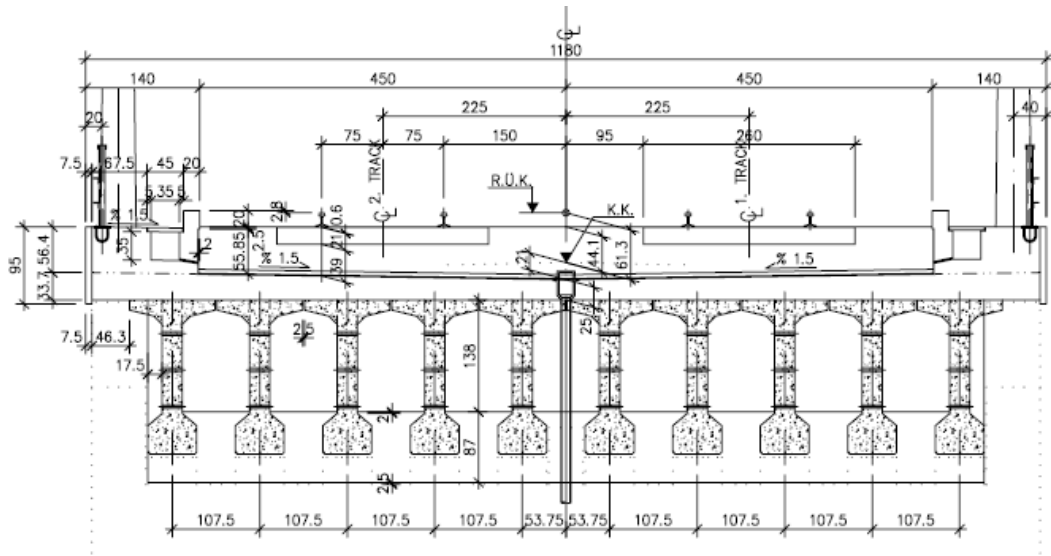


Figure 4.1 Composite section for L=30 m

Cross section area	= 11.26 m ²
Moment of inertia	= 6.185 m ⁴
Total superstructure weight	= 426.34 kN / m
Total superstructure mass	= 43.473 t / m

4.2.2 Project Speed

The maximum operating speed for Ankara-Sivas high-speed railway project is 250 km/h and design speed according to the Eurocode is taken as;

$$1.2 \times 250 \text{ km/h} = 300 \text{ km/h} = 83.33 \text{ m/s}$$

4.2.3 Type of Structure

The structure is considered that it has negligible skew effects and is constituted from simple span prestressed beams with rigid supports at the end. Therefore, the bridge can be considered as simple structure.

After the determination of the type of structure, the next step is comparing the span length according to the flow chart presented in Chapter 3.

4.2.4 Span Length

Since the span length of the bridge is less than 40 m, the ratio of torsional frequency of the structure to the natural bending frequency should be checked. Therefore, there is a need for eigenvalue analysis of the structure.

4.2.5 Damping Ratio of the Structure

From Table 3.3 damping ratio for span length of 30 m is found as;

$$\varepsilon = 1.0 \%$$

According to Figure 3.7 presented in Chapter 3 damping ratio increase is 0. Therefore, damping ratio is taken as 1.0%

4.2.6 Definition of Model for SAP2000

The 3D finite element modelling of the bridge is prepared in SAP2000 by modelling beams as frame elements whereas the deck is modelled with shell members. The beam and deck is connected with rigid frame members. The supports are modelled as elastomeric bearings. A figure that shows the finite element modelling of the bridge structure is shown below;

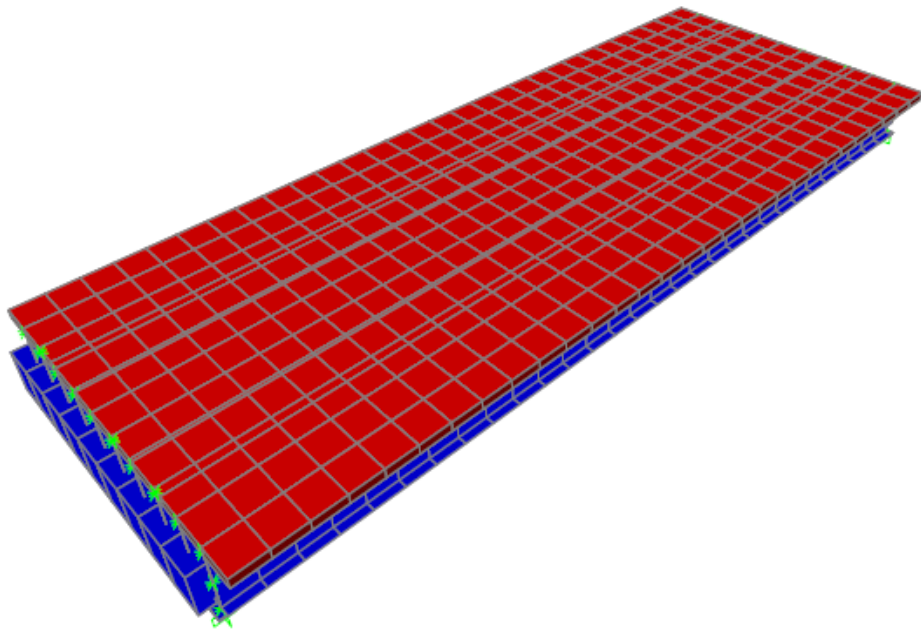


Figure 4.2 Analysis model of the bridge structure

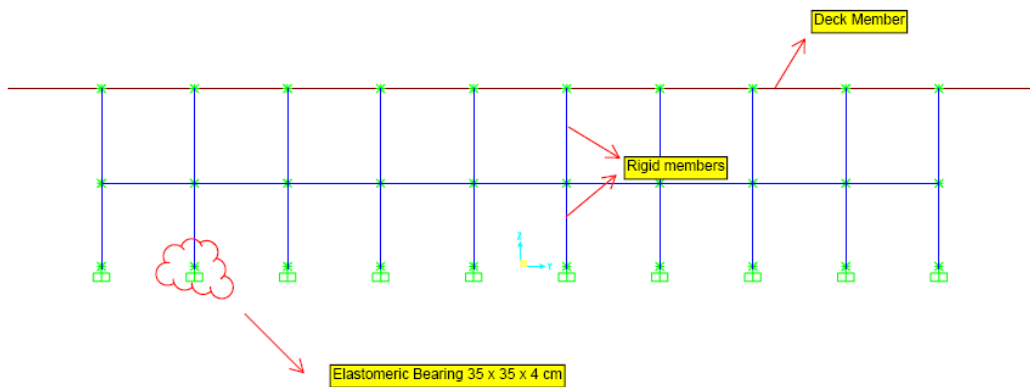


Figure 4.3 Section View of Analysis Model

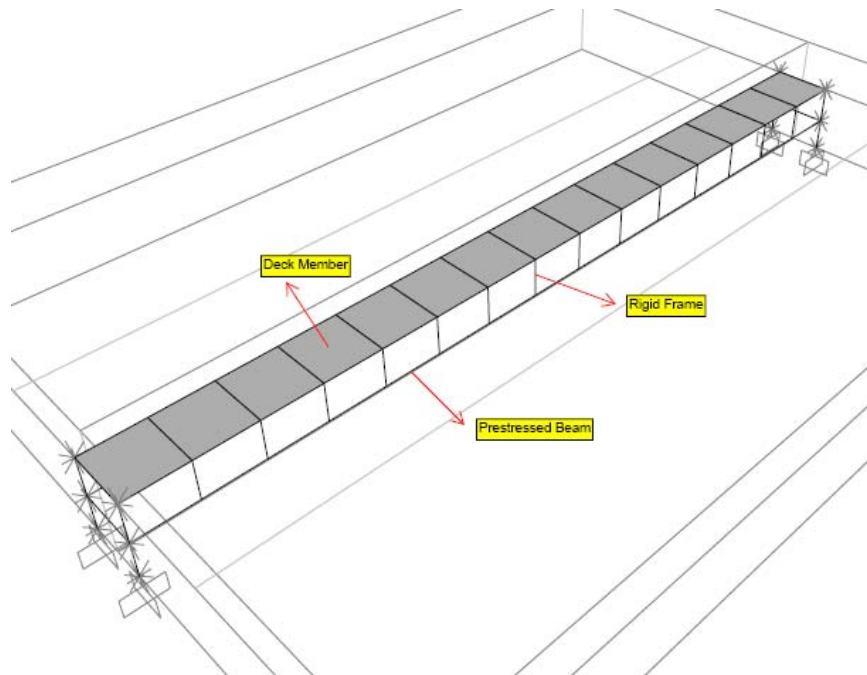


Figure 4.4 Marking of members in the analysis model

4.2.7 Eigenvalue Analysis for the Bridge

Modal analysis for the bridge was performed and the results for the first natural bending period are presented in the Figure 4.5 below;

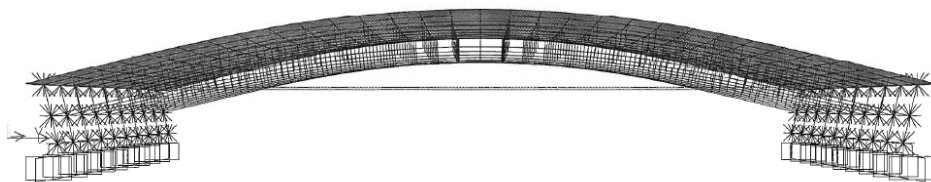


Figure 4.5 First bending mode shape

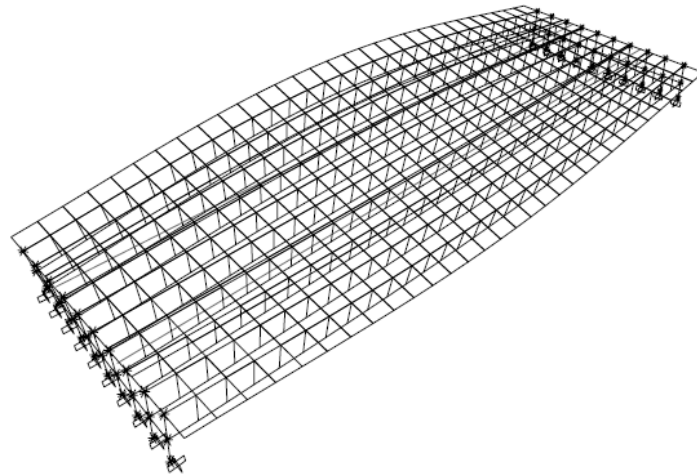


Figure 4.6 First torsional mode shape

First bending period for the structure is obtained as 0.28 sec while the torsional mode is 0.24 sec. And correspondingly the first natural bending frequency and torsional frequency are;

$$n_0 = 1 / 0.28 = 3.57 \text{ Hz and } n_T = 1 / 0.24 = 4.17 \text{ Hz.}$$

Since $n_T < 1.2 \times n_0$ dynamic analysis is required according to the flow chart.

4.2.8 Determination of Critical Wavelength of Exication

In order to determine the critical wavelength of exication, the maximum design speed wavelength of exication should be found according to the formula that is defined in Section 3.

$$\lambda_v = V_{ds} / n_0 = 83.33 \text{ (m/s)} / 3.57 \text{ Hz} = 23.34 \text{ m}$$

Then from figure 3.18 in Chapter 3, the critical wavelength of exication is found as 23.34 m.

4.2.9 Determination of Critical Train Loading

After finding the critical wavelength of excitation, the critical train loading can easily be chosen using Figure 3.22 or using the DER method spectra for the HSLM trains that is presented in Chapter 2.

For $\lambda_c = 23.34$ m, the critical train model is chosen as HSLM A6. HSLM A7 train may also be critical according to Eurocode. HSLM A6 will be used for finite element analysis whereas all trains will be analysed analytically.

4.2.10 Determination of Critical Train Speed

The first bending frequency of the structure is 3.57 Hz. Then the critical speed is found as;

$$V_{cr} = \lambda_1 \times n_0 = 23 \text{ m} \times 3.57 = 82.11 \text{ m/s (HSLM A6)}$$

$$V_{cr2} = \lambda_2 \times n_0 = 18.7 \text{ m} \times 3.57 = 66.76 \text{ m/s (TGV)}$$

4.2.11 Determination of Load Case and Analysis Case in SAP2000

The train loading is determined as multi step moving load in SAP2000 and linear modal history analysis is performed. Damping coefficient is chosen as 1% for all modes. The HSLM A6 train is determined by using the Bridge vehicle menu in program as shown below;

Vehicle Name A6

Use BD 37/01 (2002) for Uniform Load Length Effects
 Vehicle Applies To Straddle (Adjacent) Lanes Only
 Straddle Reduction Factor

Usage
 Lane Negative Moments at Supports
 Interior Vertical Support Forces
 All other Responses

Floating Axle Loads
 Value Width Type Axle Width
 For Lane Moments 0. One Point
 For Other Responses 0. One Point
 Double the Lane Moment Load when Calculating Negative Span Moments

Loads

Load Length Type	Minimum Distance	Maximum Distance	Uniform Load	Uniform Width Type	Uniform Width	Axle Load	Axle Width Type	Axle Width
Fixed Length	1,000E-04		0.	Zero Width		180.	One Point	
Fixed Length	1,000E-04		0.	Zero Width		180.	One Point	
Fixed Length	3.		0.	Zero Width		180.	One Point	
Fixed Length	111.		0.	Zero Width		180.	One Point	
Fixed Length	3.		0.	Zero Width		180.	One Point	
Fixed Length	3,525		0.	Zero Width		180.	One Point	
Fixed Length	2.		0.	Zero Width		180.	One Point	
Fixed Length	18,2375		0.	Zero Width		180.	One Point	

Add Insert Modify Delete

OK Cancel Units KN, m, C

Figure 4.7 Vehicle Definition in SAP2000

The train speed is determined in Load Case menu and the lane is assigned to related loading.

Vehicle	Lane	Start Dist	Start Time	Direction	Speed
A6	LANE1	0.	0.	Forward	82.11
A6	LANE1	0.	0.	Forward	82.11

Add
Modify
Delete

Note: Vehicles that are defined using a uniform load will not be included in the program generated multi-step analysis case. Click this note to see a list of vehicles defined using uniform loads.

Load Discretization Information
 Duration of Loading is 10.108 seconds
 Discretize Load every 0.01 seconds

Units
 KN, m, C

OK Cancel

Figure 4.8 Moving Load Definition in SAP2000

And finally the linear modal history analysis case is determined. Linear modal history case is acceptable for the dynamic analysis procedure, especially for the

models in which there is no element that shows nonlinear behaviour. Linear modal history analysis in SAP2000 is determined as shown below;

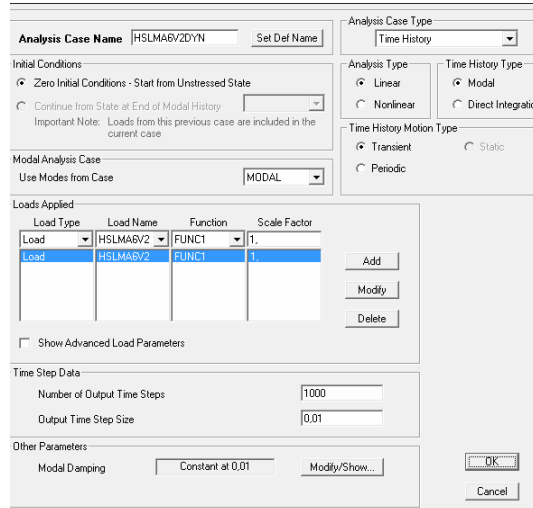


Figure 4.9 Linear Modal History Analysis Definition in SAP2000

After defining all the model features, the analysis is performed and obtained results are presented.

4.2.12 Analysis Results

The displacement and acceleration graphs that are found from analysis in SAP2000 are presented below;

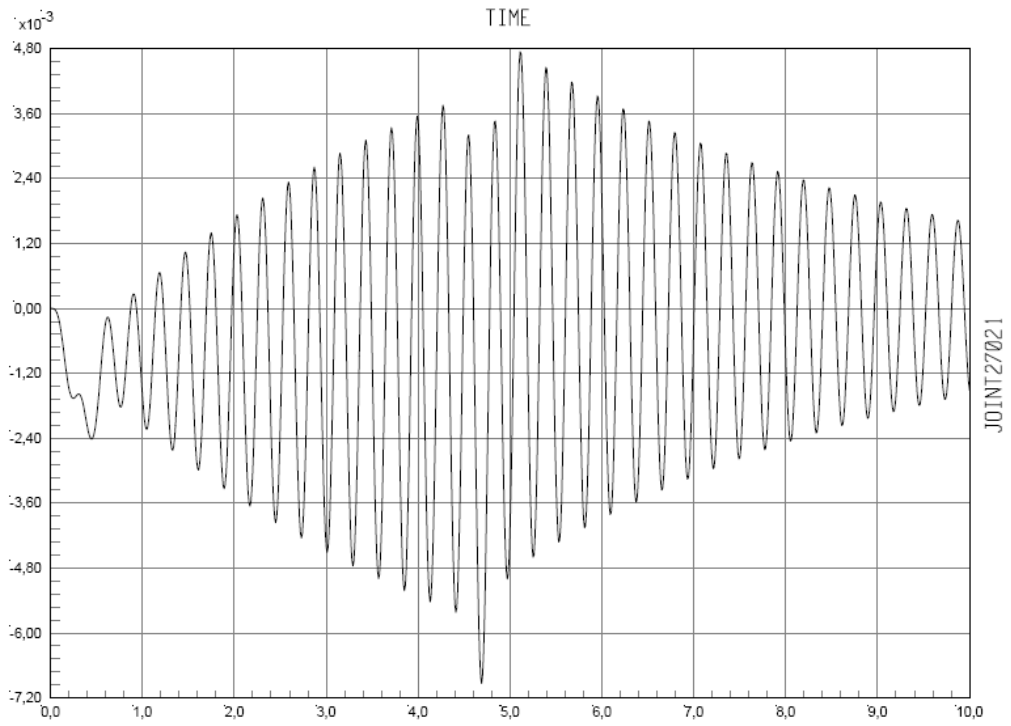


Figure 4.10 Displacement v.s. Time for HSLMA6 (from SAP2000)

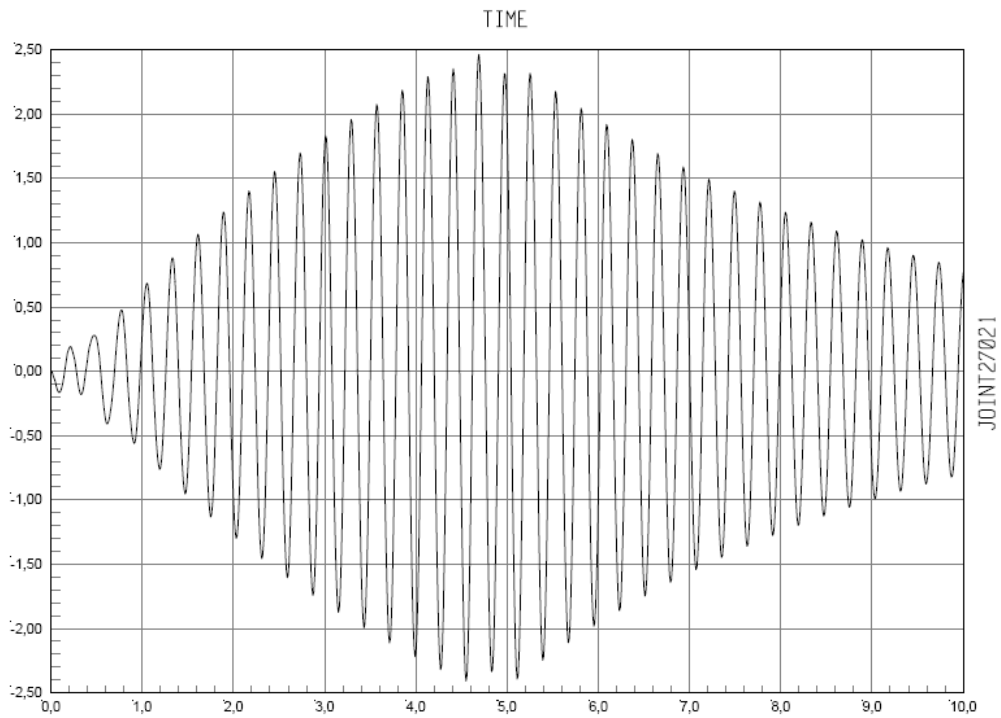


Figure 4.11 Acceleration v.s. Time for HSLMA6 (from SAP2000)

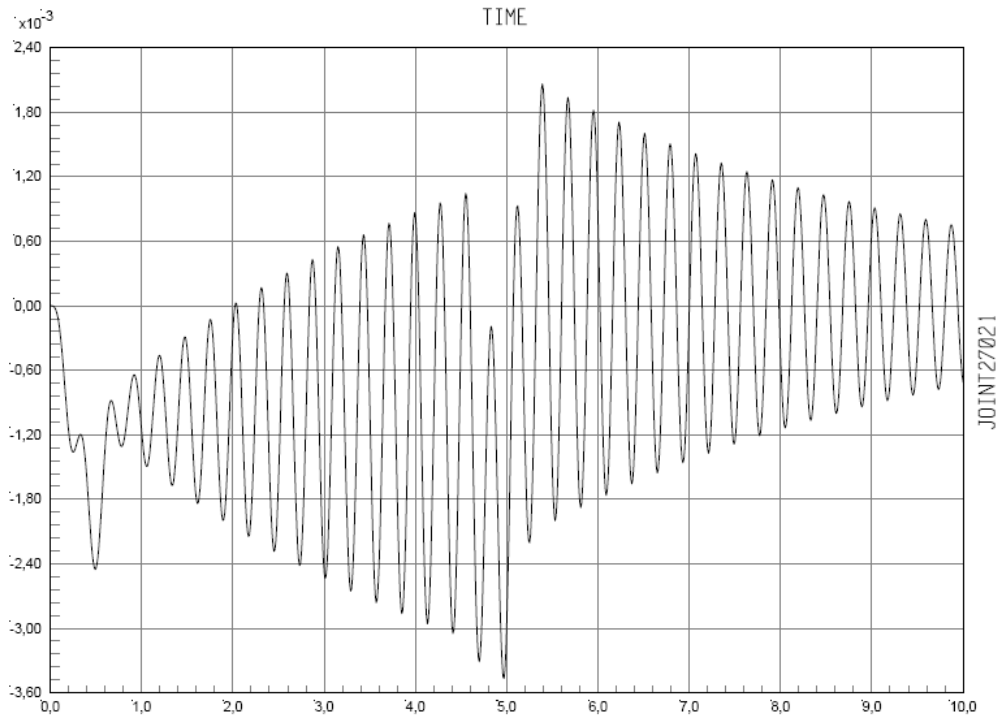


Figure 4.12 Displacement v.s. Time for French TGV (from SAP2000)

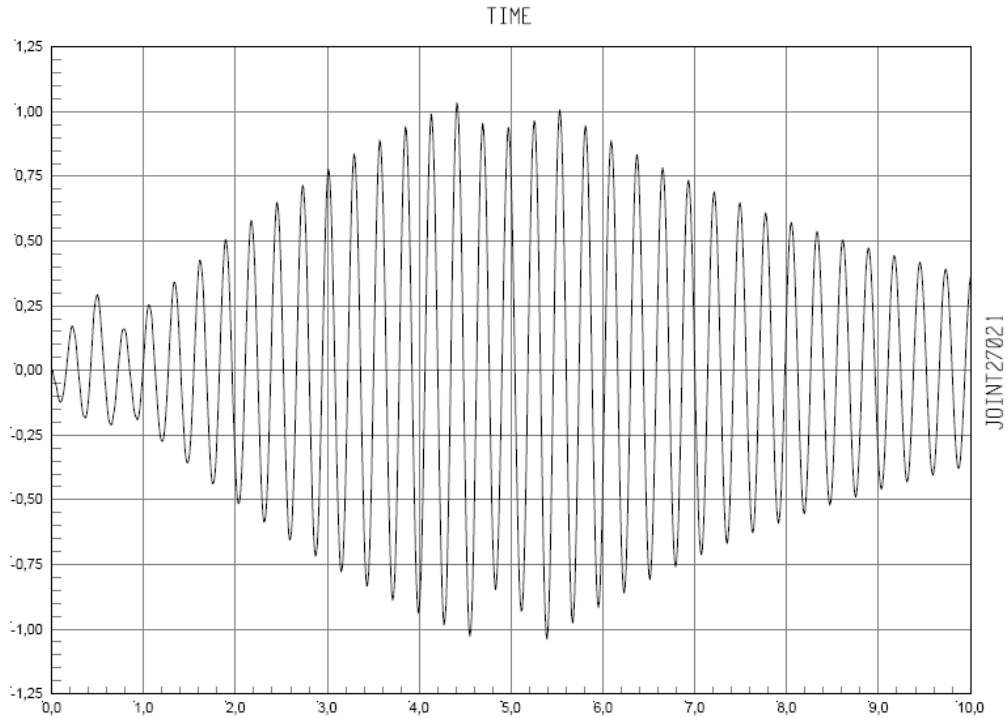


Figure 4.13 Acceleration v.s. Time for French TGV (from SAP2000)

4.2.13 Analytical Approach to the Problem

The same bridge for the Ankara-Sivas High-Speed Railway Project is also analysed using analytical approach explained in Chapter 2. The analyses are performed for all HSLM trains and for different speeds with 5 m/s range and between 40 m/s and 83.33 m/s. The speed v.s. maximum acceleration graphs for all trains at 5 m/s speed range and displacement v.s. time, acceleration v.s. time graphs at critical speed for HSLM A6 and French TGV trains are shown below whereas the related acceleration and displacement graphs for the remaining are given in Appendix B.

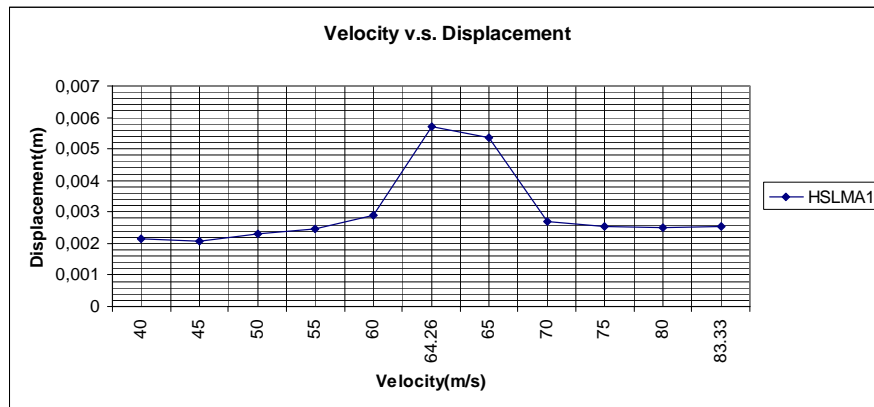


Figure 4.14 Displacement v.s. Speed for HSLMA1

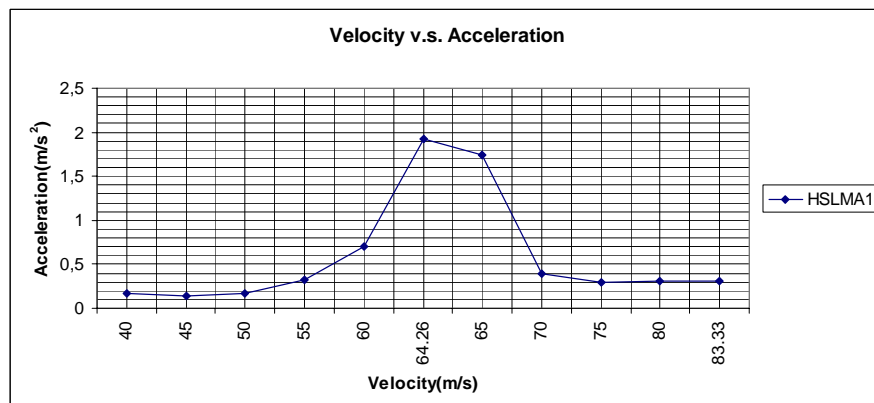


Figure 4.15 Acceleration v.s. Speed for HSLMA1

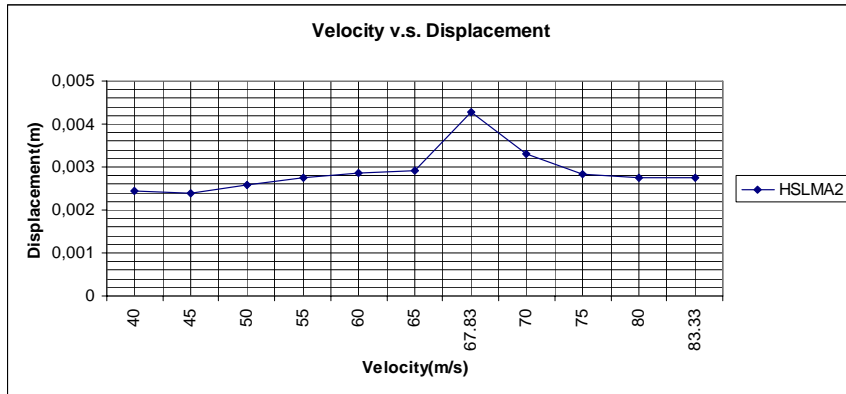


Figure 4.16 Displacement v.s. Speed for HSLMA2

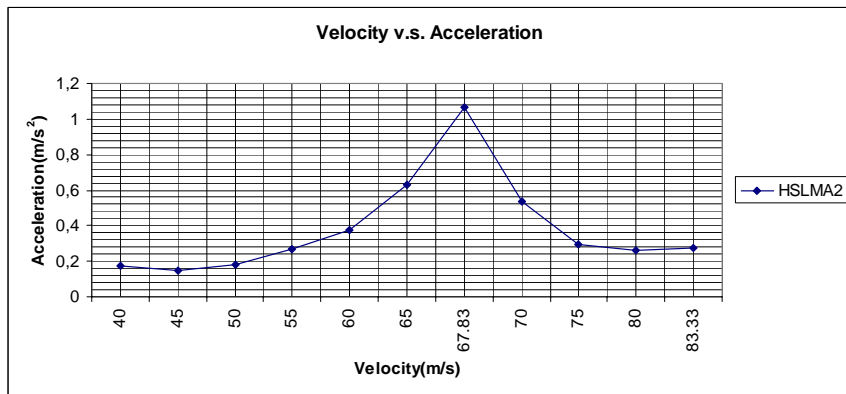


Figure 4.17 Acceleration v.s. Speed for HSLMA2

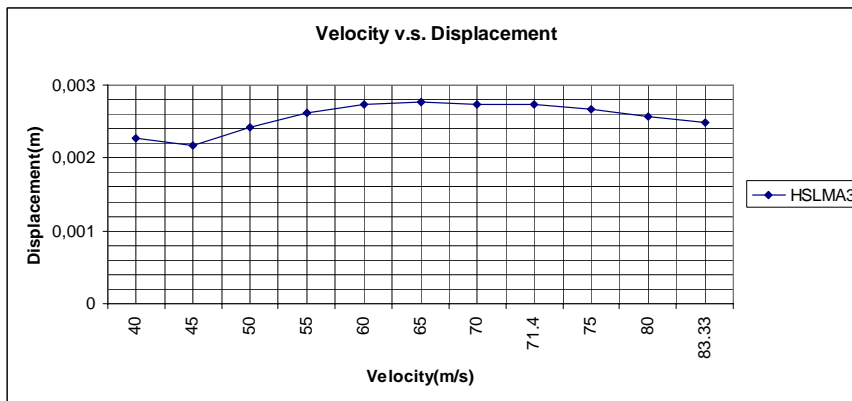


Figure 4.18 Displacement v.s. Speed for HSLMA3

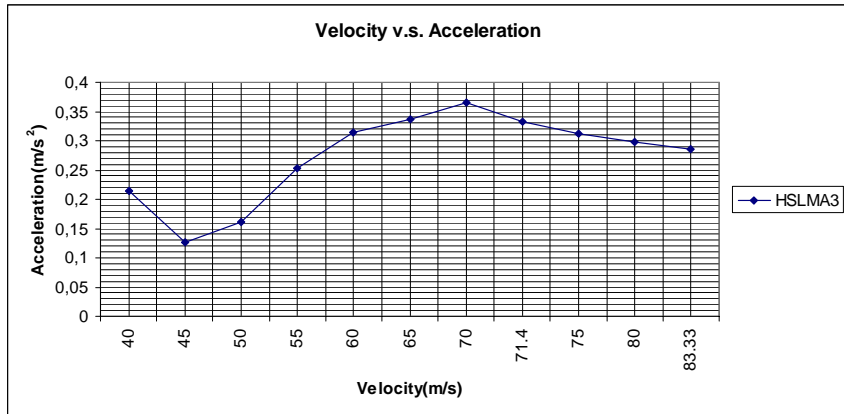


Figure 4.19 Acceleration v.s. Speed for HSLMA3

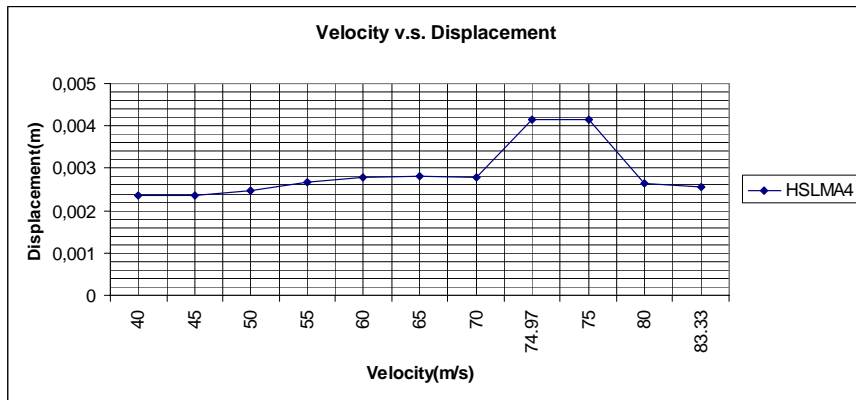


Figure 4.20 Displacement v.s. Speed for HSLMA4

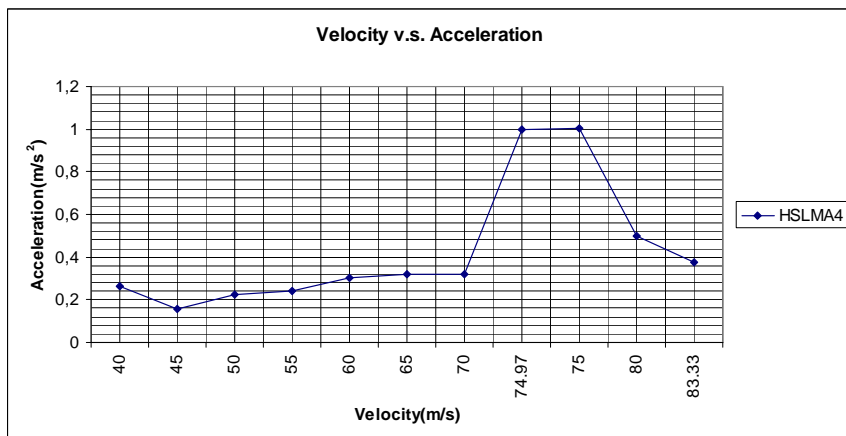


Figure 4.21 Acceleration v.s. Speed for HSLMA4

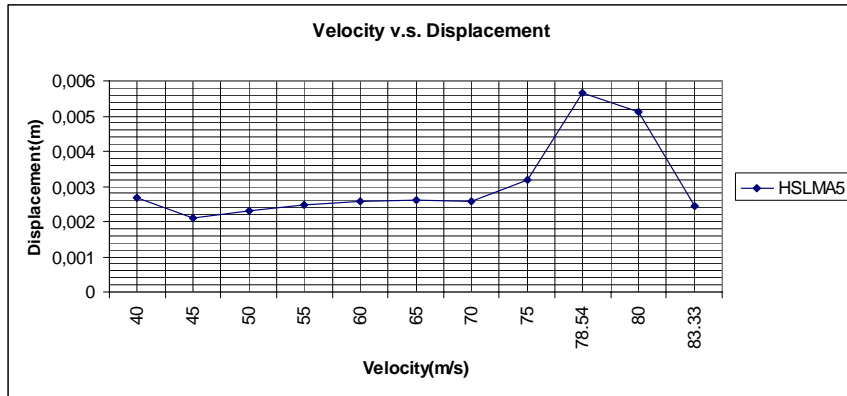


Figure 4.22 Displacement v.s. Speed for HSLMA5

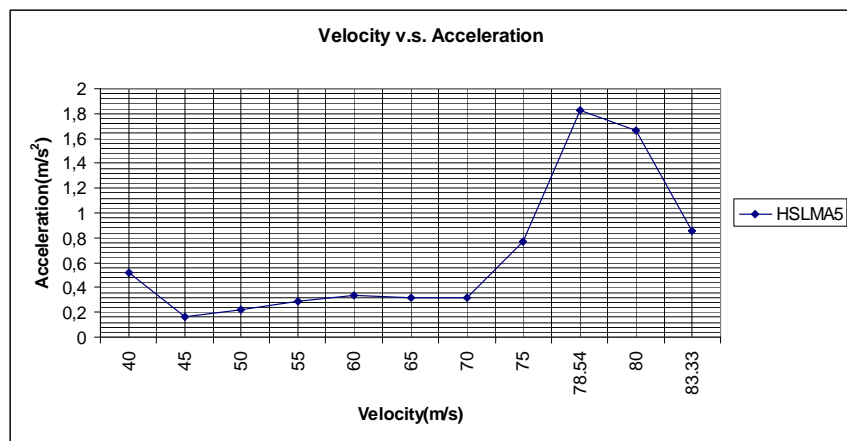


Figure 4.23 Acceleration v.s. Speed for HSLMA5

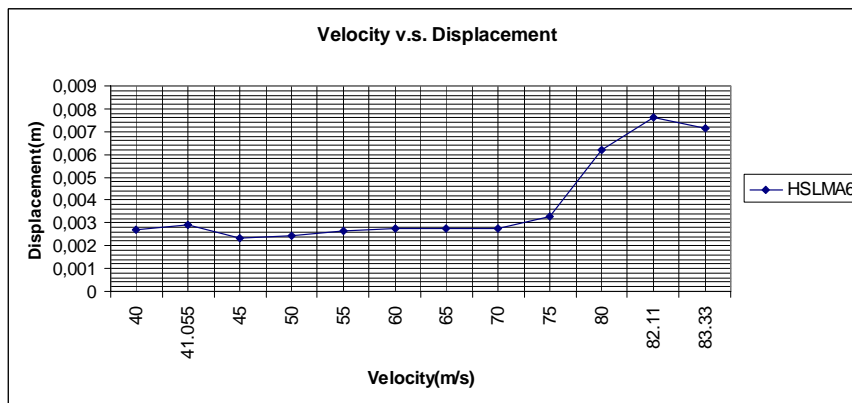


Figure 4.24 Displacement v.s. Speed for HSLMA6

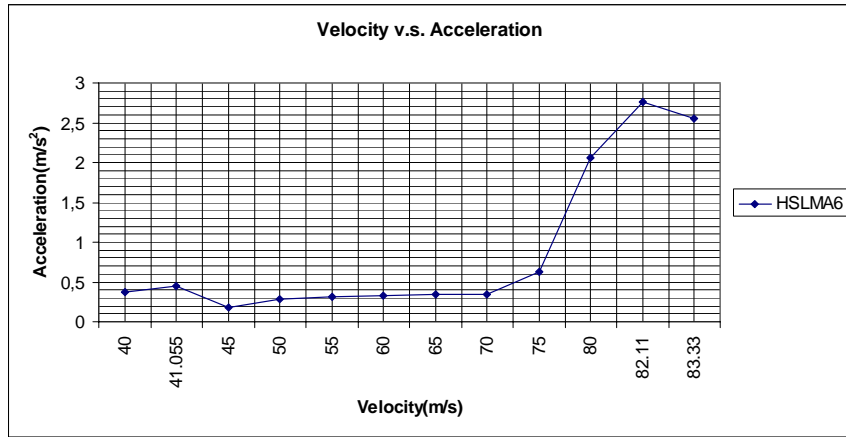


Figure 4.25 Acceleration v.s. Speed for HSLMA6

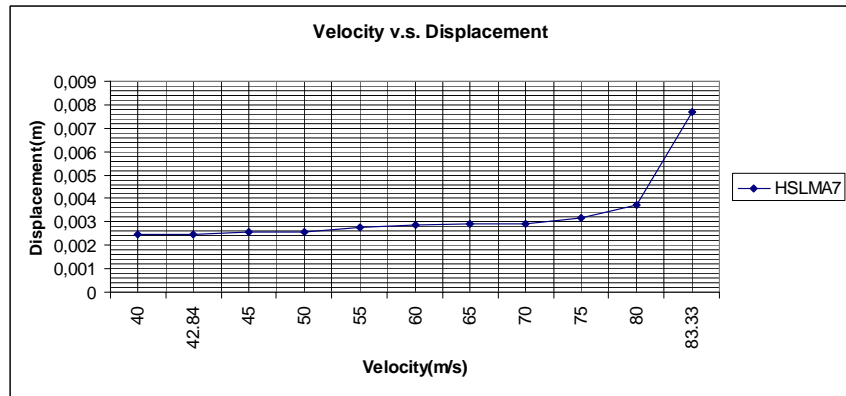


Figure 4.26 Displacement v.s. Speed for HSLMA7

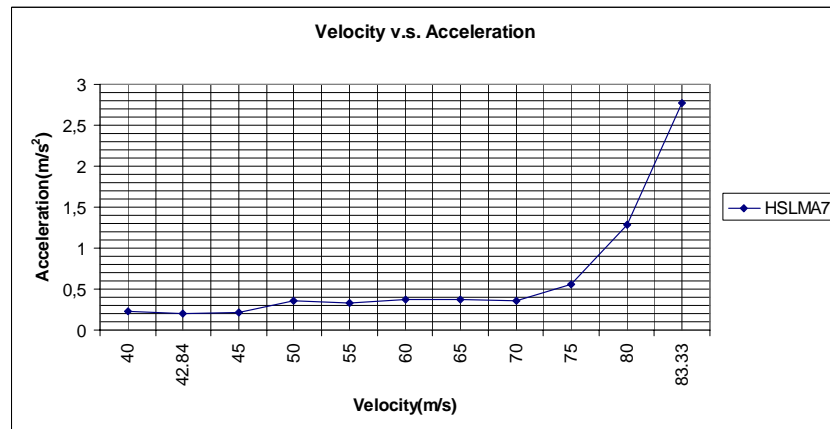


Figure 4.27 Acceleration v.s. Speed for HSLMA7

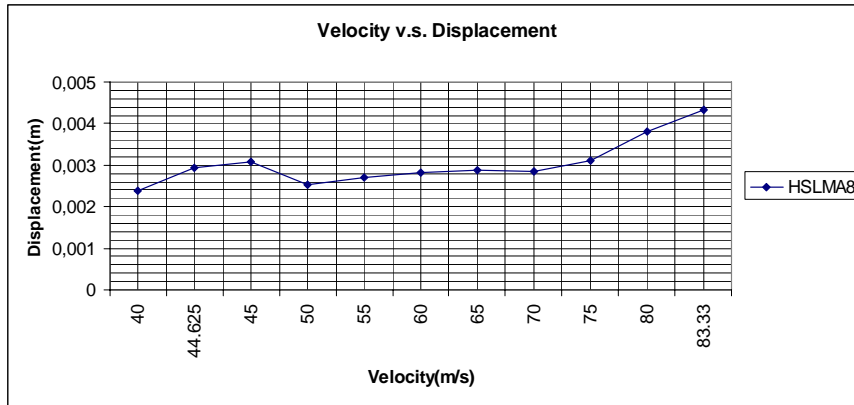


Figure 4.28 Displacement v.s. Speed for HSLMA8

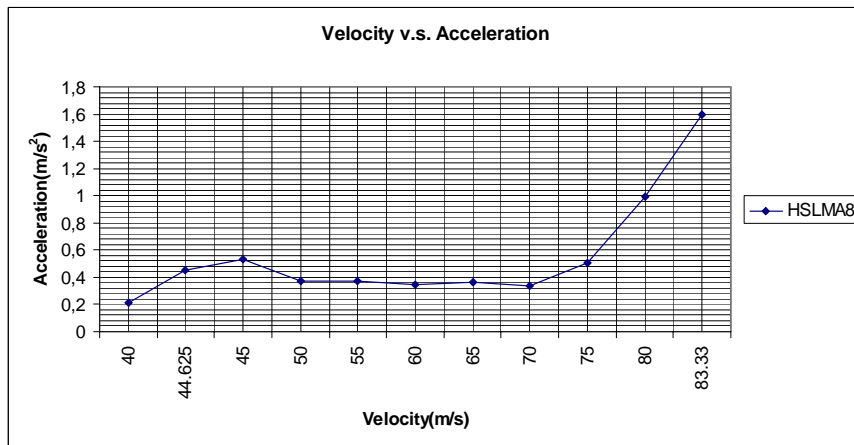


Figure 4.29 Acceleration v.s. Speed for HSLMA8

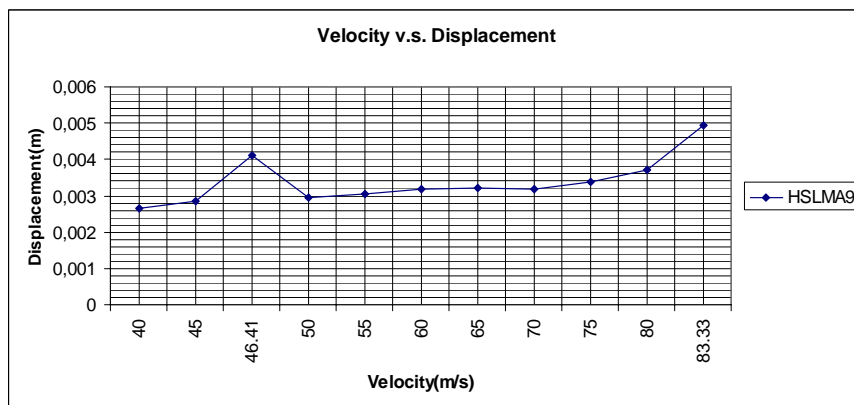


Figure 4.30 Displacement v.s. Speed for HSLMA9

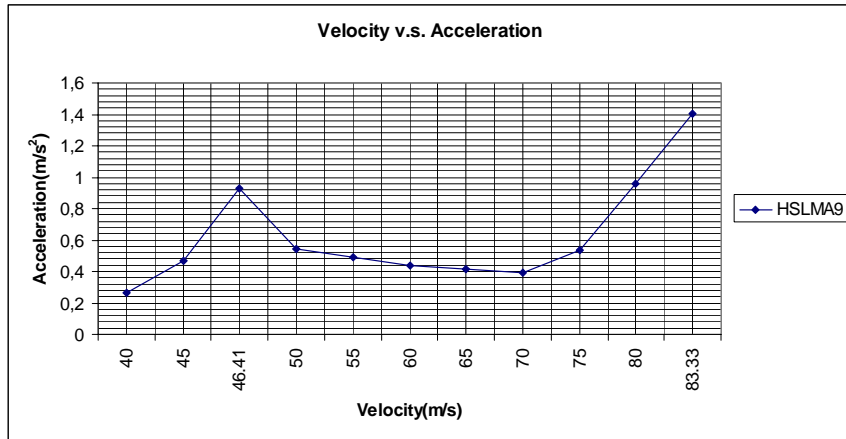


Figure 4.31 Acceleration v.s. Speed for HSLMA9

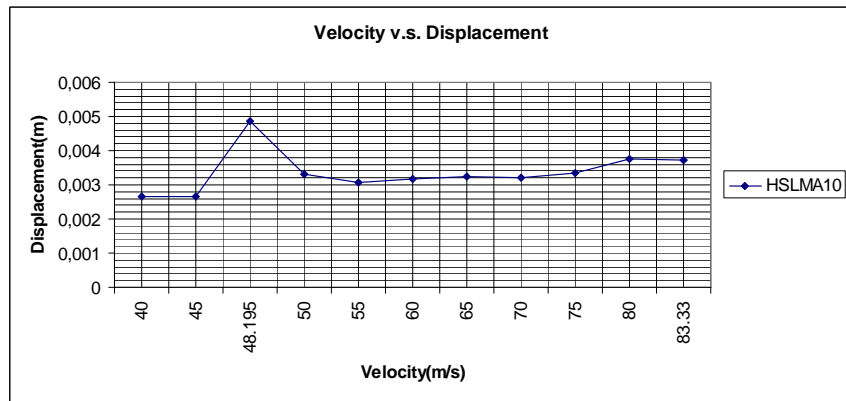


Figure 4.32 Displacement v.s. Speed for HSLMA10

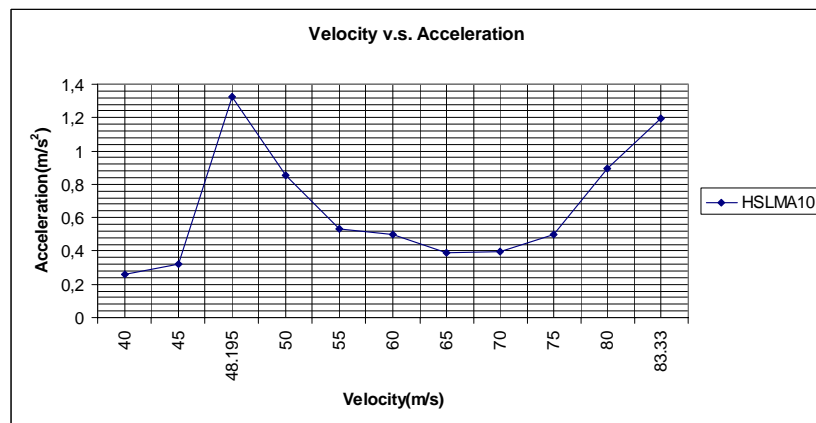


Figure 4.33 Acceleration v.s. Speed for HSLMA10

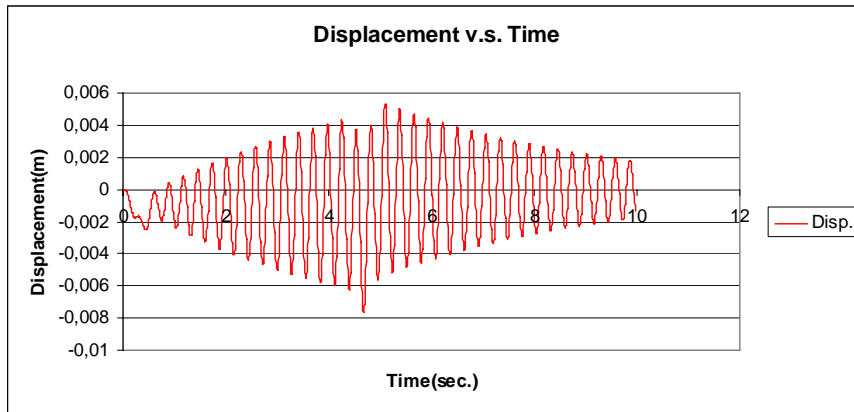


Figure 4.34 Displacement v.s. Time Graph for HSLMA6 (Analytical Approach)

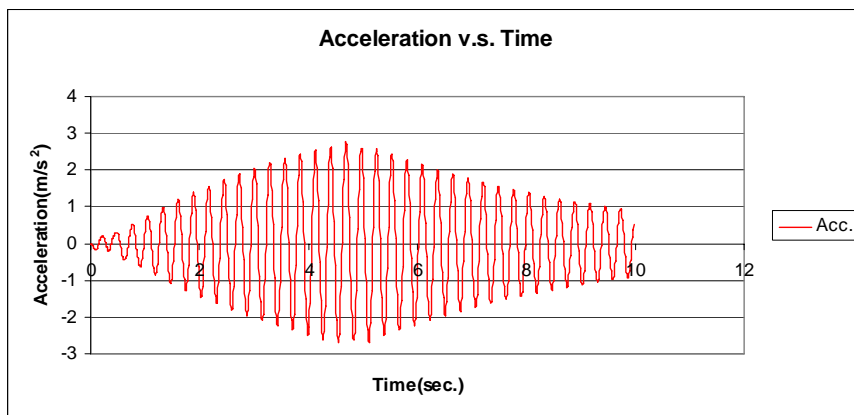


Figure 4.35 Acceleration v.s. Time Graph for HSLMA6 (Analytical Approach)

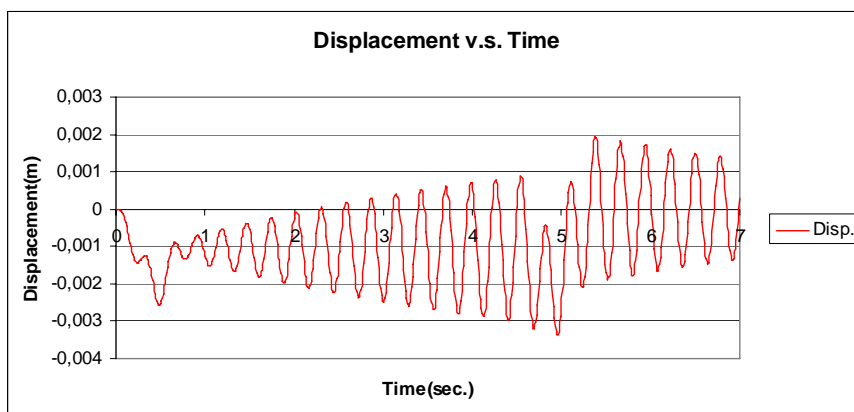


Figure 4.36 Displacement v.s. Time Graph for TGV (Analytical Approach)

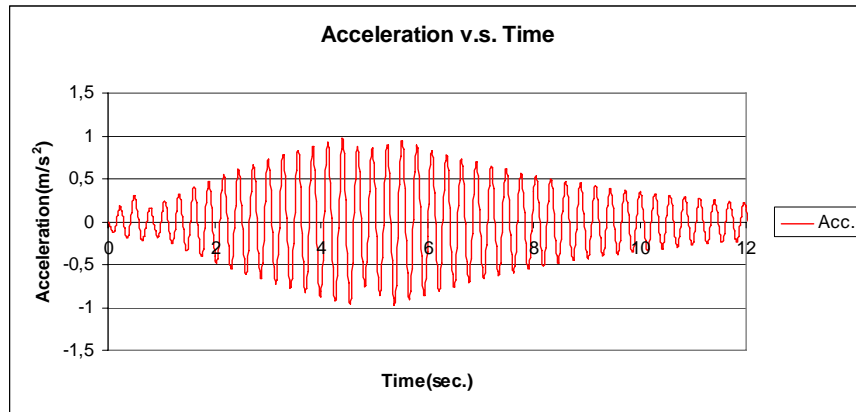


Figure 4.37 Acceleration v.s. Time Graph for TGV (Analytical Approach)

4.2.14 Comparison of the Results

In this part obtained results from finite element method and analytical approach are compared. The graphs for the comparison of the results are presented below;

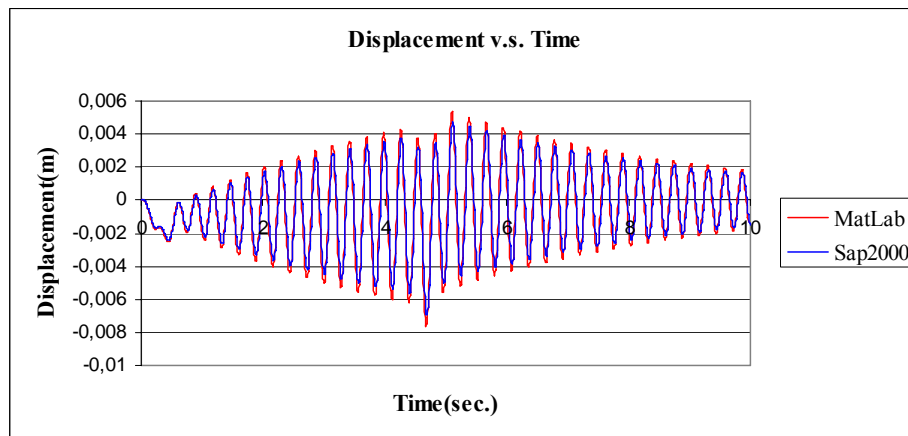


Figure 4.38 Comparison of Displacement responses of SAP2000 and Analytical Solution for HSLM A6 train

In Figure 4.38 presented above, Displacement responses from finite element analysis and analytical approach are drawn in same graph. In other words, Figure 4.10 and Figure 4.34 are presented together.

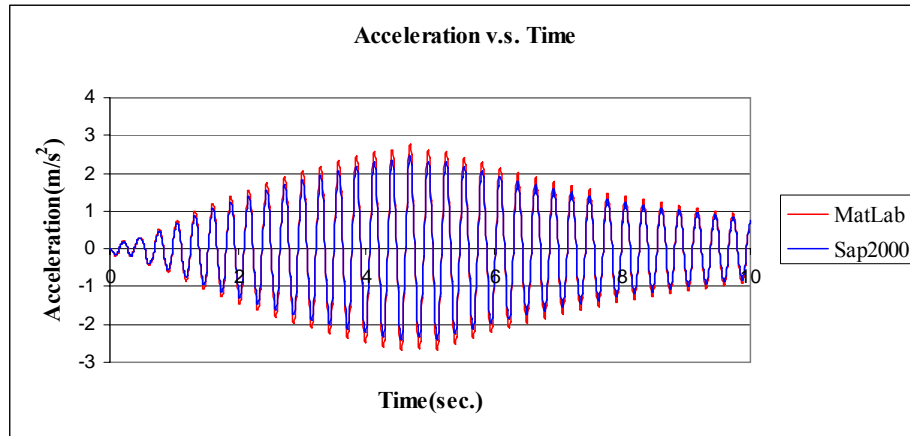


Figure 4.39 Comparison of Acceleration responses of SAP2000 and Analytical Solution for HSLM A6 train

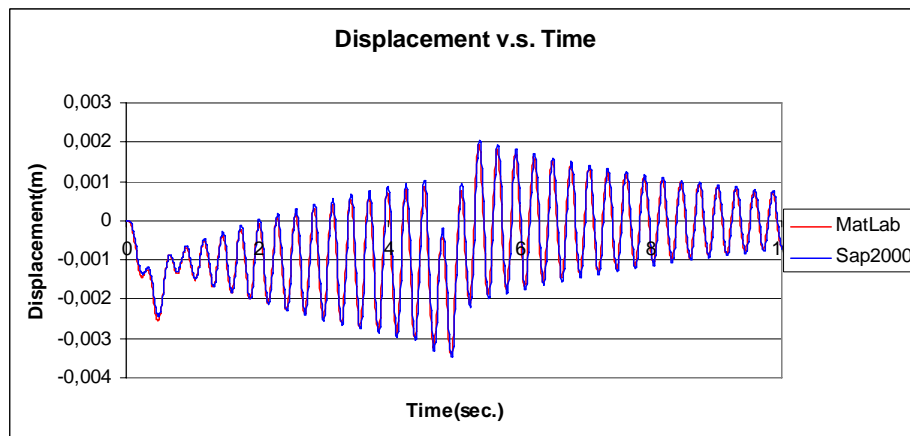


Figure 4.40 Comparison of Displacement responses of SAP2000 and Analytical Solution for TGV train

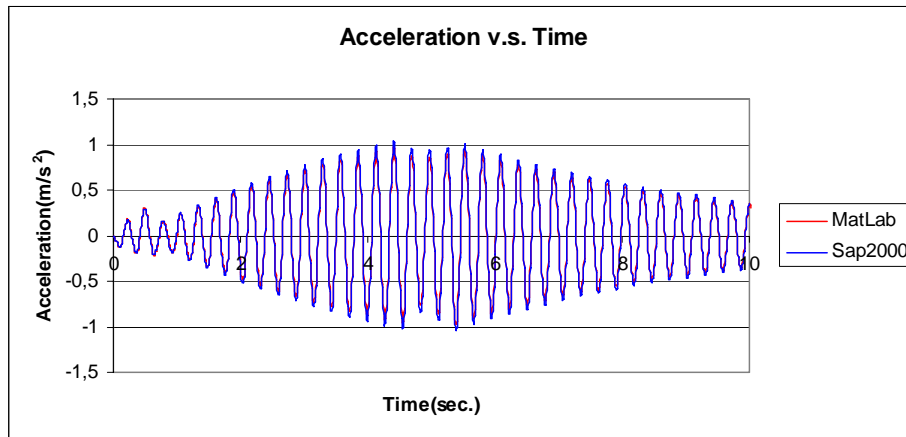


Figure 4.41 Comparison of Acceleration responses of SAP2000 and Analytical Solution for TGV train

In addition to the presented figures above, tabular presentation of the results are shown below;

Table 4.1 Tabular presentation of the obtained results from SAP2000 and analytical approach

Analysis Results Comparison				
Response	Finite Element Program		Analytical Approach	
	HSLMA6	TGV	HSLMA6	TGV
Displacement(mm)	6.90	3.47	7.63	3.38
Acceleration(m/s ²)	2.50	1.04	2.76	0.98

The analysis with finite element method and analytical approach are performed by neglecting the effect of torsional mode. The values are not too much different from each other. Small differences can be considered according to that the loading is not centering the bridge in finite element model and also 3d modelling is used in finite element approach. In 3d analysis, there is probability of girders to show local response. However, since the differences are not too much, analytical approach can

be used to define the critical parameters that affect the dynamic responses. In order to see the effect of torsional mode, comparisons for HSLM A6 train are provided by taking the torsional mode together with higher bending modes into consideration in SAP 2000. The related comparisons are shown below;

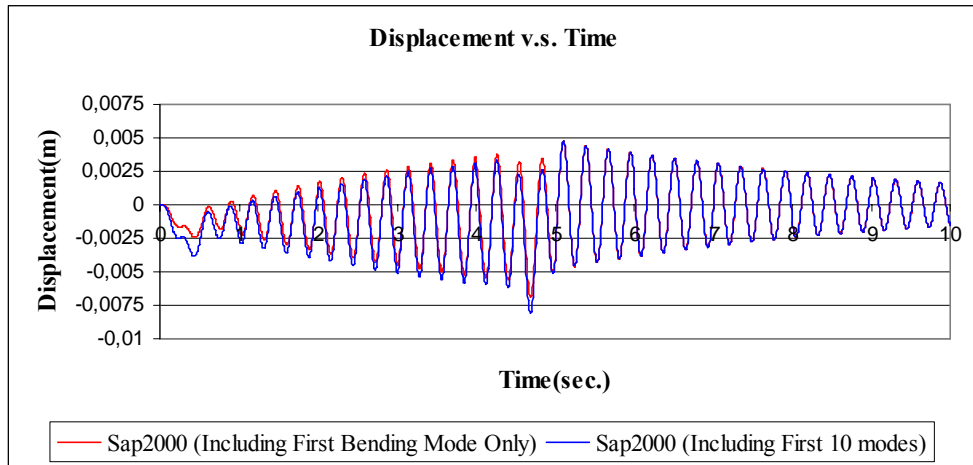


Figure 4.42 Comparison of Displacement responses of SAP2000 With and Without Torsion for HSLM A6 train

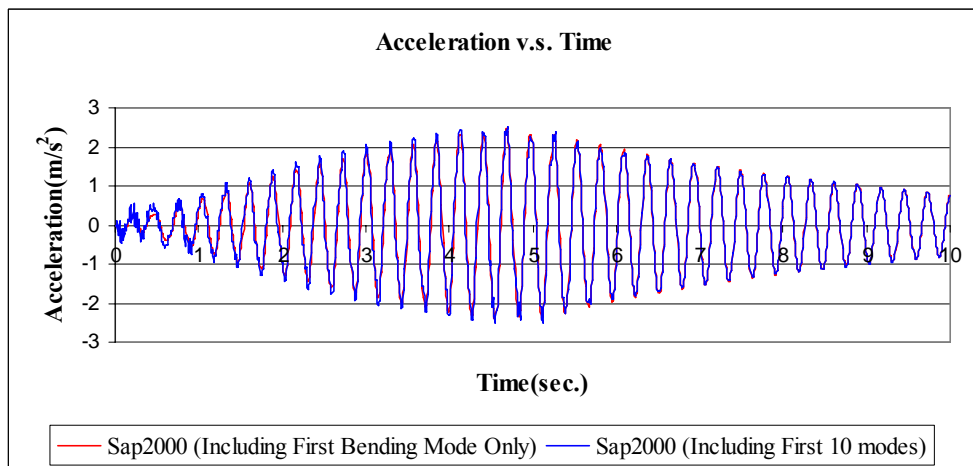


Figure 4.43 Comparison of Acceleration responses of SAP2000 With and Without Torsion for HSLM A6 train

It can be seen from Figure 4.42 and Figure 4.43, effect of higher modes including torsion are negligible. The datas obtained from both cases are very similar to eachother.

The results from analytical approach and finite element method is also compared with the initial predictions found from the formulas presented in Section 2.6 in DER method below ;

For HSLM A6 train;

$$C_t = 4 / (43.473 \times \pi) = 0.03$$

$$A(L/\lambda) \times G(\lambda) = 96 \text{ (from Figure 2.3 in Section 2.6)}$$

$$\ddot{y} \leq C_t \cdot A(L/\lambda) \cdot G(\lambda) = 96 \times 0.03 = 2.88 \text{ m/s}^2$$

For French TGV train;

$$C_t = 4 / (43.473 \times \pi) = 0.03$$

$$A(L/\lambda) \times G(\lambda) = 37 \text{ (from Figure 2.3 in Section 2.6)}$$

$$\ddot{y} \leq C_t \cdot A(L/\lambda) \cdot G(\lambda) = 37 \times 0.03 = 1.11 \text{ m/s}^2$$

Table 4.2 Comparison of Results with DER method

Analysis Type	HSLM A6	French TGV
	Acceleration (m/s ²)	Acceleration (m/s ²)
Analytical Approach	2.76	0.98
Finite Element Method	2.5	1.04
DER method	2.88	1.11

It can be seen from Table 4.2, DER method predicts the response in good accuracy.

If we check the displacement and acceleration responses with respect to different velocities obtained from analytical approach, we can see that the maximum response is obtained for HSLM A6 train at the speed of 82.11 m/s and for HSLM A7 at the speed of 83.33 m/s. As explained before Eurocode suggests HSLM A6 and HSLM A7 trains to be analysed. The critical train can also be found from Figure 2.3 in Chapter 2 which shows the aggressivity values for each HSLM train. And it can also be seen from the Figures between 4.14 and 4.33, the critical trains that are shown in Table 4.3 below for different speed values gives maximum response when compared to others in the design speed range.

Table 4.3 Critical trains for different maximum design speeds

Maksimum Design Speed (m/s)	λ_v (m)	λ_c (m)	Critical Train
60	16.81	13.50	A10
70	19.61	18.00	A1
80	22.41	22.40	A5 and A6

Therefore, it can be concluded that suggested HSLM trains by Eurocode can be used for the parametric study that will be performed in next chapter by analytical approach.

CHAPTER 5

PARAMETRIC STUDY

5.1 General

In this chapter, effect of different parameters such as mass, stiffness, modal frequency and corresponding modal displacements are studied in order to define the effect of these parameters on the dynamic response of the bridge. Analytical approach is used in parametric study which is considered as acceptable from other studies performed about the subject and also proven to be consistent in Chapter 4 of this study. Taiwan high-speed railway bridge is chosen as the basis for parametric study which has been checked for dynamic response in Chapter 2. However the damping ratio of 2.5% is decreased to 1% in parametric study and kept constant for each cases. 7 different stiffness values is analysed for 3 different mass values. Analyses are performed for critical HSLM trains and TGV train and results are presented. Then the necessary comments about the obtained results are also presented in this section. The definition of the parameters is described for each one in the following parts.

5.2 Stiffness Values for Parametric Study

As previously mentioned in Section 5.1, Taiwan high-speed railway bridge is taken as basis for stiffness determination. As shown in Figure 2.10 in Chapter 2 the flexural stiffness of the Taiwan high speed railway bridge is found as $E \times I = 2.82 \times 10^7 \times 17.9 \text{ m}^4 = 504780000 \text{ kNm}^2$.

The other stiffness values are determined as multiplying the stiffness of Taiwan high-speed railway bridge with 1/100, 1/20, 1/5, 2.50, 3.0 and final stiffness value is determined according to the obtained results from the previous stiffness values.

5.3 Mass Values for Parametric Study

Mass values for the parametric study are determined by considering the minimum and maximum practical mass for concrete bridges. In the light of this assumption mass values are determined as 25 t/m, 35 t/m and 45 t/m for parametric study.

5.4 Speeds Considered in Parametric Study

Analyses are performed for different speed values in parametric study. Maximum design speed is chosen as 350 km/h (97.22 m/s). Together with the determined speeds by Eurocode, additional analysis speeds are determined. The speeds are defined according to the formula stated below;

$$V_{cr} = d / i \times (n_0, \dots, n_k) \quad \text{where } i = 1, 2, 3, 4$$

d = axle distance for critical train

i = resonance number

n_0 = first natural bending frequency

n_k = k^{th} natural bending frequency

n_k is considered for the values obtained from the formula stated below where;

$$40 \text{ m/s} < V_{cr} < 97.22 \text{ m/s}$$

5.5 Train Model Considered for Parametric Study

The critical trains for each analysis are determined from the procedure defined in Eurocodes. And all analyses are also performed for French TGV train to compare the results obtained from HSLM trains in safety point of view.

5.6 Summary of the Parameters

Analyses are performed for constant 1% damping and span length of 40 m. The analysis no, stiffness, mass, critical trains and speed values for each analysis are summarized in table shown below;

Table 5.1 Analysis Parameters

ANALYSIS NO	EI (kNm ²)	m (t/m)	Critical Train	Analysis Speeds (m/s)
1	5047800	25	HSLMA3	(40) / (55.12) / (73.49) / (79.40) / (97.22)
2	5047800	35	HSLMA3	(40) / (46.59) / (62.12) / (67.10) / (93.17) / (97.22)
3	5047800	45	HSLMA3	(40) / (41.09) / (54.78) / (59.18) / (82.17) / (97.22)
4	25239000	25	HSLMA3	(40) / (44.39) / (59.19) / (88.78) / (97.22)
5	25239000	35	HSLMA3	(40) / 50 / 75 / (97.22)
6	25239000	45	HSLMA3	(40) / (44.11) / (58.82) / (66.17) / (91.89) / (97.22)
7	100955600	25	HSLMA3	(40) / (78.91) / (88.77) / (97.22)
8	100955600	35	HSLMA3	(40) / (66.70) / (75) / (97.22)
9	100955600	45	HSLMA3	(40) / (58.82) / (66.17) / (88.23) / (97.22)
10	504780000	25	HSLMA3	(40) / (88.23) / (97.22)
11	504780000	35	HSLMA3	(40) / (74.56) / (97.22)
12	504780000	45	HSLMA3	(40) / (65.80) / (97.22)
13	1261950000	25	HSLMA10	(40) / (47.08) / (62.78) / (94.16) / (97.22)
14	1261950000	35	HSLMA10	(40) / (53) / (79.58) / (97.22)
15	1261950000	45	HSLMA2	(40) / (49.39) / (97.22)

Table 5.1 Analysis Parameters Cont'd

ANALYSIS NO	EI (kNm ²)	m (t/m)	Critical Train	Analysis Speeds (m/s)
16	1499196630	25	HSLMA9	(40) / (49.42) / (65.89) / (97.22)
17	1499196630	35	HSLMA10	(40) / (43,37) / (57,83) / (86,74) / (97,22)
18	1499196630	45	HSLMA10	(40) / (51) / (76,55) / (97,22)
19	2089789200	25	HSLMA3	(40) / (44,88) / (59,84) / (89,76) / (97,22)
20	2089789200	35	HSLMA9	(40) / (49,31) / (65,75) / (97,22)
21	2089789200	45	HSLMA10	(40) / (45,16) / (60,21) / (90,32) / (97,22)

The speeds marked as red are critical speeds determined by Eurocode while others are analytically determined critical speeds.

5.7 Analysis Results

The displacement and acceleration responses obtained for each case will be presented in this part. The results will be given as tables in this part. The related graphs for the analysis performed for selected critical speeds are given in Appendix C.

5.7.1 Results and Discussion on Results for Critical Speed

The results for the first three analysis performed in the scope in this study are summarized in the tables shown below in which the obtained acceleration and displacement values are shown for each analysed speed value. The displacement-time and acceleration-time graphs for selected critical speed are presented in Appendix C of this study. In this part, displacement-time and acceleration-time graphs for the case of maximum response are presented.

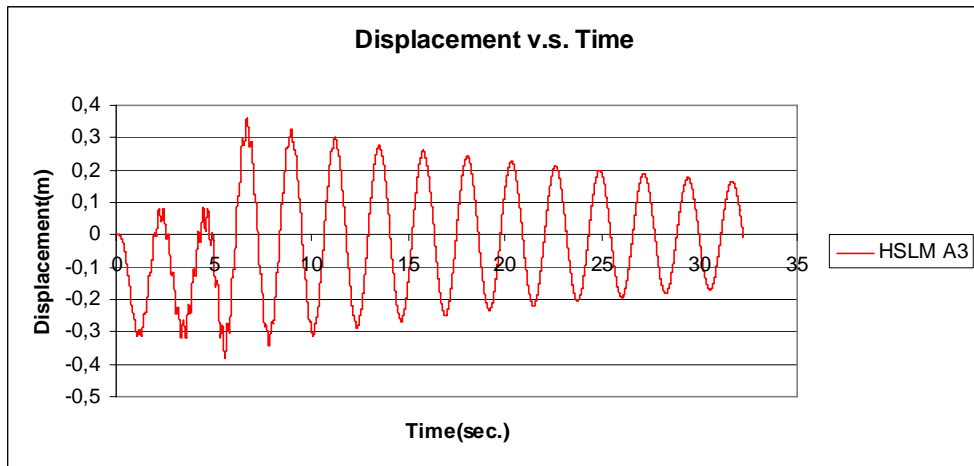


Figure 5.1 Displacement v.s. Time graph for $EI = 5047800 \text{ kNm}^2$, $m=25 \text{ t/m}$ and $V=79.40 \text{ m/s}$

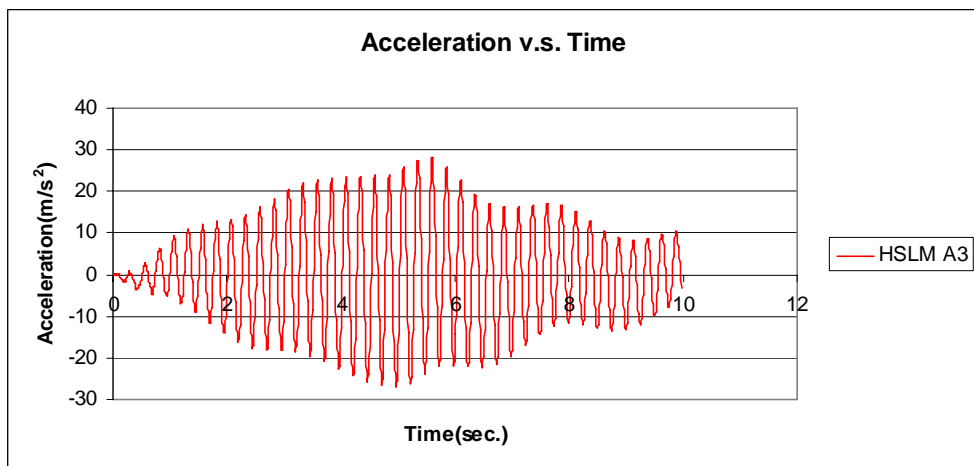


Figure 5.2 Acceleration v.s. Time graph for $EI = 5047800 \text{ kNm}^2$, $m=25 \text{ t/m}$ and $V=79.40 \text{ m/s}$

The values obtained for the first three analyses are summarized in the tables shown below;

Table 5.2 Analysis results for different speed values, EI=5047800, m= 25 t/m

V (m/s)	u (cm)	a (m/s²)
40	46	5.35
55.12	37.8	3.45
73.49	36.47	9.2
79.40	38.15	28.02
97.22	29	4.04

Table 5.3 Analysis results for different speed values, EI=5047800, m= 35 t/m

V (m/s)	u (cm)	a (m/s²)
40	35.8	2
46.59	37.83	2.5
62.12	36.47	6.56
67.10	38.15	20.25
93.17	28.2	7
97.22	27.89	3.7

Table 5.4 Analysis results for different speed values, EI=5047800, m= 45 t/m

V (m/s)	u (cm)	a (m/s²)
40	41.42	2
41.09	37.8	1.95
54.78	36.47	5.11
59.18	38.15	15.75
82.17	28.22	5.51
97.22	29.76	2.16

As can be seen from the tables, maximum responses are obtained at non-resonant speeds. In other words, peak responses are obtained for the speeds that are found from the bending modes different than the first mode. This may occur when the first natural bending mode does not have peak modal displacement in the design frequency range. The frequency and modal displacement graph for the first analysis is presented below;

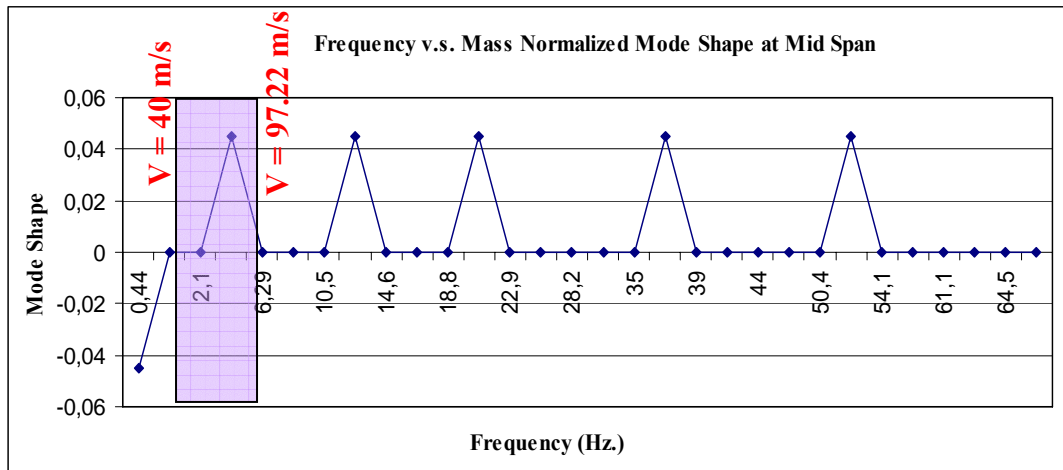


Figure 5.3 Frequency v.s. Mode Shapes for $EI = 5047800 \text{ kNm}^2$, $m=25 \text{ t/m}$

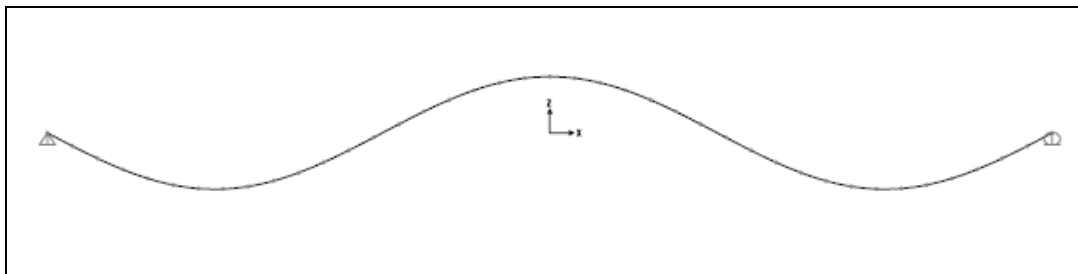


Figure 5.4 Modal Shape in Design Frequency Range for $EI = 5047800 \text{ kNm}^2$, $m=25 \text{ t/m}$

The frequency value that leads to peak modal displacement shown in Figure 5.3 is 3.97 Hz. And critical speed value that gives the maximum response for the HSLM A3 train ($d=20 \text{ m}$), $V_{cr} = 20 \times 3.97 = 79.40 \text{ m/s}$

The results for the analyses between 4 and 6 are presented below. The displacement v.s. time graph is given for the analysis 4 together with acceleration v.s. time graph in this part while the same graphs for other analyses are given in Appendix C.

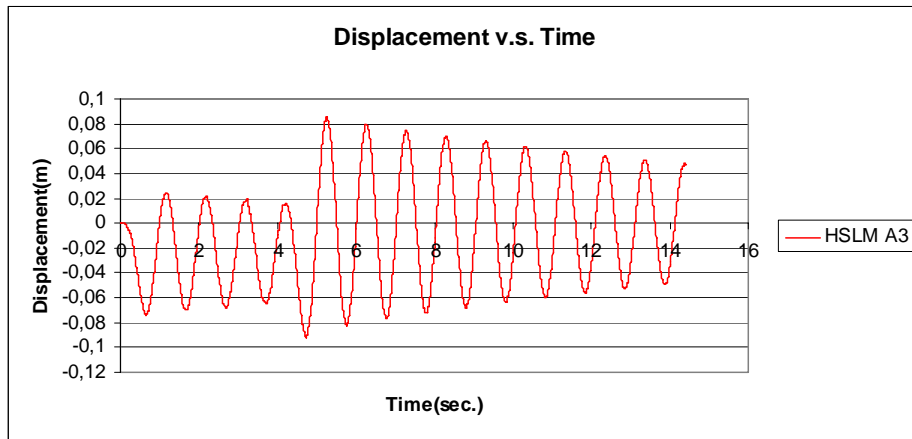


Figure 5.5 Displacement v.s. Time graph for $EI = 25239000 \text{ kNm}^2$, $m=25 \text{ t/m}$ and $V=88.78 \text{ m/s}$

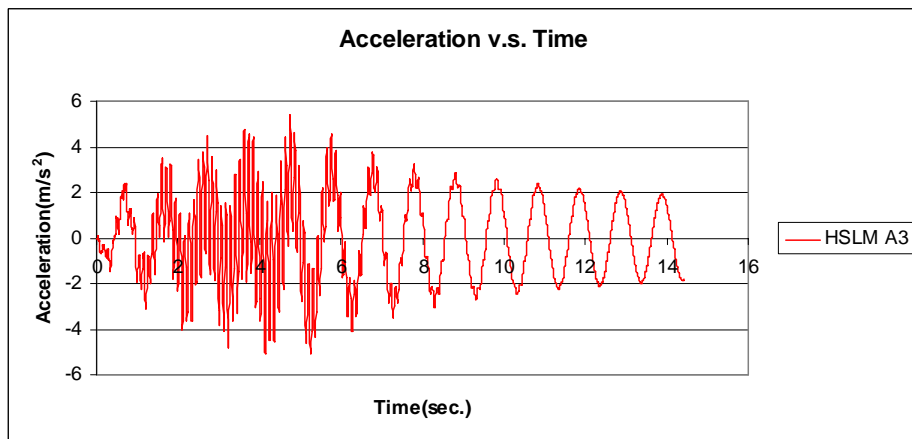


Figure 5.6 Acceleration v.s. Time graph for $EI = 25239000 \text{ kNm}^2$, $m=25 \text{ t/m}$ and $V=88.78 \text{ m/s}$

Table 5.5 Analysis results for different speed values, $EI=25239000$, $m= 25 \text{ t/m}$

V (m/s)	u (cm)	a (m/s²)
40	6.32	1.13
44.39	6.88	1.36
59.19	8.38	2.76
88.78	9.18	5.4
97.22	7.3	2.84

Table 5.6 Analysis results for different speed values, EI=25239000, m= 35 t/m

V (m/s)	u (cm)	a (m/s²)
40	6.54	0,97
50	8.38	1.98
75	9.18	3.9
97.22	8.42	2.46

Table 5.7 Analysis results for different speed values, EI=25239000, m= 45 t/m

V (m/s)	u (cm)	a (m/s²)
40	6.84	1.12
44.11	8.37	1.54
58.82	7.38	1.35
66.17	9.18	3
91.89	7.56	1.92
97.22	6.81	1.64

In Figure 5.3, there is a peak modal displacement in the design frequency range. However, in case of that there is no peak modal displacement in the design frequency range, it is obvious that the acceleration response of the bridge will be smaller when compared to the condition that there is a peak modal displacement in the design frequency range. The closer resonant speeds where the peak modal displacements are obtained should be considered in these cases. Results of the analyses between 4 and 9 can be example for the related condition. The results for the analyses between 4 and 6 are presented in Table 5.5 to Table 5.7 whereas the related frequency v.s. modal displacement graph for analysis 4 can be seen in Figure 5.7. Same condition can be seen for analysis between 5 and 9 from the presented acceleration v.s. time graphs in Appendix C and frequency v.s. modal displacement graphs in Appendix D.

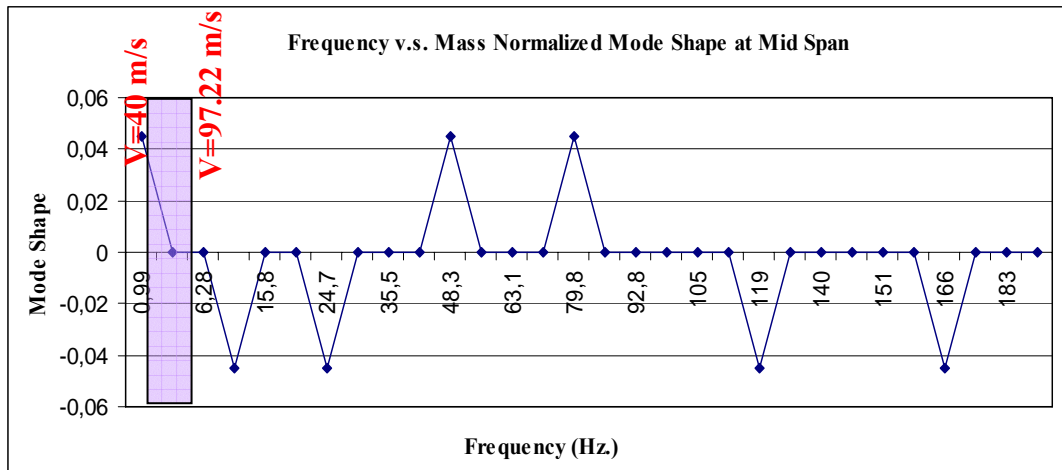


Figure 5.7 Frequency v.s. Mode Shape for $EI = 25239000 \text{ kNm}^2$, $m=25 \text{ t/m}$

As can be seen from Figure 5.7, there is no peak modal displacement in the design frequency range. However there is a peak modal displacement for the frequency value of 8.878 Hz. And, maximum response is obtained for 88.78 m/s speed as presented in Table 5.5. This non-resonant speed is obtained with the calculation for HSLM A3 train such that, $V_{cr} = (d / i) \times 8.878 = (20 / 2) \times 8.877 = 88.87 \text{ m/s}$.

In the calculation shown above, the “i” value is taken as 2. This means that the bridge shows two cycles of oscillations between the passage of two consecutive loads. However, it is obvious that the situation that the bridge shows one cycle of oscillation between the passage of two consecutive loads is more probable. And there can be higher acceleration results in that case. Since, in the analytical approach, the effect of torsional frequency is not considered, the responses obtained for the cases where there is no peak modal displacements in the design frequency range may be underestimated. If detailed analysis is performed for a bridge, there is a probability of that the second mode is torsional mode. And obviously there will be a peak modal displacement in the design frequency range according to torsion. In that case, the non-resonant speed should be calculated from the torsional frequency together with the closer bending frequencies. From this explanation, it can be said that the probable critical modes should be considered for

the cases where the peak modal displacements are not obtained from the first natural bending mode in design frequency range.

5.7.2 Results and Discussion on Results for Displacement and Acceleration

The displacement and acceleration values will be discussed by presenting peak values for all analyses together. The peak responses obtained from the analysis are summarized in the table shown below;

Table 5.8 Summary of results for peak responses

ANALYSES NO	STIFFNESS AND MASS		CRITICAL TRAIN	PEAK RESPONSES	
	EI(kNm ²)	m(t/m)		a(m/s ²)	u(cm)
1	5047800	25	HSLMA3	28	45.99
2	5047800	35	HSLMA3	20.25	38.15
3	5047800	45	HSLMA3	15.74	41.42
4	25239000	25	HSLMA3	5.4	9.18
5	25239000	35	HSLMA3	3.9	9.18
6	25239000	45	HSLMA3	3.05	9.18
7	100955600	25	HSLMA3	3.65	3.4
8	100955600	35	HSLMA3	1.45	2.96
9	100955600	45	HSLMA3	1.52	2.09
10	504780000	25	HSLMA3	4.14	0.73
11	504780000	35	HSLMA3	2.97	0.73
12	504780000	45	HSLMA3	2.31	0.73
13	1261950000	25	HSLMA10	1.56	0.18
14	1261950000	35	HSLMA10	1.13	0.18
15	1261950000	45	HSLMA2	1.71	0.25
16	1499196630	25	HSLMA9	1.1	0.13
17	1499196630	35	HSLMA10	1.12	0.153
18	1499196630	45	HSLMA10	0.87	0.155
19	2089789200	25	HSLMA3	1	0.081
20	2089789200	35	HSLMA9	0.83	0.093
21	2089789200	45	HSLMA10	0.87	0.110

The peak responses from the analyses 1 to 9 are based on the occurrence of peak modal displacements in the design frequency range. And the acceleration responses are decreased with increasing stiffness. The first natural bending frequency is in the design frequency range for the other analysis. The effect of mass and critical train on the response of the bridge can be understood better from the analysis between 10 and 21. This is because of the fact that, the responses obtained in the first nine analyses are much more affected from the frequency range. The results will also be compared with the initial estimations according to the DER method to understand the effect of each parameter.

With the increase in mass, it is expected to obtain lower acceleration responses for constant train spectrum values. As can be seen from Table 5.8, the acceleration responses decrease with the increase in mass for the analysis 10, 11 and 12 for all of which the critical train is HSLM A3 and the aggressivity is same. However, the displacement responses are same as 0.73 cm. This is due to the fact that the displacement values are affected from the stiffness, bridge influence line and dynamic signature of train, mass and frequency together. The first three parameters are same for the analyses 10, 11 and 12. The displacement is inversely proportional to mass and frequency. It is expected to have less displacement with the increasing mass value. However, the frequency is decreasing with the increase in mass. Therefore, the total response is balanced and the displacement values are same for the three analysis.

For analyses 13, 14 and 15, it can be seen that the acceleration response decrease with the increase in mass for analysis 13 and 14. However, the acceleration value of analysis 15 is higher than analysis 13 and 14 although the mass is more than others. This is due to the change of the critical train and the value of the train excitation correspondingly. The critical train for analysis 15 is HSLM A2 when it is HSLM A10 for the other two analyses. In order to understand the effect of train excitation in the response of the bridge, the critical wavelength values together with

the aggressivity as explained in DER method in Section 2 is presented in the table shown below;

Table 5.9 Aggressivity values for the analysis

ANALYSIS NO	PARAMETERS		Critical Train	d (m)	n ₀	V (m/s)	λ _c (m)	AxG
	EI (kNm ²)	m (t/m)						
10	504780000	25	HSLMA3	20	4.411	88.23	20.00	83.897
11	504780000	35	HSLMA3	20	3.728	74.56	20.00	83.897
12	504780000	45	HSLMA3	20	3.288	65.80	20.01	83.897
13	1261950000	25	HSLMA10	27	6.975	94.16	13.50	31.2
14	1261950000	35	HSLMA10	27	5.895	79.58	13.50	31.2
15	1261950000	45	HSLMA2	19	5.199	97.22	18.70	60
16	1499196630	25	HSLMA9	26	7.603	97.22	12.79	22.8
17	1499196630	35	HSLMA10	27	6.425	86.74	13.50	31.2
18	1499196630	45	HSLMA10	27	5.667	76.55	13.51	31.2
19	2089789200	25	HSLMA3	20	8.976	89.76	10.00	18.91
20	2089789200	35	HSLMA9	26	7.586	97.22	12.82	23
21	2089789200	45	HSLMA10	27	6.690	90.32	13.50	31.2

As can be seen from the Table 5.9 above, the aggressivity value for analysis 15 is 60 when it is 31.2 for the analysis 13 and 14. Therefore, the response obtained in analysis 15 is larger than the responses from analyses 13 and 14.

It can be seen from Table 5.8 that the acceleration responses of analyses 14 and 17 are the same although the stiffness values are different. The mass for each analysis is 35 t/m and aggressivity is 31.2. Same situation is also valid between analyses 18 and 21. Therefore, it can be concluded that the acceleration does not mainly depend on the stiffness for high stiffness values. The acceleration responses are same for the bridges with same aggressivity and mass values after a stiffness limit that lead to natural frequencies of the bridge to be shifted from the frequencies that are induced by train.

From the displacement point of view, it can be seen from table 5.8 and 5.9, the displacement values change according to the stiffness for same mass and aggressivity. The displacement response decrease with the increase in stiffness as expected.

5.7.3 Comparison of Results with Initial Estimations by DER Method

In this part, the results obtained from the analyses will be compared with the initial estimations found by using decomposing the excitation at resonance method. The responses of the bridge at resonance can be estimated by initial input parameters such as mass and aggressivity. Given the stiffness and mass of the bridge, we can determine the aggressivity by using equation (2.24) and (2.26) presented in Section 2. After the determination of aggressivity, the initial estimation for the acceleration value can be made by using equation (2.23) as explained in Section 2.

Table 5.10 Comparison of analysis results with DER method

ANALYSIS NO	ANALYSIS PARAMETERS		a(m/s ²)	V (m/s)	λ_c (m)	AxG	4/m π	Acceleration DER method a _{der}
	EI (kNm ²)	m (t/m)						
10	504780000	25	4.14	88.23	20.00	83.897	0.051	4.27
11	504780000	35	2.97	74.56	20.00	83.897	0.036	3.05
12	504780000	45	2.31	65.80	20.01	83.897	0.028	2.37
13	1261950000	25	1.56	94.16	13.50	31.2	0.051	1.59
14	1261950000	35	1.13	79.58	13.50	31.2	0.036	1.14
15	1261950000	45	1.71	97.22	18.70	60	0.028	1.70
16	1499196630	25	1.1	97.22	12.79	22.8	0.051	1.16
17	1499196630	35	1.12	86.74	13.50	31.2	0.036	1.14
18	1499196630	45	0.87	76.55	13.51	31.2	0.028	0.88
19	2089789200	25	1	89.76	10.00	18.91	0.051	0.96
20	2089789200	35	0.83	97.22	12.82	23	0.036	0.84
21	2089789200	45	0.87	90.32	13.50	31.2	0.028	0.88

As can be seen from Table 5.10, the dynamic response of the bridge can be predicted in sufficient accuracy by DER method. Therefore, it can be concluded that the DER method can be used for the prediction of the dynamic response before performing detailed analysis for the cases where the peak responses are obtained at resonance conditions. The limitations of the DER method, which were explained in Chapter 2, shall also be considered.

5.7.4 Comparison of Results with a Real Train, French TGV

The analyses are also performed for the French TGV train and the levels of safety of the HSLM trains are obtained. The axle arrangement for French TGV train is shown in Figure 2.11 and the properties of the train are presented in Figure 2.14. The critical speeds for French TGV train are determined as explained in Section 5.4. The critical speeds used in the related analysis for French TGV train is shown in the Table 5.11 below. Analysis are performed for all possible critical speeds and peak responses found from analysis are presented in the Table 5.12 below together with the peak responses from HSLM trains obtained for same analysis.

Table 5.11 Comparison of analysis results HSLM and TGV trains

NO	ANALYSIS PARAMETERS		Critical train	V (HSLM) (m/s)	Acc. (HSLM)	V (TGV) (m/s)	Acc. (TGV)	Diff. %
	EI (kNm ²)	m (t/m)			a(m/s ²)		a(m/s ²)	
1	5047800	25	HSLMA3	79.40	28	74.24	17.2	63%
2	5047800	35	HSLMA3	67.10	20.25	62.74	12.3	65%
3	5047800	45	HSLMA3	59.18	15.74	55.33	9.6	64%
4	25239000	25	HSLMA3	88.78	5.4	73.78	3.1	74%
5	25239000	35	HSLMA3	75.03	3.9	62.36	2.2	77%
6	25239000	45	HSLMA3	66.17	3.05	97.22	1.69	80%
7	100955600	25	HSLMA3	40.00	3.65	97.22	1.86	96%
8	100955600	35	HSLMA3	97.22	1.45	93.54	1.09	33%
9	100955600	45	HSLMA3	88.23	1.52	97.22	1.11	37%

Table 5.11 Comparison of analysis results HSLM and TGV trains Cont'd

NO	ANALYSIS PARAMETERS		Critical train	V (HSLM) (m/s)	Acc. (HSLM)	V (TGV) (m/s)	Acc. (TGV)	Diff. %
	EI (kNm ²)	m (t/m)			a(m/s ²)		a(m/s ²)	
10	504780000	25	HSLMA3	88.23	4.14	82.49	2.73	52%
11	504780000	35	HSLMA3	74.56	2.97	69.72	1.95	52%
12	504780000	45	HSLMA3	65.80	2.31	61.50	1.52	52%
13	1261950000	25	HSLMA10	94.16	1.56	65.22	0.383	300%
14	1261950000	35	HSLMA10	79.58	1.13	55.12	0.28	300%
15	1261950000	45	HSLMA2	97.22	1.71	97.22	1.52	13%
16	1499196630	25	HSLMA9	97.22	1.1	71.10	0.384	186%
17	1499196630	35	HSLMA10	86.74	1.12	60.10	0.275	300%
18	1499196630	45	HSLMA10	76.55	0.87	97.22	0.257	239%
19	2089789200	25	HSLMA3	89.76	1	83.93	0.375	167%
20	2089789200	35	HSLMA9	97.22	0.83	70.93	0.275	202%
21	2089789200	45	HSLMA10	90.32	0.87	62.55	0.213	308%

As can be seen from Table 5.11, HSLM trains give conservative solutions for all of the cases. The degree of conservativity changes for the analyses performed. If the properties of critical HSLM train and TGV train are different, HSLM trains give higher responses and are in the safe side. However, as can be seen in Table 5.11 for analysis 15, the acceleration response of the HSLM train is only 13% larger than the response of TGV train. This is mainly due to that characteristic properties of HSLM A2 train and TGV train is close to each other. Therefore, it can be concluded that more optimum design can be performed by using the real train to be operated for the railway line for some cases. However, Eurocode does not lead more conservative design for the cases where the real train and HSLM train properties match with each other.

CHAPTER 6

CONCLUSIONS

6.1 Summary

The high-speed railway lines became popular all around the world. With the introduction of the high-speed railway lines, the new considerations for the design of bridges were also introduced. A lot of researches have been conducted throughout the history and analytical approaches were developed about the subject in order to define the critical parameters that effect the dynamic response of the bridges under the passage of the moving traffic.

In this thesis study, the analytical approach developed by Fryba for the simple beam subjected to series of moving load and the corresponding presentation of the method by Y.B. Yang, J.D. Yau, Y.S. Wu was used. Analytical methods are widely used in different studies and two examples in which the analytical approach is used were explained in this study. The necessary comparisons were provided with these studies and the comformation of the process was done. Also, a case study was performed by chosing a bridge from Ankara-Sivas high-speed railway project and the design procedure that is suggested by Eurocode was clearly defined. The same bridge was also analysed by analytical approach and the obtained results were compared with the finite element method. It was concluded that the analytical method can be used with the limitations stated below;

- Vehicle-structure interaction including mass of train and inertial effects of bogies is neglected.
- Load distribution by the ballast and sleepers is neglected.
- Effect of torsional mode is neglected since the analytical approach is based on a Euler-Bernoulli beam and only the bending modes are considered.
- Excitation due to the track irregularities is neglected.

The train determination procedure that is defined by Eurocode was also investigated and the bridge in the scope of Ankara-Sivas high-speed railway project was analysed for all HSLM trains at 5 m/s speed range. It was concluded that the DER method is used for the determination of critical train in Eurocode and the critical trains determined by Eurocode can be used for the analysis of high-speed railway bridges.

DER method which is based on the decomposition of excitation at resonance was also explained in this thesis study and necessary comparisons were provided for 12 analysis performed in Chapter 5. It was concluded that this method can be used for initial predictions for the dynamic responses of the bridges given the mass and aggressivity of the bridge. However, it is important that the maximum peak response is to be obtained at resonance to predict the behaviour correctly. And also the limitations for DER method which are listed in Chapter 2.6 shall be considered.

Mass, stiffness, agressivity and moving speed are the parameters of which the effects on dynamic response were investigated in Chapter 5 of this thesis study. The values obtained were discussed in the related chapter. The obtained conclusions for all parameters are summarized in the parts below.

6.2 Mass of the Bridge

Three different mass values were used for the parametric study and it was found that the response is decreasing with the increase in mass as expected for the cases that the critical train and corresponding aggressivity values are same. In other words, mass is an important parameter for the acceleration responses of the bridges when the dynamic signature of the train is same. The displacement responses are mainly based on stiffness and they are constant for same stiffness and aggressivity values.

6.3 Stiffness of the Bridge

Increasing stiffness of a flexible system helps to reduce excessive accelerations induced by vibration. At a threshold stiffness, additional increase in stiffness do not decrease the accelerations furthermore due to shift of structural critical frequency from the range of frequencies of trains that are induced by axle spacing and speed. The stiffness v.s. acceleration and stiffness v.s. displacement graphs are shown below;

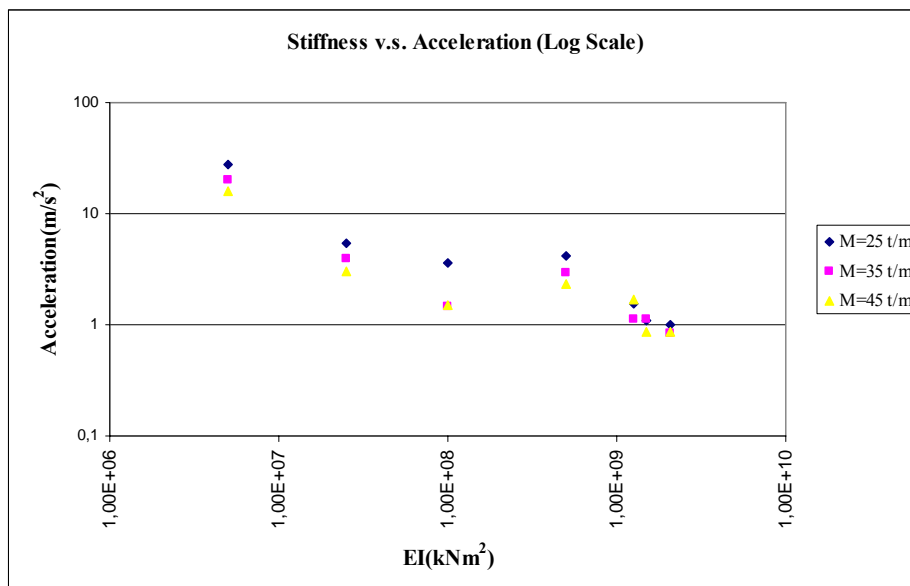


Figure 6.1 Stiffness v.s. Acceleration Graph

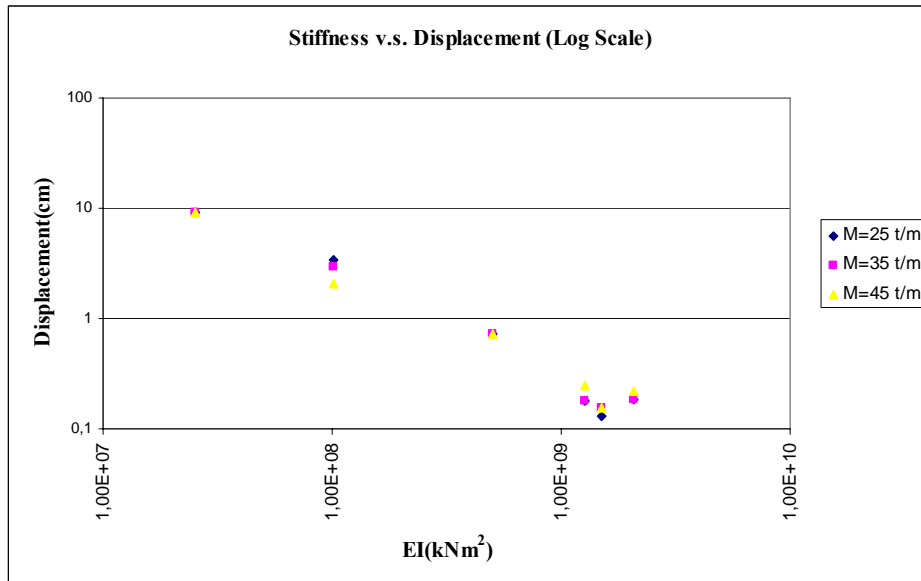


Figure 6.2 Stiffness v.s. Displacement Graph

As can be seen from Figure 6.1, acceleration values are decreasing with the increase in stiffness for low stiffness values. For high stiffness values the change due to stiffness loses its effectivity.

6.4 Aggressivity from the Bridge and Train Properties

Aggressivity is also an important parameter for the dynamic response of the bridge. It is based on the train characteristics together with the bridge properties. Although the change in mass and stiffness for two bridges in such a manner that the responses are decreased or increased with the change in these properties, aggressivity is also an important parameter that can change the behaviour in reverse to the effect of mass and stiffness. Therefore, it is not possible to consider only the influence of bridge characteristics on the dynamic response. The aggressivity value shall also be considered which is obtained by the multiplication of bridge influence line effect and dynamic signature of the train as explained in Chapter 2.

6.5 Critical Speed

As explained before, the maximum responses are required to occur at resonance conditions and resonant speeds correspondingly. However, it can be seen from the results that are obtained from the analysis 1 to 9, there may be some cases where there is a peak modal displacement in the design frequency range for modes higher than first natural bending mode. And this situation leads to obtain peak responses at non-resonant speeds and brings the need for consideration of other modes where the peak modal displacements are obtained. Therefore, it is important to define the modal behaviour of the bridge considered and decide about the critical speed values accordingly.

REFERENCES

Cheng, Y.S. Au, F.T.K, Cheung, Y.K. (2001). "Vibration of railway bridges under a moving train by using bridge-track-vehicle element". *Engineering Structures*, 23(12), 1597-1606.

Clough, R., Penzien, J. (2003). *Dynamic of Structures*, Computers & Structures, Inc, Berkeley.

Delgado, R.M. Cruz, S (1997). "Modelling of railway bridge-vehicle interaction on high speed tracks". *Computers & Structures*, 63(3), 511-523.

EN1990-A2. (2005). "Basis of Structural Design – Annex A2: Applications for bridges (Normative)." Final Version, European Committee for Standardization (CEN), Brussels.

EN1991-2. (2003). "Actions on Structures – Part 2: Traffic loads on bridges." European Committee for Standardization (CEN), Brussels.

EN1992-1-1. (2003). "Design of concrete structures." European Committee for Standardization (CEN), Brussels.

ERRI D214/RP6 Rail Bridges for speeds > 200 km/h - Calculation for bridges with simply-supported beams during the passage of a train, December 1999.

Fryba, L., (1996). *Dynamics of Railway Bridges*, Thomas Telford, Prague.

Fryba, L., (1999). *Vibration of Solids and Structures under Moving Loads*, Thomas Telford, Prague.

Fryba, L., (2001). "A rough assesment of railway bridges for high speed trains." *Engineering Structures*, 23, 548-556.

Goicolea, J., Dominguez, J., Navarro, J., et al. (2002). "New Dynamic Analysis Methods For Railway Bridges In Codes IAPF and Eurocode 1." *Congreso de Puentes de Ferrocarril, Grupo Espanol de IABSE*, Madrid.

K. Liu, G. De Roeck, and G. Lombaert. "The effect of dynamic train-bridge interaction on the bridge response during a train passage". *Journal of Sound and Vibration*, 325(1-2):240-251, 2009.

Lin, C.C., Wang, J.F., Chen, B.L., 2005, "Train-Induced Vibration Control of High Speed Railway Bridges Equipped with Multiple Tuned Mass Dampers", *Civil Engineering*, ASCE

Myung-Kwan Song, Hyuk-Chun Noh, Chang-Koon Choi, "A new three dimensional finite element analysis model of high-speed train-bridge interactions", *Engineering Structures*, Vol. 25, No. 13, November 2003, pp. 1611-1626.

P. Museros, E. Alarcon. "Influence of the second bending mode on the response of high speed railway bridges at resonance". *Journal of Structural Engineering*, Vol. 131, No. 3, March 2005, pp. 405-415.

SAP2000 (v9.0.3). *Integrated software for structural analysis & Design. User's Manual*, http://www.csiberkeley.com/products_SAP.html, September 2009.

Xia, H., De Roeck, G., Zhang, N., et al. (2003a). "Experimental analysis of a high-speed railway bridge under THALYS trains." *Journal of Sound and Vibration*, 268(1), 103-113

Xia, H., Zhang, N., De Roeck, G., (2003b). “Dynamic analysis of high speed railway bridge under articulated trains.” *Computers & Structures*,, 81(26-27), 2467-2478.

Xia, H., Zhang, N., Guo, W.W., (2006). “Analysis of resonance mechanism and conditions of train-bridge system.” *Journal of Sound and Vibration*, 297(3-5), 810-822.

Yang, Y.B., Yau, J.D., Wu, Y. (2004). *Vehicle-Bridge Interaction Dynamics: With Applications to High-Speed Railways*, World Scientific Publishing Co. Pte. Ltd., Singapore

APPENDIX A

CRITICAL WAVELENGTH V.S. DYNAMIC SIGNATURE OF TRAIN GRAPHS

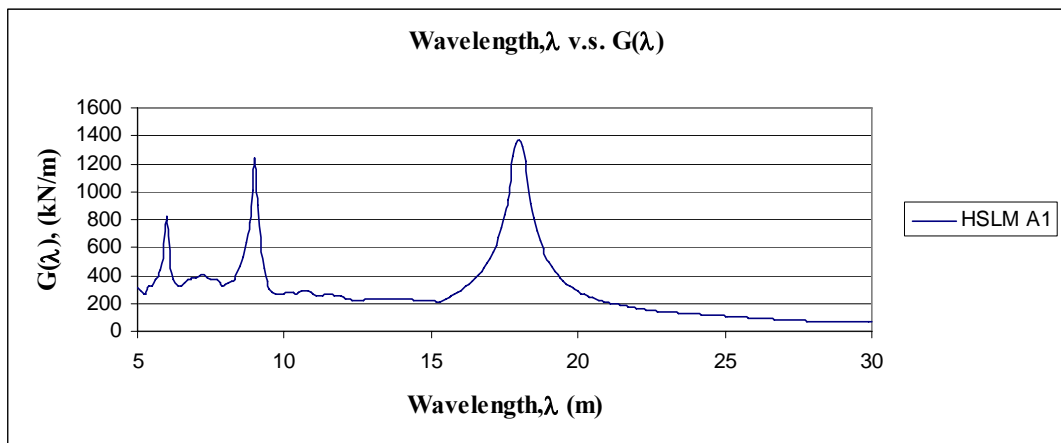


Figure A.1 Wavelength v.s. Dynamic Signature $L=30$ m, $\epsilon=0.01$ (HSLM A1)

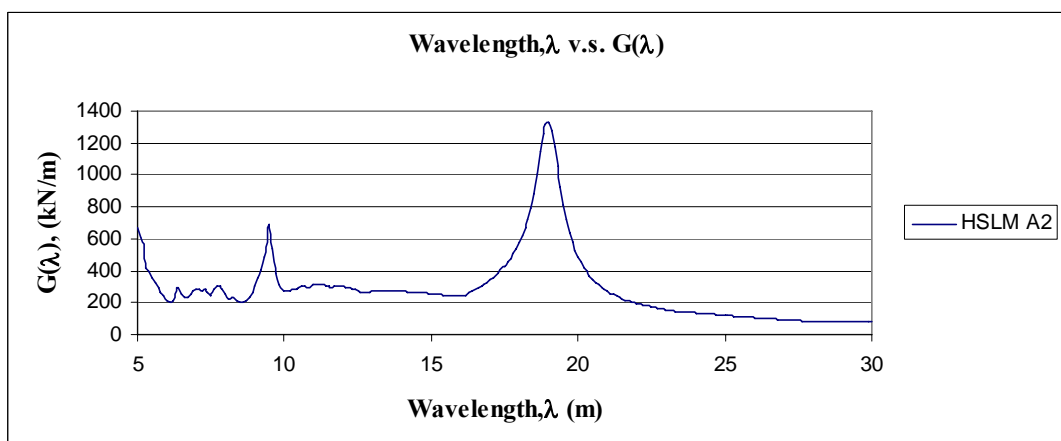


Figure A.2 Wavelength v.s. Dynamic Signature $L=30$ m, $\epsilon=0.01$ (HSLM A2)

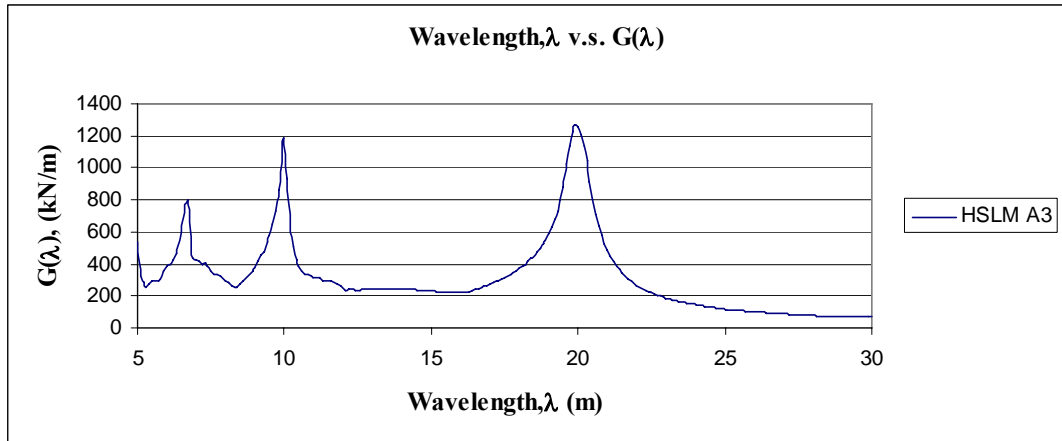


Figure A.3 Wavelength v.s. Dynamic Signature $L=30$ m, $\epsilon=0.01$ (HSLM A3)

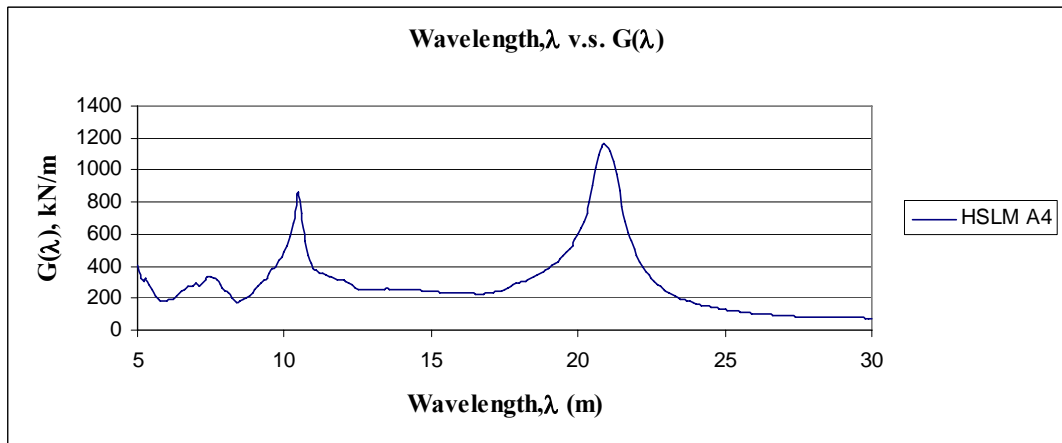


Figure A.4 Wavelength v.s. Dynamic Signature $L=30$ m, $\epsilon=0.01$ (HSLM A4)

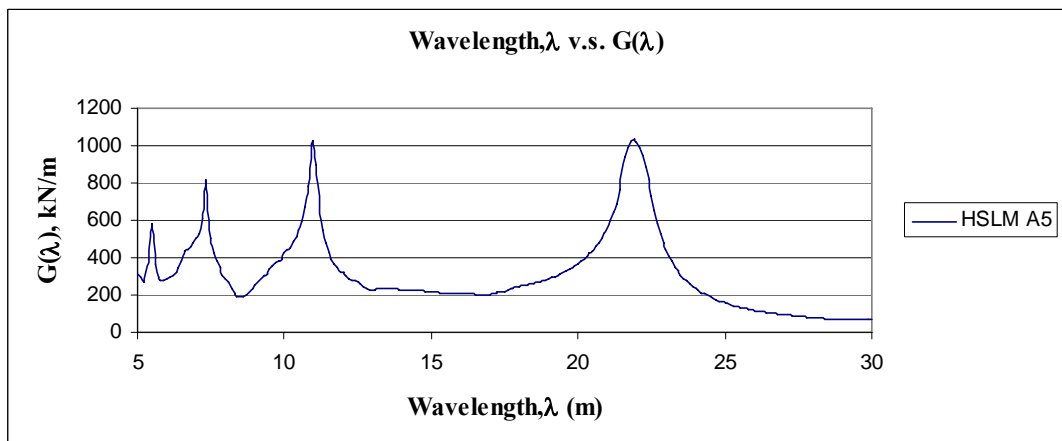


Figure A.5 Wavelength v.s. Dynamic Signature $L=30$ m, $\epsilon=0.01$ (HSLM A5)

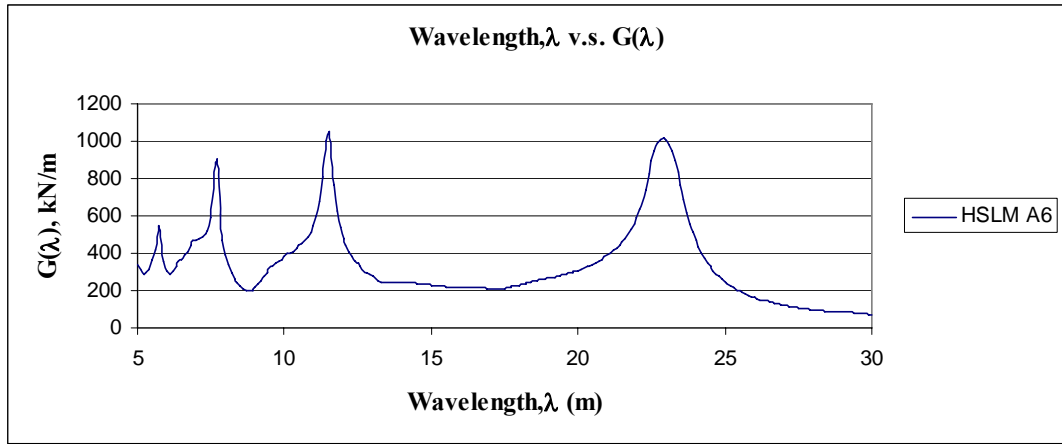


Figure A.6 Wavelength v.s. Dynamic Signature $L=30$ m, $\epsilon=0.01$ (HSLM A6)

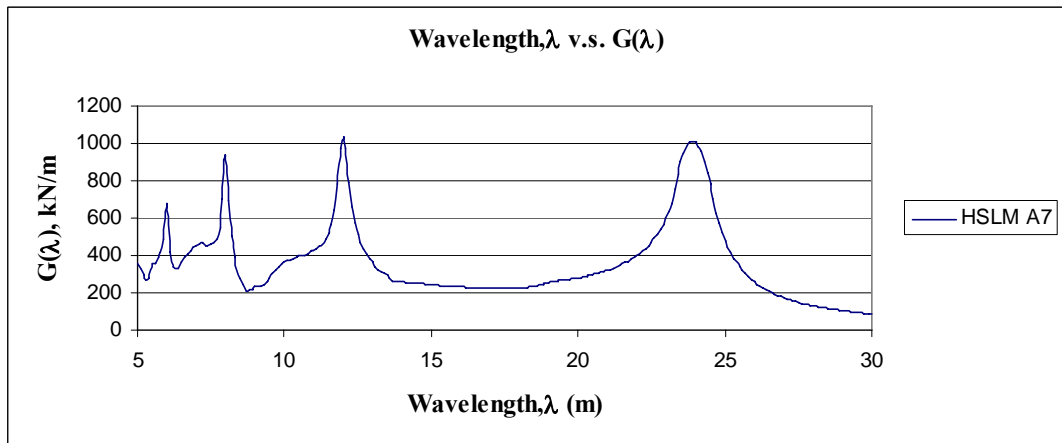


Figure A.7 Wavelength v.s. Dynamic Signature $L=30$ m, $\epsilon=0.01$ (HSLM A7)

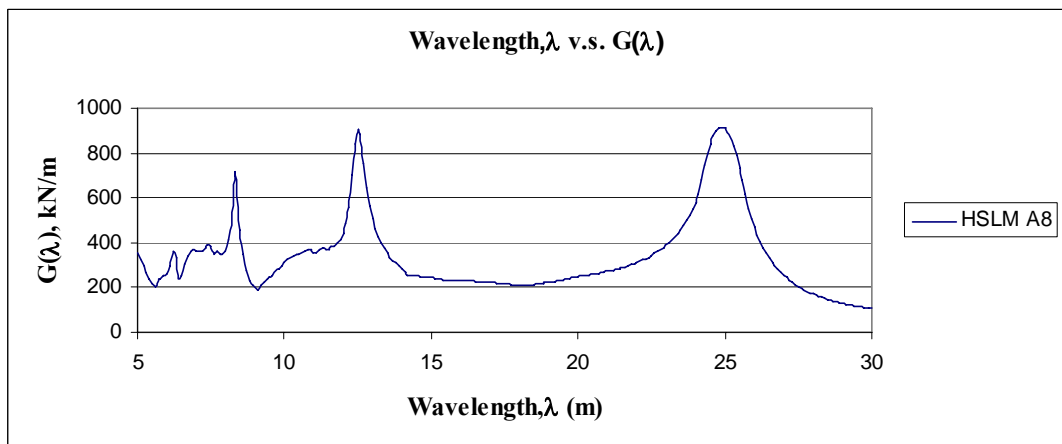


Figure A.8 Wavelength v.s. Dynamic Signature $L=30$ m, $\epsilon=0.01$ (HSLM A8)

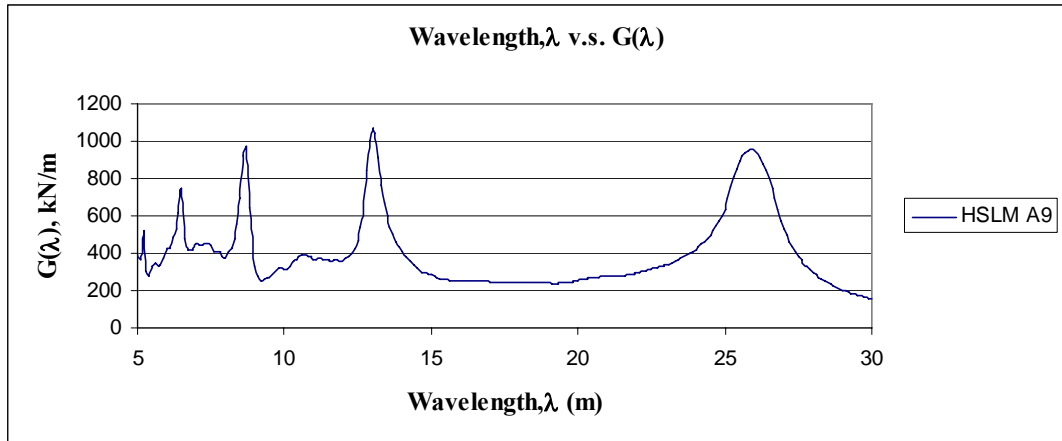


Figure A.9 Wavelength v.s. Dynamic Signature $L=30$ m, $\epsilon=0.01$ (HSLM A9)

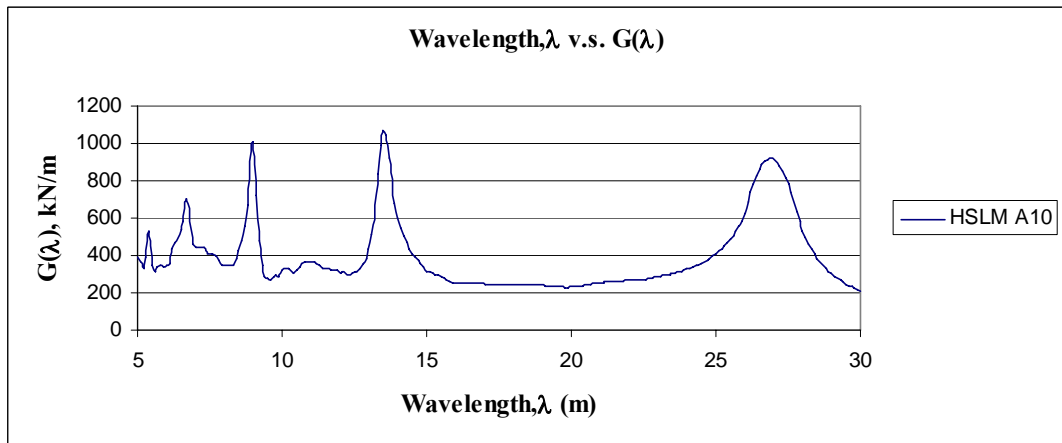


Figure A.10 Wavelength v.s. Dynamic Signature $L=30$ m, $\epsilon=0.01$ (HSLM A10)

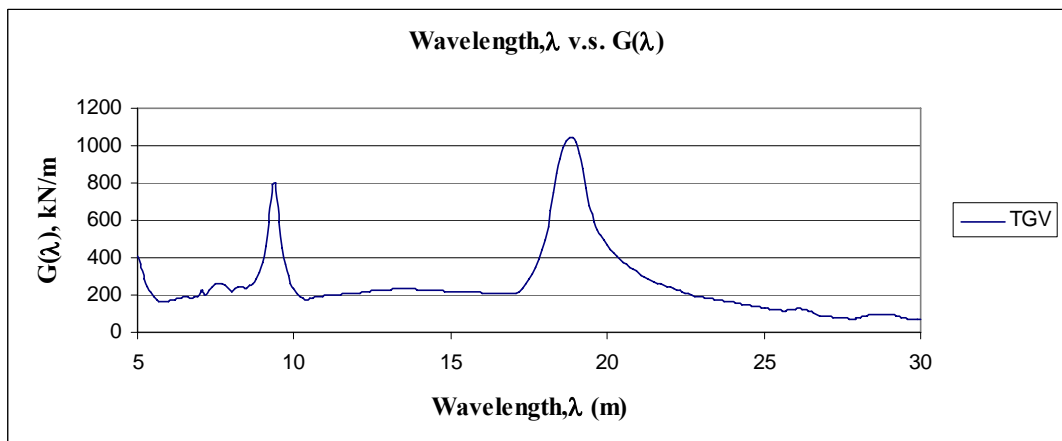


Figure A.11 Wavelength v.s. Dynamic Signature $L=30$ m, $\epsilon=0.01$ (TGV)

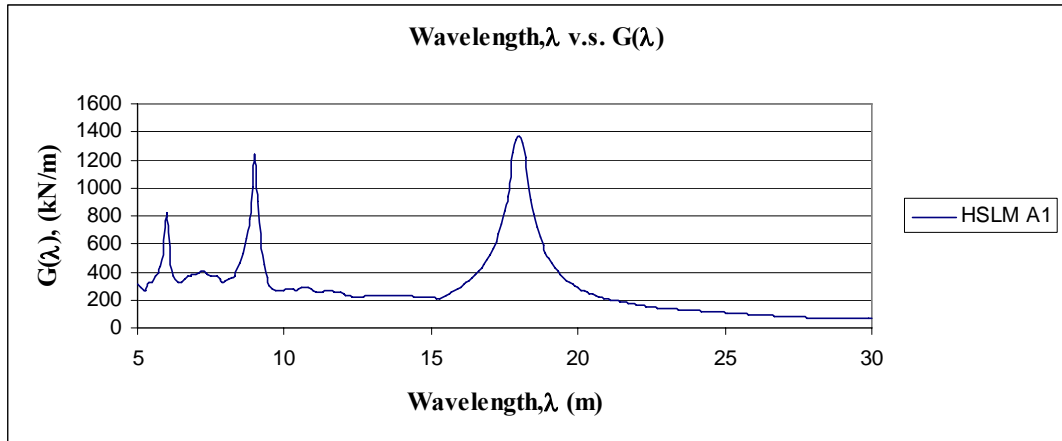


Figure A.12 Wavelength v.s. Dynamic Signature $L=40$ m, $\epsilon=0.01$ (HSLM A1)

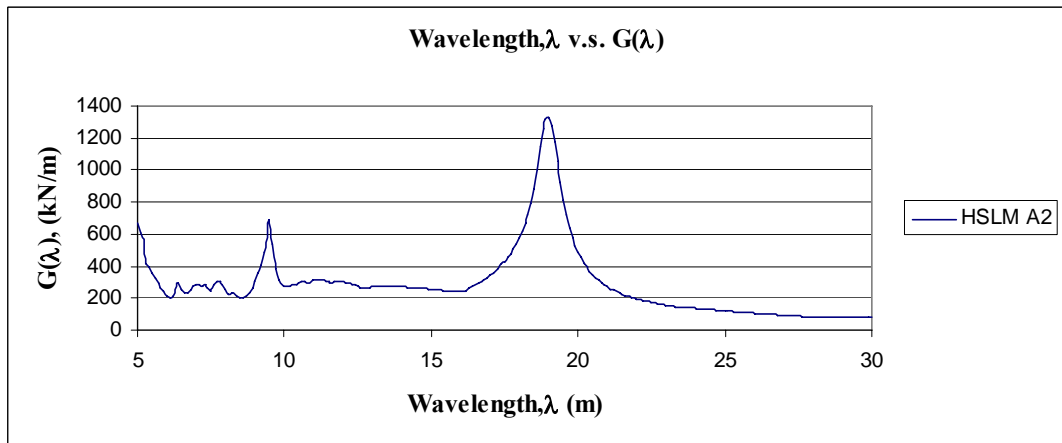


Figure A.13 Wavelength v.s. Dynamic Signature $L=40$ m, $\epsilon=0.01$ (HSLM A2)

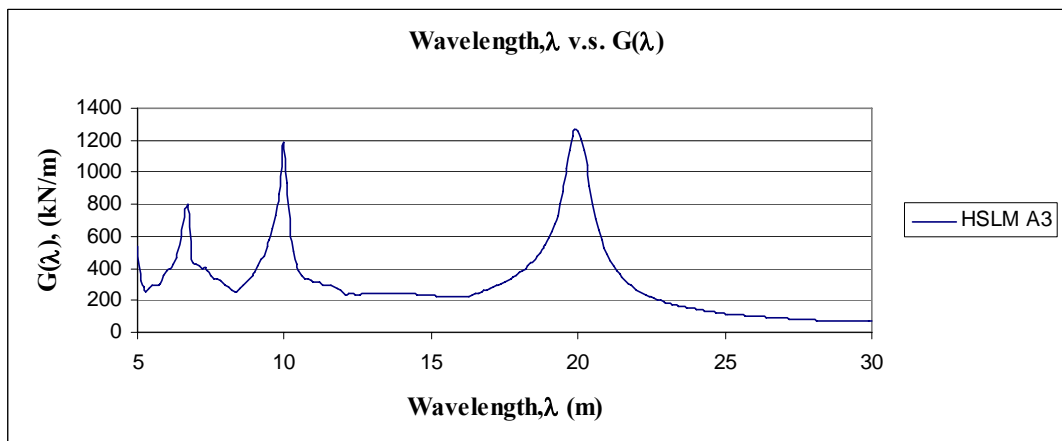


Figure A.14 Wavelength v.s. Dynamic Signature $L=40$ m, $\epsilon=0.01$ (HSLM A3)

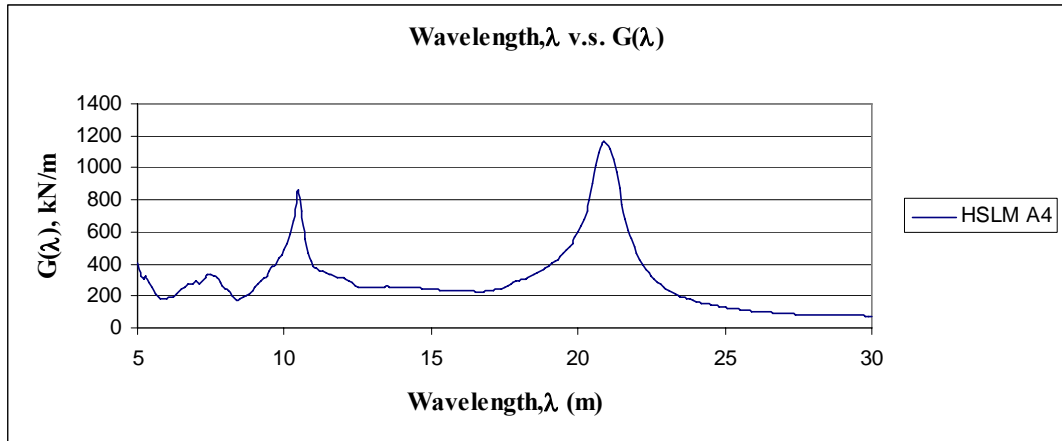


Figure A.15 Wavelength v.s. Dynamic Signature $L=40$ m, $\varepsilon=0.01$ (HSLM A4)

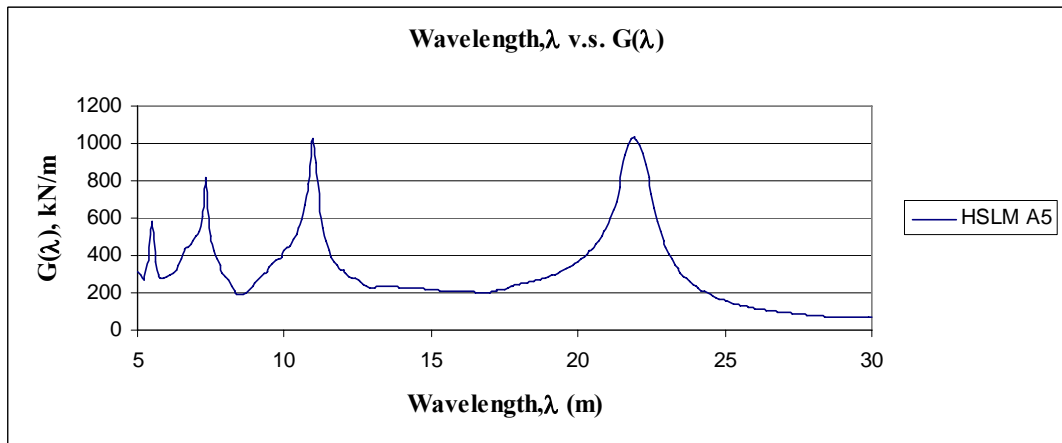


Figure A.16 Wavelength v.s. Dynamic Signature $L=40$ m, $\varepsilon=0.01$ (HSLM A5)

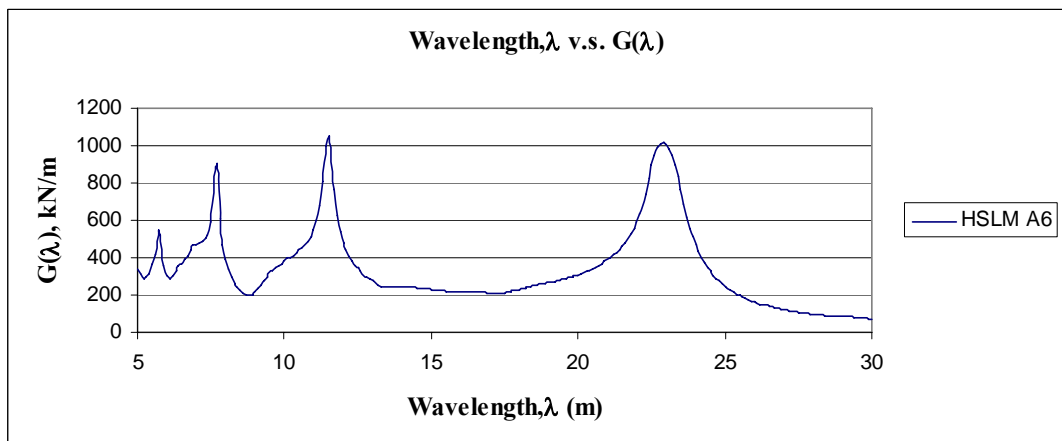


Figure A.17 Wavelength v.s. Dynamic Signature $L=40$ m, $\varepsilon=0.01$ (HSLM A6)

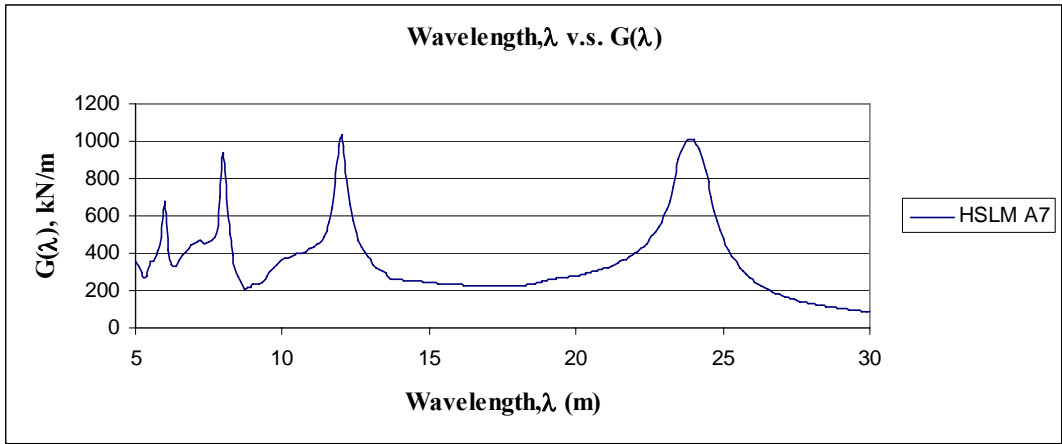


Figure A.18 Wavelength v.s. Dynamic Signature $L=40$ m, $\varepsilon=0.01$ (HSLM A7)

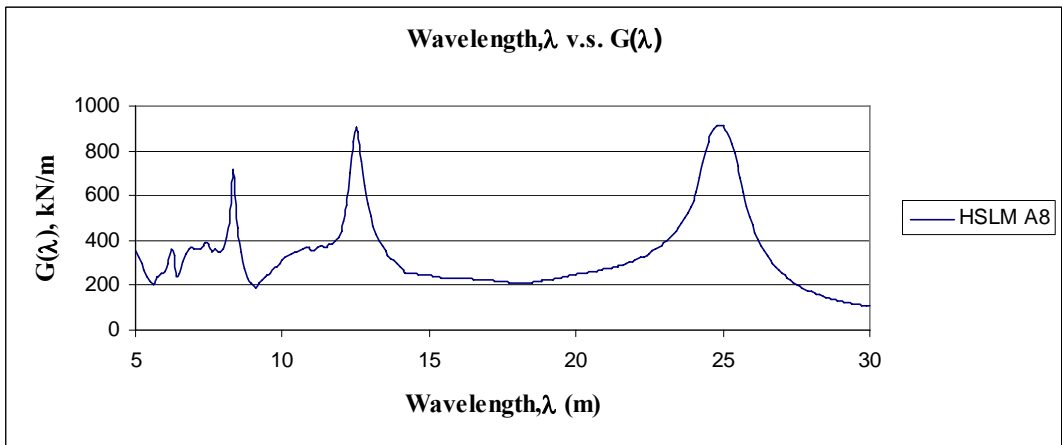


Figure A.19 Wavelength v.s. Dynamic Signature $L=40$ m, $\varepsilon=0.01$ (HSLM A8)

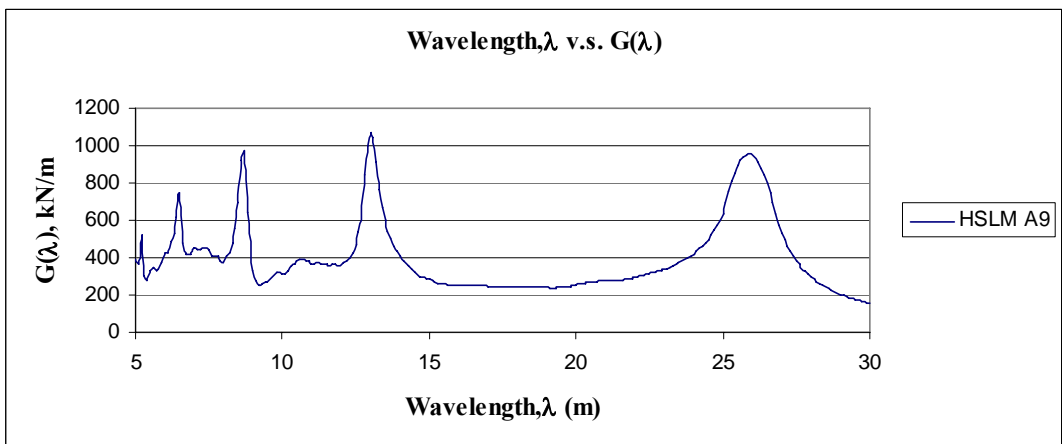


Figure A.20 Wavelength v.s. Dynamic Signature $L=40$ m, $\varepsilon=0.01$ (HSLM A9)

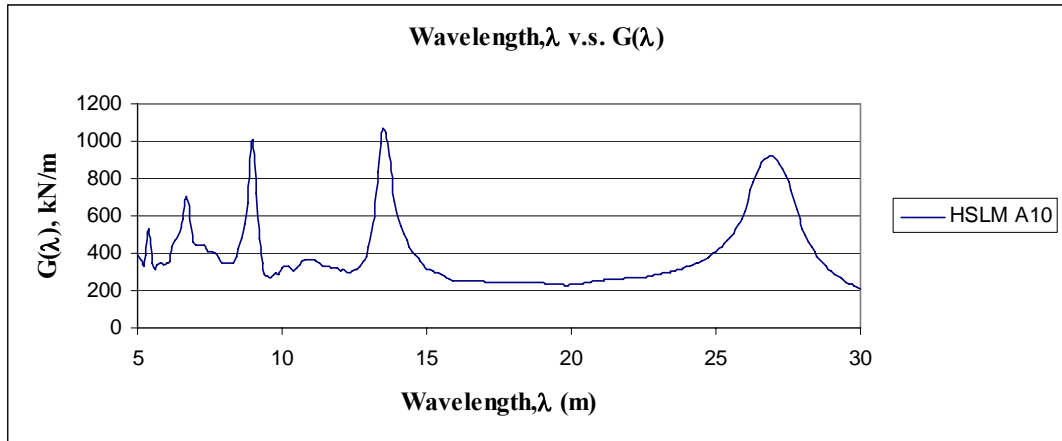


Figure A.21 Wavelength v.s. Dynamic Signature $L=40$ m, $\epsilon=0.01$ (HSLM A10)

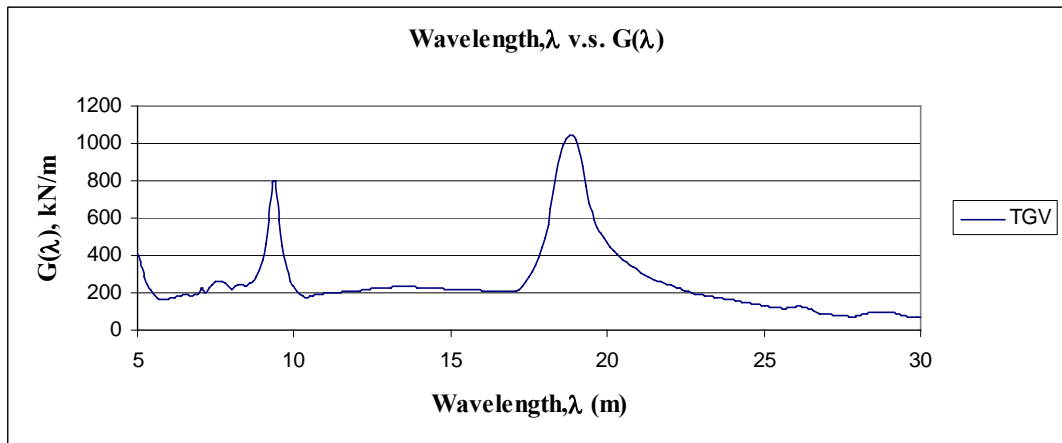


Figure A.22 Wavelength v.s. Dynamic Signature $L=40$ m, $\epsilon=0.01$ (TGV)

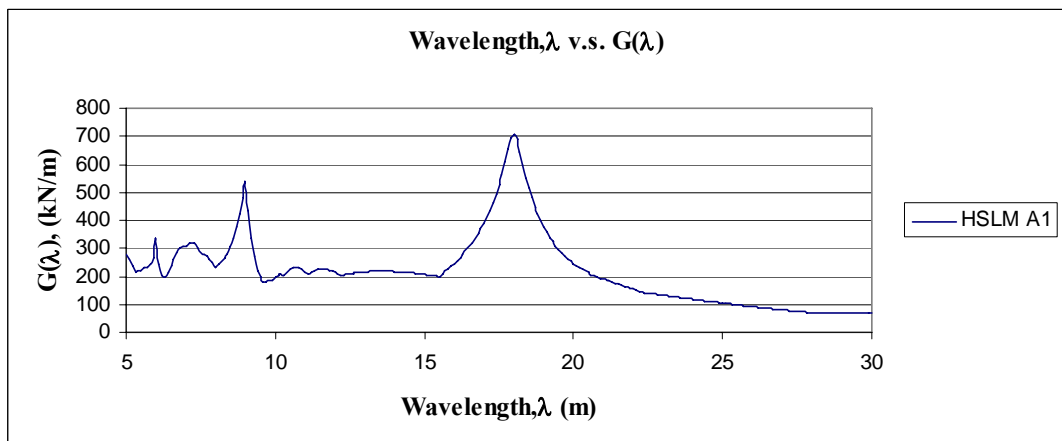


Figure A.23 Wavelength v.s. Dynamic Signature $L=40$ m, $\epsilon=0.025$ (HSLM A1)

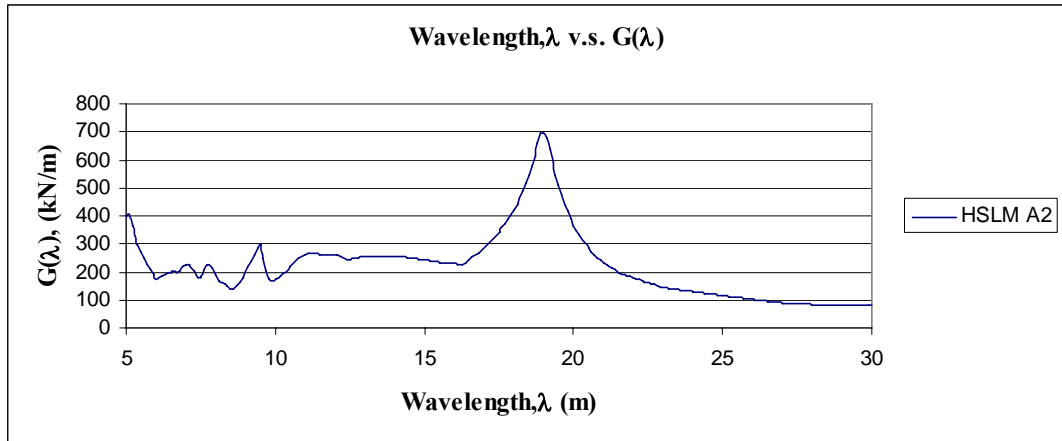


Figure A.24 Wavelength v.s. Dynamic Signature $L=40$ m, $\epsilon=0.025$ (HSLM A2)

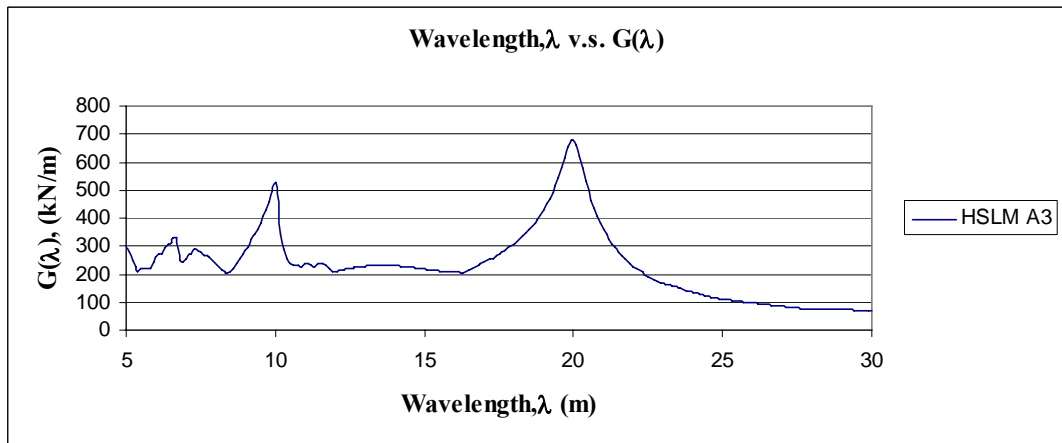


Figure A.25 Wavelength v.s. Dynamic Signature $L=40$ m, $\epsilon=0.025$ (HSLM A3)

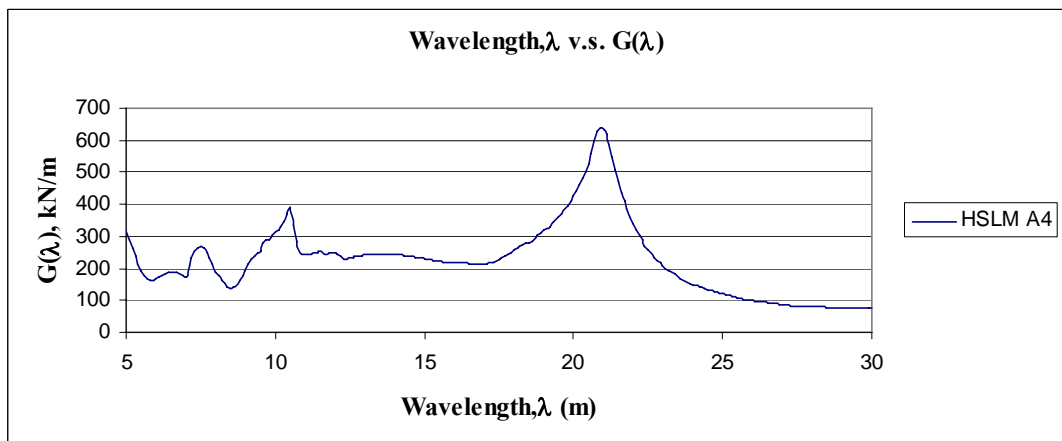


Figure A.26 Wavelength v.s. Dynamic Signature $L=40$ m, $\epsilon=0.025$ (HSLM A4)

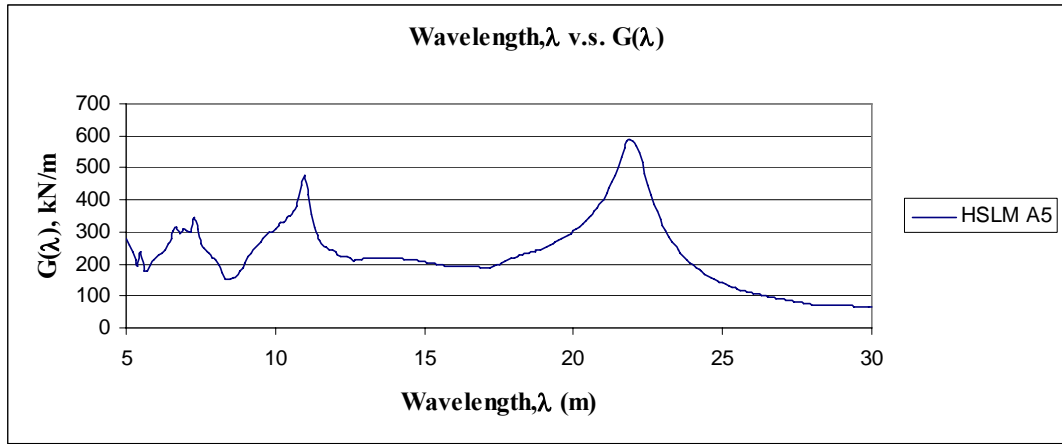


Figure A.27 Wavelength v.s. Dynamic Signature $L=40$ m, $\epsilon=0.025$ (HSLM A5)

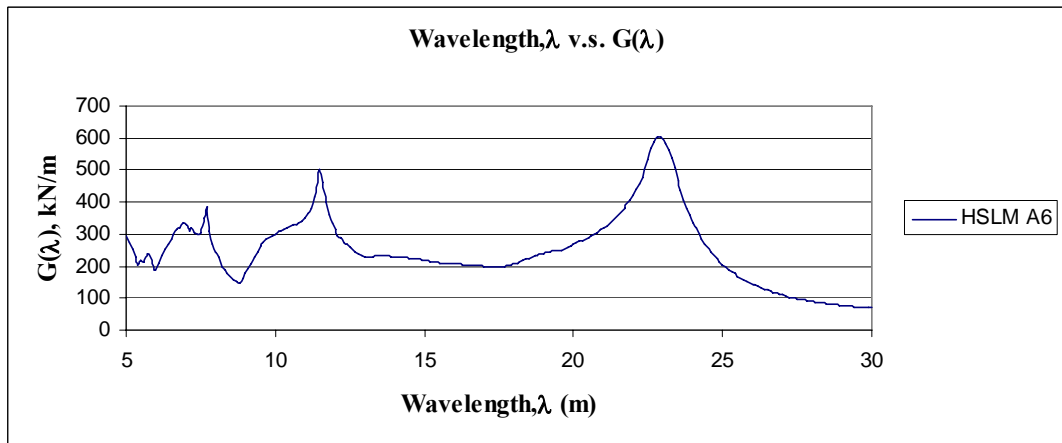


Figure A.28 Wavelength v.s. Dynamic Signature $L=40$ m, $\epsilon=0.025$ (HSLM A6)

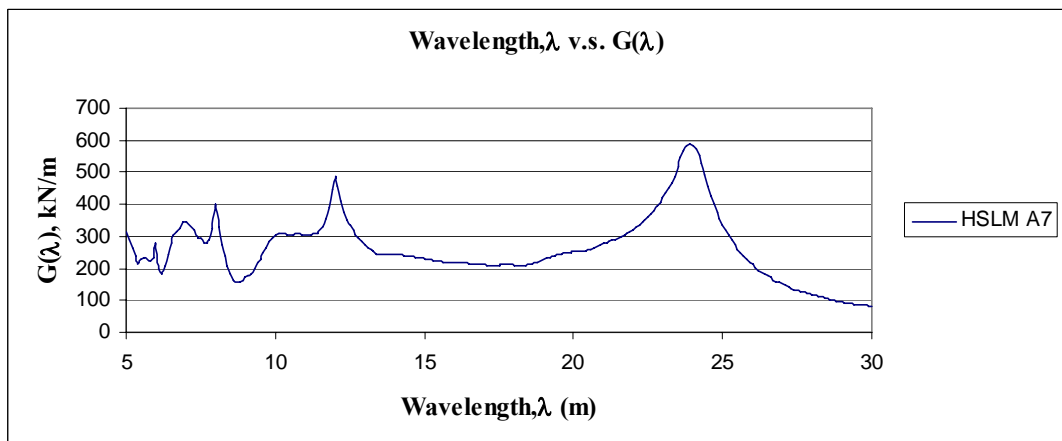


Figure A.29 Wavelength v.s. Dynamic Signature $L=40$ m, $\epsilon=0.025$ (HSLM A7)

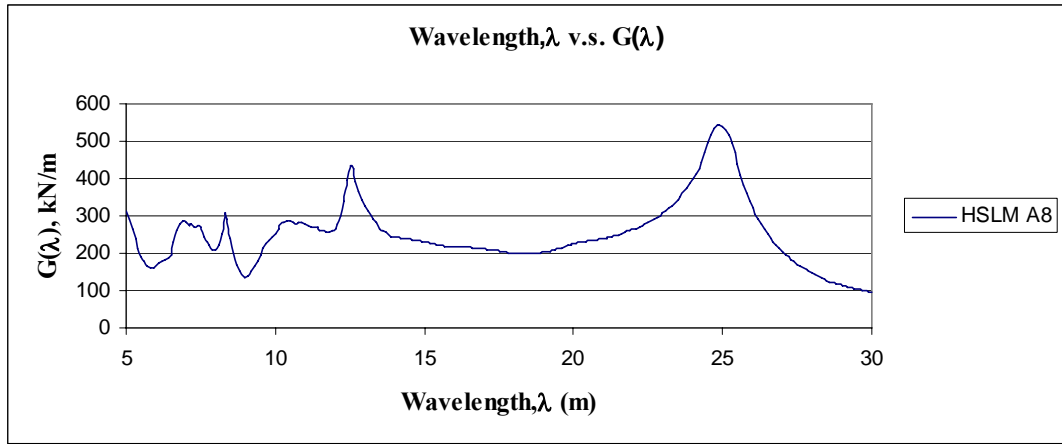


Figure A.30 Wavelength v.s. Dynamic Signature $L=40$ m, $\epsilon=0.025$ (HSLM A8)

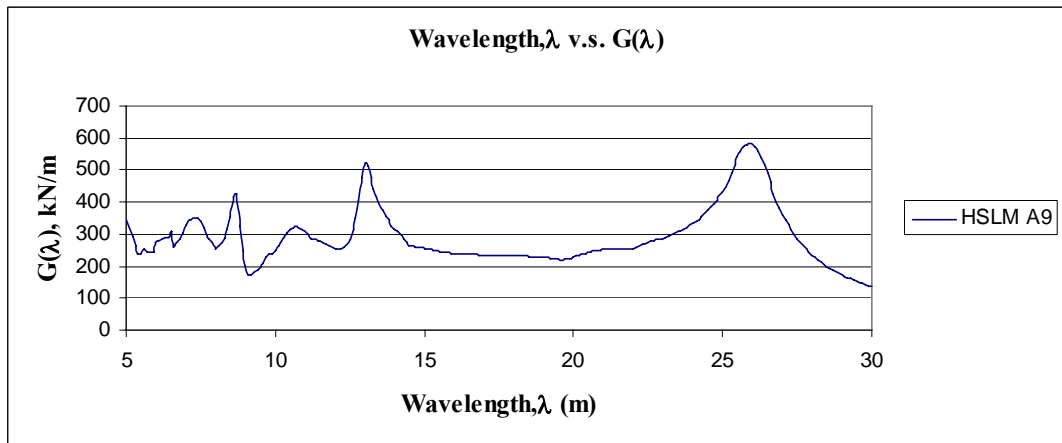


Figure A.31 Wavelength v.s. Dynamic Signature $L=40$ m, $\epsilon=0.025$ (HSLM A9)

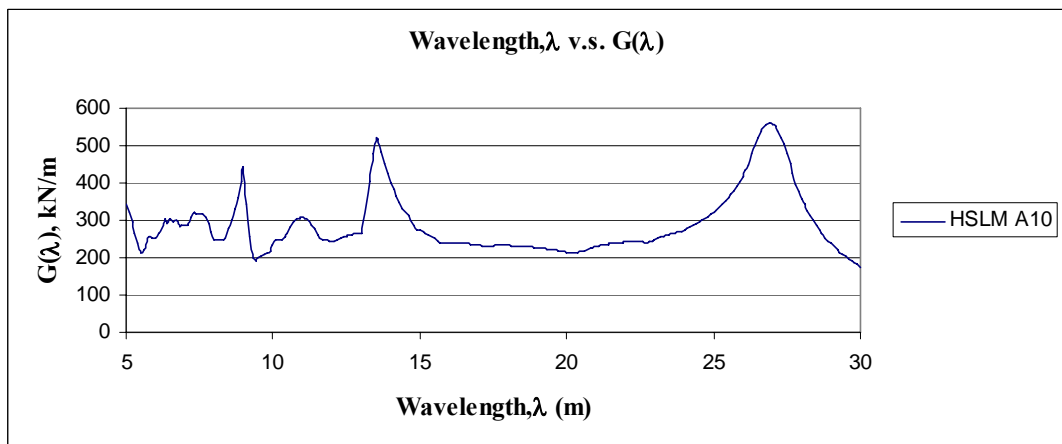


Figure A.32 Wavelength v.s. Dynamic Signature $L=40$ m, $\epsilon=0.025$ (HSLM A10)

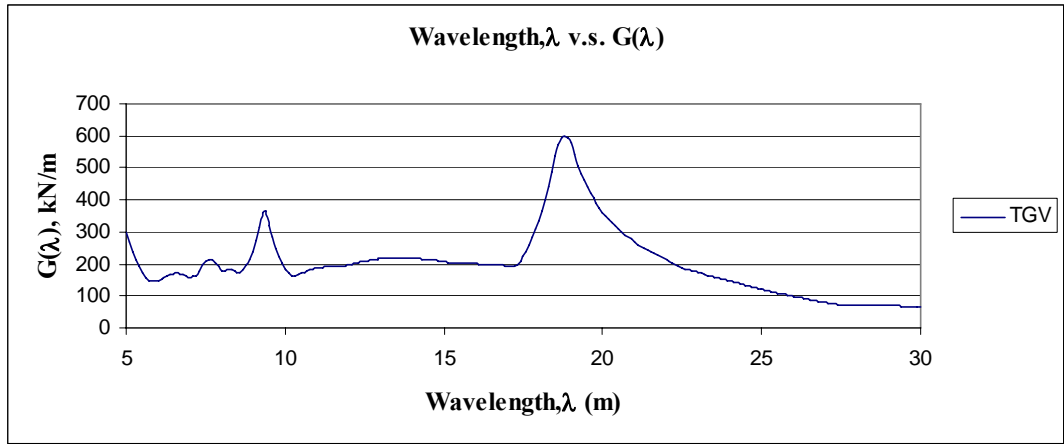


Figure A.33 Wavelength v.s. Dynamic Signature $L=40$ m, $\varepsilon=0.025$ (TGV)

APPENDIX B

DISPLACEMENT V.S. TIME AND ACCELERATION V.S. TIME GRAPHS FOR CASE STUDY

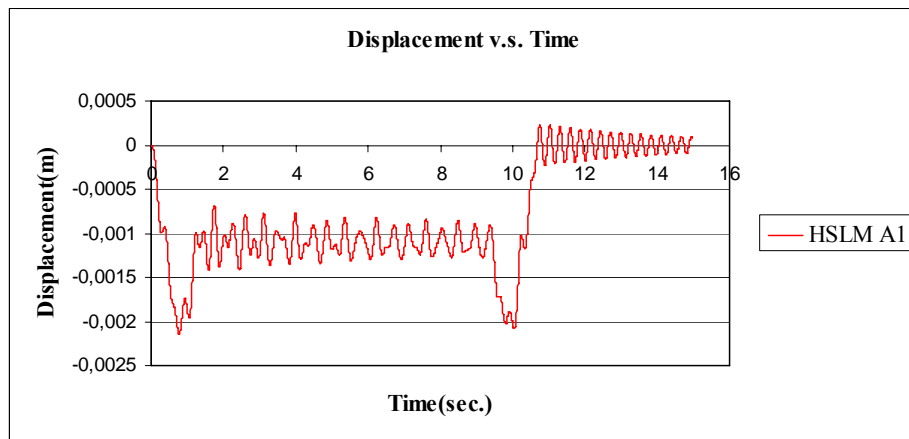


Figure B.1 Displacement v.s. Time graph $V = 40$ m/s, for HSLM A1

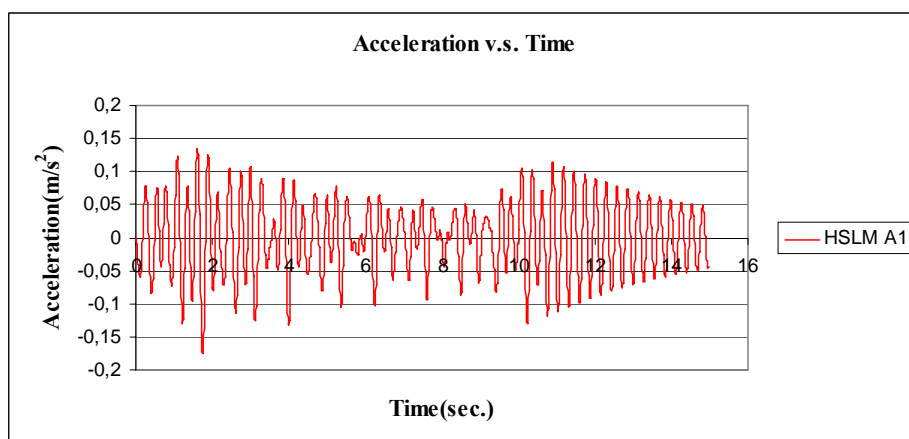


Figure B.2 Acceleration v.s. Time graph $V = 40$ m/s, for HSLM A1

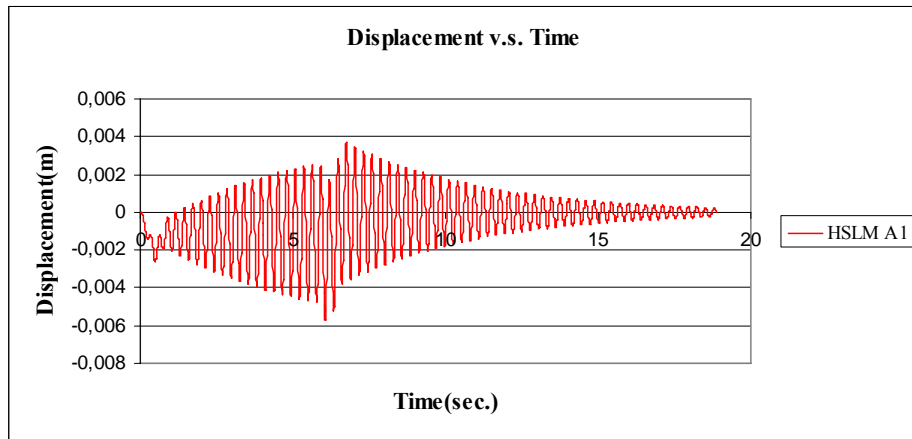


Figure B.3 Displacement v.s. Time graph $V = 64.26$ m/s, for HSLM A1

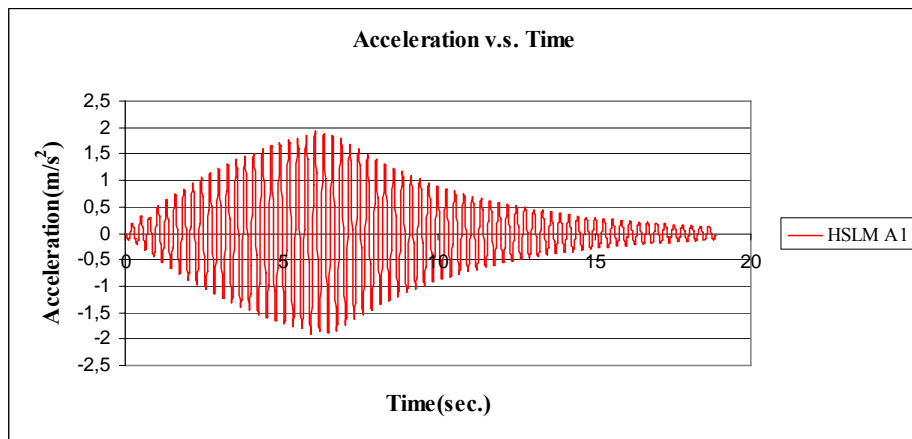


Figure B.4 Acceleration v.s. Time graph $V = 64.26$ m/s, for HSLM A1

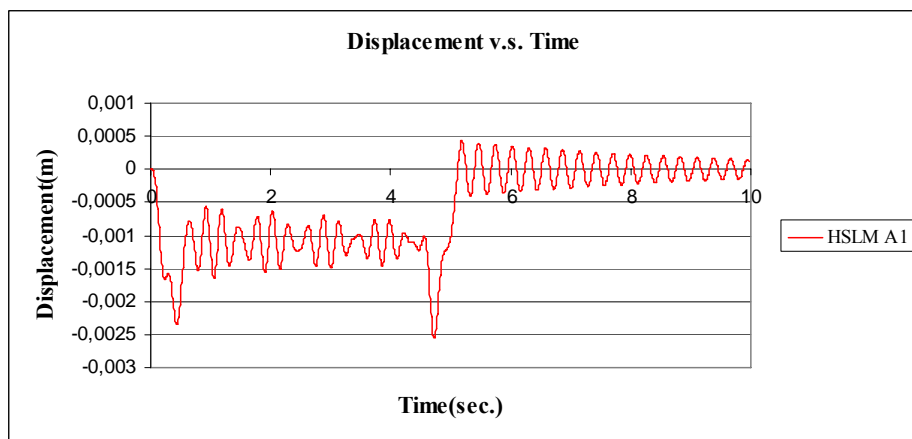


Figure B.5 Displacement v.s. Time graph $V = 83.33$ m/s, for HSLM A1

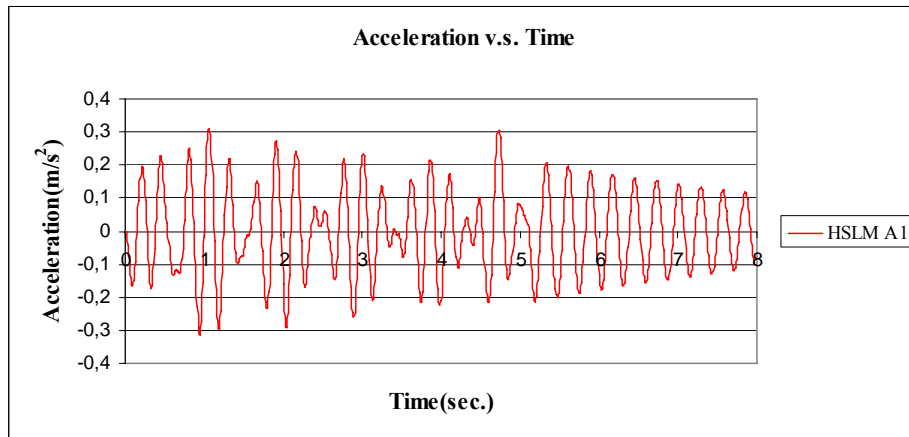


Figure B.6 Acceleration v.s. Time graph $V = 83.33 \text{ m/s}$, for HSLM A1

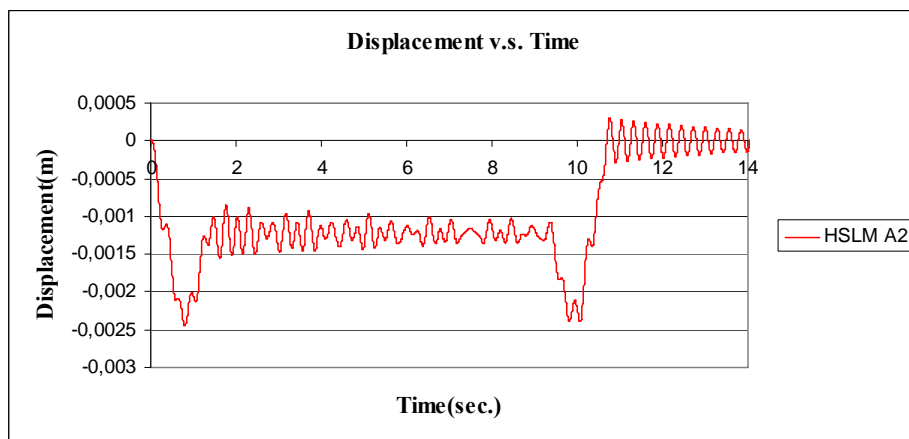


Figure B.7 Displacement v.s. Time graph $V = 40 \text{ m/s}$, for HSLM A2

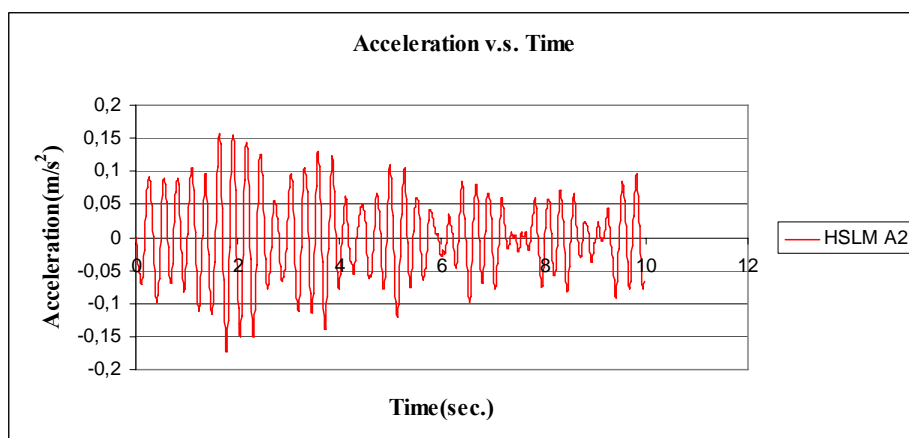


Figure B.8 Acceleration v.s. Time graph $V = 40 \text{ m/s}$, for HSLM A2

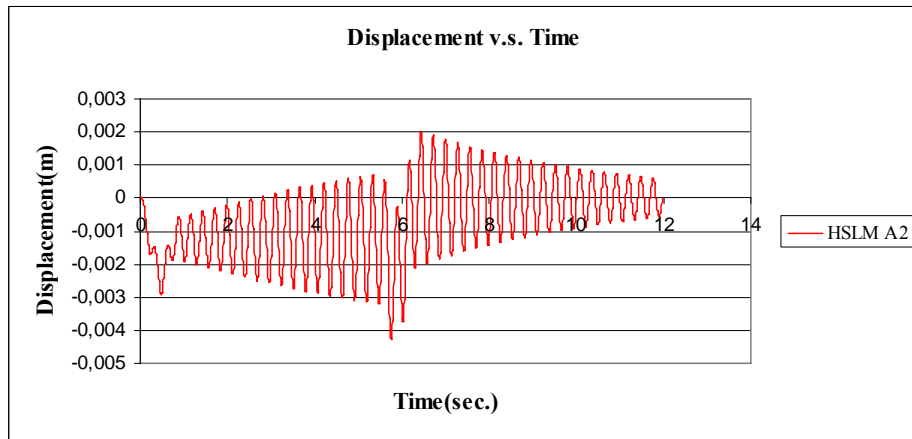


Figure B.9 Displacement v.s. Time graph $V = 67.83$ m/s, for HSLM A2

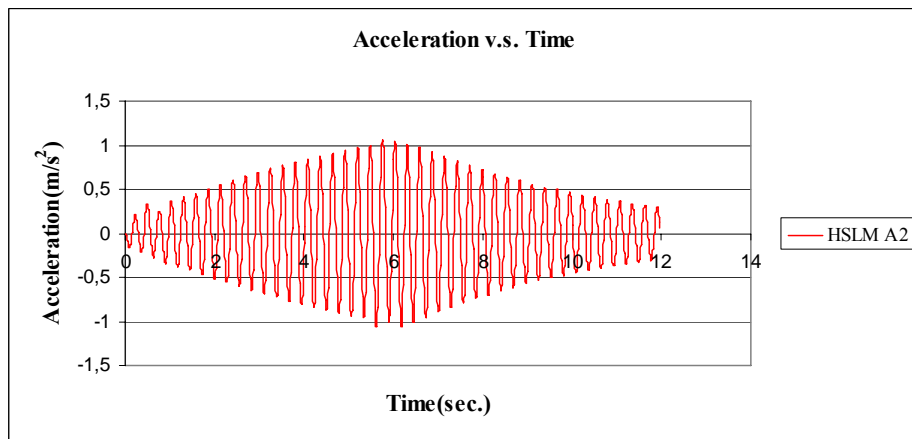


Figure B.10 Acceleration v.s. Time graph $V = 67.83$ m/s, for HSLM A2

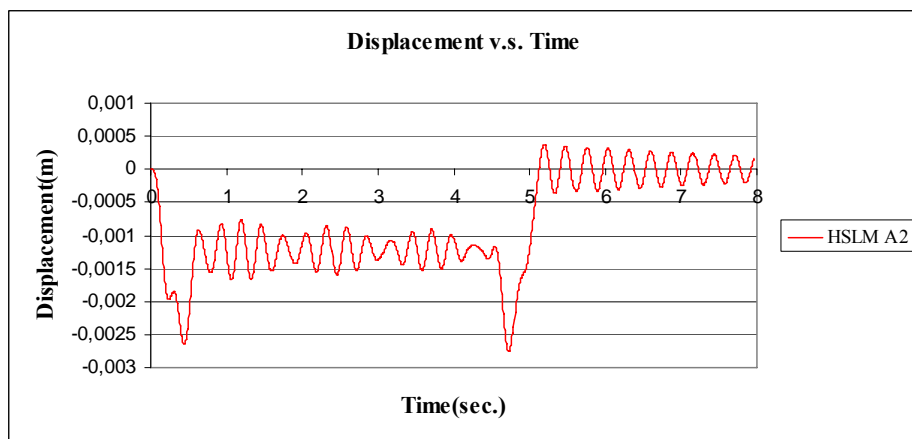


Figure B.11 Displacement v.s. Time graph $V = 83.33$ m/s, for HSLM A2

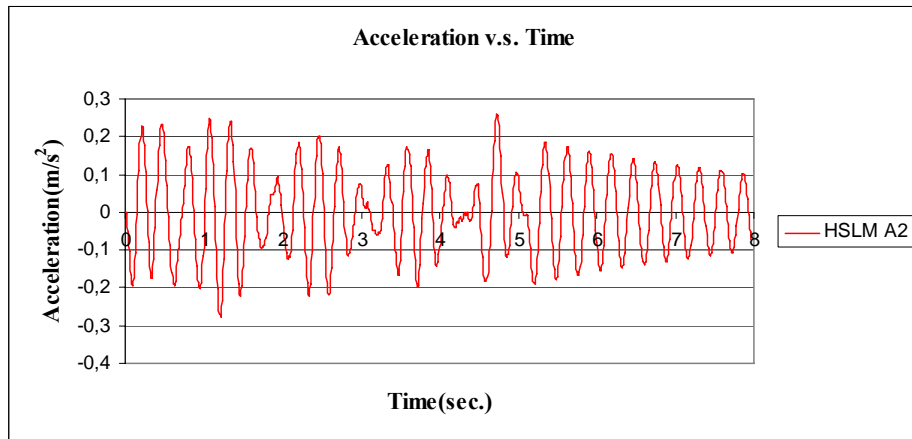


Figure B.12 Acceleration v.s. Time graph $V = 83.33$ m/s, for HSLM A2

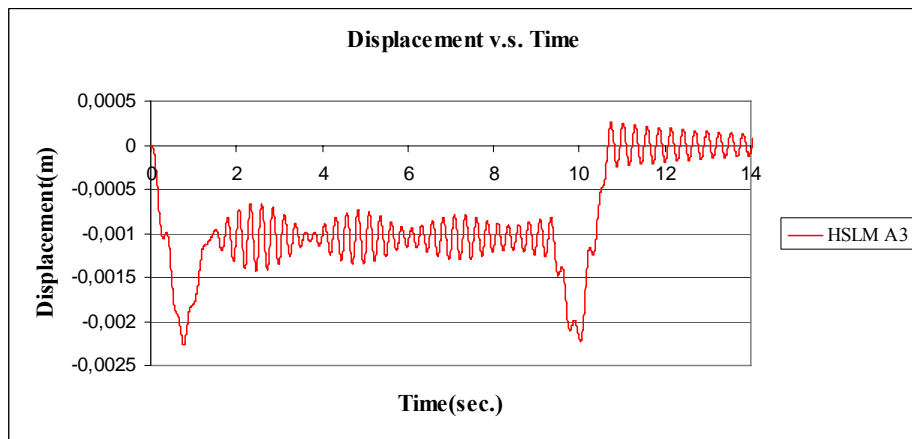


Figure B.13 Displacement v.s. Time graph $V = 40$ m/s, for HSLM A3

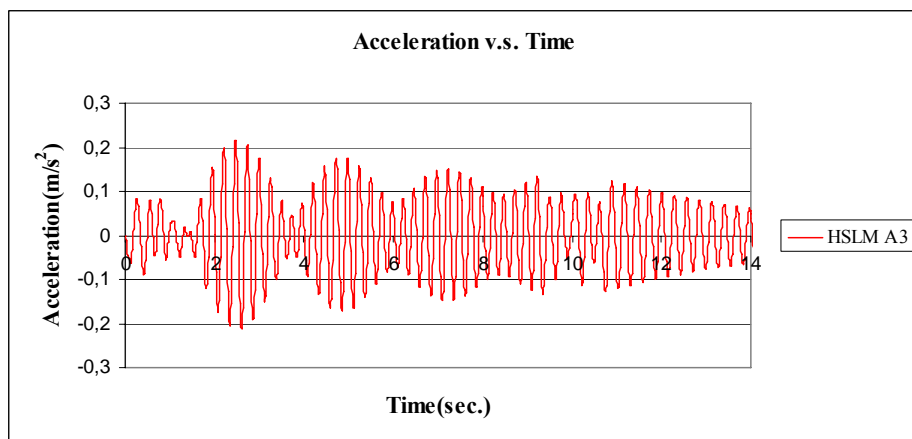


Figure B.14 Acceleration v.s. Time graph $V = 40$ m/s, for HSLM A3

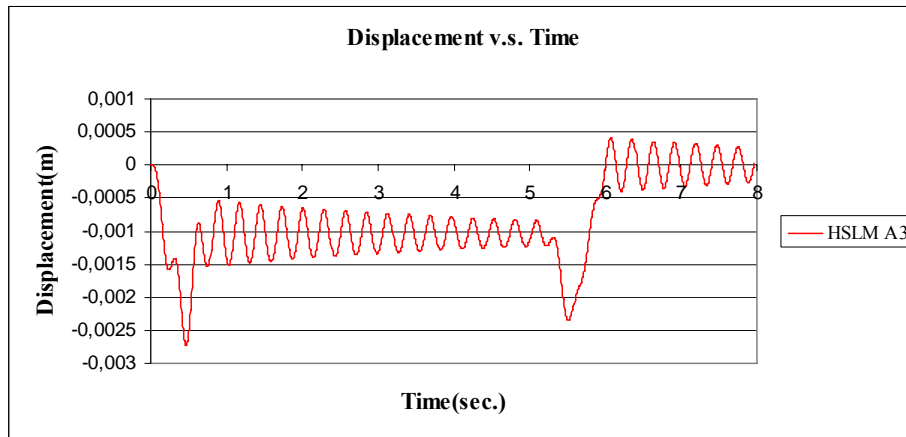


Figure B.15 Displacement v.s. Time graph $V = 71.40$ m/s, for HSLM A3

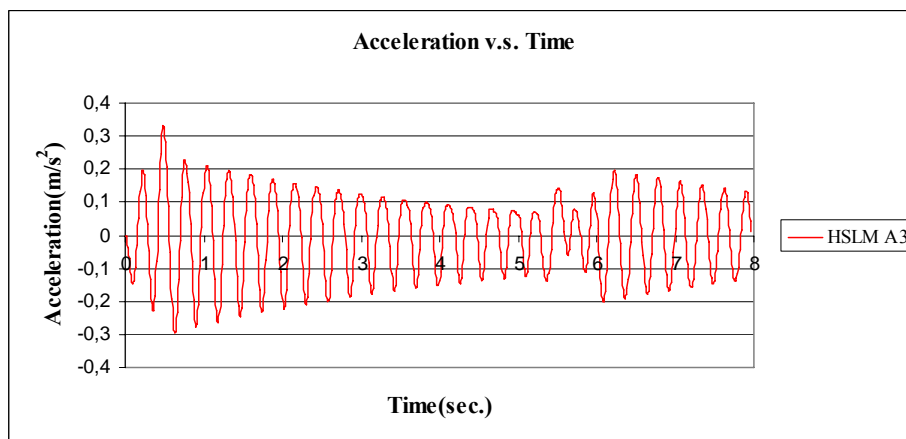


Figure B.16 Acceleration v.s. Time graph $V = 71.40$ m/s, for HSLM A3

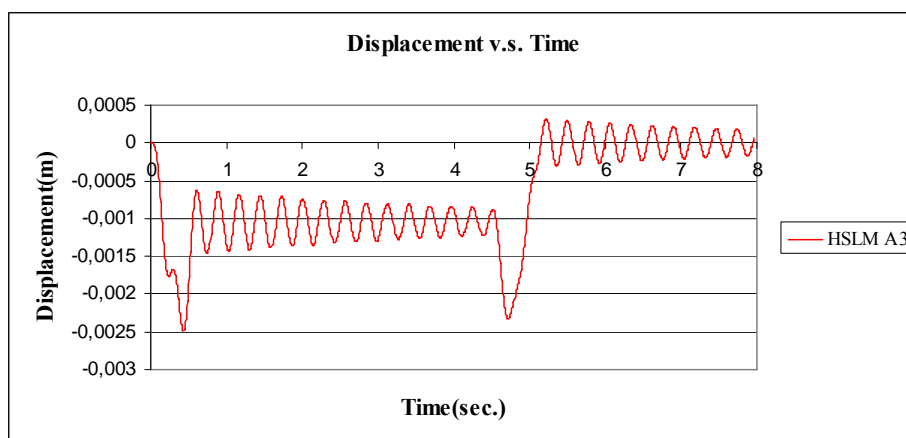


Figure B.17 Displacement v.s. Time graph $V = 83.33$ m/s, for HSLM A3

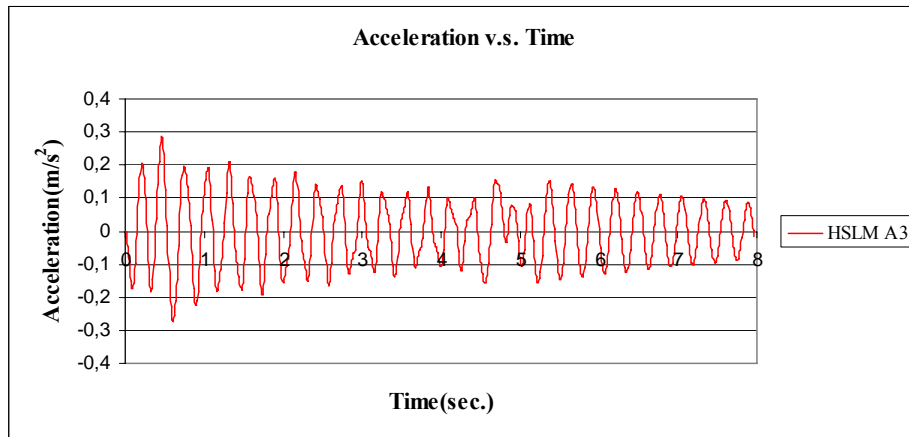


Figure B.18 Acceleration v.s. Time graph $V = 83.33$ m/s, for HSLM A3

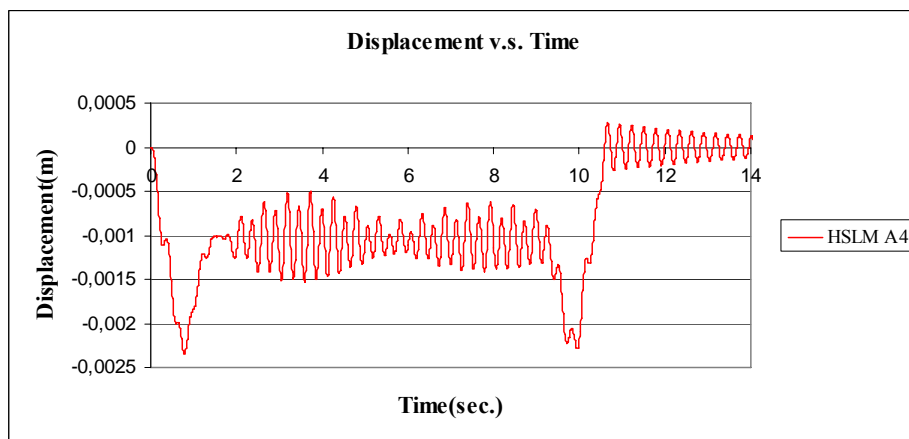


Figure B.19 Displacement v.s. Time graph $V = 40$ m/s, for HSLM A4

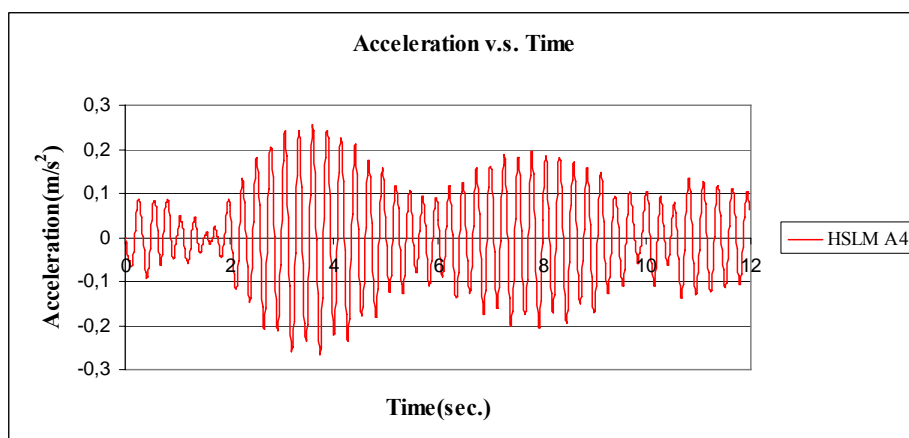


Figure B.20 Acceleration v.s. Time graph $V = 40$ m/s, for HSLM A4

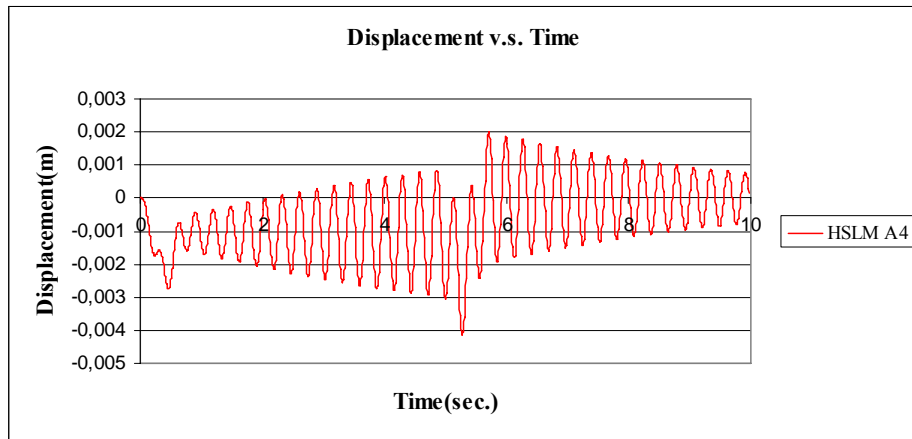


Figure B.21 Displacement v.s. Time graph $V = 74.97$ m/s, for HSLM A4

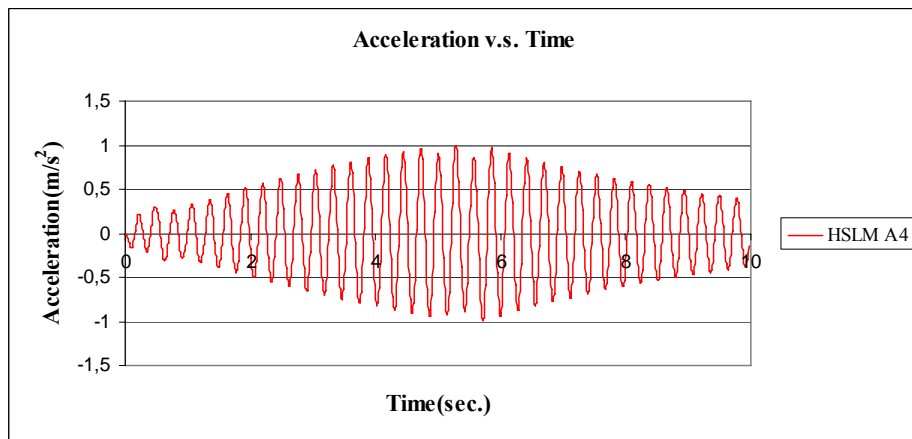


Figure B.22 Acceleration v.s. Time graph $V = 74.97$ m/s, for HSLM A4

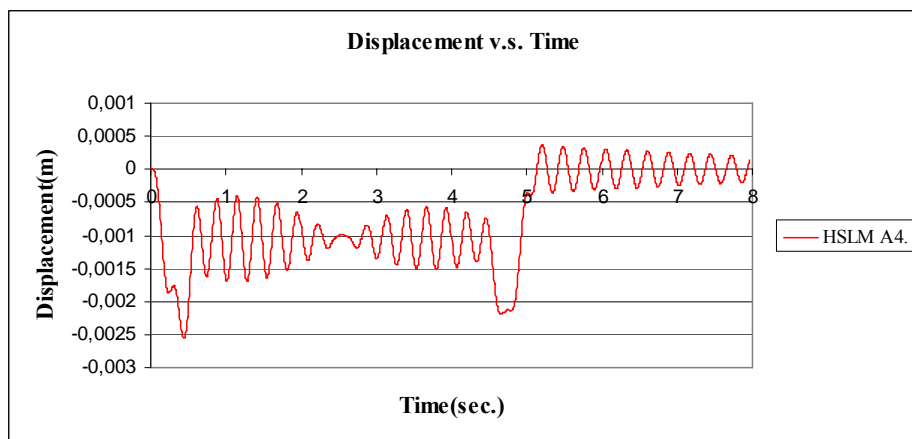


Figure B.23 Displacement v.s. Time graph $V = 83.33$ m/s, for HSLM A4

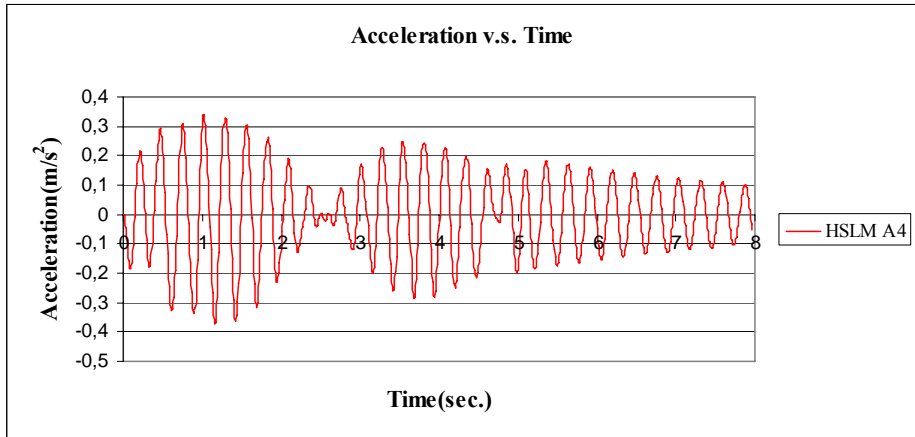


Figure B.24 Acceleration v.s. Time graph $V = 83.33$ m/s, for HSLM A4

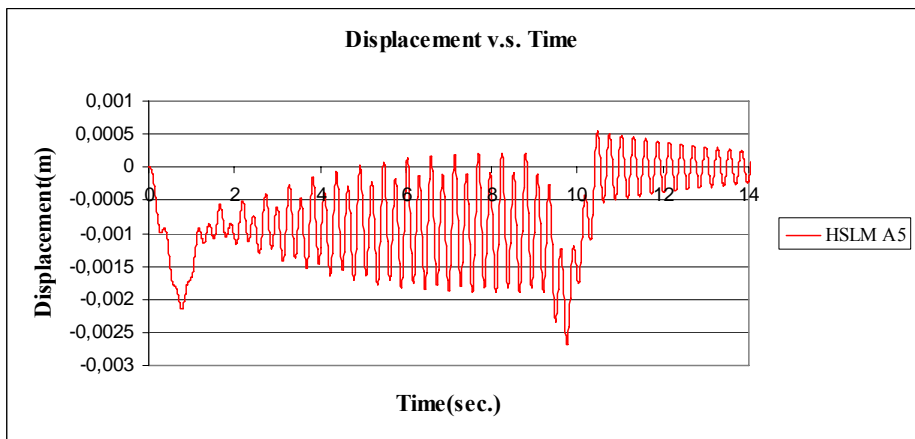


Figure B.25 Displacement v.s. Time graph $V = 40$ m/s, for HSLM A5

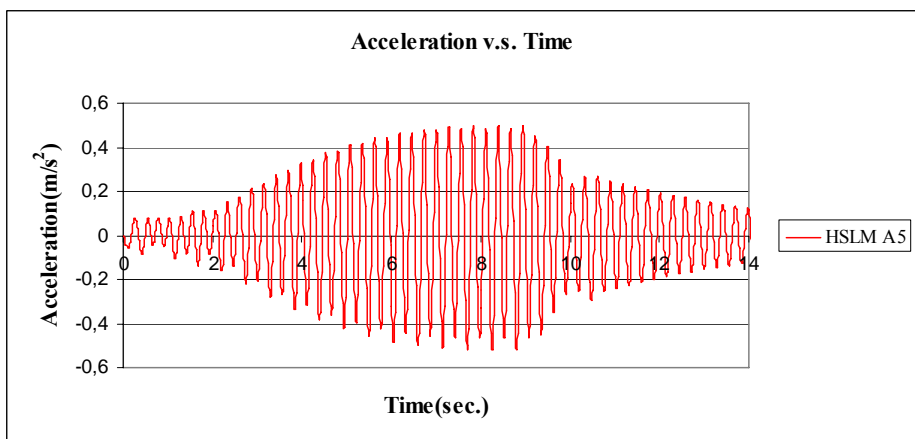


Figure B.26 Acceleration v.s. Time graph $V = 40$ m/s, for HSLM A5

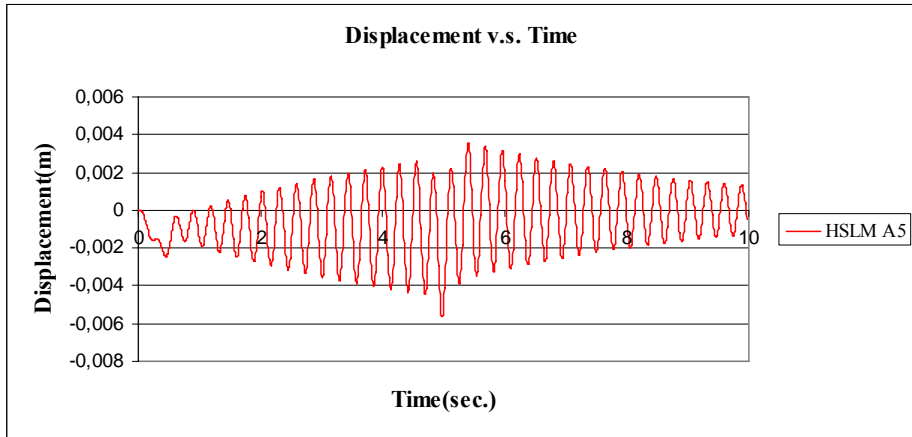


Figure B.27 Displacement v.s. Time graph $V = 78.54$ m/s, for HSLM A5

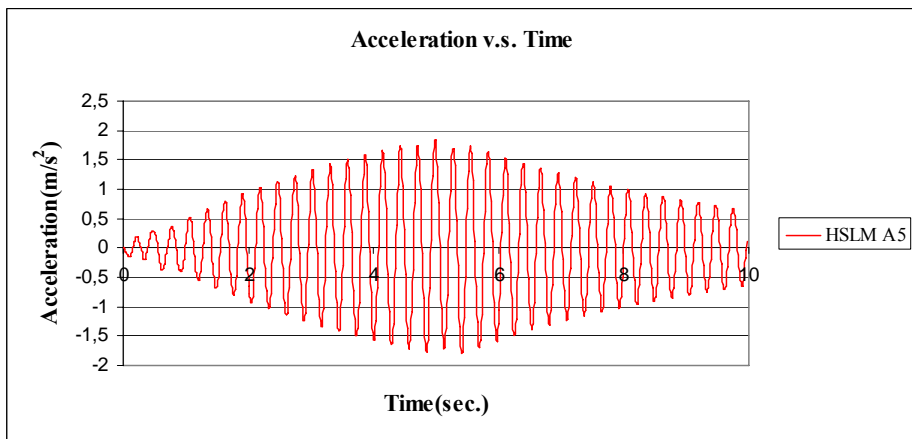


Figure B.28 Acceleration v.s. Time graph $V = 78.54$ m/s, for HSLM A5

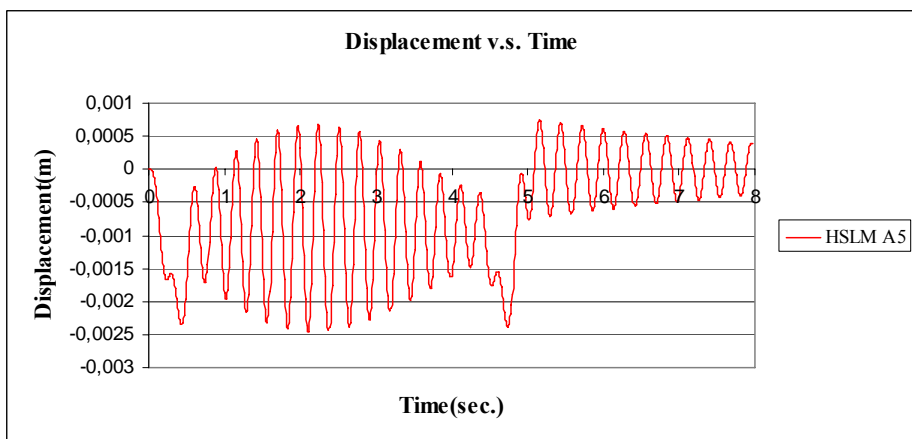


Figure B.29 Displacement v.s. Time graph $V = 83.33$ m/s, for HSLM A5

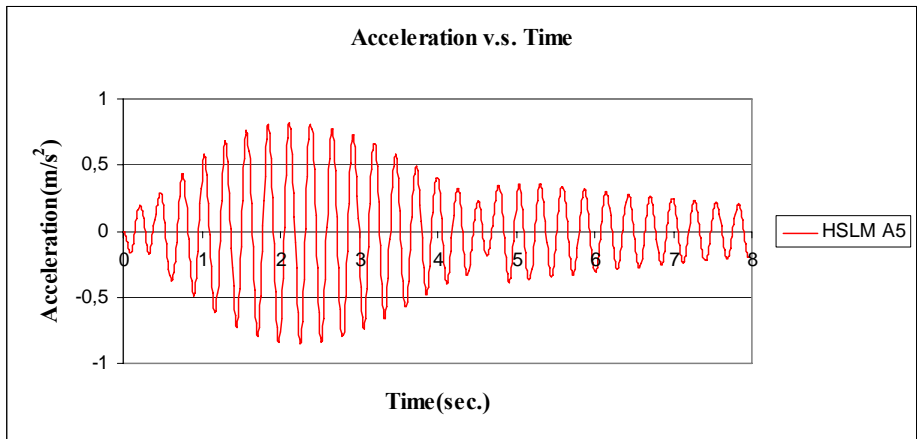


Figure B.30 Acceleration v.s. Time graph $V = 83.33$ m/s, for HSLM A5

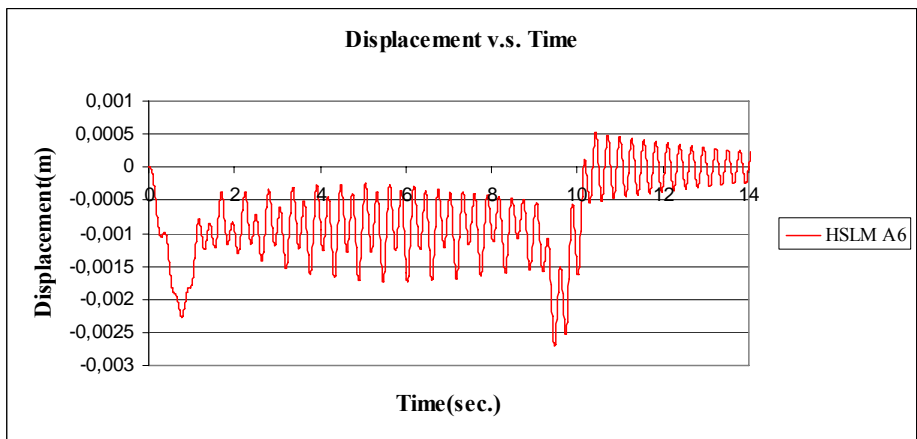


Figure B.31 Displacement v.s. Time graph $V = 40$ m/s, for HSLM A6

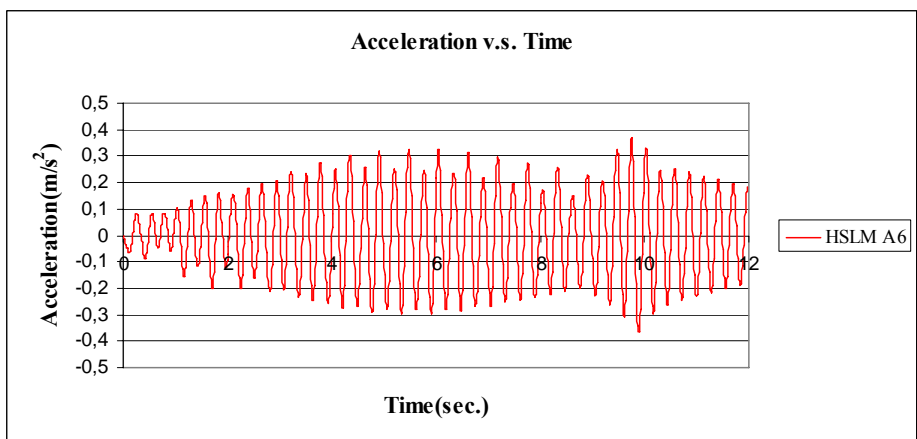


Figure B.32 Acceleration v.s. Time graph $V = 40$ m/s, for HSLM A6

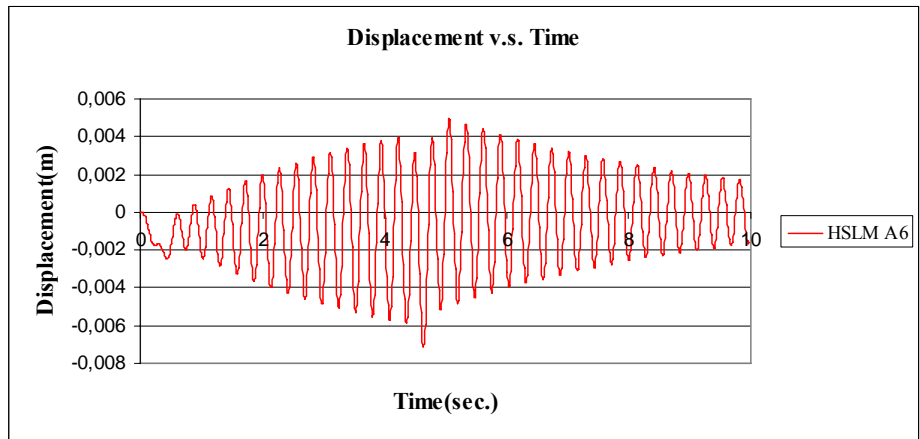


Figure B.33 Displacement v.s. Time graph $V = 83.33$ m/s, for HSLM A6

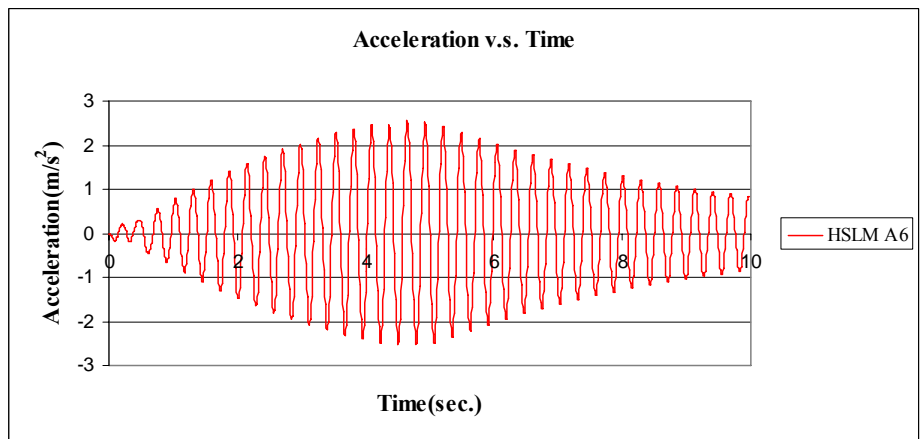


Figure B.34 Acceleration v.s. Time graph $V = 83.33$ m/s, for HSLM A6

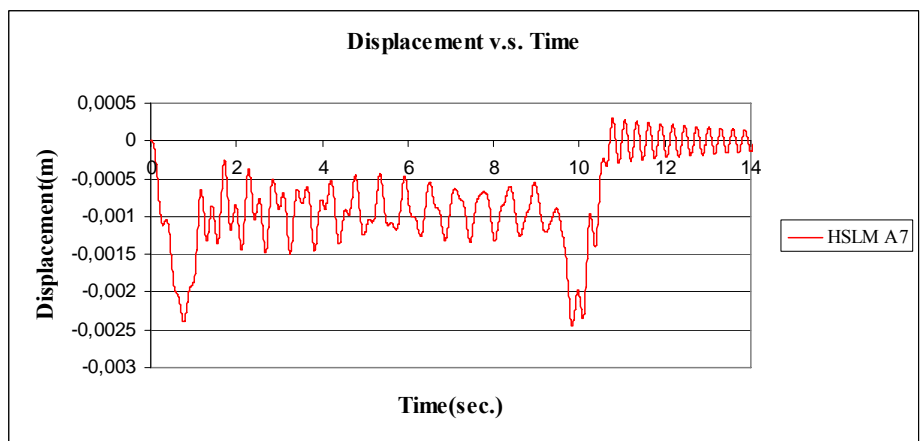


Figure B.35 Displacement v.s. Time graph $V = 40$ m/s, for HSLM A7

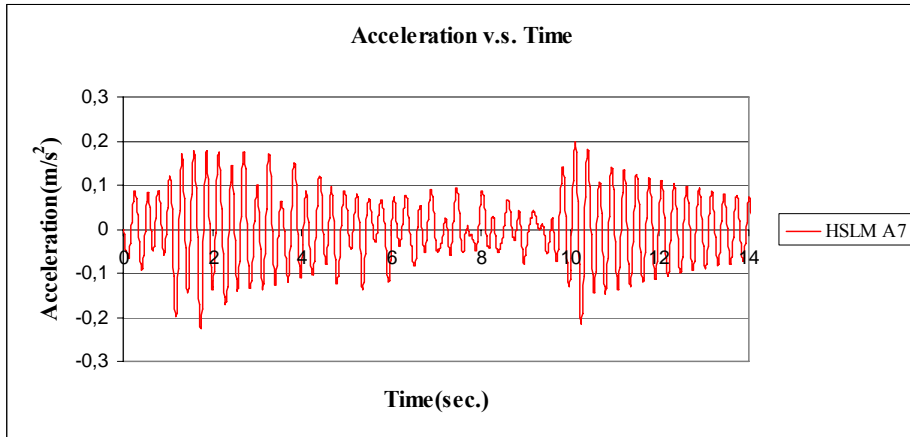


Figure B.36 Acceleration v.s. Time graph $V = 40$ m/s, for HSLM A7

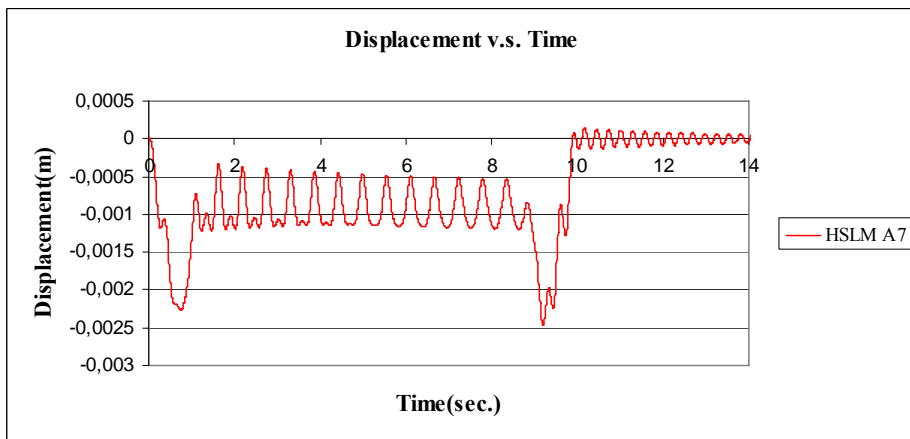


Figure B.37 Displacement v.s. Time graph $V = 42.84$ m/s, for HSLM A7

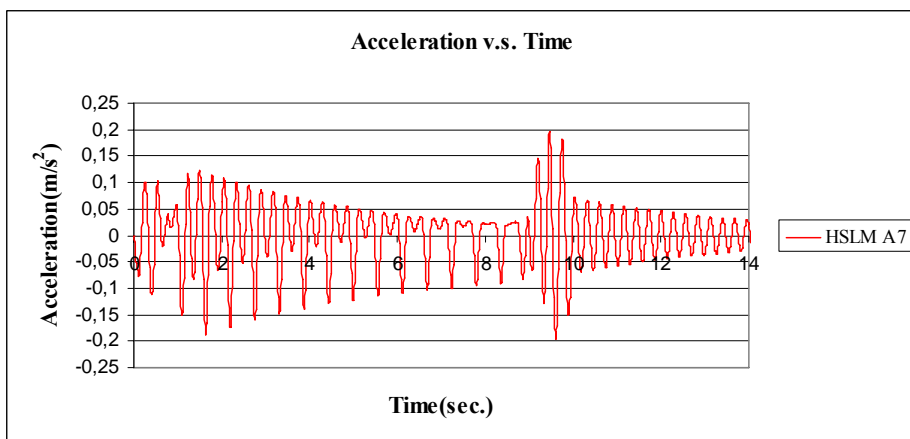


Figure B.38 Acceleration v.s. Time graph $V = 42.84$ m/s, for HSLM A7

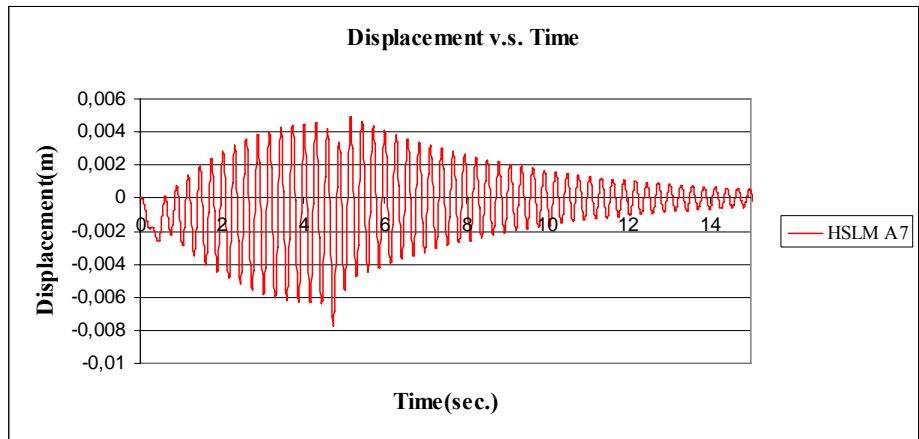


Figure B.39 Displacement v.s. Time graph $V = 83.33$ m/s, for HSLM A7

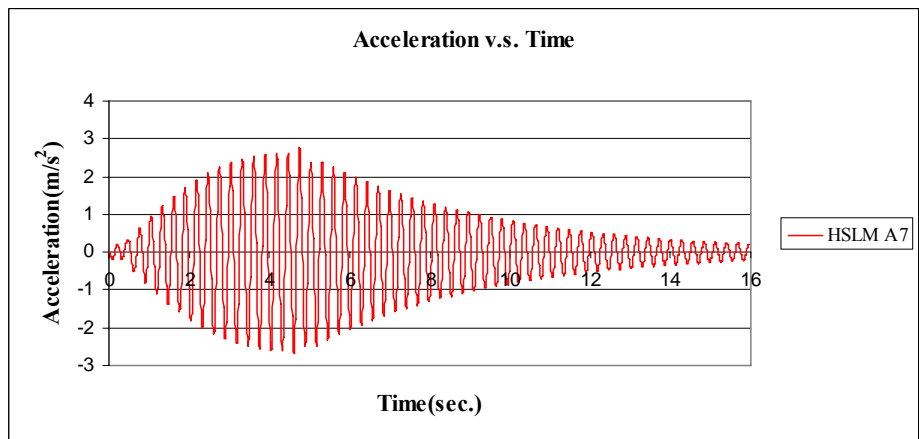


Figure B.40 Acceleration v.s. Time graph $V = 83.33$ m/s, for HSLM A7

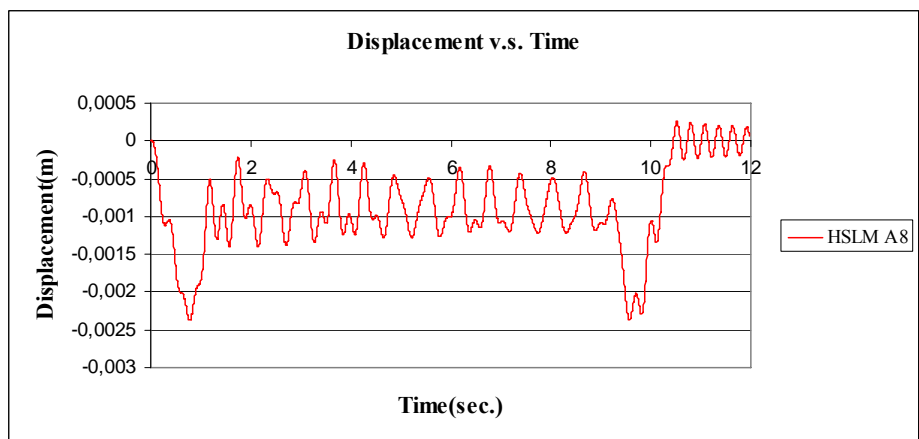


Figure B.41 Displacement v.s. Time graph $V = 40$ m/s, for HSLM A8

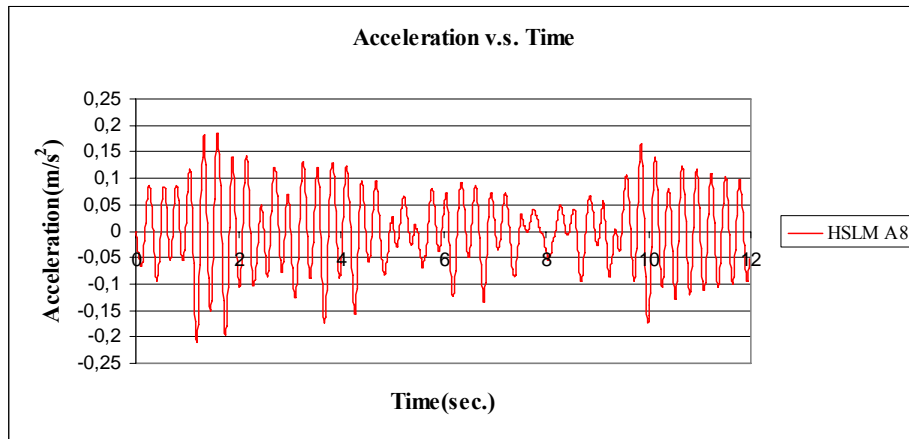


Figure B.42 Acceleration v.s. Time graph $V = 40$ m/s, for HSLM A8

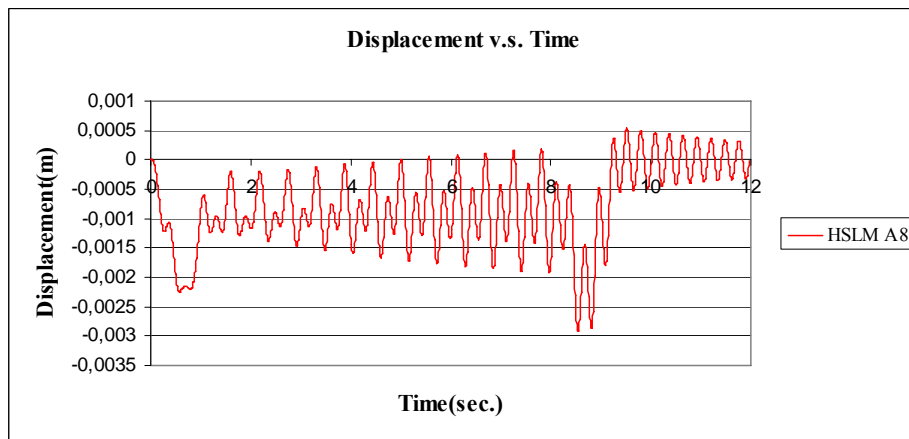


Figure B.43 Displacement v.s. Time graph $V = 44.625$ m/s, for HSLM A8

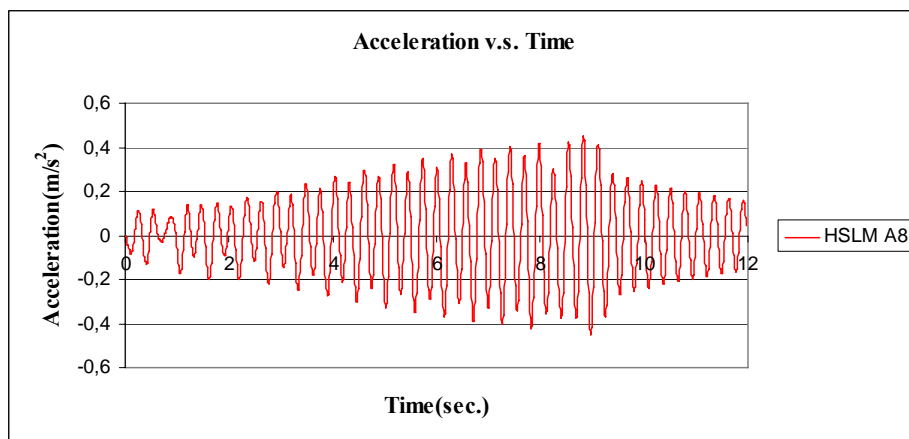


Figure B.44 Acceleration v.s. Time graph $V = 44.625$ m/s, for HSLM A8

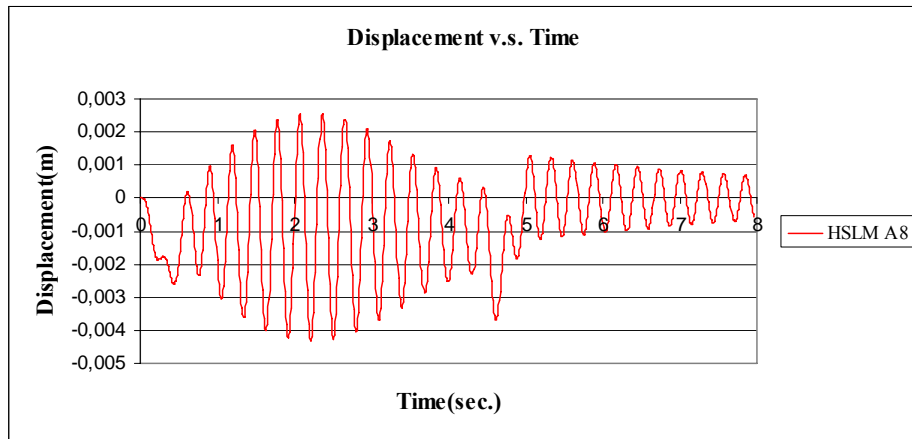


Figure B.45 Displacement v.s. Time graph $V = 83.33$ m/s, for HSLM A8

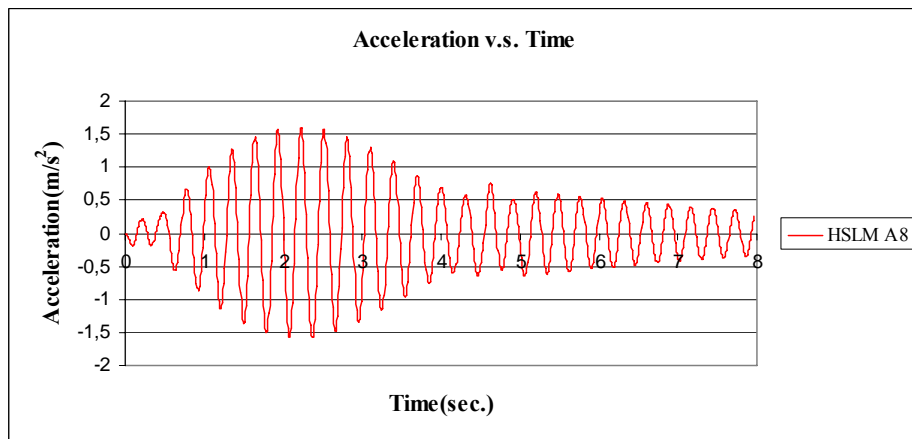


Figure B.46 Acceleration v.s. Time graph $V = 83.33$ m/s, for HSLM A8

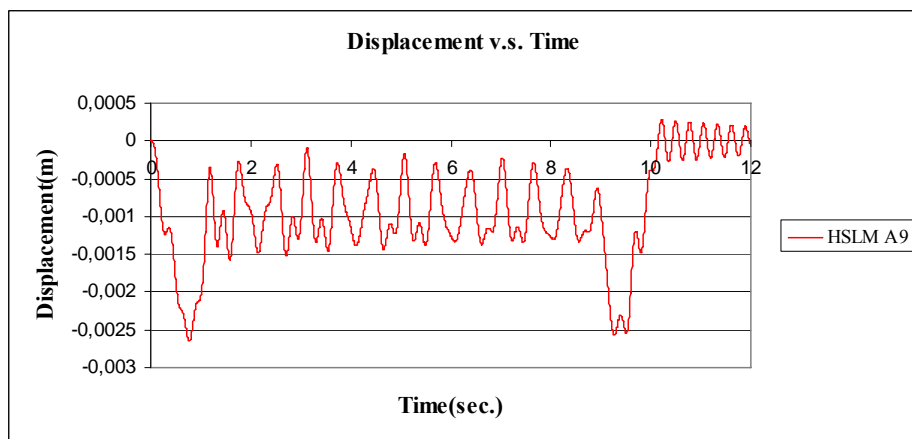


Figure B.47 Displacement v.s. Time graph $V = 40$ m/s, for HSLM A9

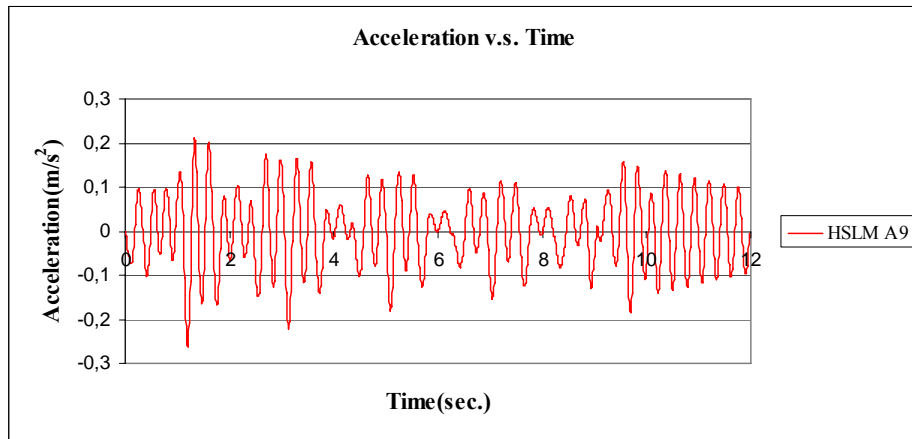


Figure B.48 Acceleration v.s. Time graph $V = 40$ m/s, for HSLM A9

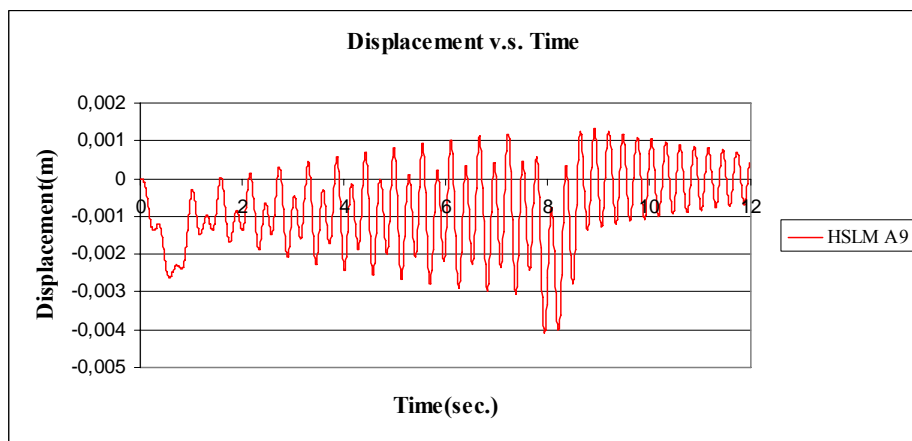


Figure B.49 Displacement v.s. Time graph $V = 46.41$ m/s, for HSLM A9

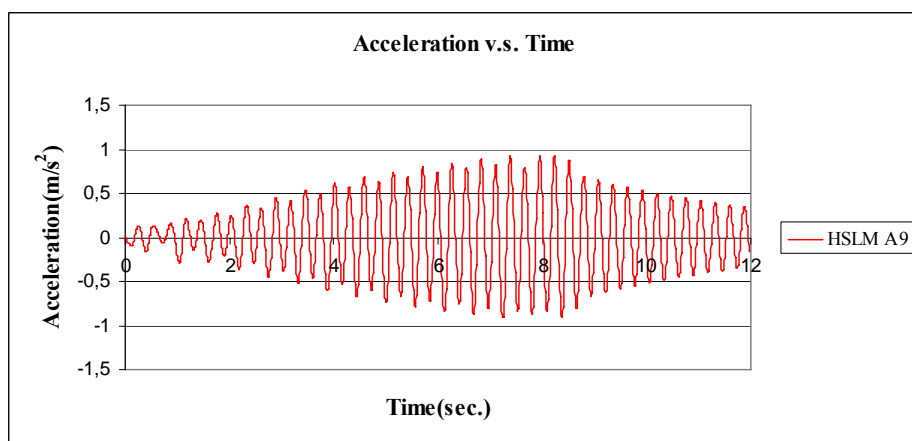


Figure B.50 Acceleration v.s. Time graph $V = 46.41$ m/s, for HSLM A9

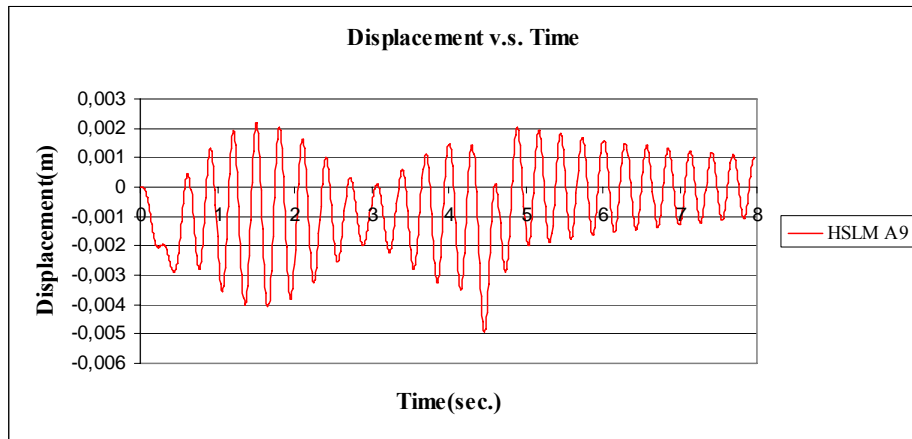


Figure B.51 Displacement v.s. Time graph $V = 83.33$ m/s, for HSLM A9

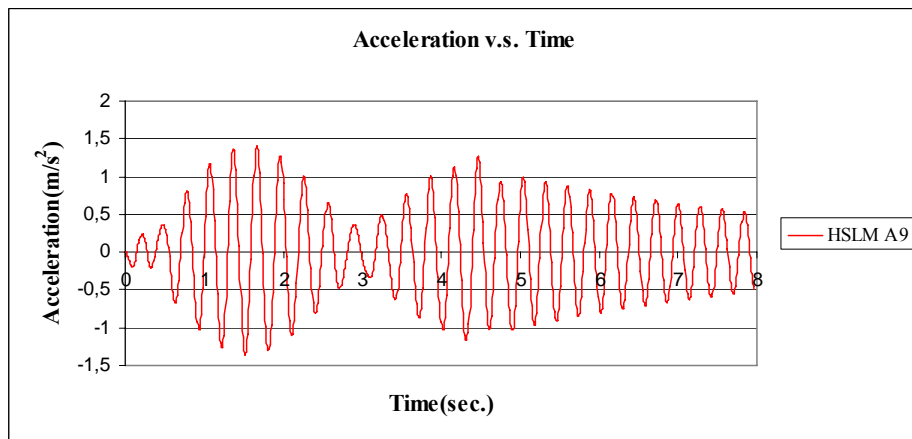


Figure B.52 Acceleration v.s. Time graph $V = 83.33$ m/s, for HSLM A9

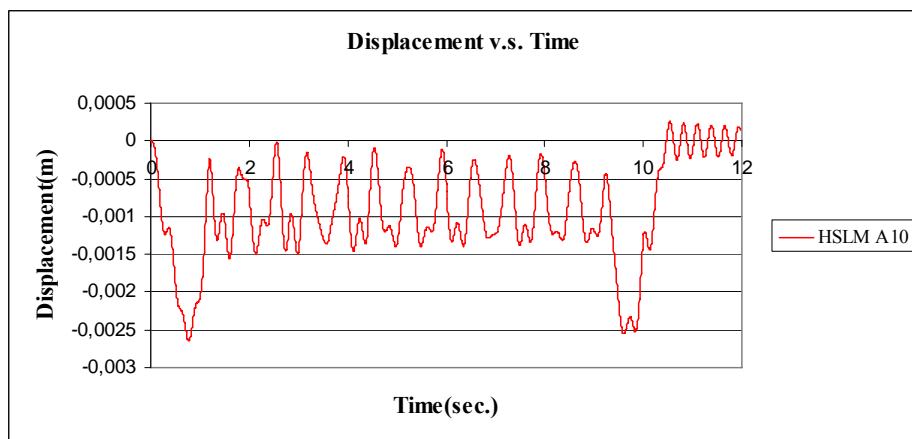


Figure B.53 Displacement v.s. Time graph $V = 40$ m/s, for HSLM A10

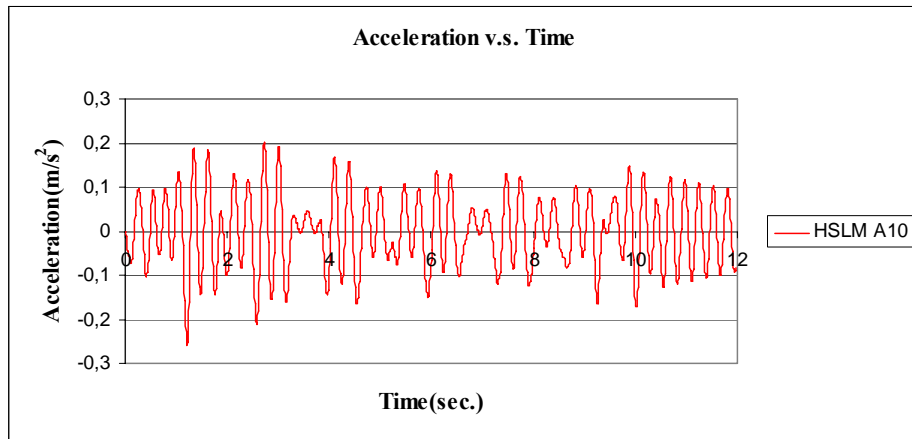


Figure B.53 Acceleration v.s. Time graph $V = 40$ m/s, for HSLM A10

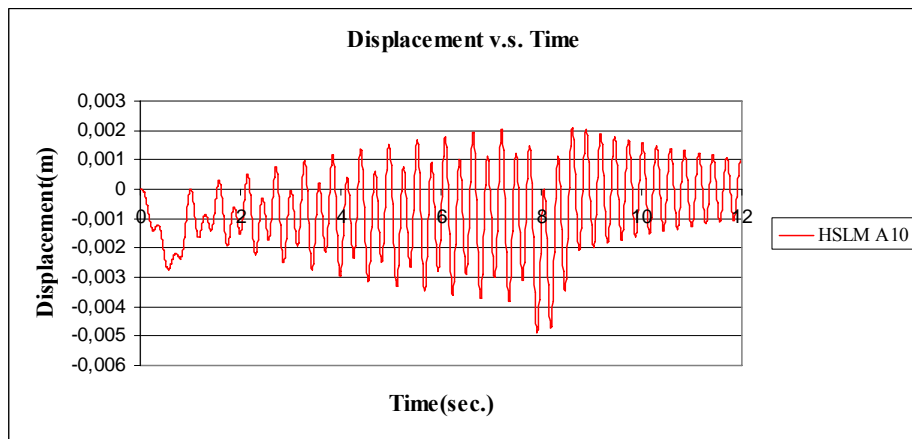


Figure B.54 Displacement v.s. Time graph $V = 48.195$ m/s, for HSLM A10

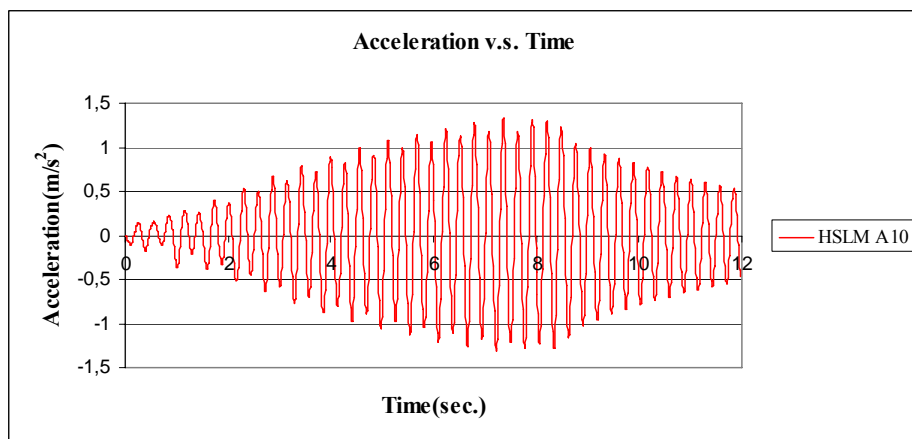


Figure B.54 Acceleration v.s. Time graph $V = 48.195$ m/s, for HSLM A10

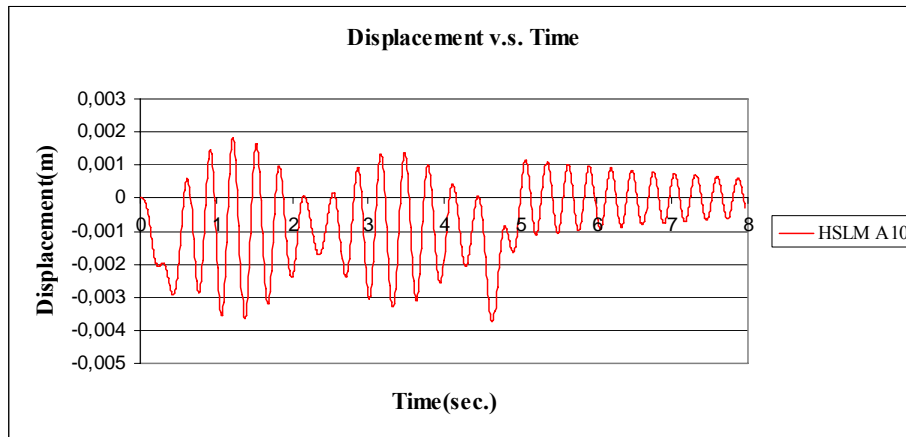


Figure B.55 Displacement v.s. Time graph $V = 83.33 \text{ m/s}$, for HSLM A10

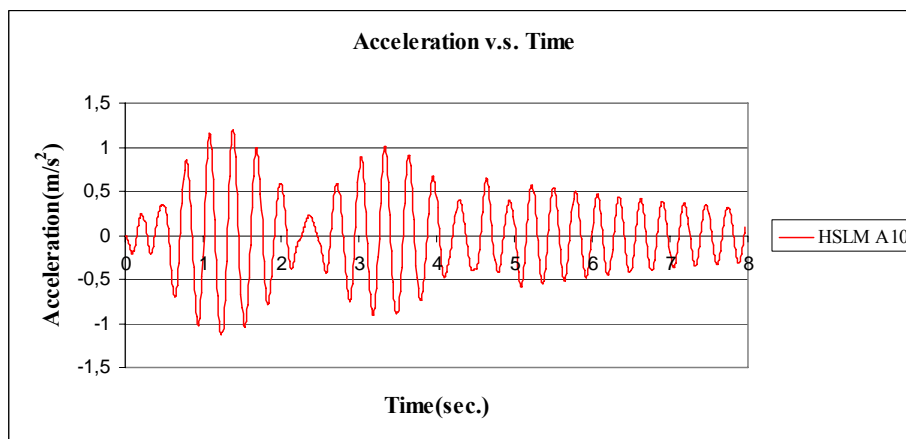


Figure B.56 Acceleration v.s. Time graph $V = 83.33 \text{ m/s}$, for HSLM A10

APPENDIX C

DISPLACEMENT V.S. TIME AND ACCELERATION V.S. TIME GRAPHS FOR PARAMETRIC STUDY

C1. GRAPHS FOR HSLM TRAIN

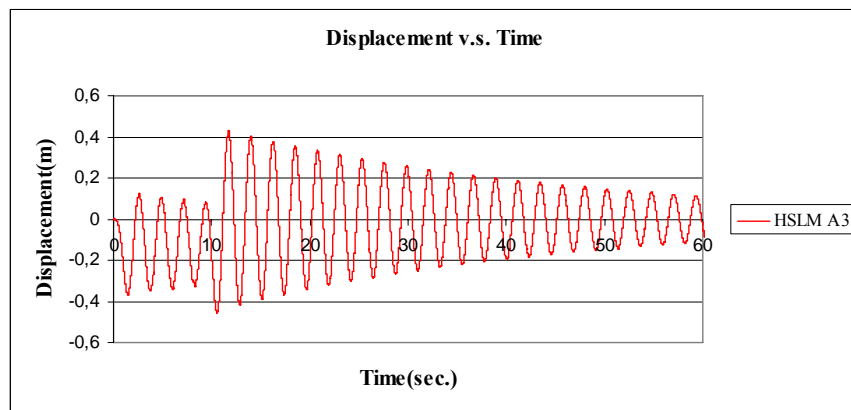


Figure C.1 Displacement v.s. Time graph, (Analysis 1, V = 40 m/s)

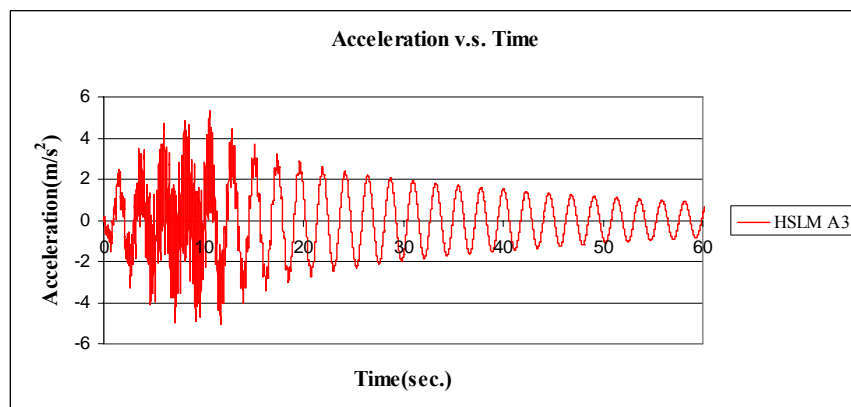


Figure C.2 Acceleration v.s. Time graph, (Analysis 1, V = 40 m/s)

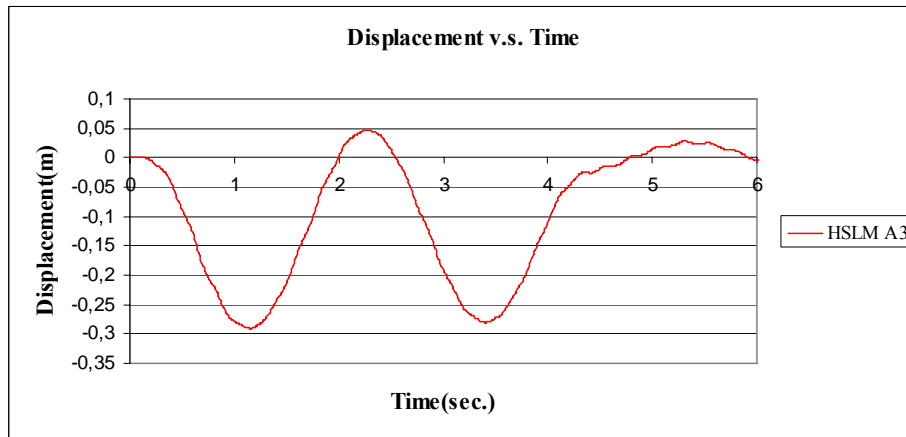


Figure C.3 Displacement v.s. Time graph, (Analysis 1, $V = 97.22$ m/s)

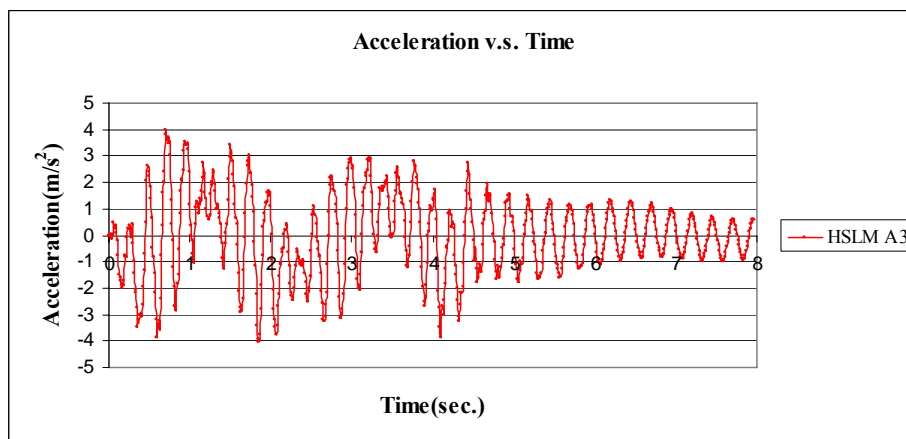


Figure C.4 Acceleration v.s. Time graph, (Analysis 1, $V = 97.22$ m/s)

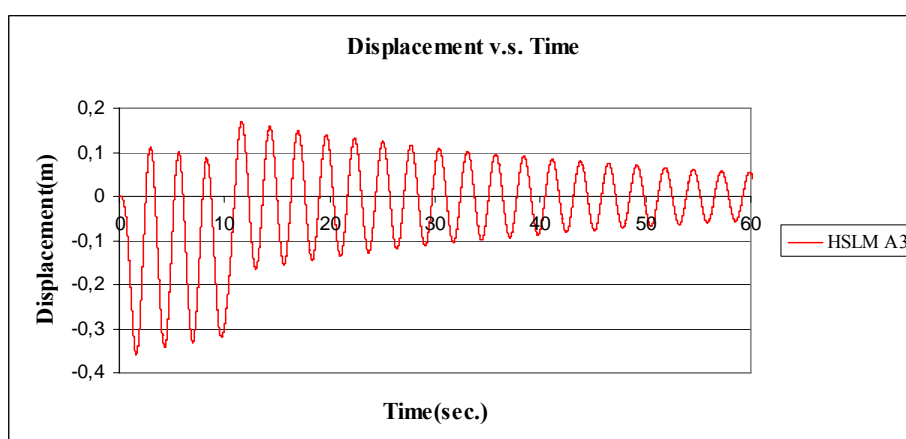


Figure C.5 Displacement v.s. Time graph, (Analysis 2, $V = 40$ m/s)

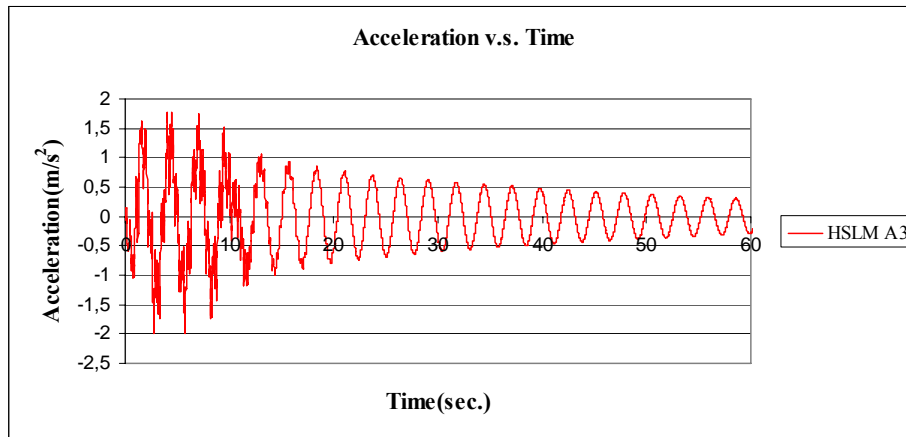


Figure C.6 Acceleration v.s. Time graph, (Analysis 2, V = 40 m/s)

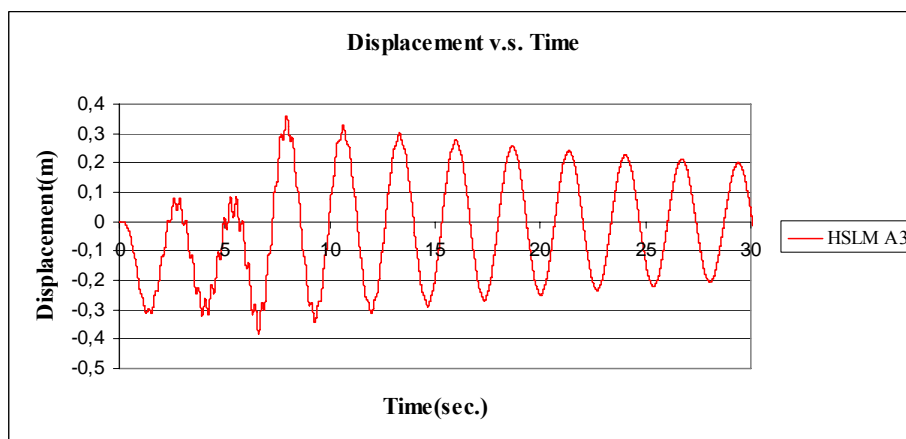


Figure C.7 Displacement v.s. Time graph, (Analysis 2, V = 67.10 m/s)

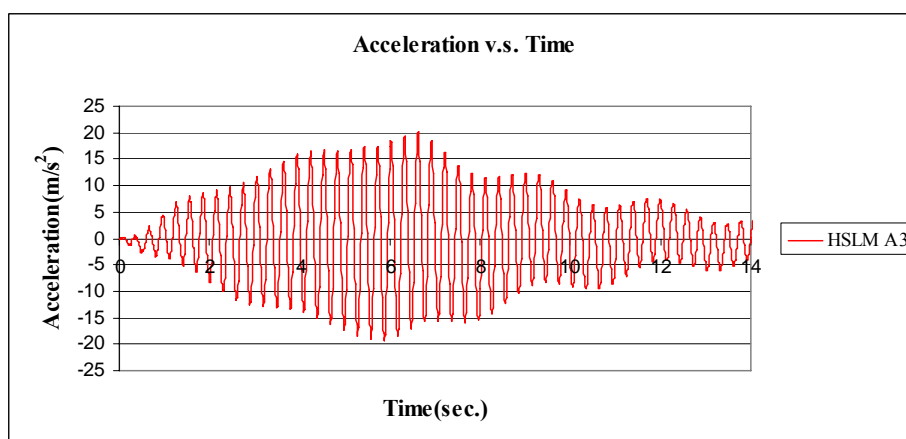


Figure C.8 Acceleration v.s. Time graph, (Analysis 2, V = 67.10 m/s)

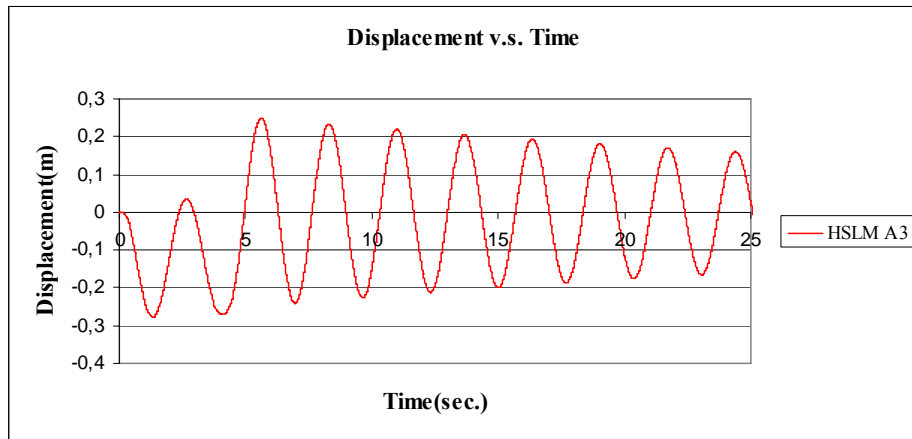


Figure C.9 Displacement v.s. Time graph, (Analysis 2, $V = 97.22$ m/s)

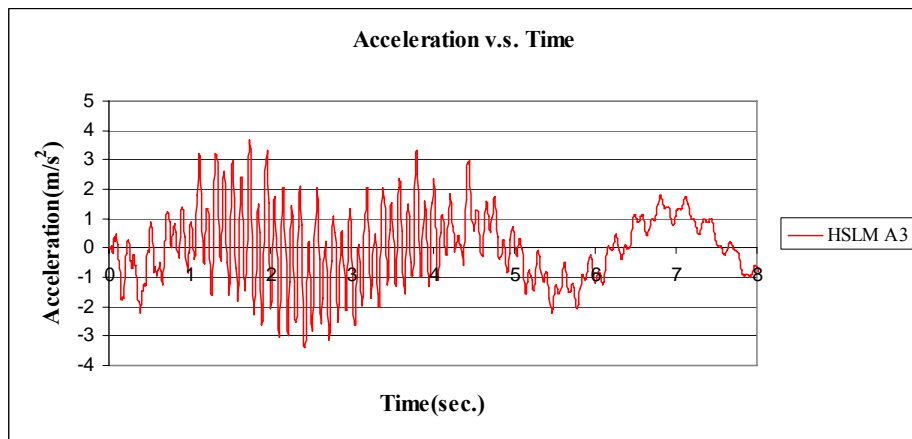


Figure C.10 Acceleration v.s. Time graph, (Analysis 2, $V = 97.22$ m/s)

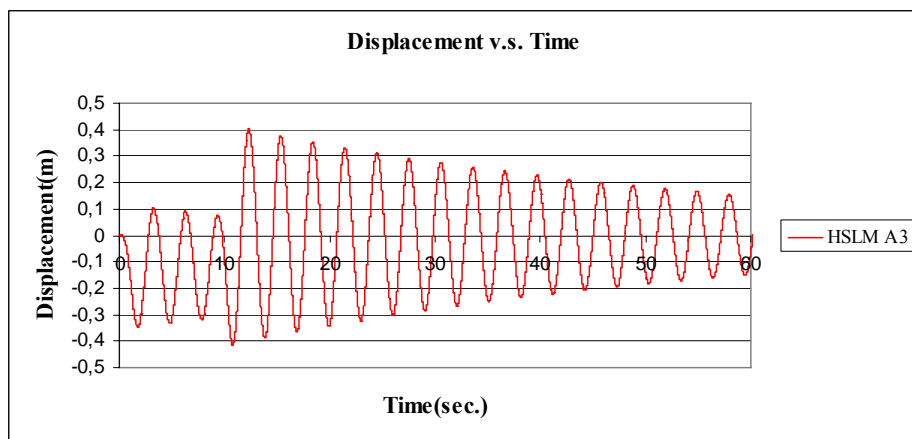


Figure C.11 Displacement v.s. Time graph, (Analysis 3, $V = 40$ m/s)

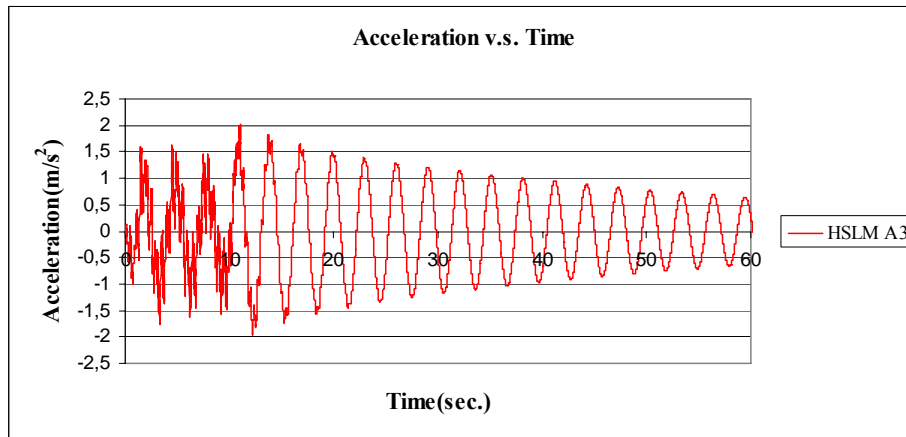


Figure C.12 Acceleration v.s. Time graph, (Analysis 3, $V = 40$ m/s)

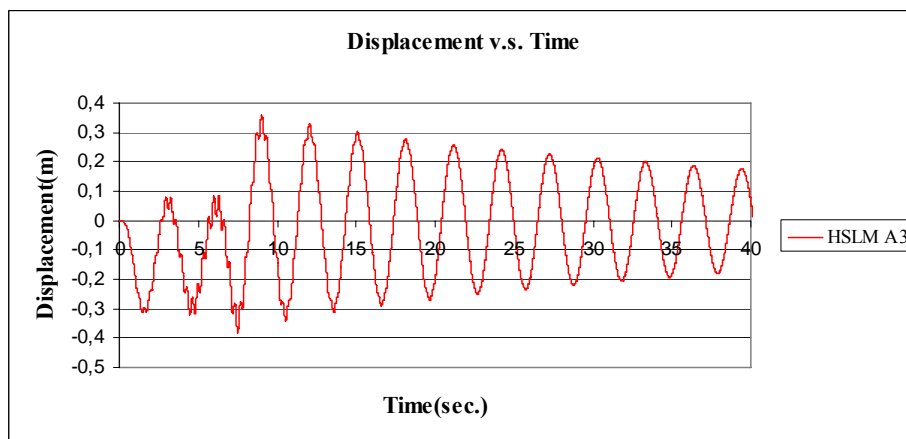


Figure C.13 Displacement v.s. Time graph, (Analysis 3, $V = 59.18$ m/s)

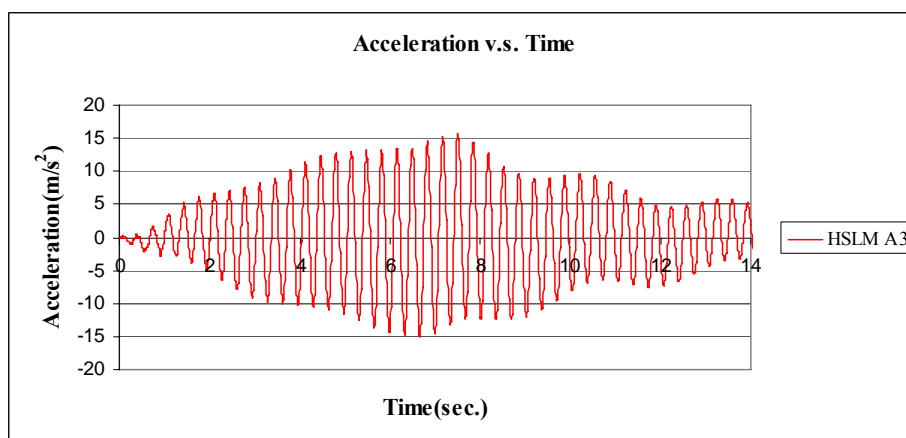


Figure C.14 Acceleration v.s. Time graph, (Analysis 3, $V = 59.18$ m/s)

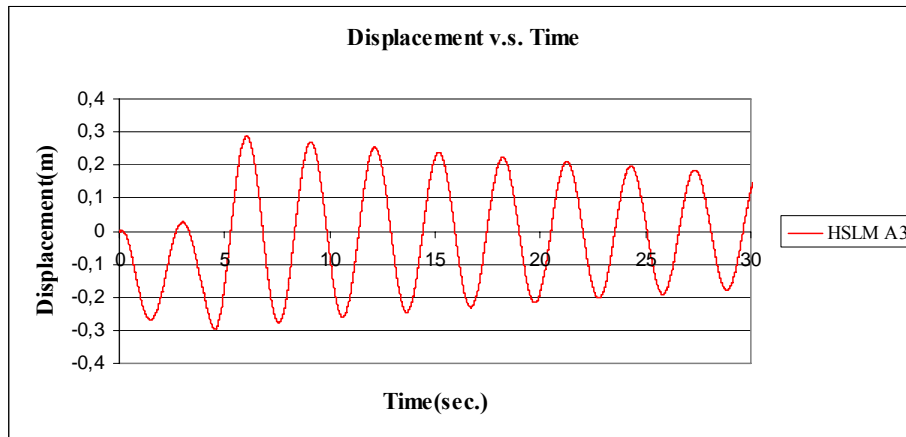


Figure C.15 Displacement v.s. Time graph, (Analysis 3, $V = 97.22$ m/s)

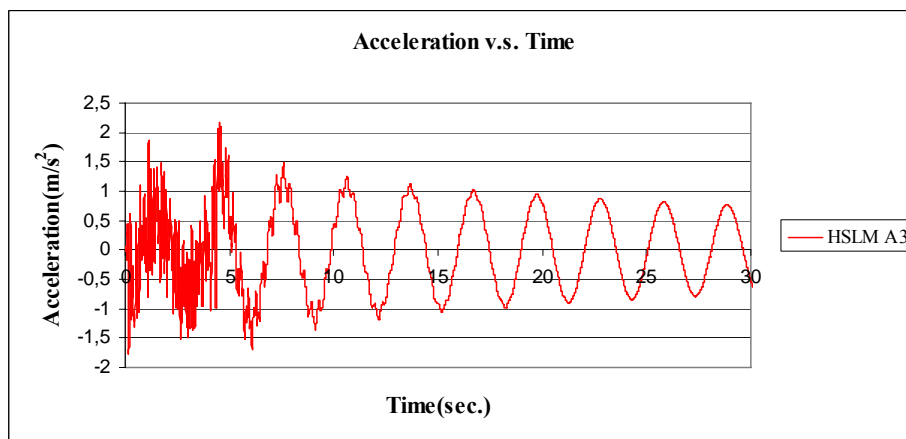


Figure C.16 Acceleration v.s. Time graph, (Analysis 3, $V = 97.22$ m/s)

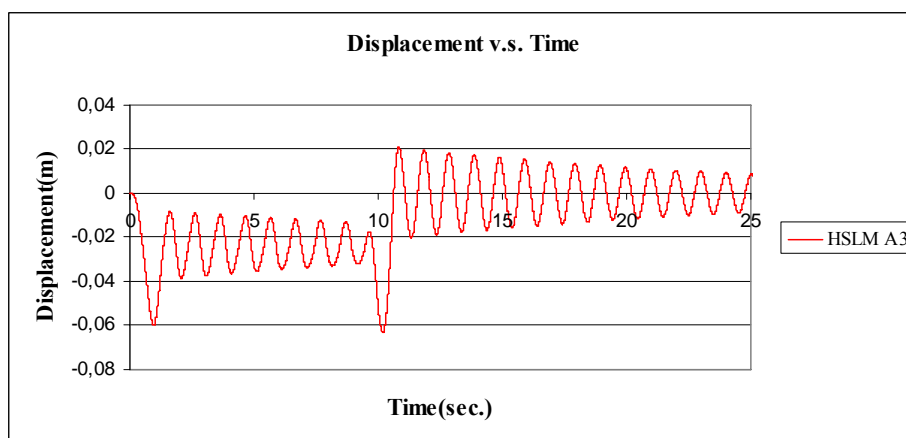


Figure C.17 Displacement v.s. Time graph, (Analysis 4, $V = 40$ m/s)

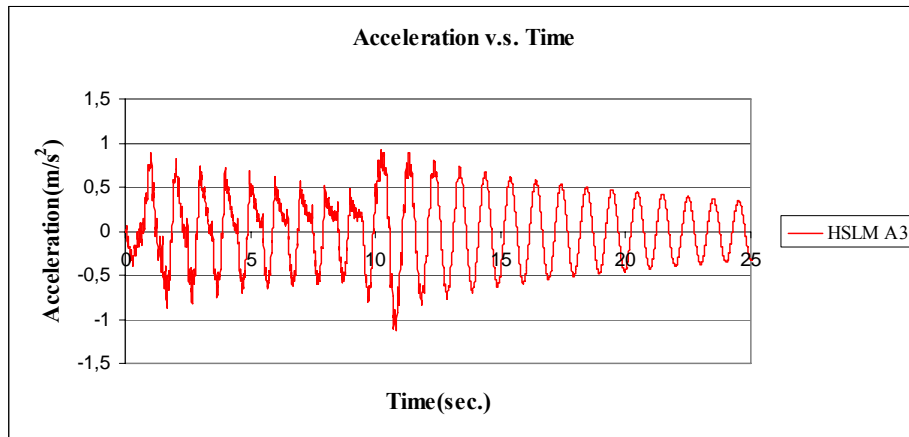


Figure C.18 Acceleration v.s. Time graph, (Analysis 4, $V = 40$ m/s)

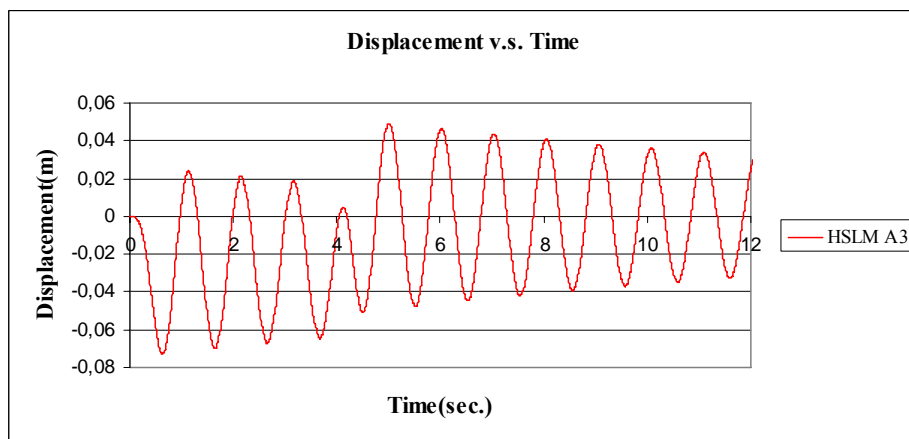


Figure C.19 Displacement v.s. Time graph, (Analysis 4, $V = 97.22$ m/s)

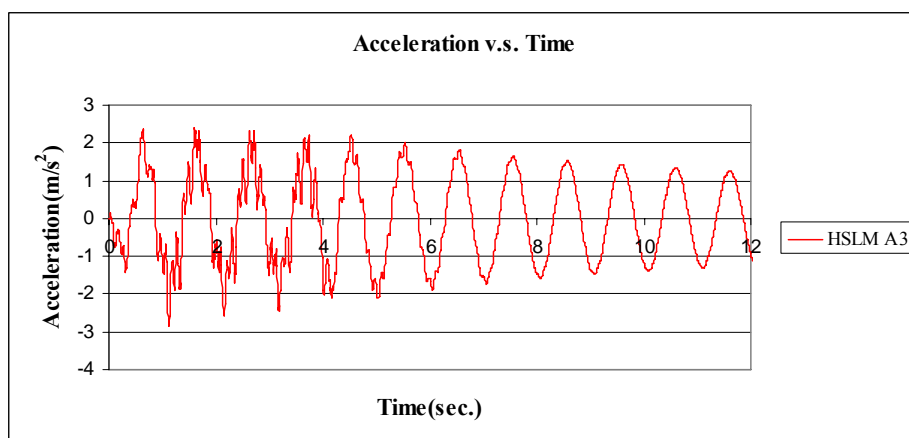


Figure C.20 Acceleration v.s. Time graph, (Analysis 4, $V = 97.22$ m/s)

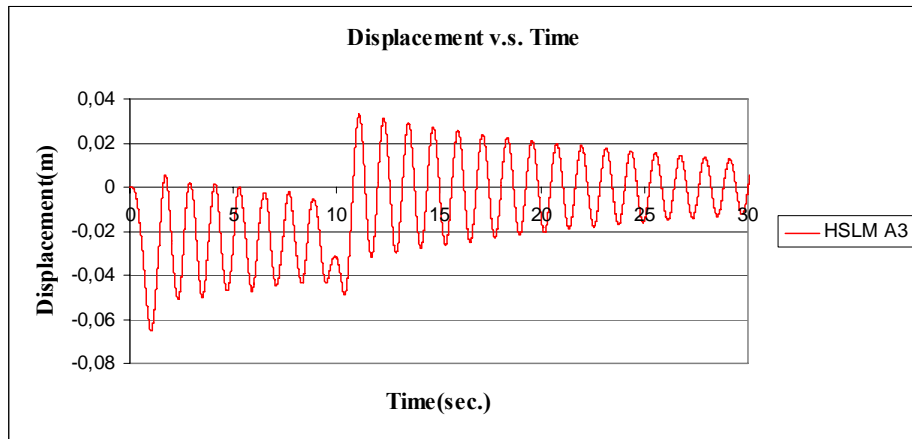


Figure C.21 Displacement v.s. Time graph, (Analysis 5, $V = 40$ m/s)

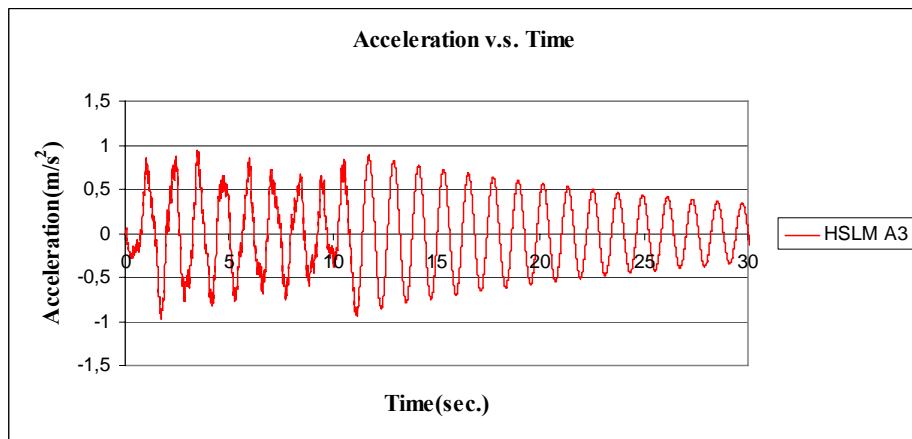


Figure C.22 Acceleration v.s. Time graph, (Analysis 5, $V = 40$ m/s)

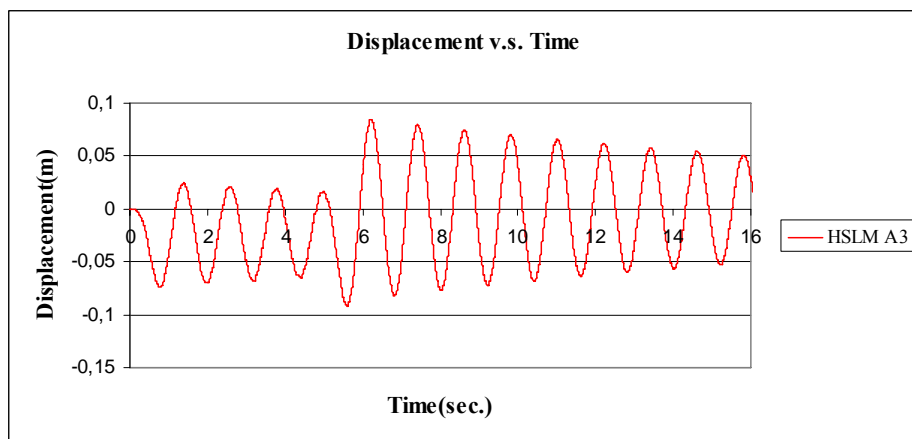


Figure C.23 Displacement v.s. Time graph, (Analysis 5, $V = 75$ m/s)

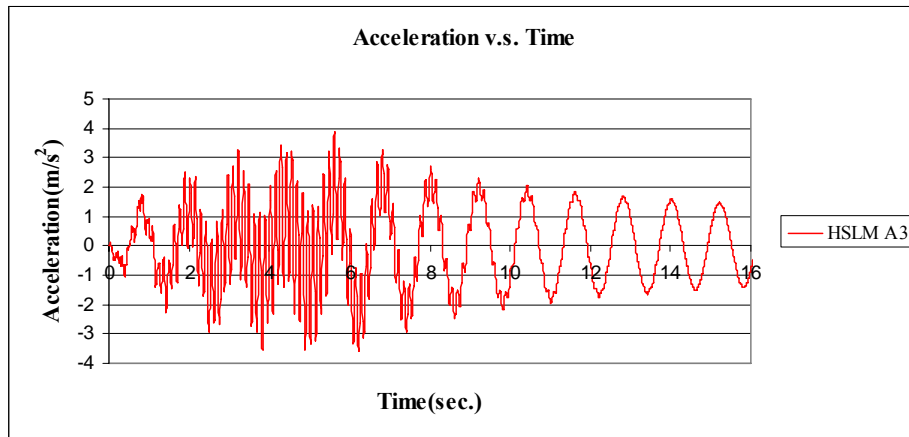


Figure C.24 Acceleration v.s. Time graph, (Analysis 5, V = 75 m/s)

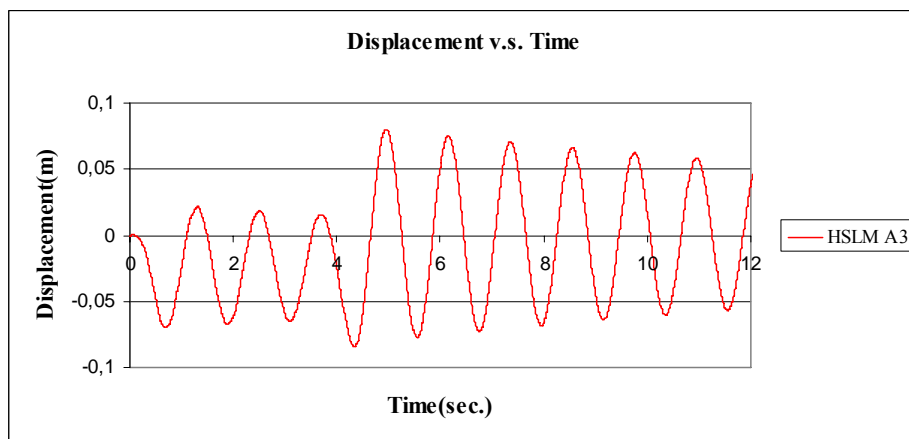


Figure C.25 Displacement v.s. Time graph, (Analysis 5, V = 97.22 m/s)

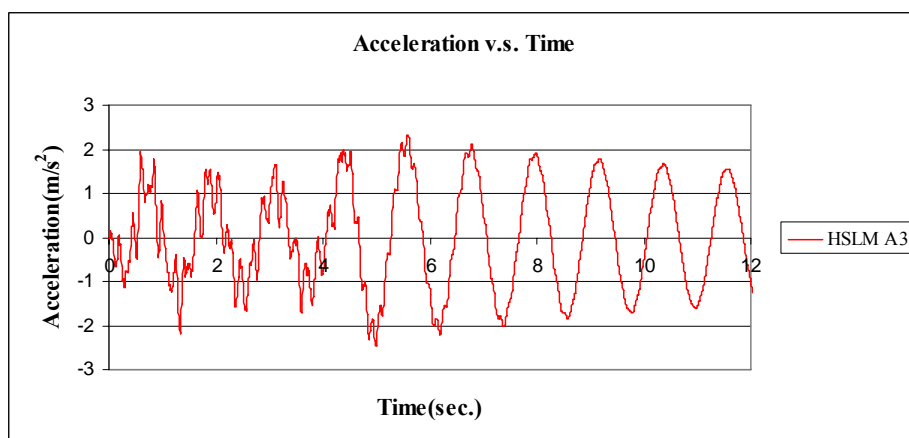


Figure C.26 Acceleration v.s. Time graph, (Analysis 5, V = 97.22 m/s)

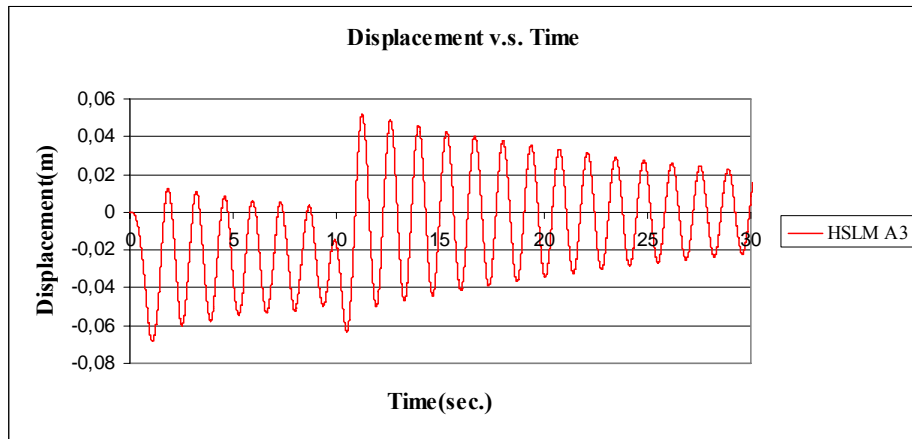


Figure C.27 Displacement v.s. Time graph, (Analysis 6, $V = 40$ m/s)

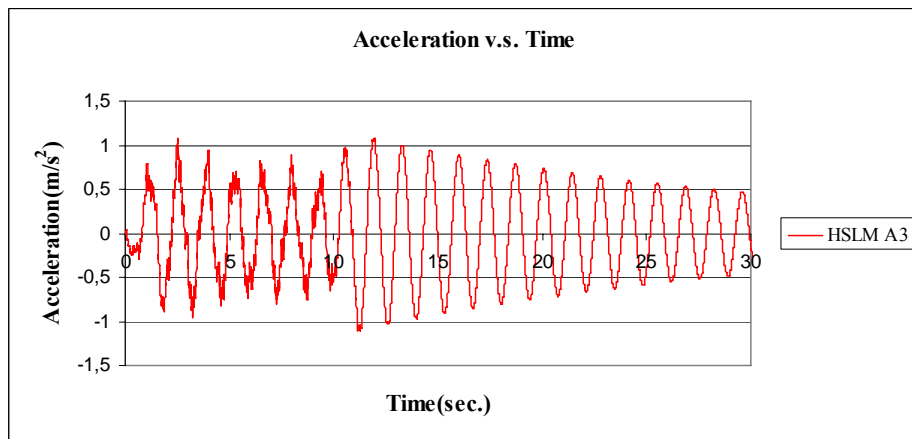


Figure C.28 Acceleration v.s. Time graph, (Analysis 6, $V = 40$ m/s)

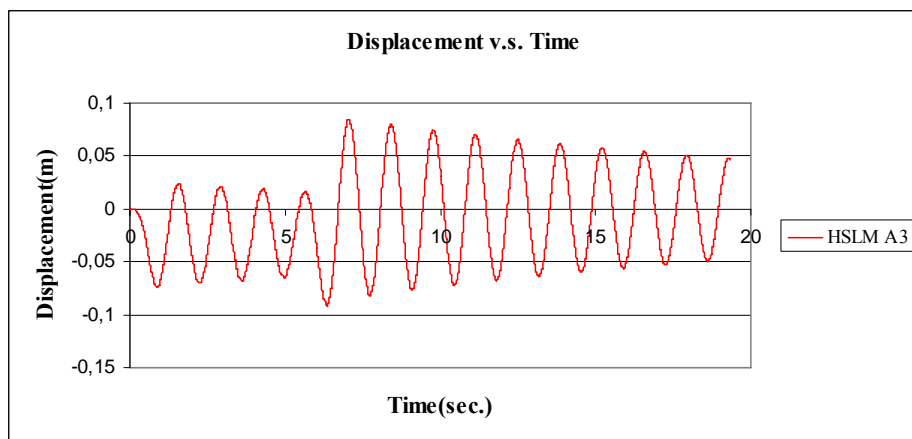


Figure C.29 Displacement v.s. Time graph, (Analysis 6, $V = 66.17$ m/s)

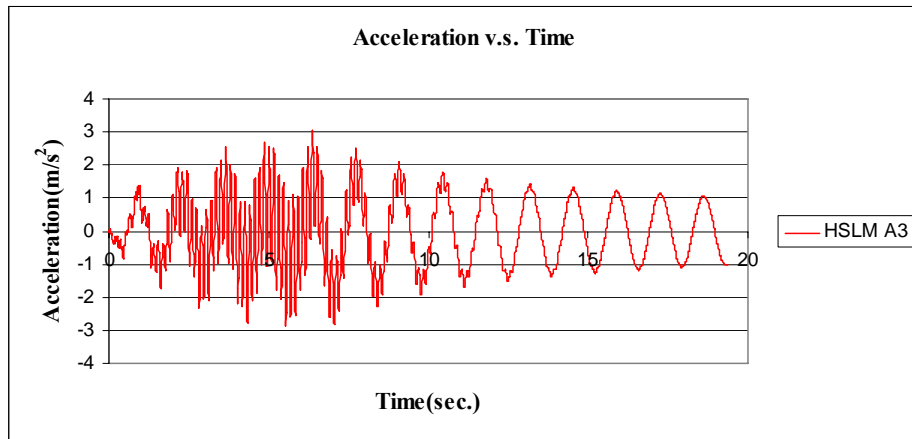


Figure C.30 Acceleration v.s. Time graph, (Analysis 6, $V = 66.17$ m/s)

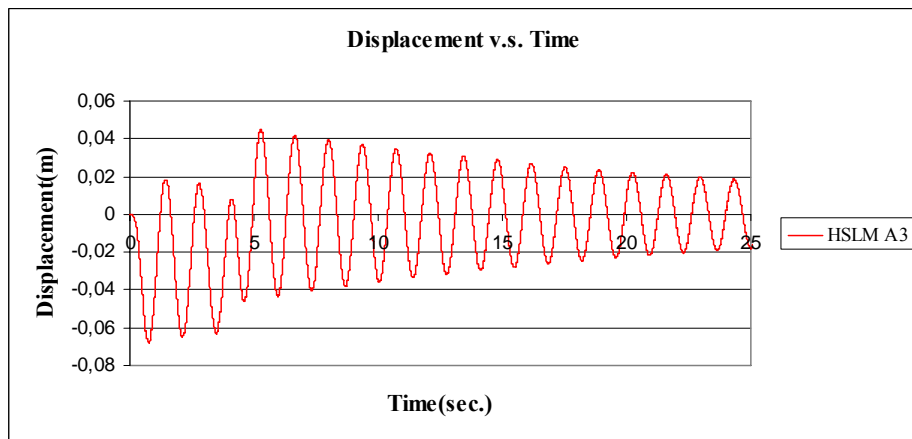


Figure C.31 Displacement v.s. Time graph, (Analysis 6, $V = 97.22$ m/s)

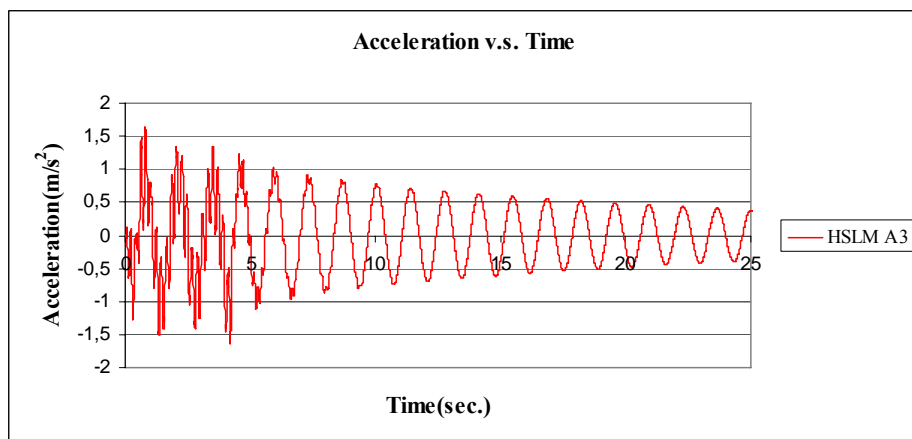


Figure C.32 Acceleration v.s. Time graph, (Analysis 6, $V = 97.22$ m/s)

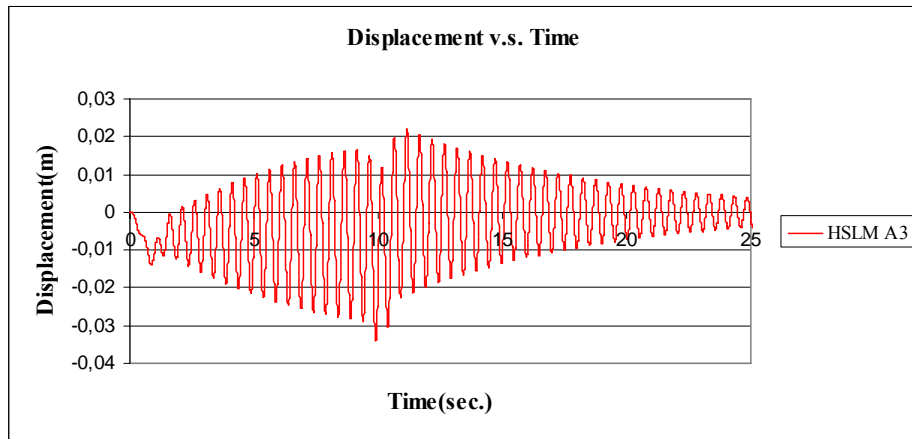


Figure C.33 Displacement v.s. Time graph, (Analysis7, V = 40 m/s)

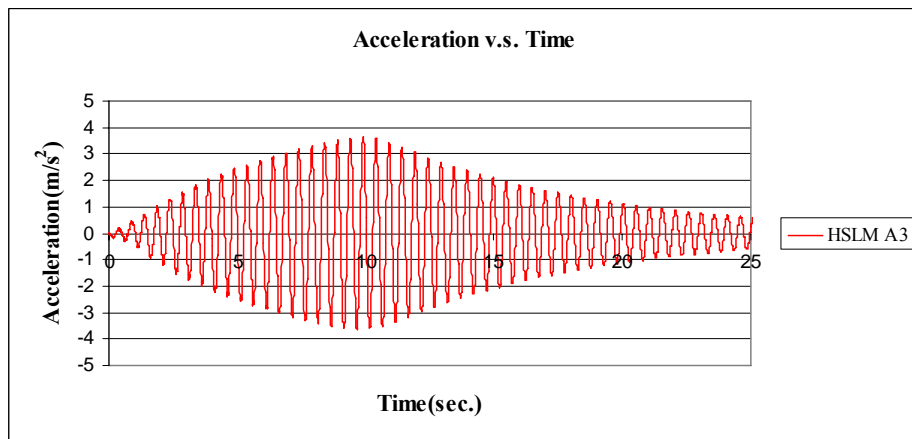


Figure C.34 Acceleration v.s. Time graph, (Analysis 7, V = 40 m/s)

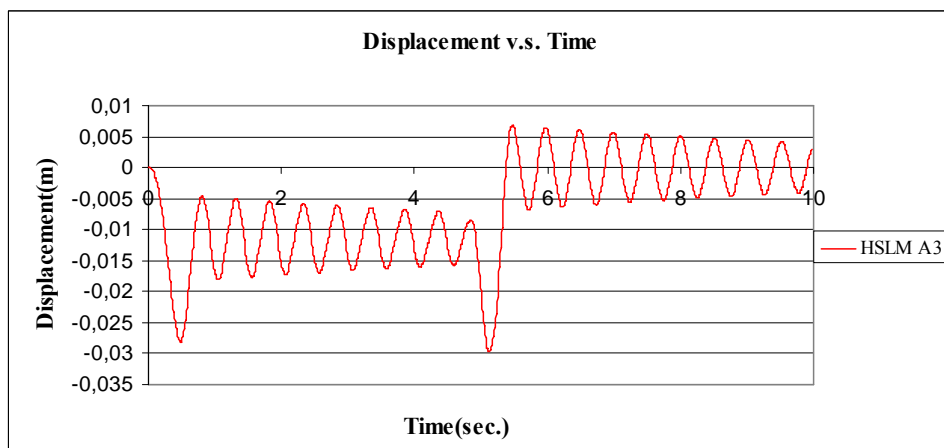


Figure C.35 Displacement v.s. Time graph, (Analysis7, V = 78.91 m/s)

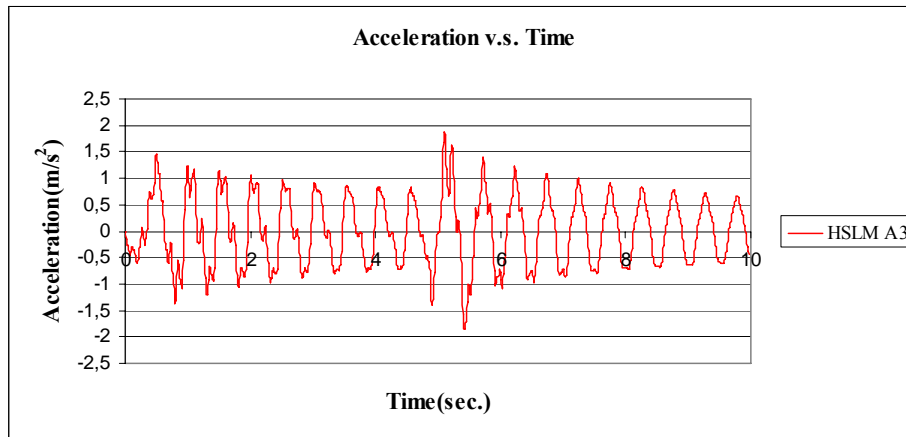


Figure C.36 Acceleration v.s. Time graph, (Analysis 7, $V = 78.91 \text{ m/s}$)

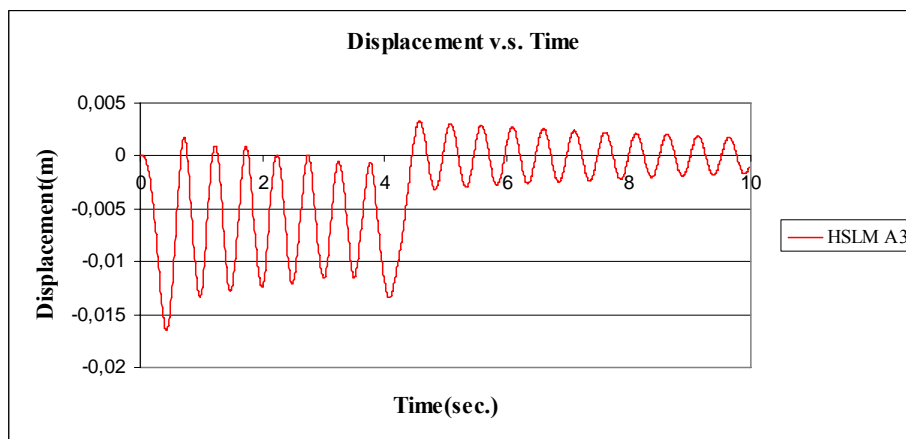


Figure C.37 Displacement v.s. Time graph, (Analysis 7, $V = 97.22 \text{ m/s}$)

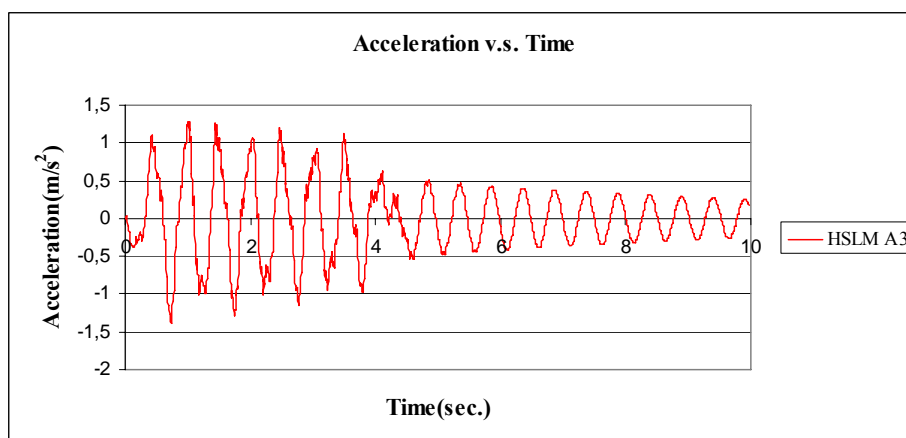


Figure C.38 Acceleration v.s. Time graph, (Analysis 7, $V = 97.22 \text{ m/s}$)

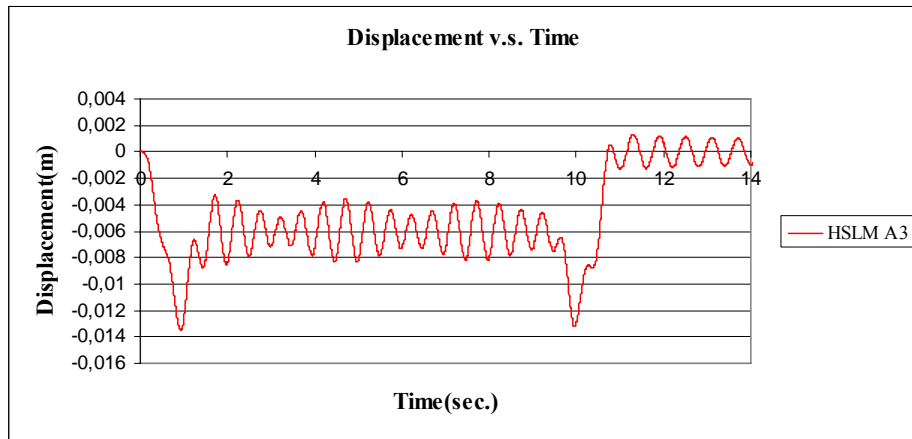


Figure C.39 Displacement v.s. Time graph, (Analysis 8, V = 40 m/s)

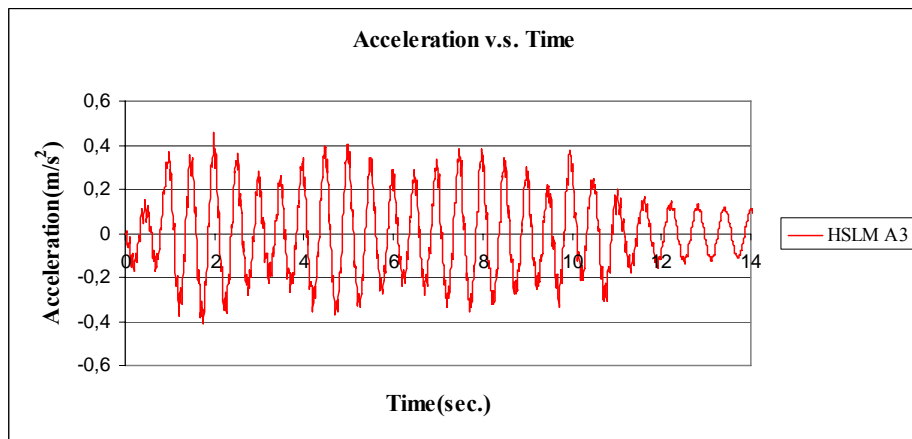


Figure C.40 Acceleration v.s. Time graph, (Analysis 8, V = 40 m/s)

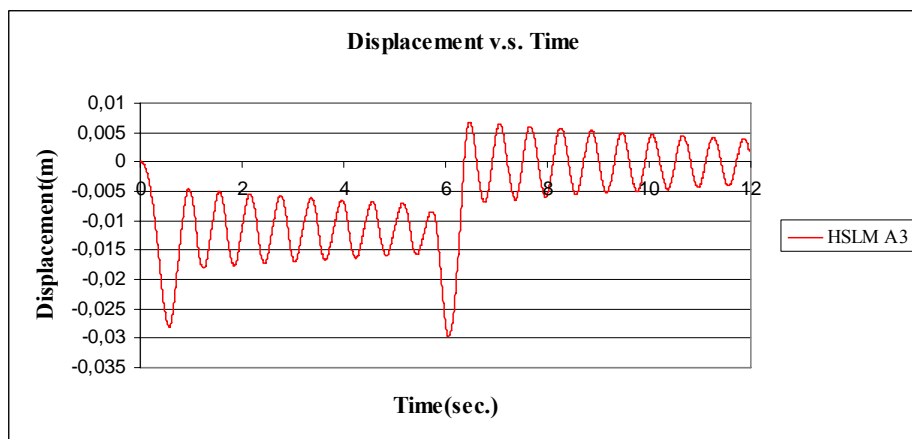


Figure C.41 Displacement v.s. Time graph, (Analysis 8, V = 66.695 m/s)

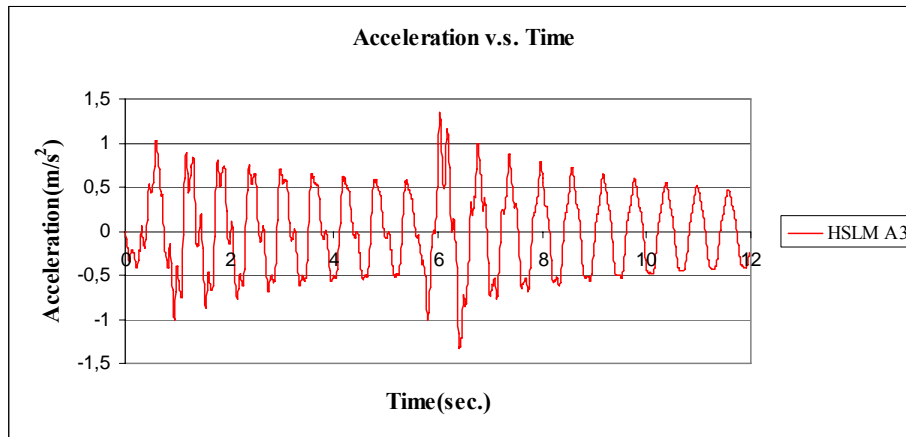


Figure C.42 Acceleration v.s. Time graph, (Analysis 8, $V = 66.695$ m/s)

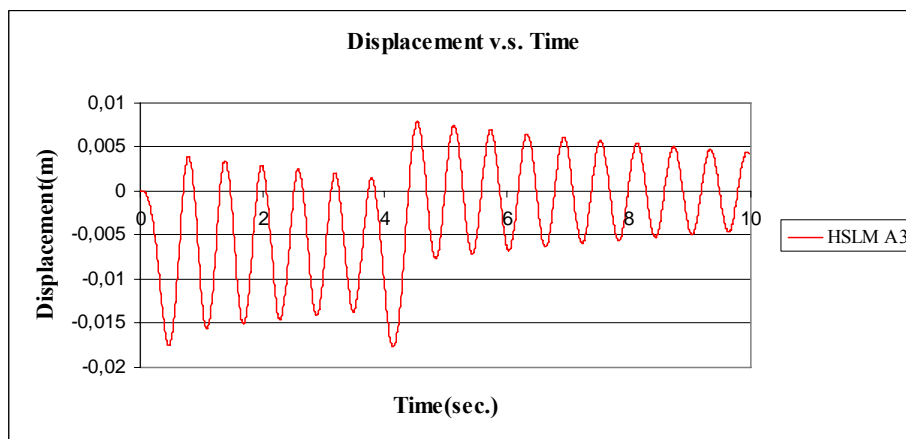


Figure C.43 Displacement v.s. Time graph, (Analysis 8, $V = 97.22$ m/s)

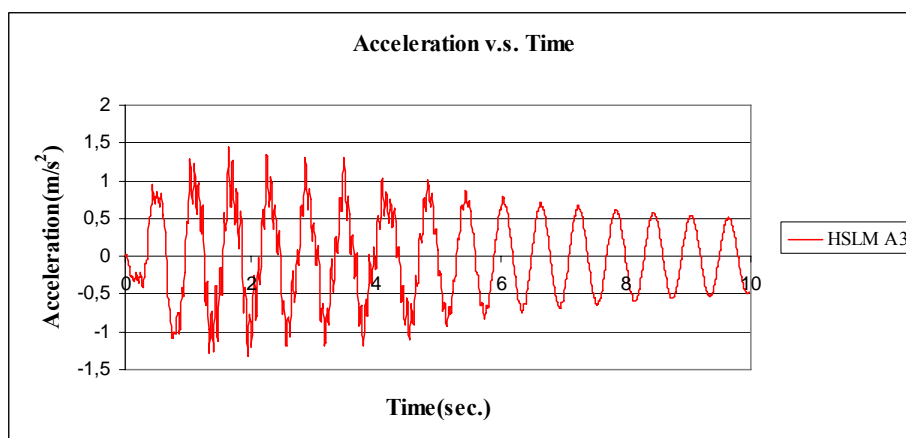


Figure C.44 Acceleration v.s. Time graph, (Analysis 8, $V = 97.22$ m/s)

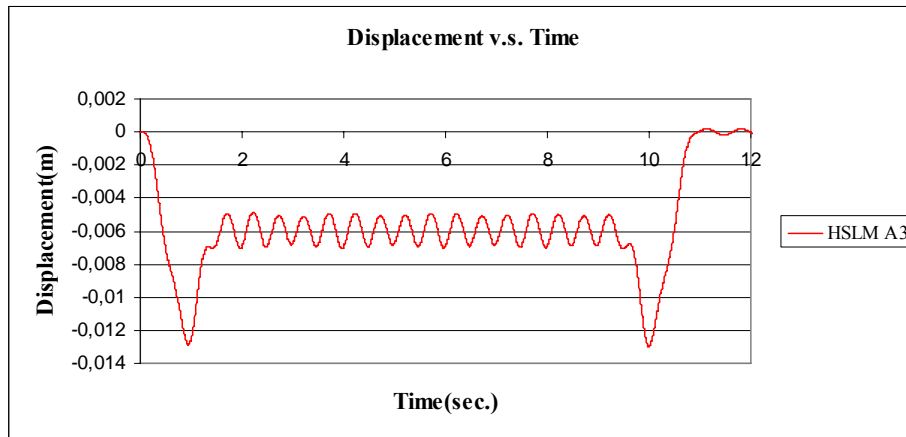


Figure C.45 Displacement v.s. Time graph, (Analysis 9, V = 40 m/s)

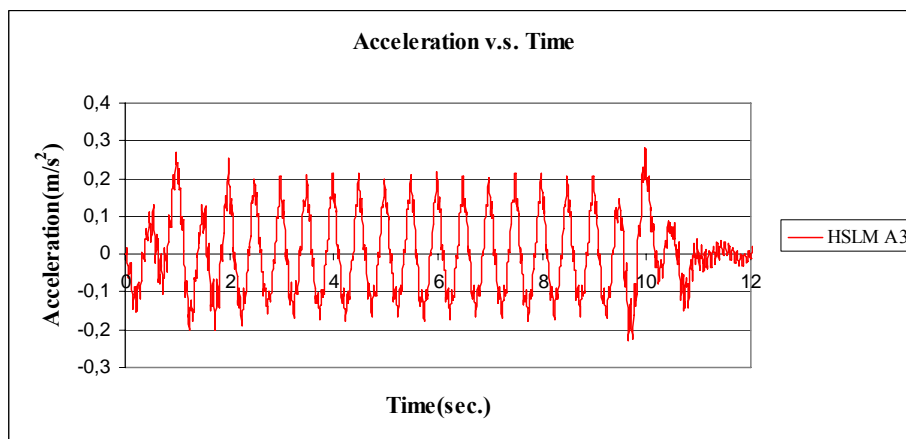


Figure C.46 Acceleration v.s. Time graph, (Analysis 9, V = 40 m/s)

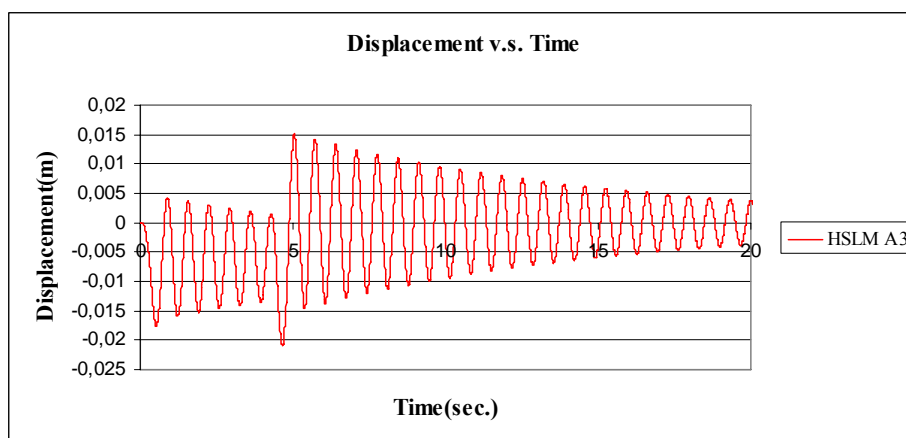


Figure C.47 Displacement v.s. Time graph, (Analysis 9, V = 88.23 m/s)

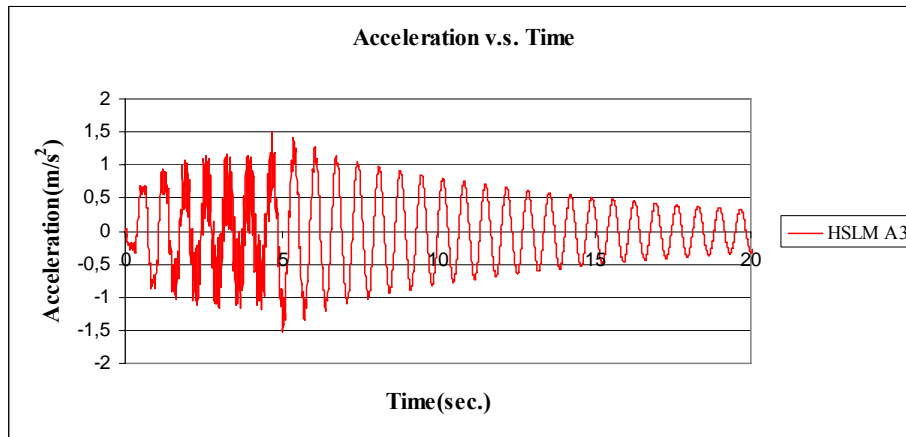


Figure C.48 Acceleration v.s. Time graph, (Analysis 9, $V = 88.23 \text{ m/s}$)

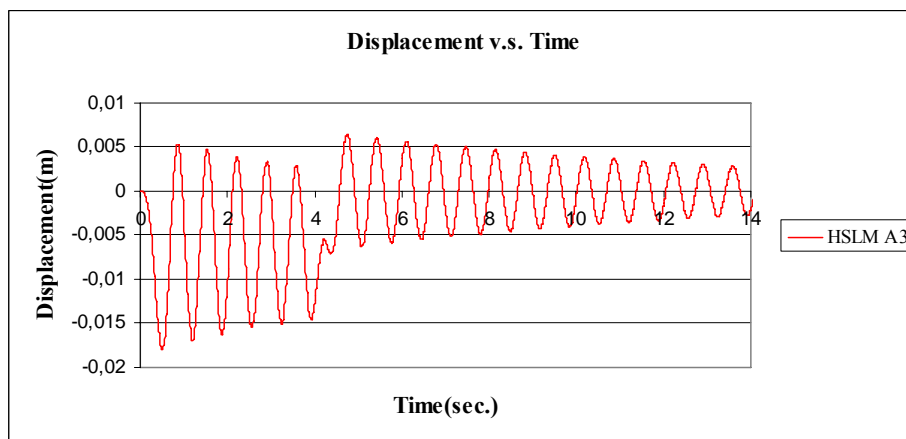


Figure C.49 Displacement v.s. Time graph, (Analysis 9, $V = 97.22 \text{ m/s}$)

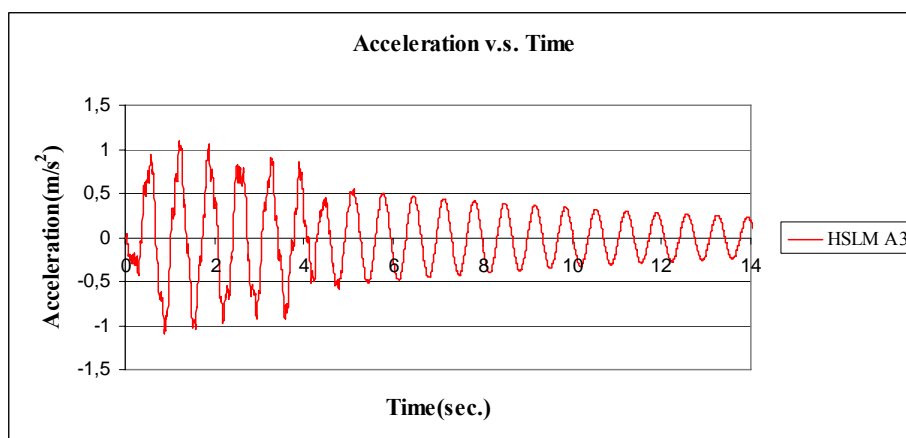


Figure C.50 Acceleration v.s. Time graph, (Analysis 9, $V = 97.22 \text{ m/s}$)

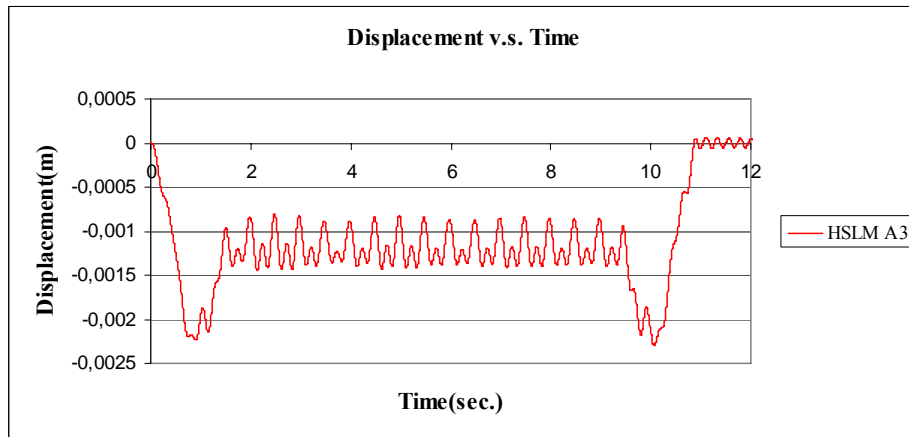


Figure C.51 Displacement v.s. Time graph, (Analysis 10, V = 40 m/s)

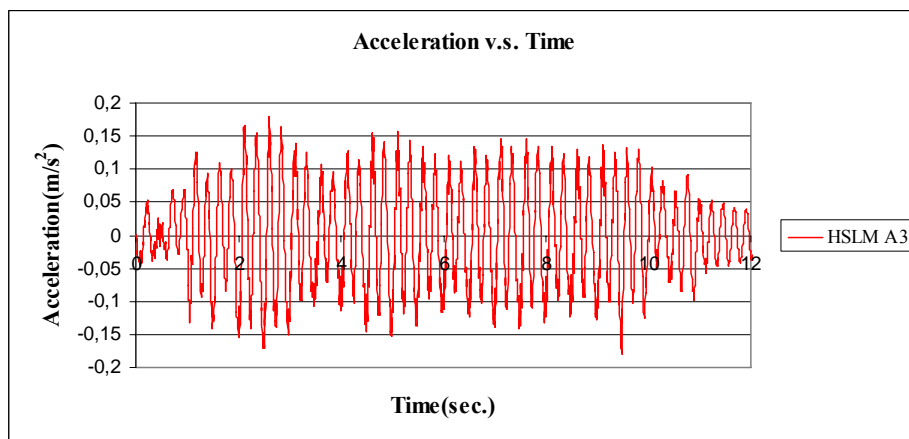


Figure C.52 Acceleration v.s. Time graph, (Analysis 10, V = 40 m/s)

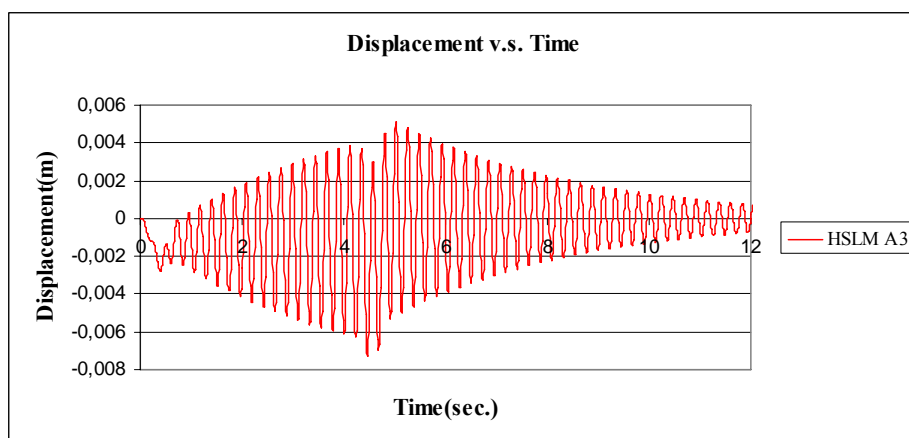


Figure C.53 Displacement v.s. Time graph, (Analysis 10, V = 88.22 m/s)

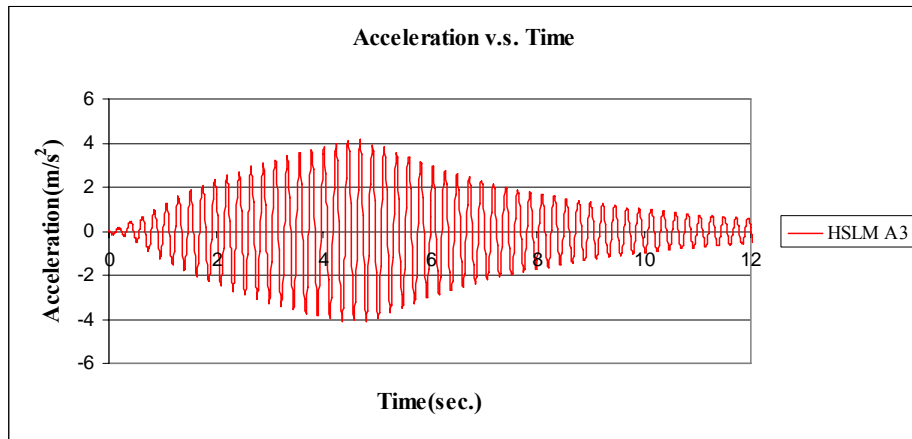


Figure C.54 Acceleration v.s. Time graph, (Analysis 10, V = 88.22 m/s)

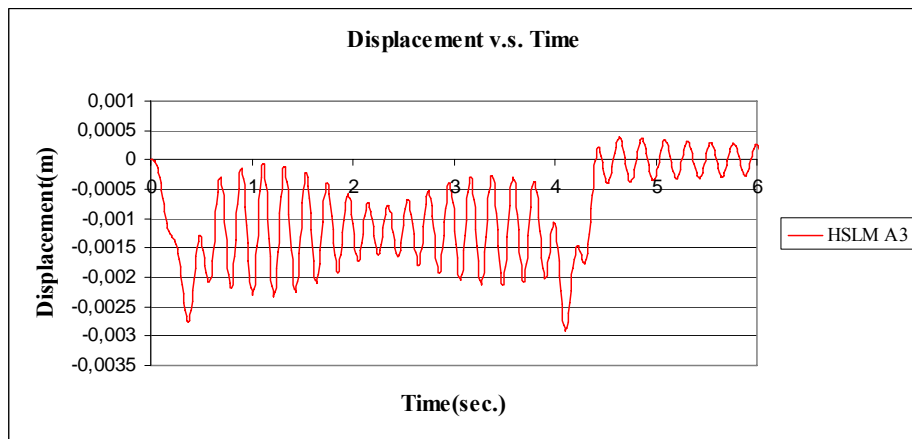


Figure C.55 Displacement v.s. Time graph, (Analysis 10, V = 97.22 m/s)

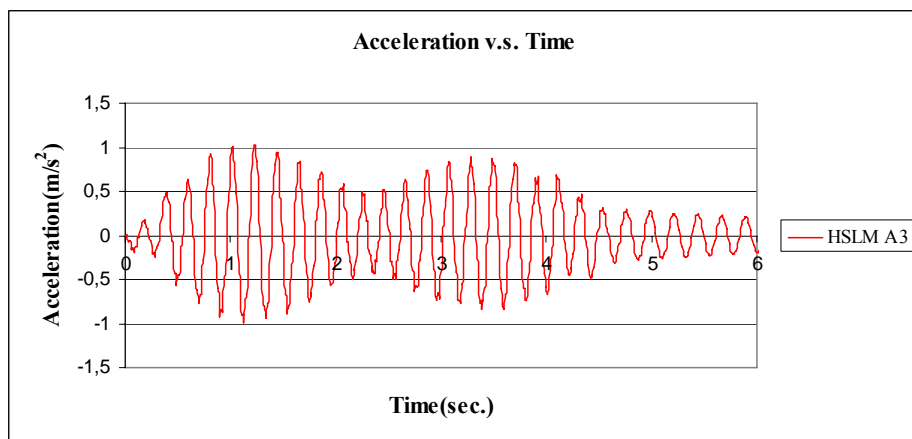


Figure C.56 Acceleration v.s. Time graph, (Analysis 10, V = 97.22 m/s)

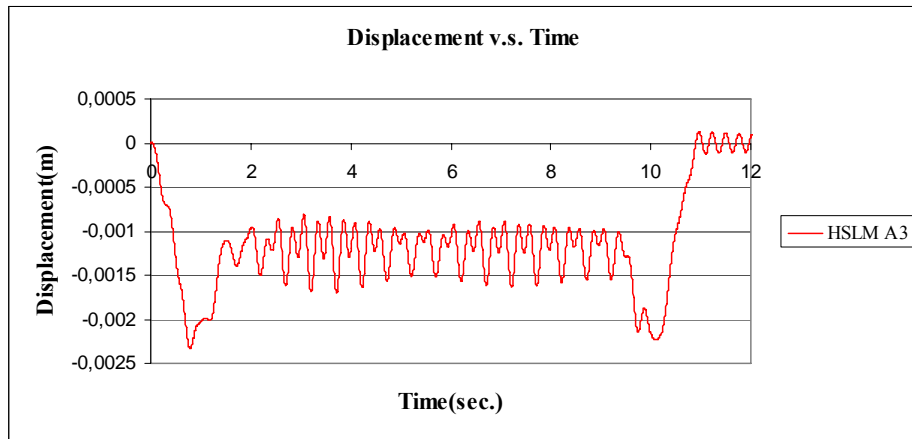


Figure C.57 Displacement v.s. Time graph, (Analysis 11, V = 40 m/s)

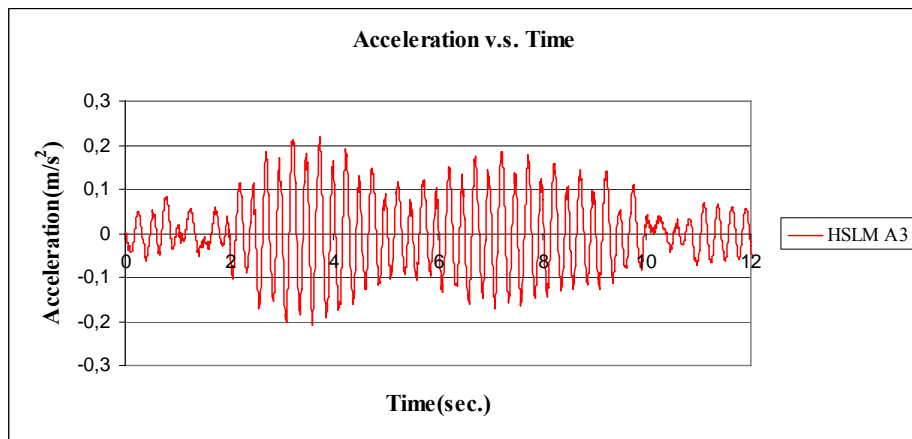


Figure C.58 Acceleration v.s. Time graph, (Analysis 11, V = 40 m/s)

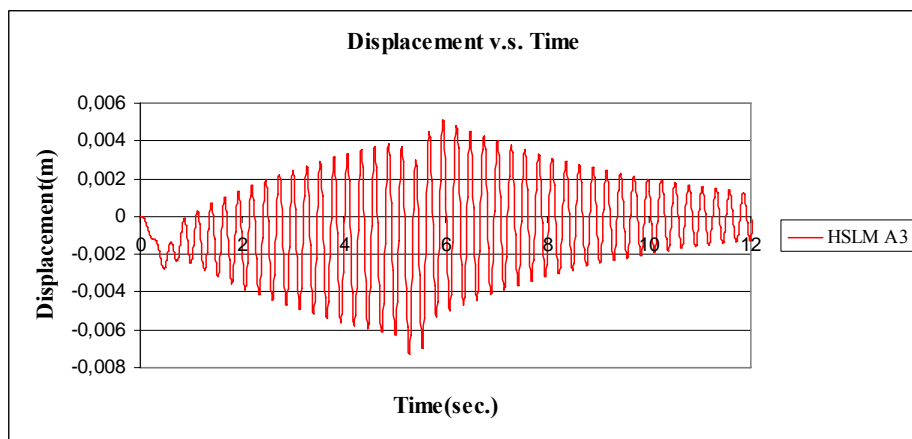


Figure C.59 Displacement v.s. Time graph, (Analysis 11, V = 74.56 m/s)

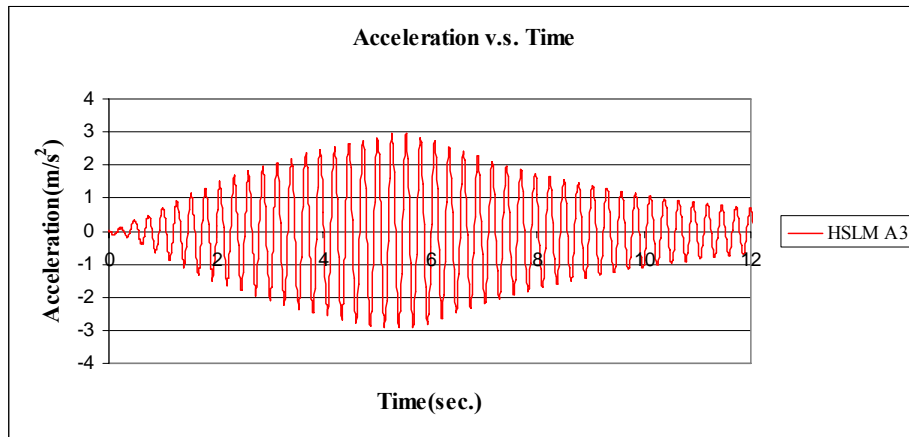


Figure C.60 Acceleration v.s. Time graph, (Analysis 11, $V = 74.56$ m/s)

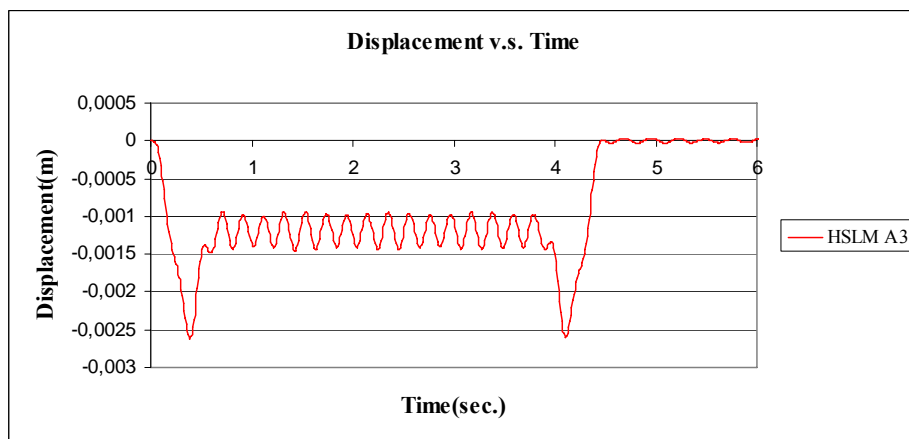


Figure C.61 Displacement v.s. Time graph, (Analysis 11, $V = 97.22$ m/s)

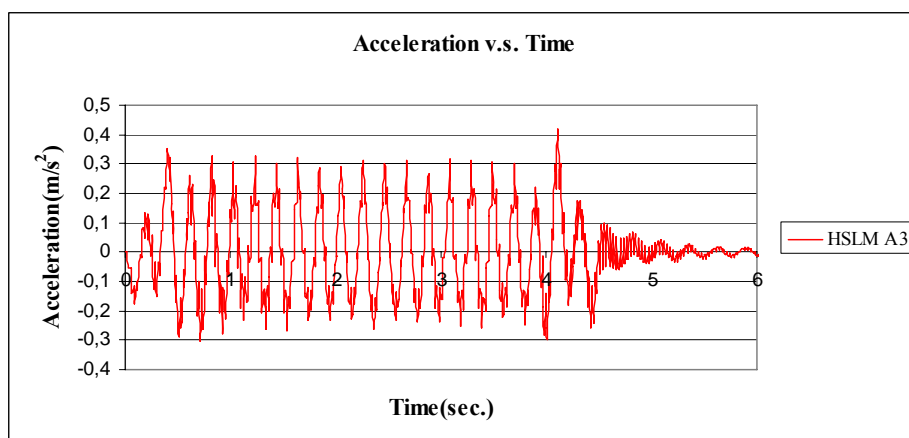


Figure C.62 Acceleration v.s. Time graph, (Analysis 11, $V = 97.22$ m/s)

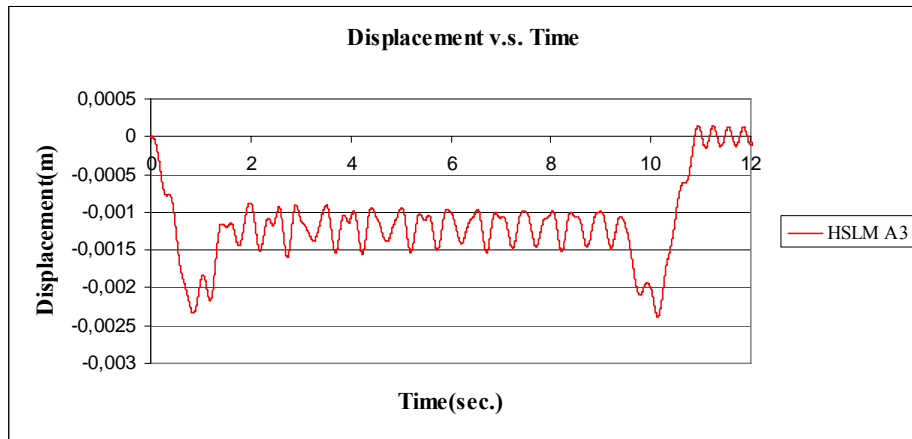


Figure C.63 Displacement v.s. Time graph, (Analysis 12, V = 40 m/s)

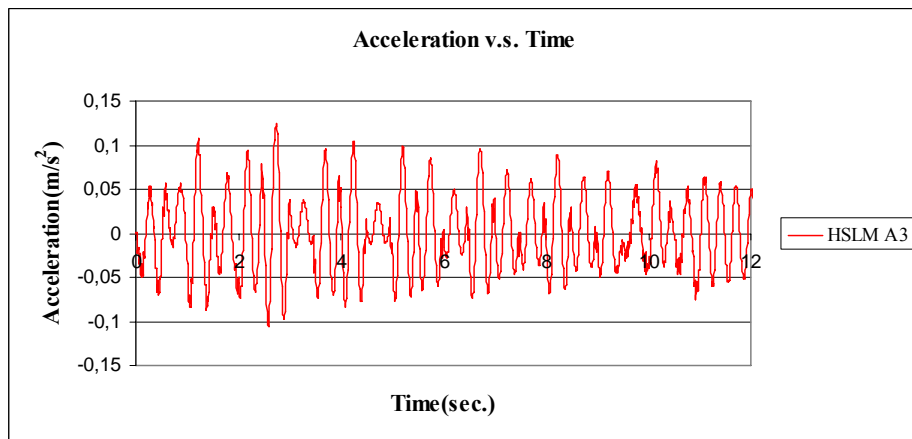


Figure C.64 Acceleration v.s. Time graph, (Analysis 12, V = 40 m/s)

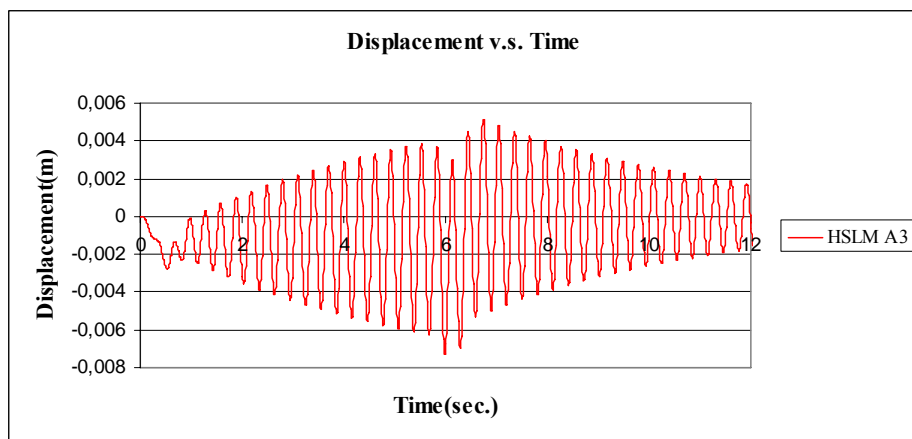


Figure C.65 Displacement v.s. Time graph, (Analysis 12, V = 65.80 m/s)

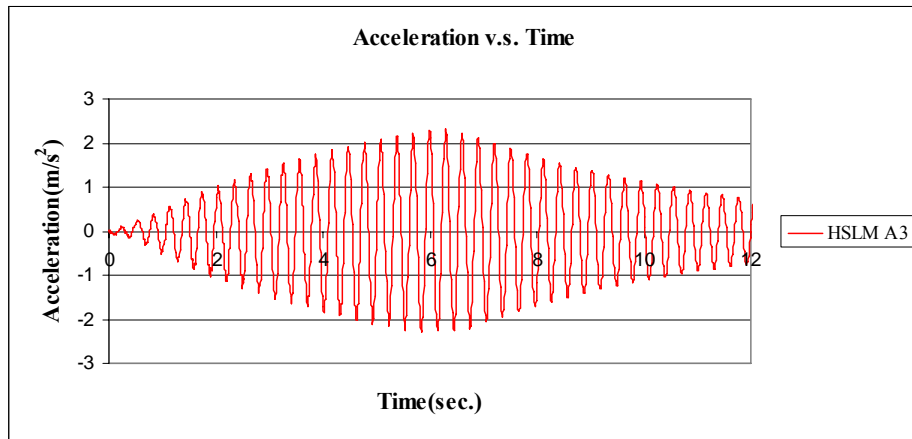


Figure C.66 Acceleration v.s. Time graph, (Analysis 12, V = 65.80 m/s)

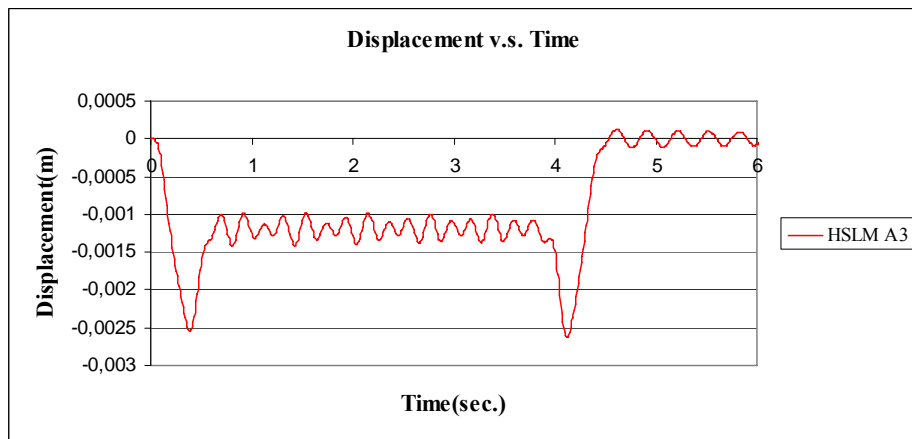


Figure C.67 Displacement v.s. Time graph, (Analysis 12, V = 97.22 m/s)

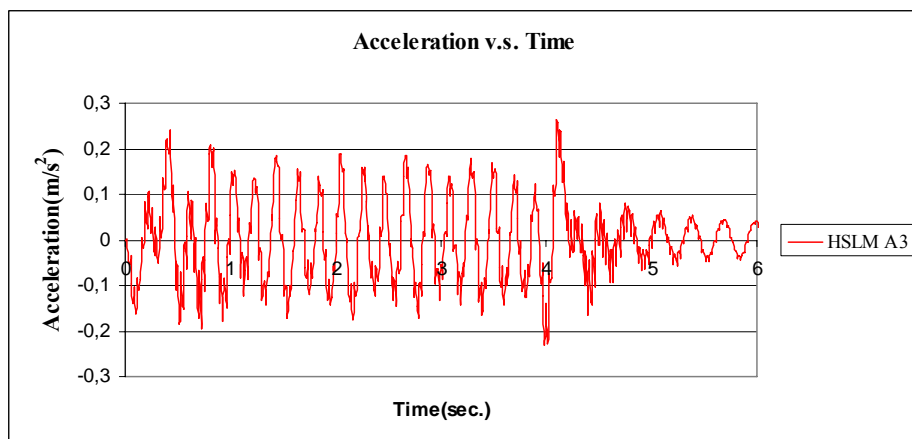


Figure C.68 Acceleration v.s. Time graph, (Analysis 12, V = 97.22 m/s)

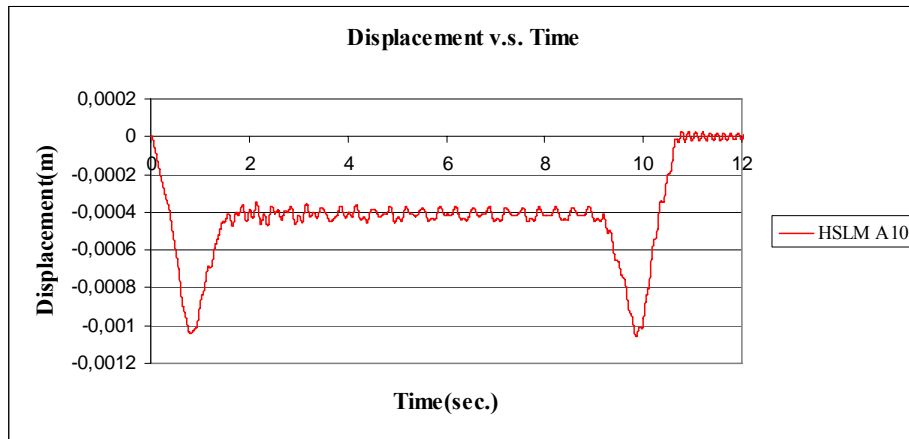


Figure C.69 Displacement v.s. Time graph, (Analysis 13, V = 40 m/s)

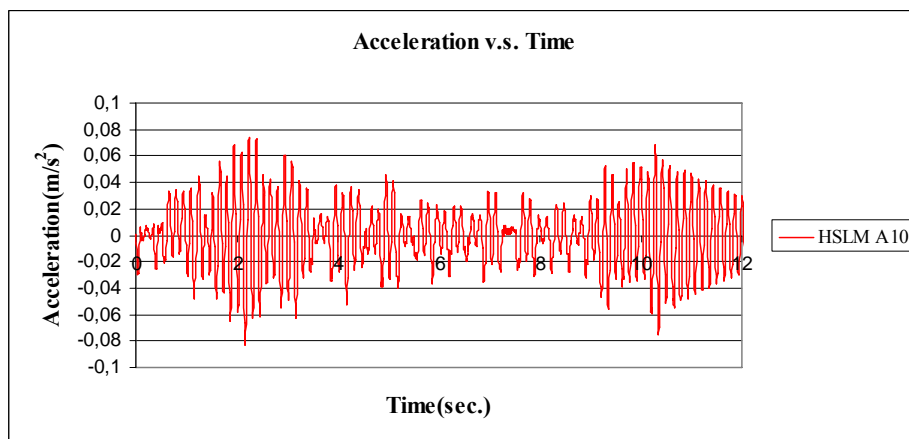


Figure C.70 Acceleration v.s. Time graph, (Analysis 13, V = 40 m/s)

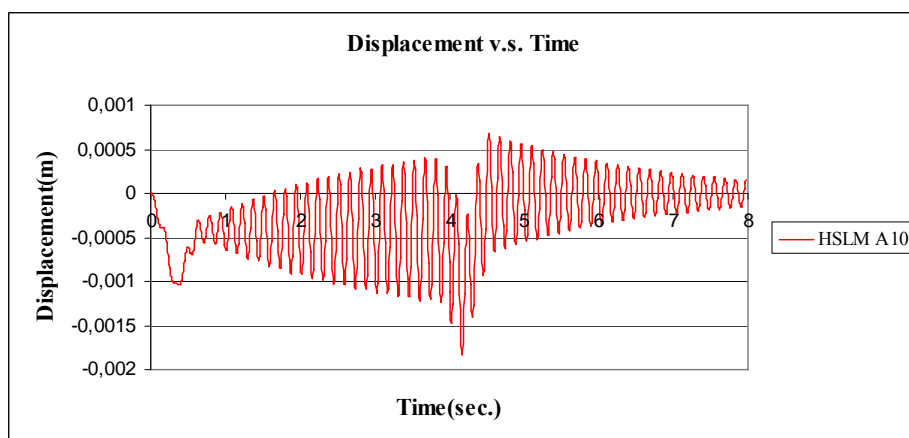


Figure C.71 Displacement v.s. Time graph, (Analysis 13, V = 94.16 m/s)

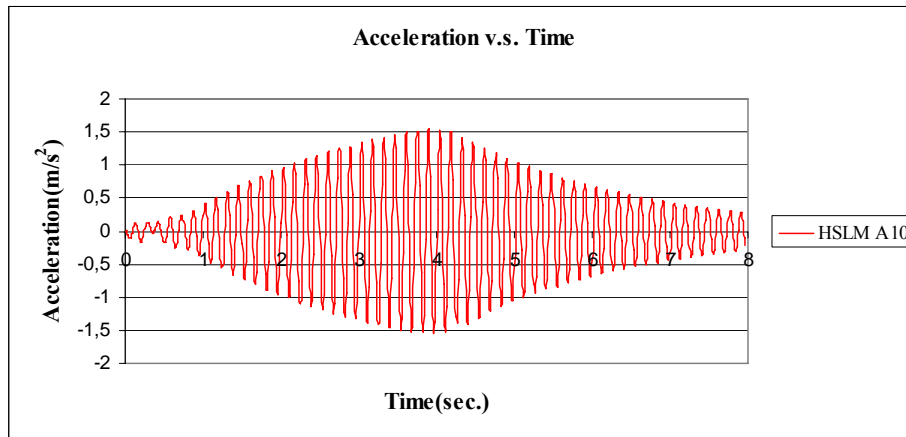


Figure C.72 Acceleration v.s. Time graph, (Analysis 13, $V = 94.16$ m/s)

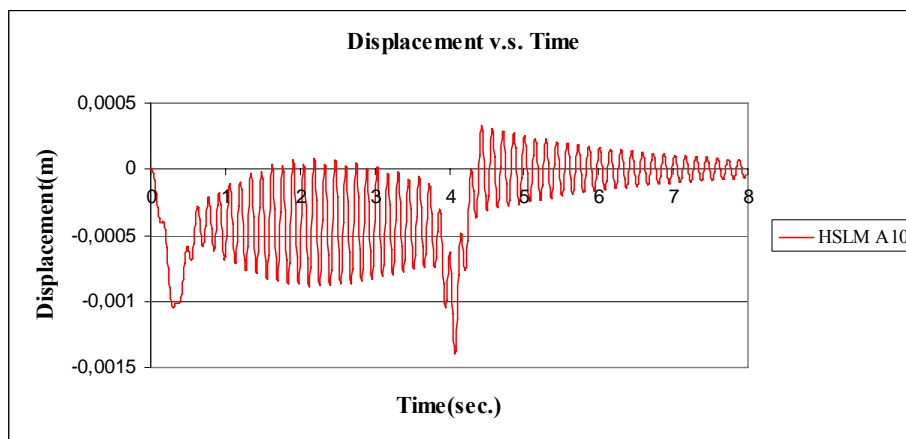


Figure C.73 Displacement v.s. Time graph, (Analysis 13, $V = 97.22$ m/s)

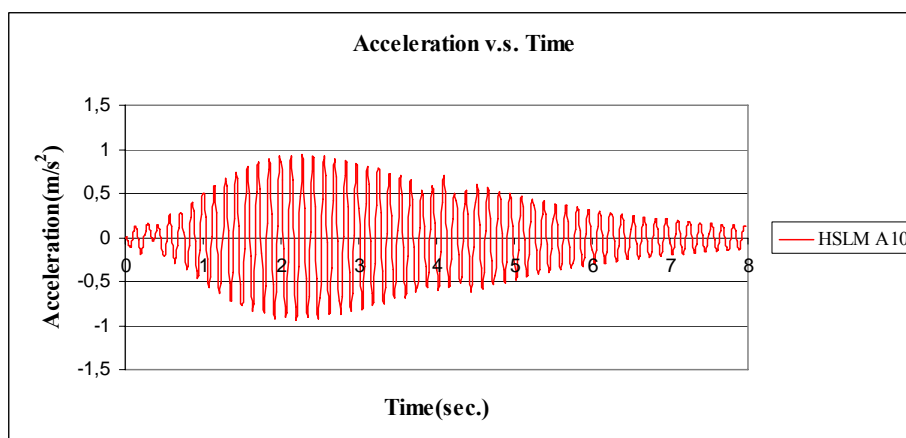


Figure C.74 Acceleration v.s. Time graph, (Analysis 13, $V = 97.22$ m/s)

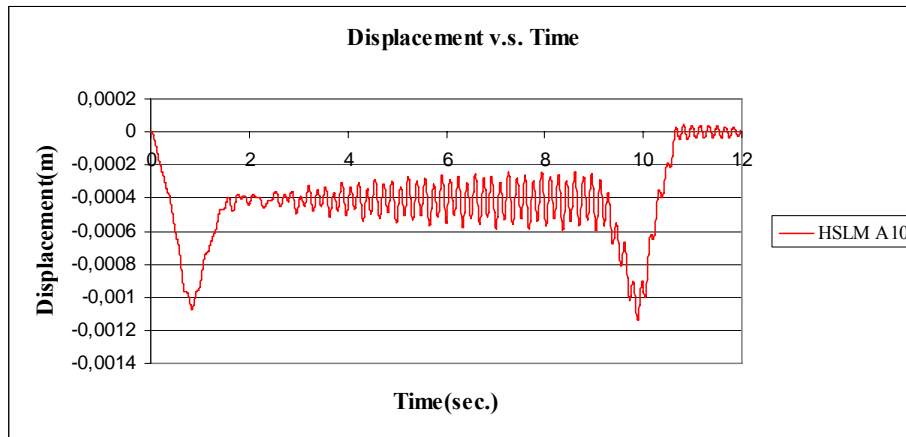


Figure C.75 Displacement v.s. Time graph, (Analysis 14, V = 40 m/s)

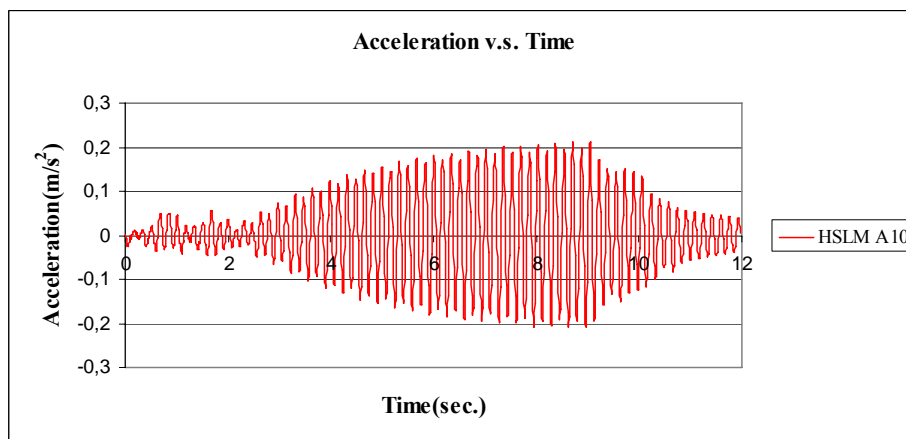


Figure C.76 Acceleration v.s. Time graph, (Analysis 14, V = 40 m/s)

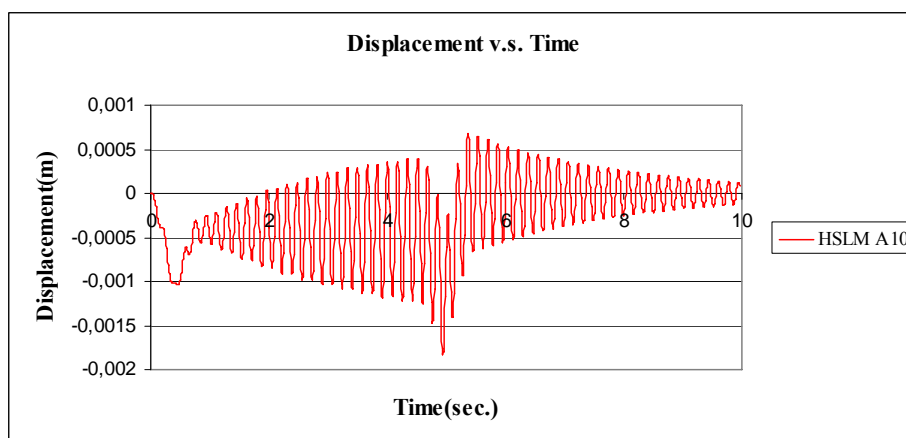


Figure C.77 Displacement v.s. Time graph, (Analysis 14, V = 79.58 m/s)

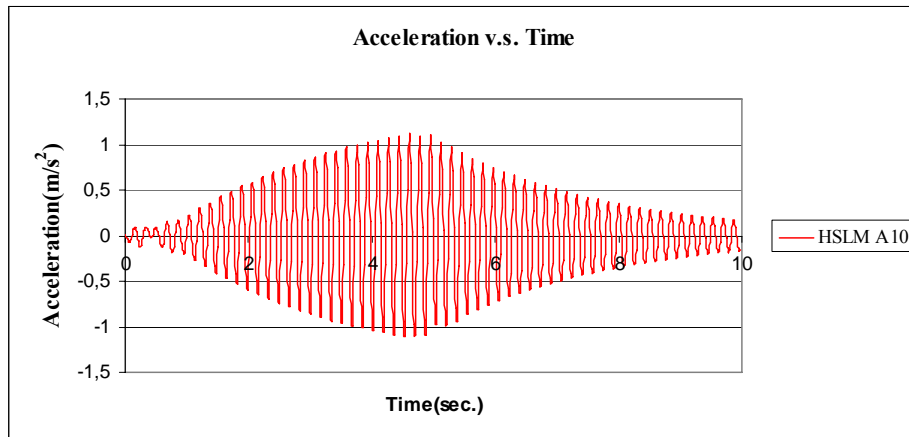


Figure C.78 Acceleration v.s. Time graph, (Analysis 14, V = 79.58 m/s)

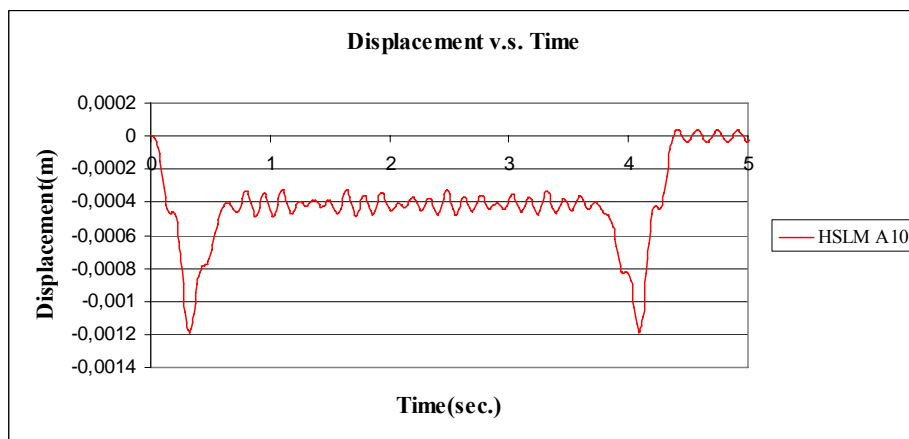


Figure C.79 Displacement v.s. Time graph, (Analysis 14, V = 97.22 m/s)

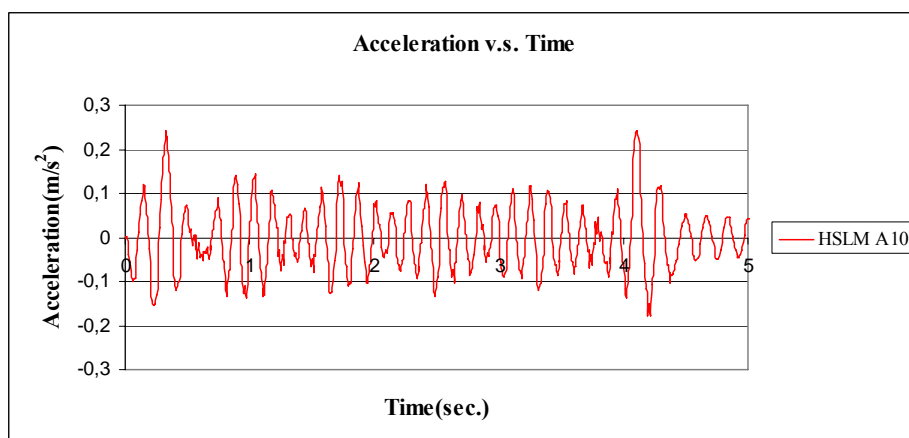


Figure C.80 Acceleration v.s. Time graph, (Analysis 14, V = 97.22 m/s)

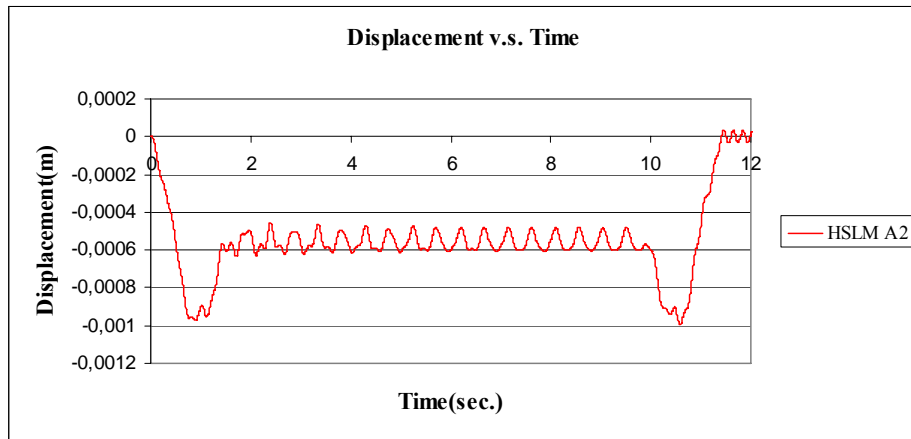


Figure C.81 Displacement v.s. Time graph, (Analysis 15, $V = 40$ m/s)

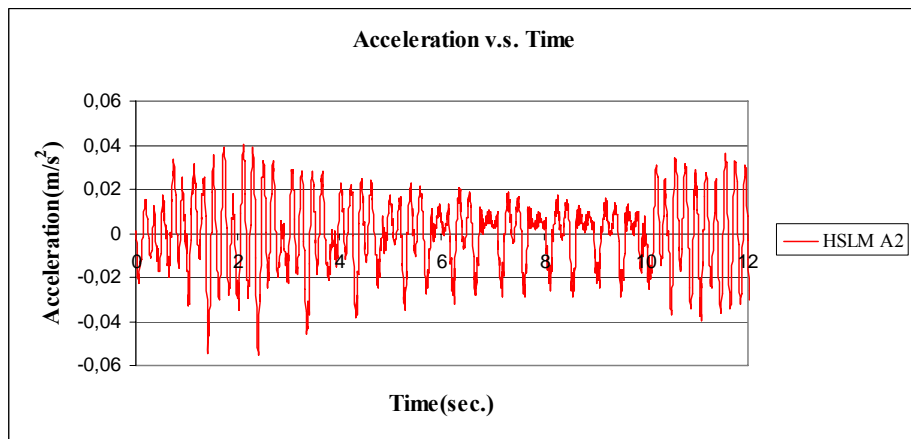


Figure C.82 Acceleration v.s. Time graph, (Analysis 15, $V = 40$ m/s)

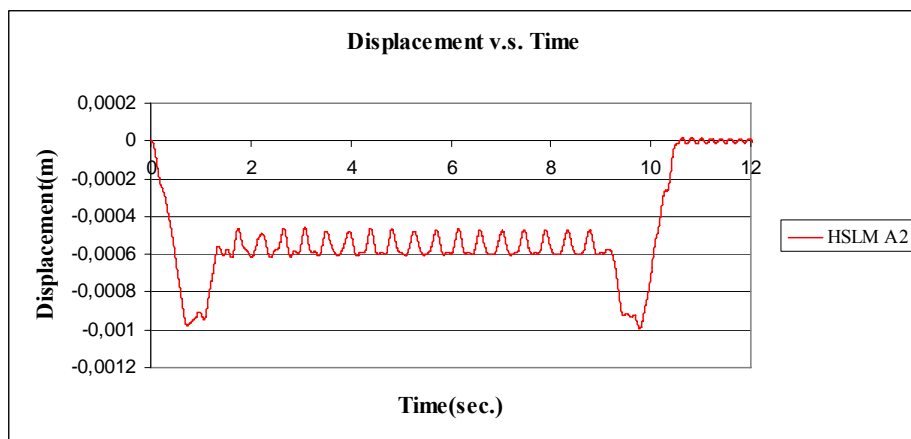


Figure C.83 Displacement v.s. Time graph, (Analysis 15, $V = 49.39$ m/s)

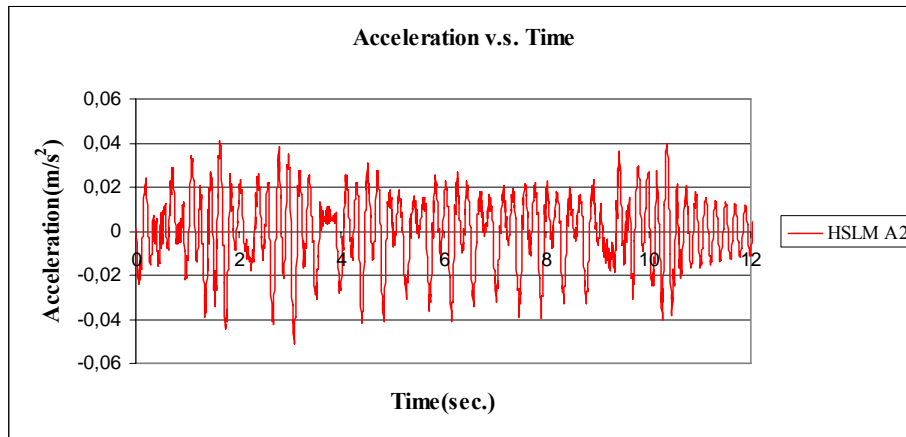


Figure C.84 Acceleration v.s. Time graph, (Analysis 15, V = 49.39 m/s)

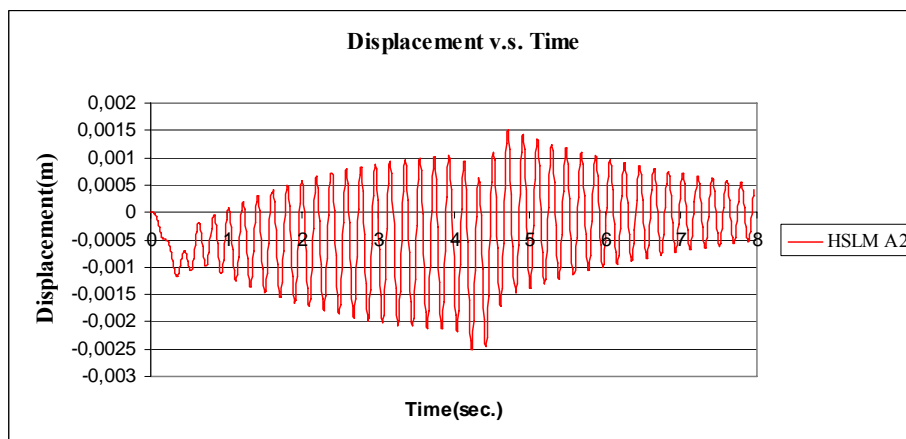


Figure C.85 Displacement v.s. Time graph, (Analysis 15, V = 97.22 m/s)

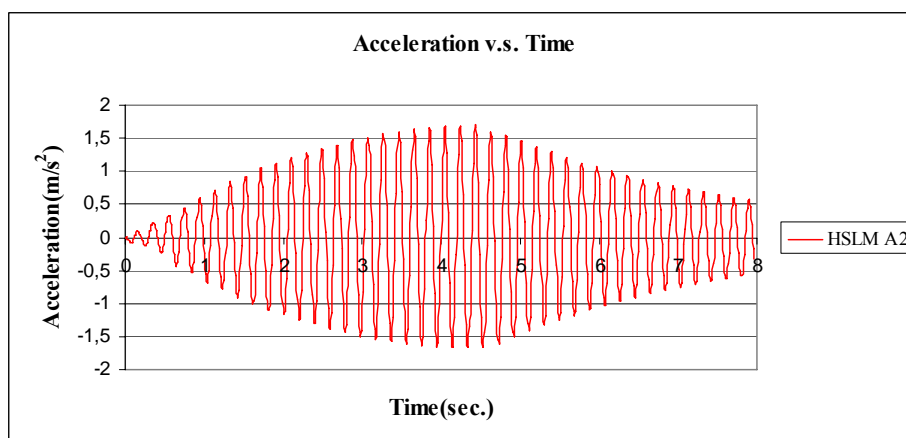


Figure C.86 Acceleration v.s. Time graph, (Analysis 15, V = 97.22 m/s)

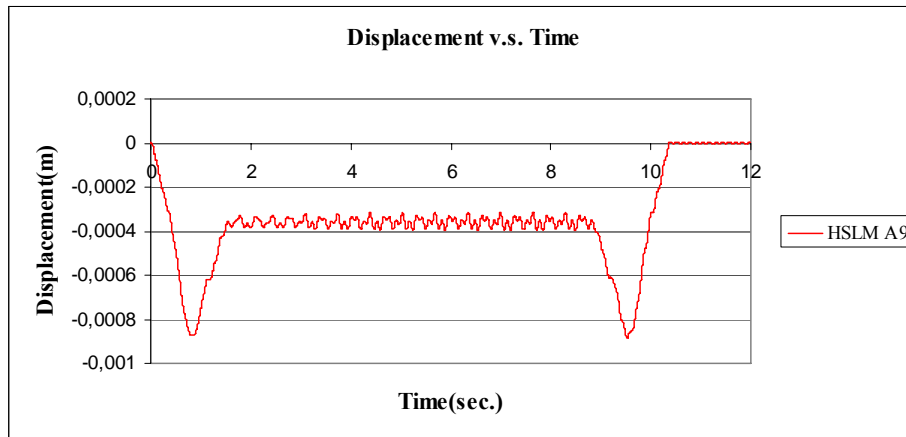


Figure C.87 Displacement v.s. Time graph, (Analysis 16, V = 40 m/s)

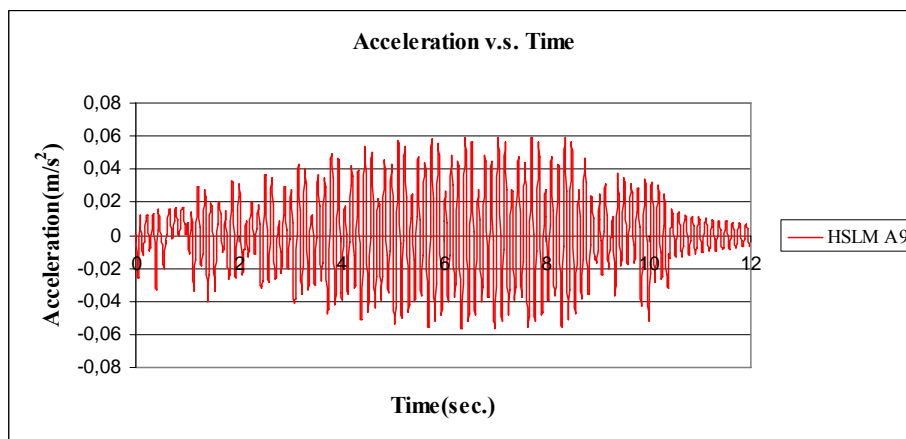


Figure C.88 Acceleration v.s. Time graph, (Analysis 16, V = 40 m/s)

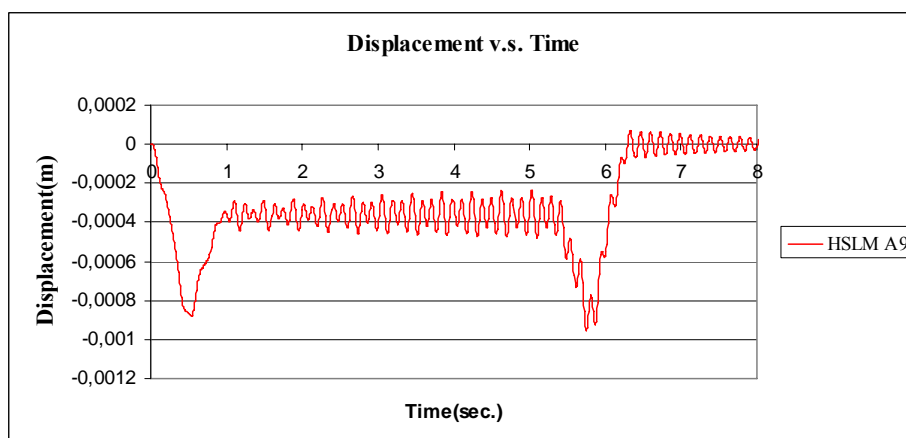


Figure C.89 Displacement v.s. Time graph, (Analysis 16, V = 65.89 m/s)

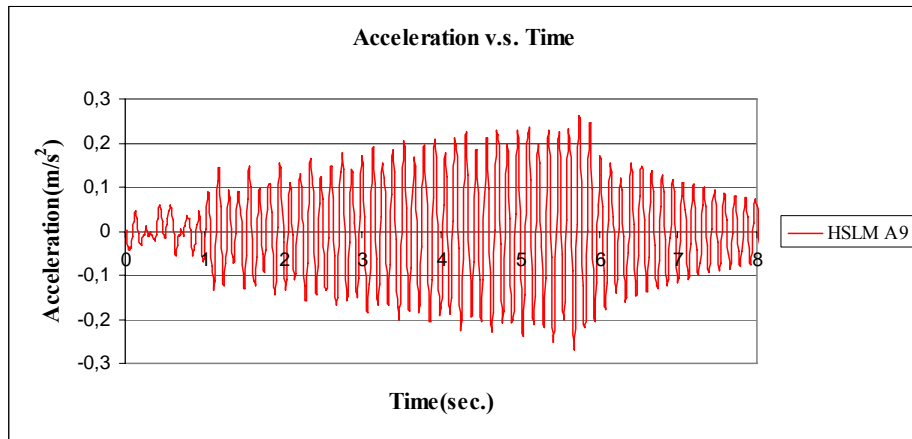


Figure C.90 Acceleration v.s. Time graph, (Analysis 16, $V = 65.89$ m/s)

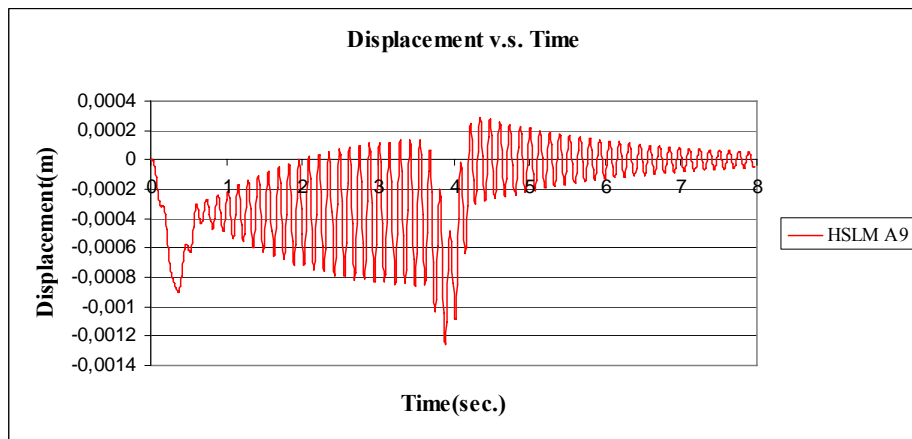


Figure C.91 Displacement v.s. Time graph, (Analysis 16, $V = 97.22$ m/s)

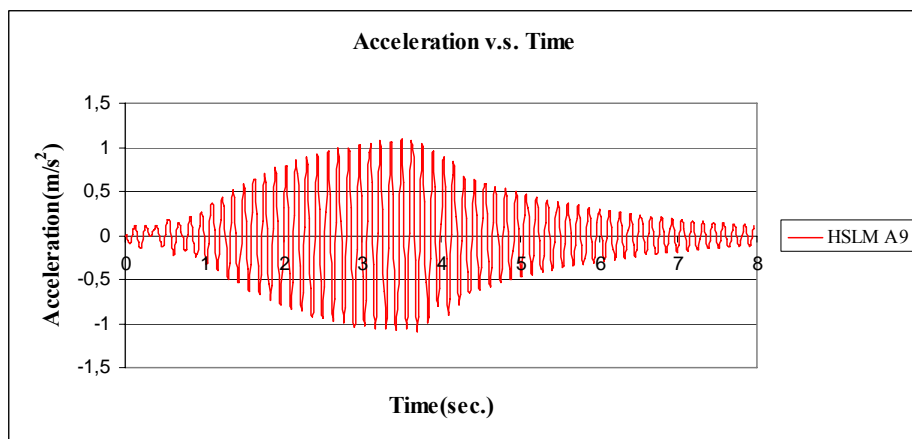


Figure C.92 Acceleration v.s. Time graph, (Analysis 16, $V = 97.22$ m/s)

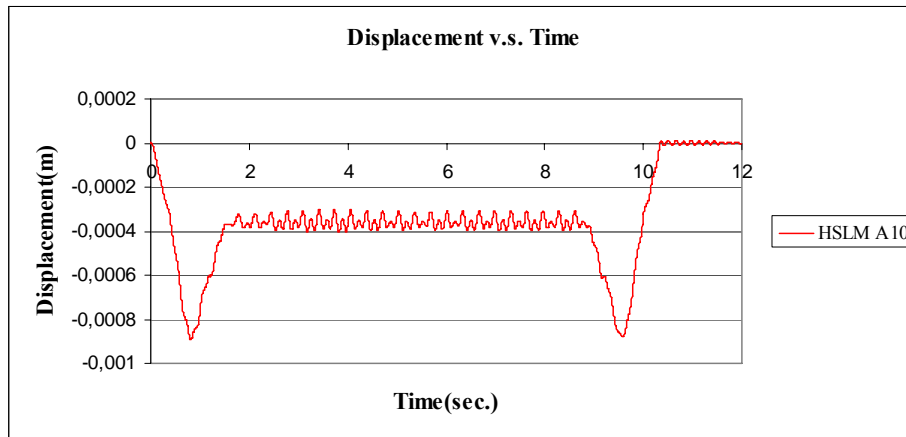


Figure C.93 Displacement v.s. Time graph, (Analysis 17, V = 40 m/s)

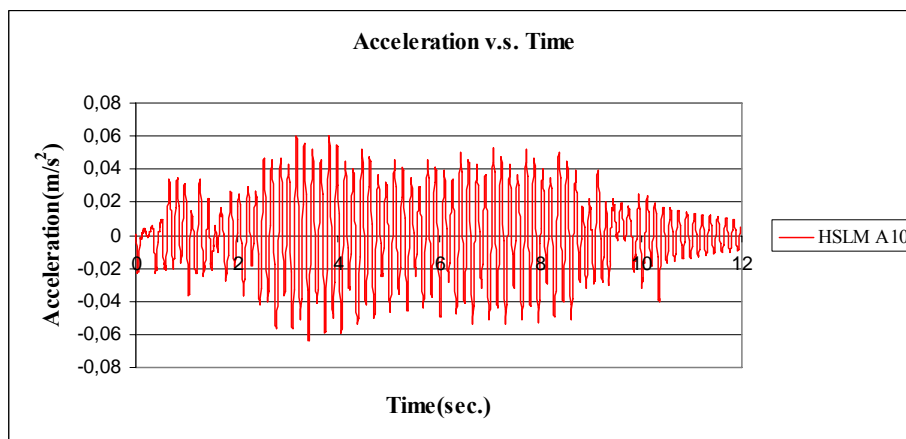


Figure C.94 Acceleration v.s. Time graph, (Analysis 17, V = 40 m/s)

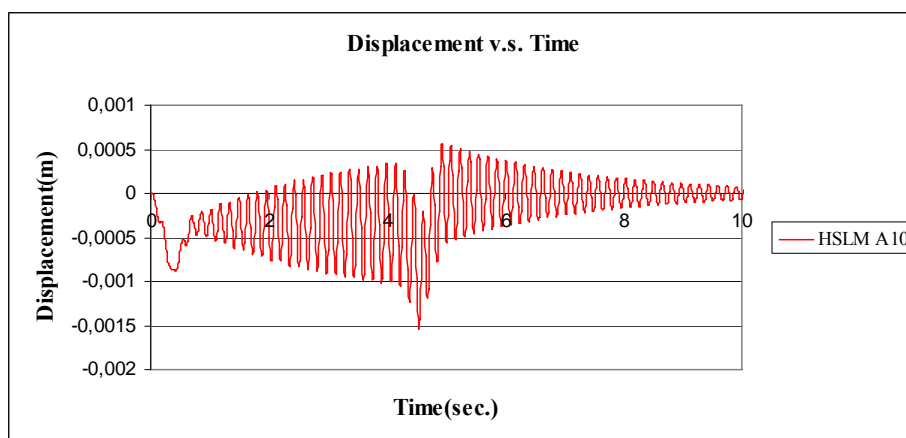


Figure C.95 Displacement v.s. Time graph, (Analysis 17, V = 86.74 m/s)

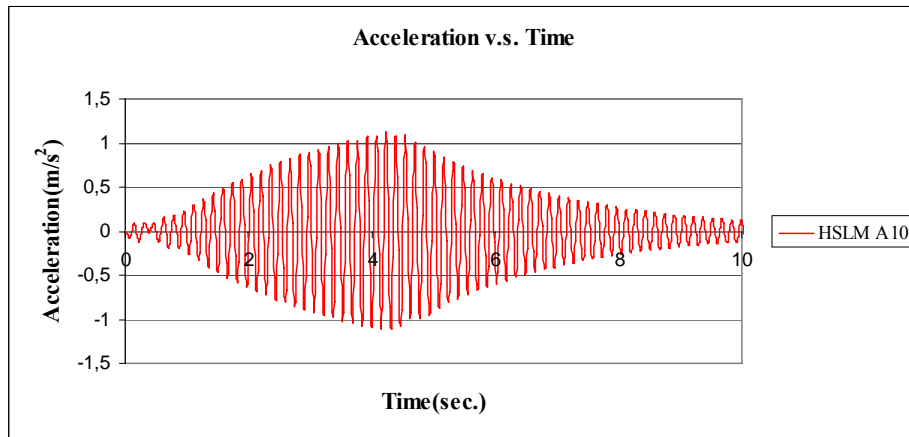


Figure C.96 Acceleration v.s. Time graph, (Analysis 17, $V = 86.74$ m/s)

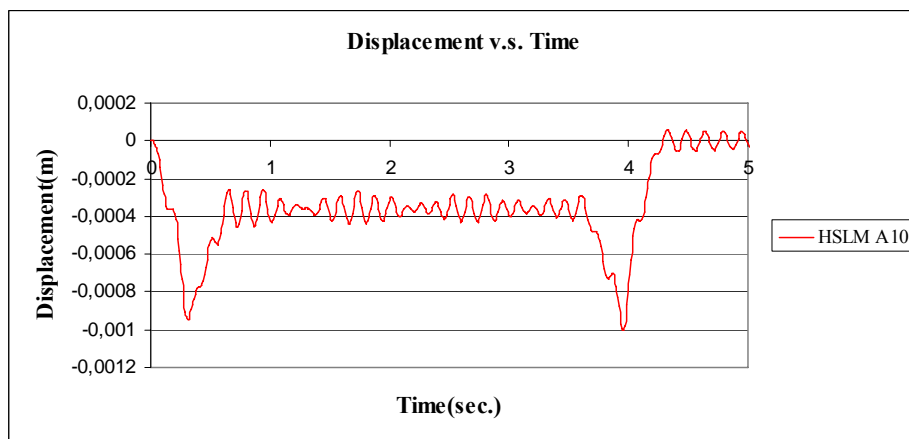


Figure C.97 Displacement v.s. Time graph, (Analysis 17, $V = 97.22$ m/s)

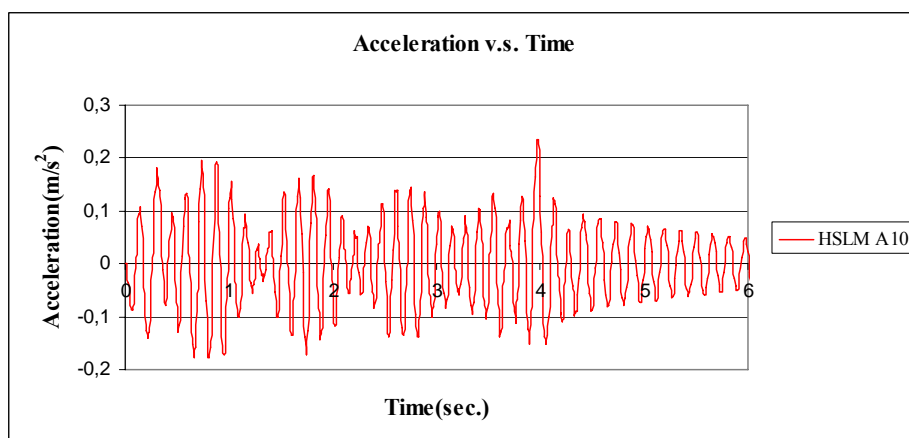


Figure C.98 Acceleration v.s. Time graph, (Analysis 17, $V = 97.22$ m/s)

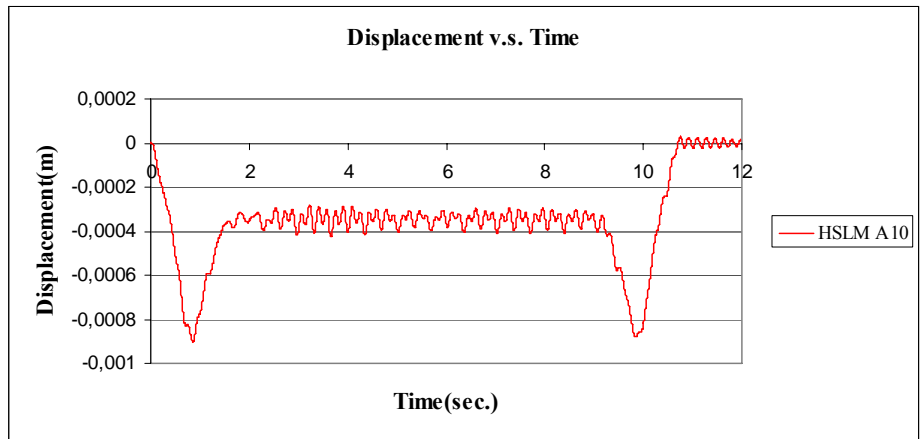


Figure C.99 Displacement v.s. Time graph, (Analysis 18, V = 40 m/s)

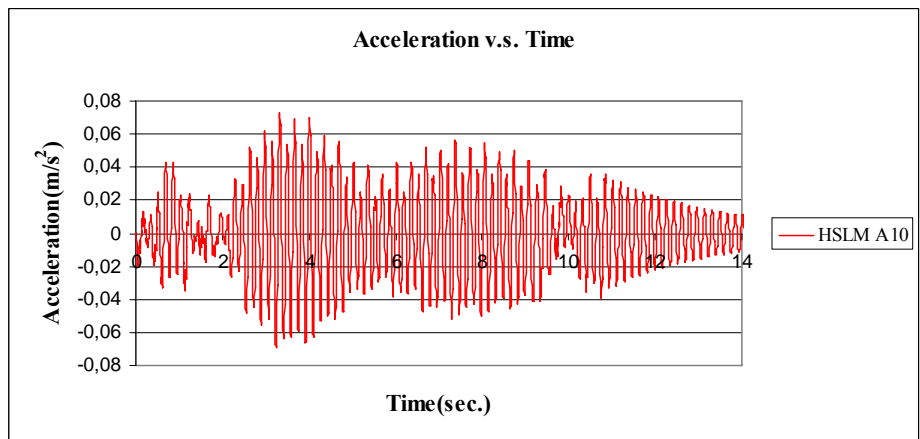


Figure C.100 Acceleration v.s. Time graph, (Analysis 18, V = 40 m/s)

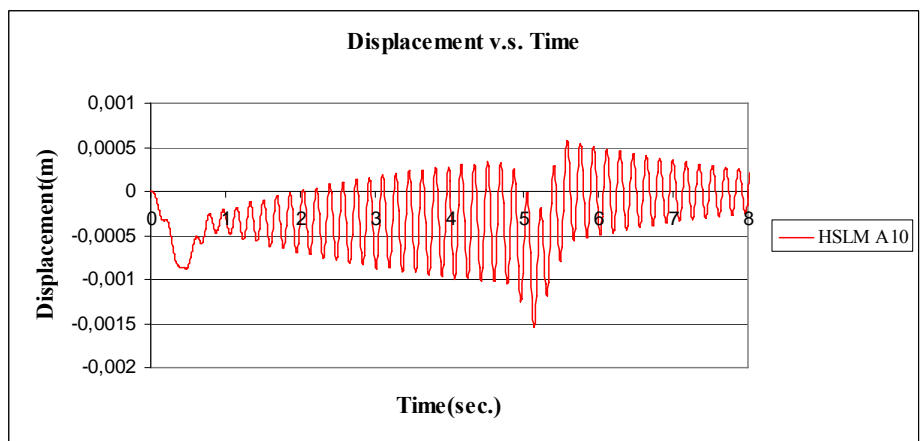


Figure C.101 Displacement v.s. Time graph, (Analysis 18, V = 76.55 m/s)

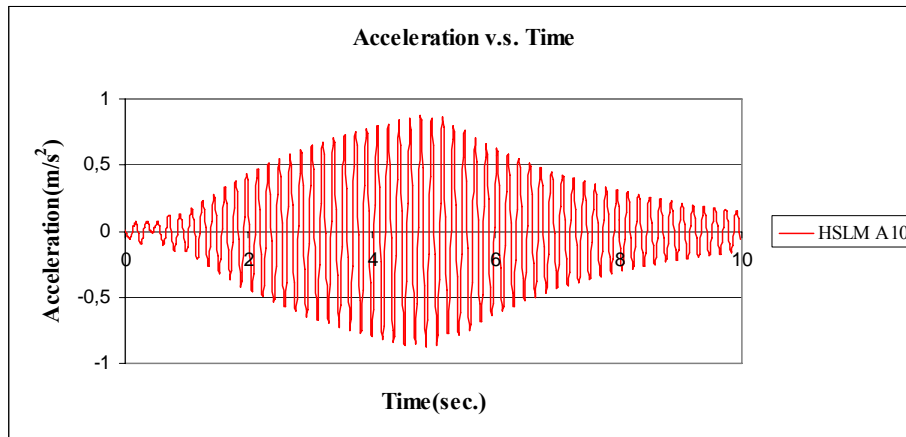


Figure C.102 Acceleration v.s. Time graph, (Analysis 18, $V = 76.55$ m/s)

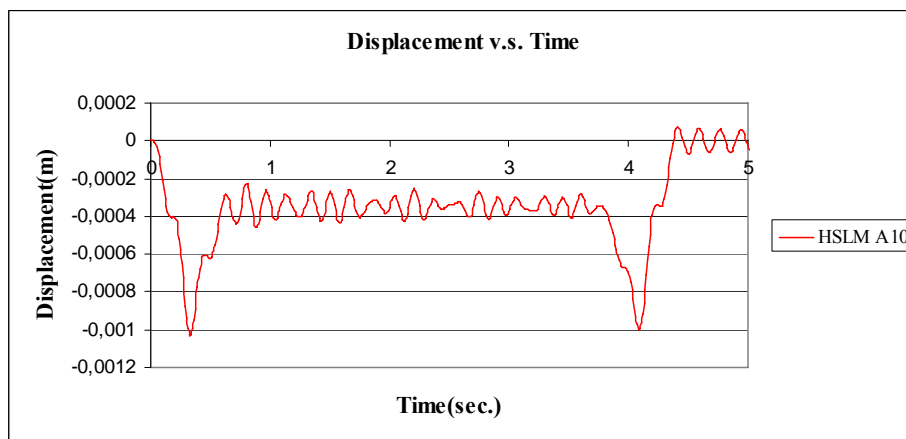


Figure C.103 Displacement v.s. Time graph, (Analysis 18, $V = 97.22$ m/s)

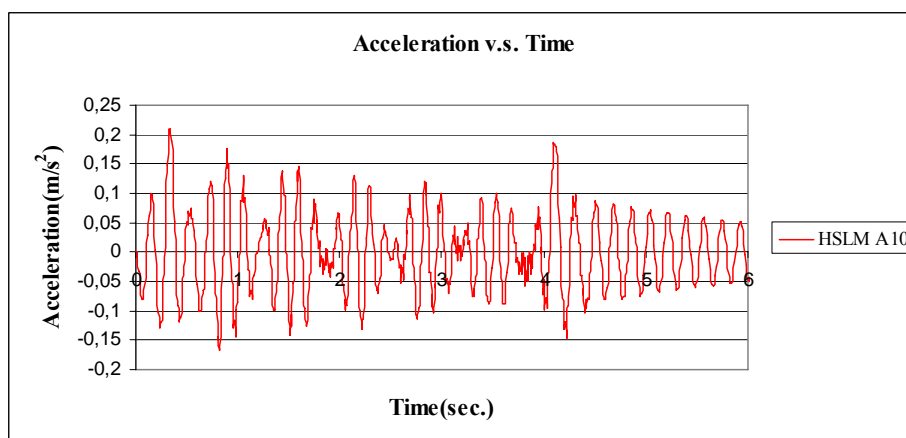


Figure C.103 Acceleration v.s. Time graph, (Analysis 18, $V = 97.22$ m/s)

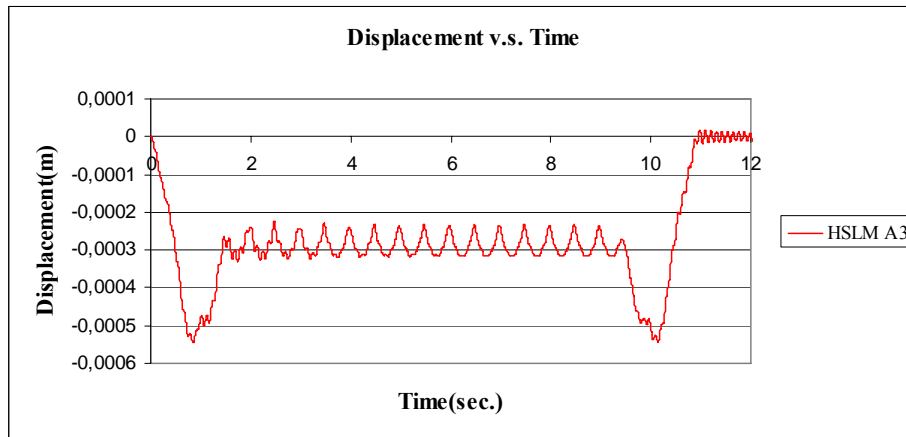


Figure C.104 Displacement v.s. Time graph, (Analysis 19, V = 40 m/s)

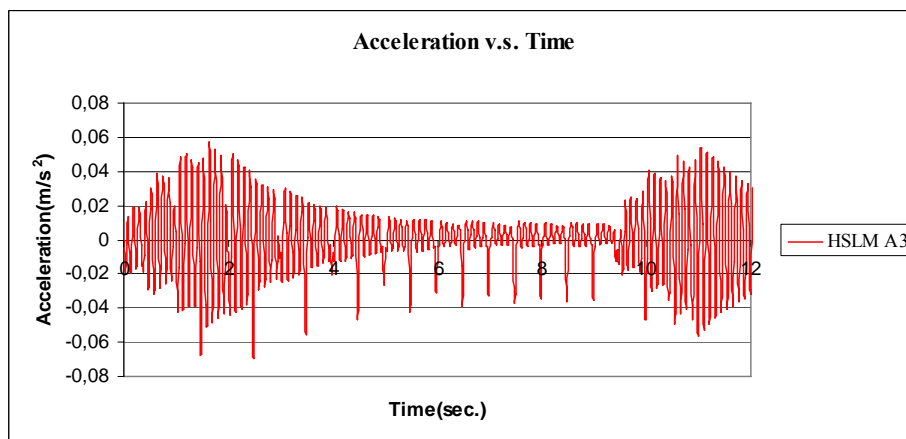


Figure C.105 Acceleration v.s. Time graph, (Analysis 19, V = 40 m/s)

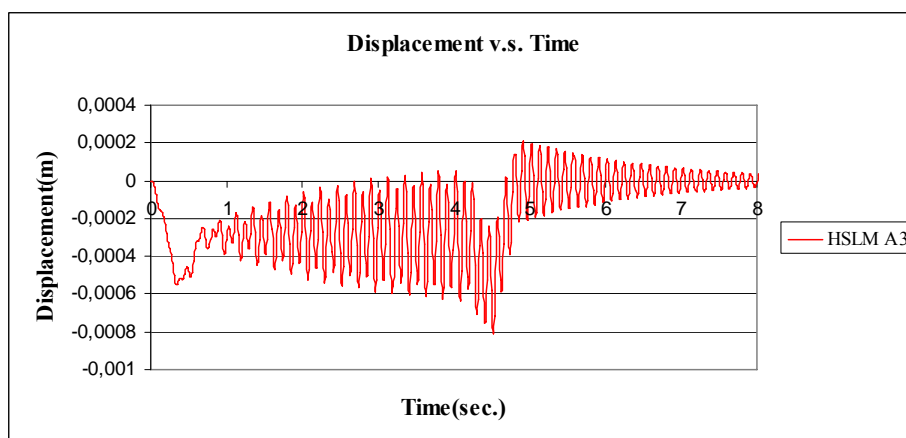


Figure C.106 Displacement v.s. Time graph, (Analysis 19, V = 89.76 m/s)

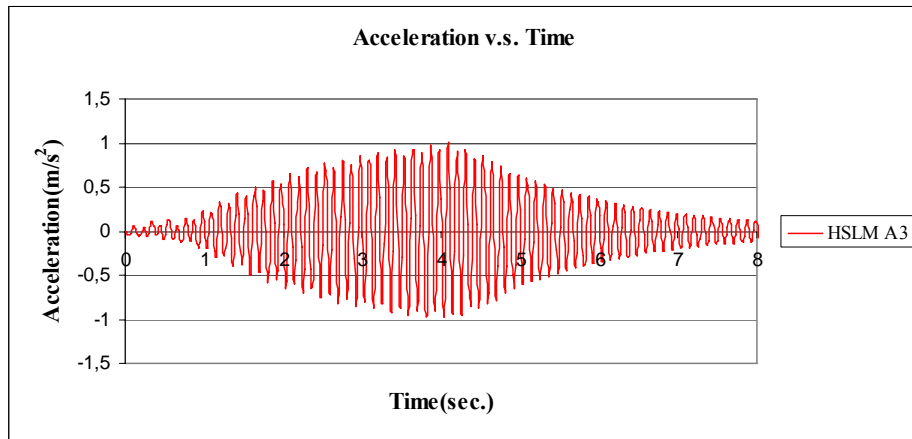


Figure C.107 Acceleration v.s. Time graph, (Analysis 19, V = 89.76 m/s)

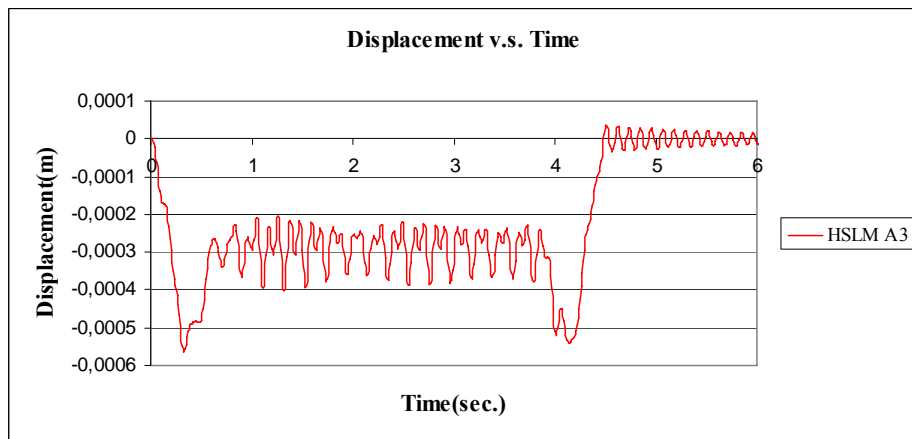


Figure C.108 Displacement v.s. Time graph, (Analysis 19, V = 97.22 m/s)

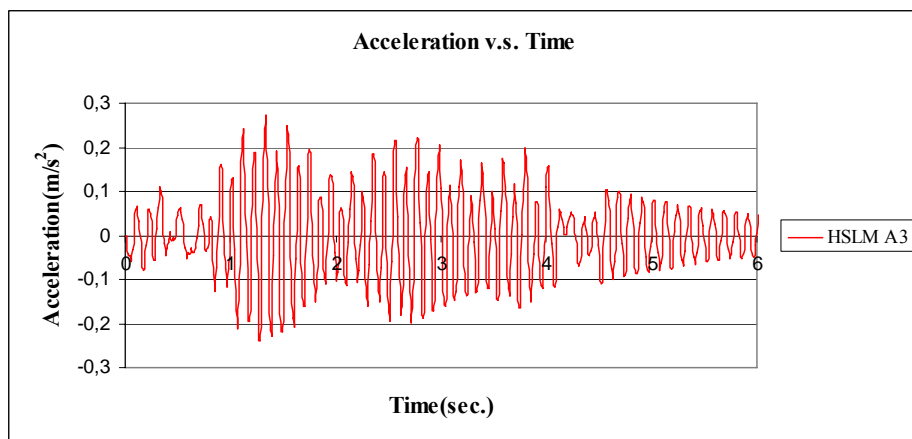


Figure C.109 Acceleration v.s. Time graph, (Analysis 19, V = 97.22 m/s)

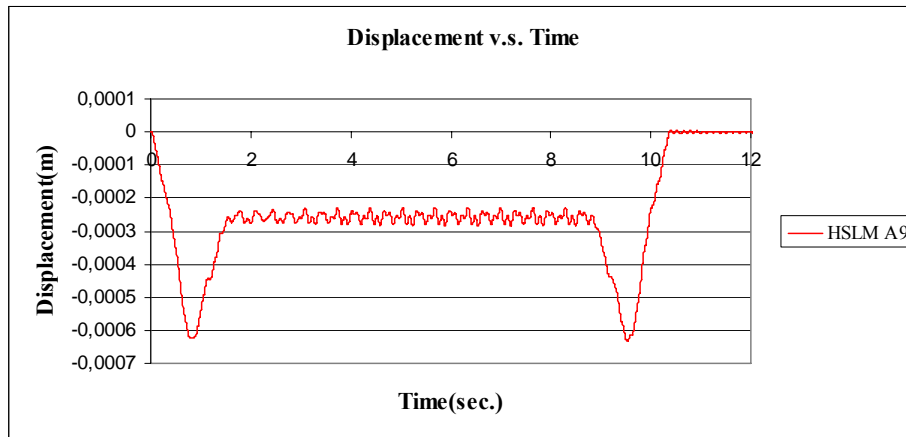


Figure C.110 Displacement v.s. Time graph, (Analysis 20, V = 40 m/s)

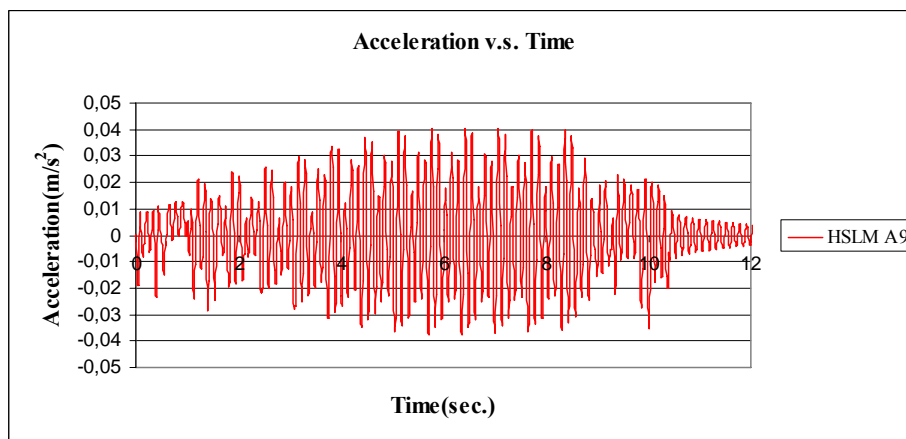


Figure C.111 Acceleration v.s. Time graph, (Analysis 20, V = 40 m/s)

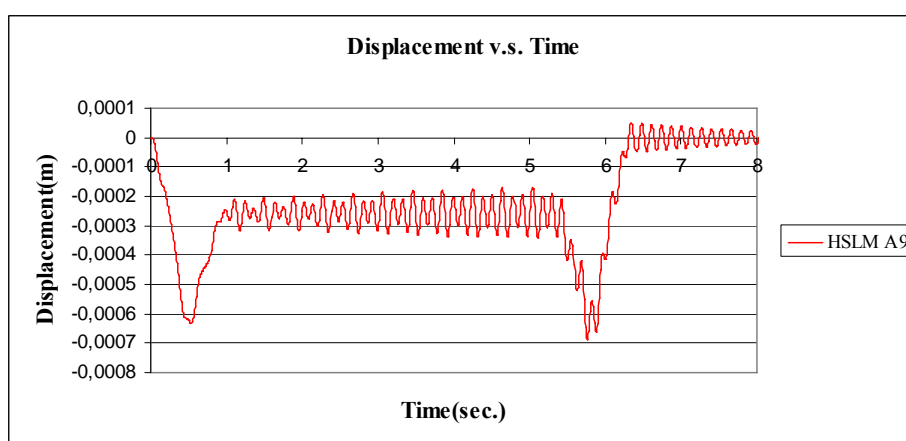


Figure C.112 Displacement v.s. Time graph, (Analysis 20, V = 65.75 m/s)

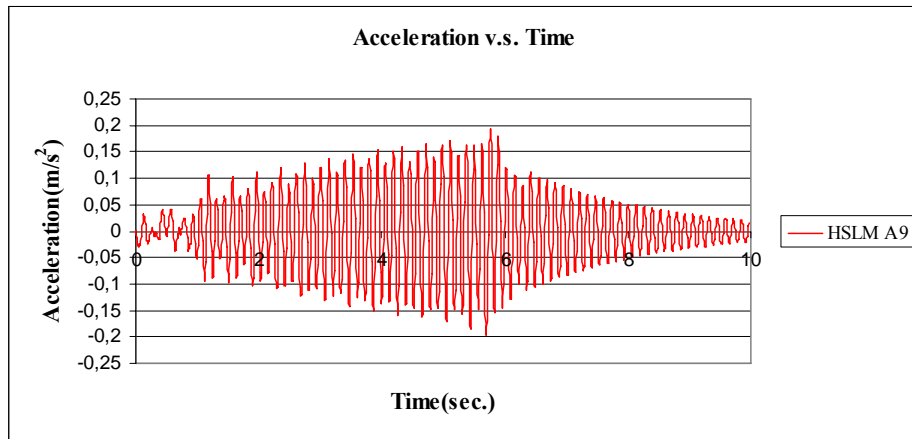


Figure C.113 Acceleration v.s. Time graph, (Analysis 20, $V = 65.75$ m/s)

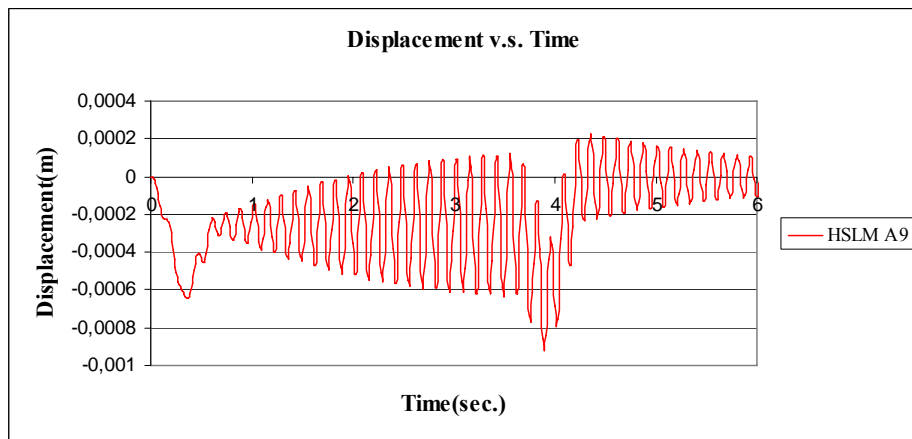


Figure C.114 Displacement v.s. Time graph, (Analysis 20, $V = 97.22$ m/s)

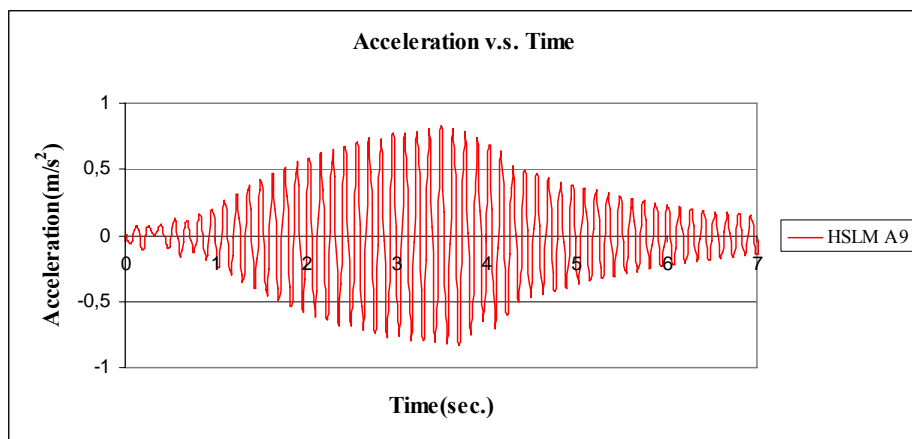


Figure C.115 Acceleration v.s. Time graph, (Analysis 20, $V = 97.22$ m/s)

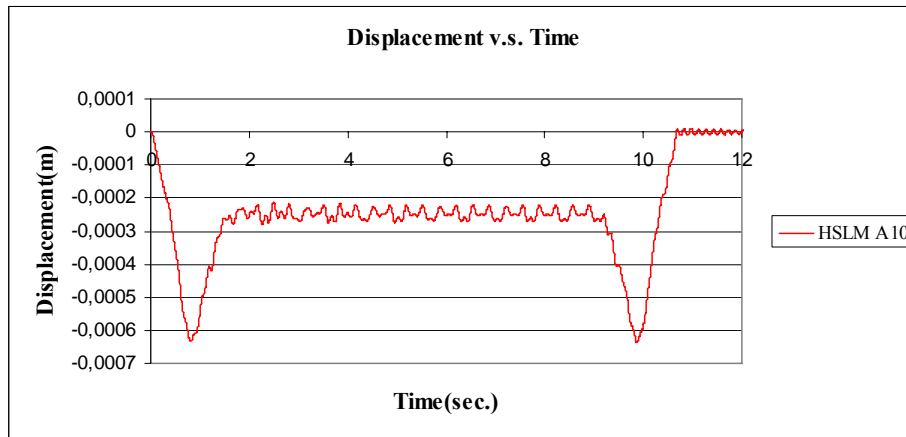


Figure C.116 Displacement v.s. Time graph, (Analysis 21, V = 40 m/s)

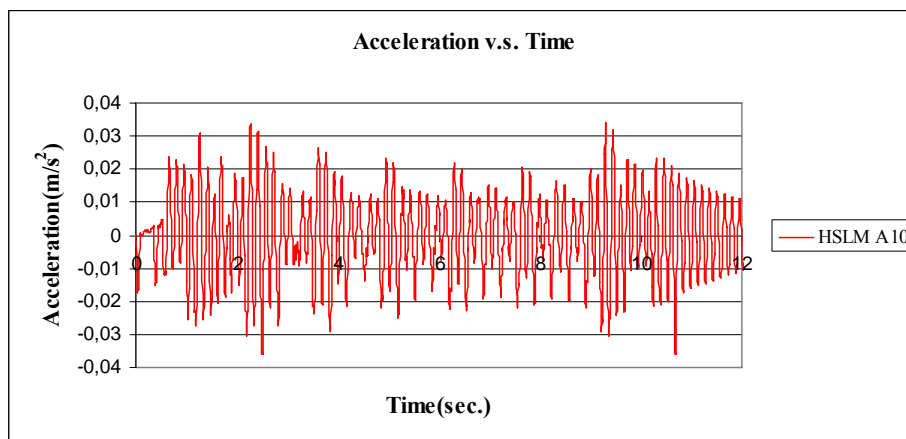


Figure C.117 Acceleration v.s. Time graph, (Analysis 21, V = 40 m/s)

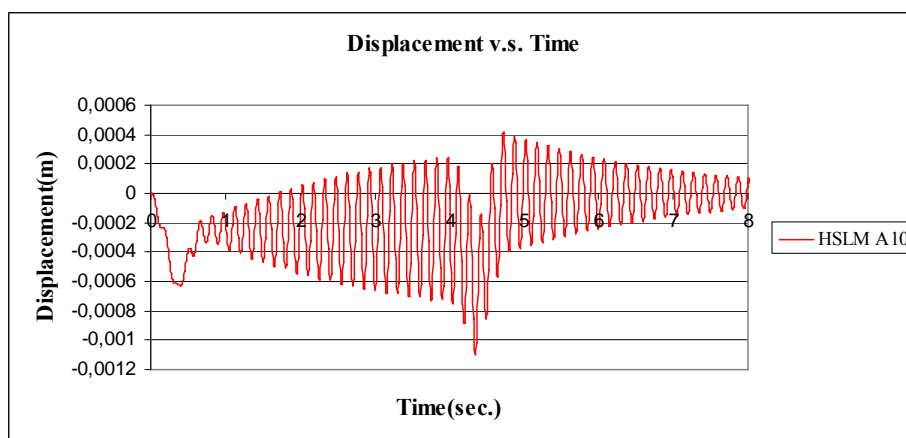


Figure C.118 Displacement v.s. Time graph, (Analysis 21, V = 90.32 m/s)

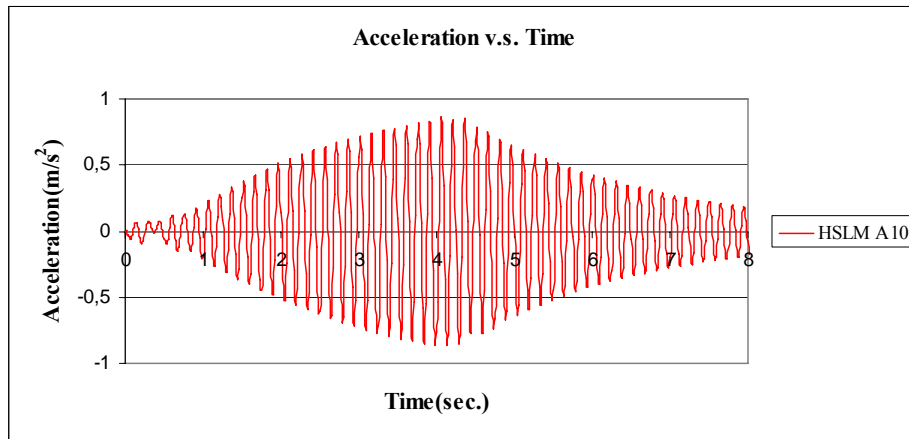


Figure C.119 Acceleration v.s. Time graph, (Analysis 21, $V = 90.32$ m/s)

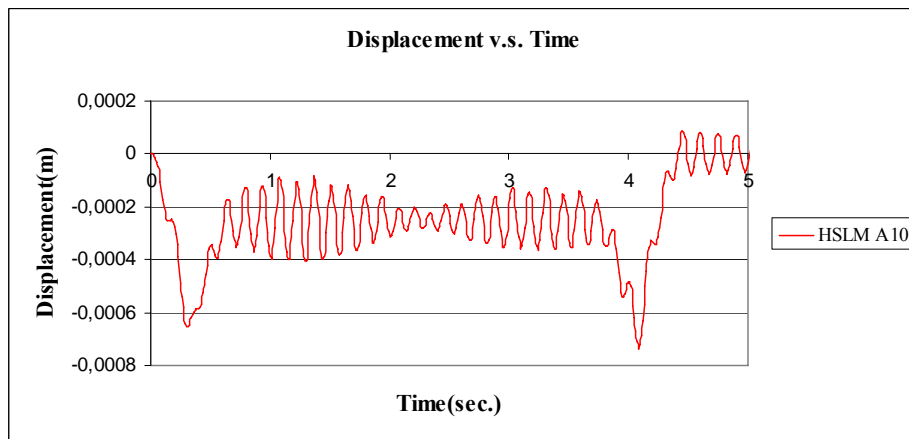


Figure C.120 Displacement v.s. Time graph, (Analysis 21, $V = 97.22$ m/s)

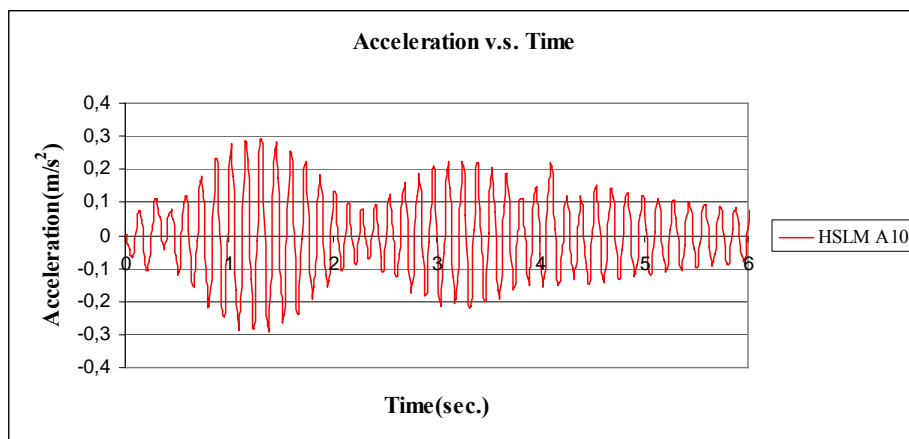


Figure C.121 Acceleration v.s. Time graph, (Analysis 21, $V = 97.22$ m/s)

C2. GRAPHS FOR TGV TRAIN

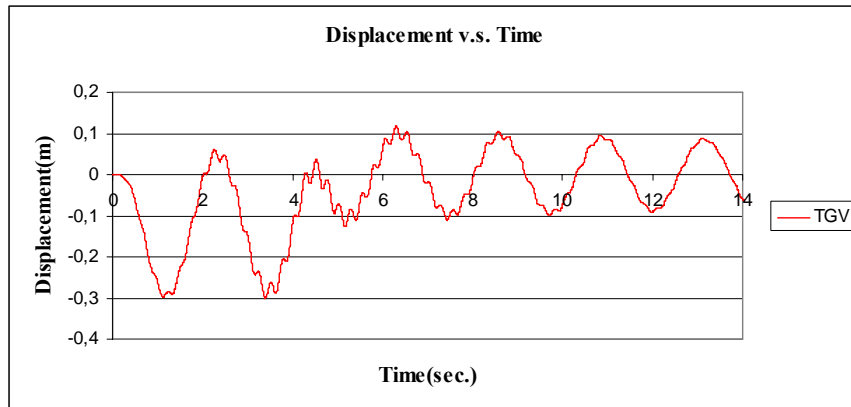


Figure C.122 Displacement v.s. Time graph, (Analysis 1, $V = 74.24$ m/s, TGV)

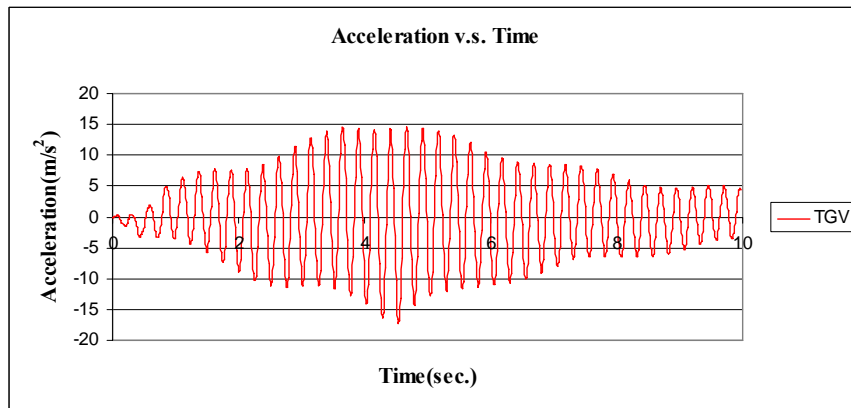


Figure C.123 Acceleration v.s. Time graph, (Analysis 1, $V = 74.24$ m/s, TGV)

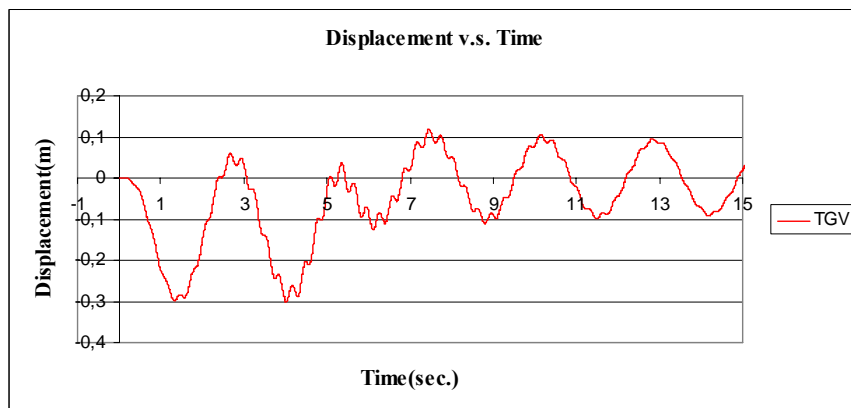


Figure C.124 Displacement v.s. Time graph, (Analysis 2, $V = 62.74$ m/s, TGV)

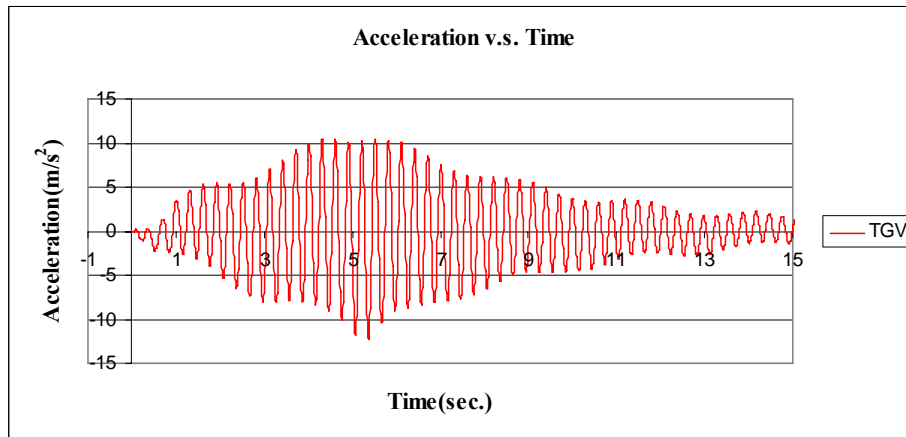


Figure C.125 Acceleration v.s. Time graph, (Analysis 2, $V = 62.74$ m/s, TGV)

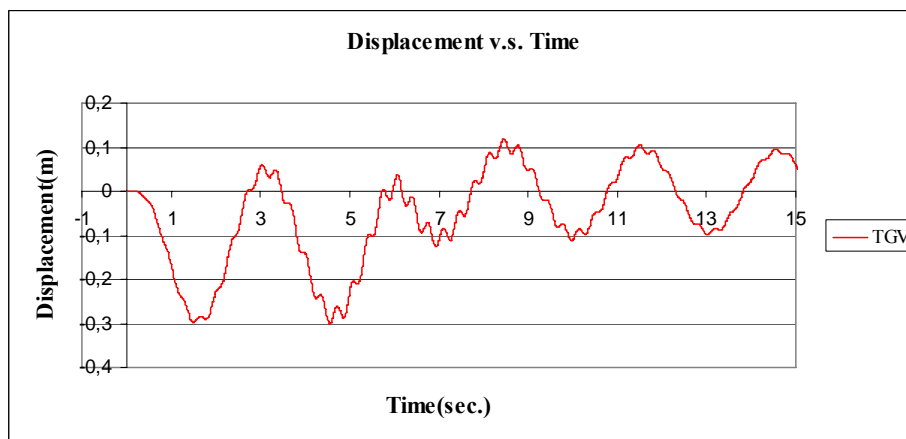


Figure C.126 Displacement v.s. Time graph, (Analysis 3, $V = 55.33$ m/s, TGV)

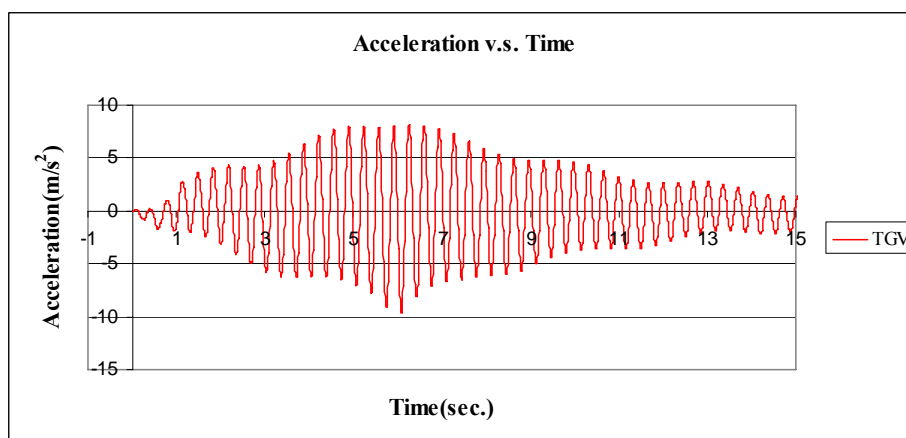


Figure C.127 Acceleration v.s. Time graph, (Analysis 3, $V = 55.33$ m/s, TGV)

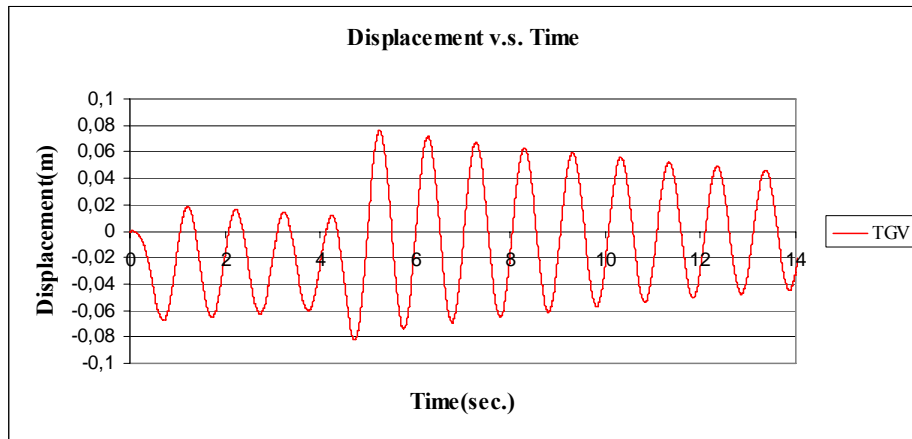


Figure C.128 Displacement v.s. Time graph, (Analysis 4, $V = 73.78$ m/s, TGV)

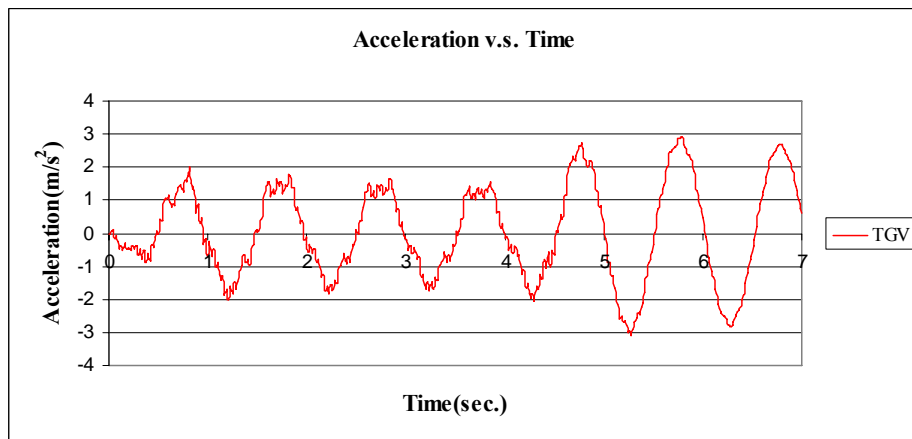


Figure C.129 Acceleration v.s. Time graph, (Analysis 4, $V = 73.78$ m/s, TGV)

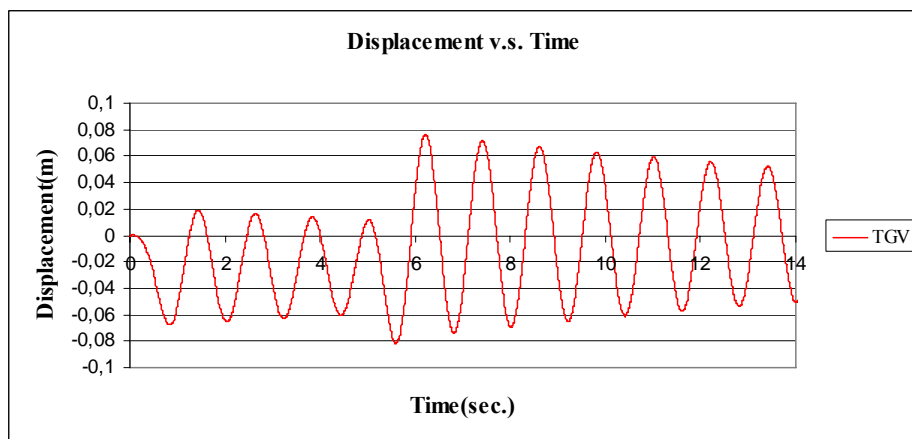


Figure C.130 Displacement v.s. Time graph, (Analysis 5, $V = 62.36$ m/s, TGV)

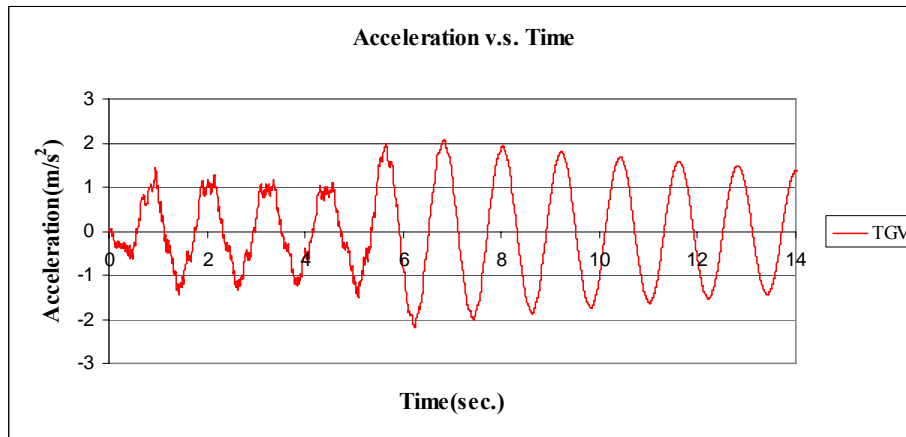


Figure C.131 Acceleration v.s. Time graph, (Analysis 5, $V = 62.36$ m/s, TGV)

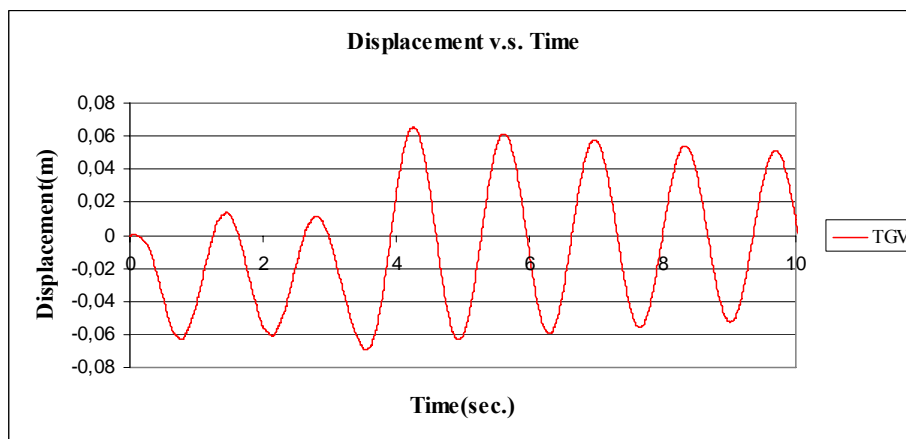


Figure C.132 Displacement v.s. Time graph, (Analysis 6, $V = 97.22$ m/s, TGV)

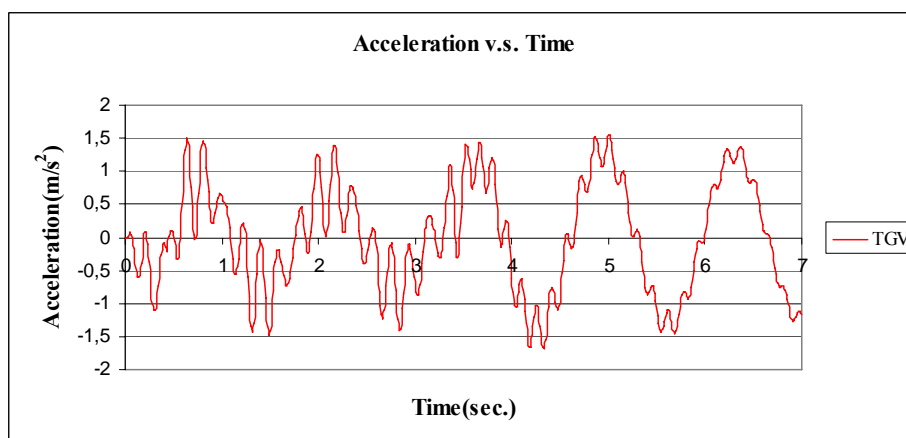


Figure C.133 Acceleration v.s. Time graph, (Analysis 6, $V = 97.22$ m/s, TGV)

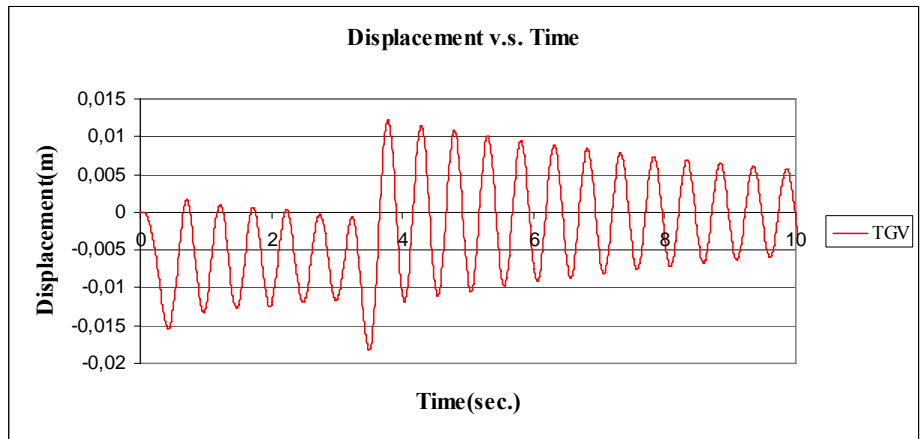


Figure C.134 Displacement v.s. Time graph, (Analysis 7, V =97.22 m/s, TGV)

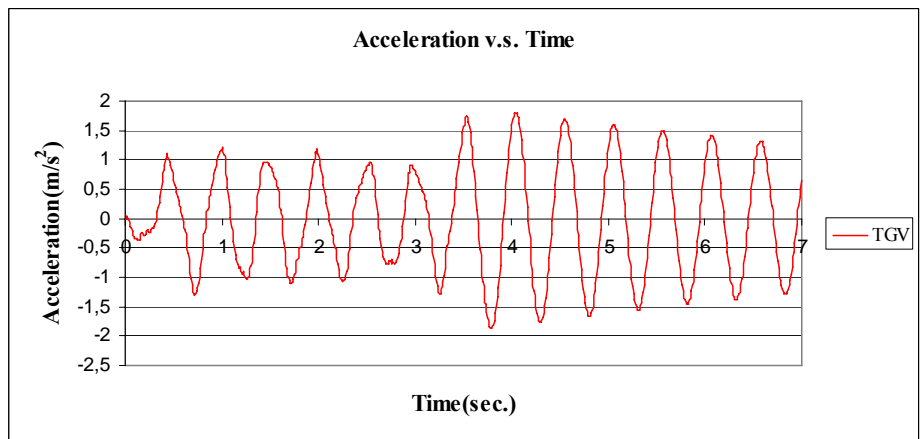


Figure C.135 Acceleration v.s. Time graph, (Analysis 7, V = 97.22 m/s, TGV)

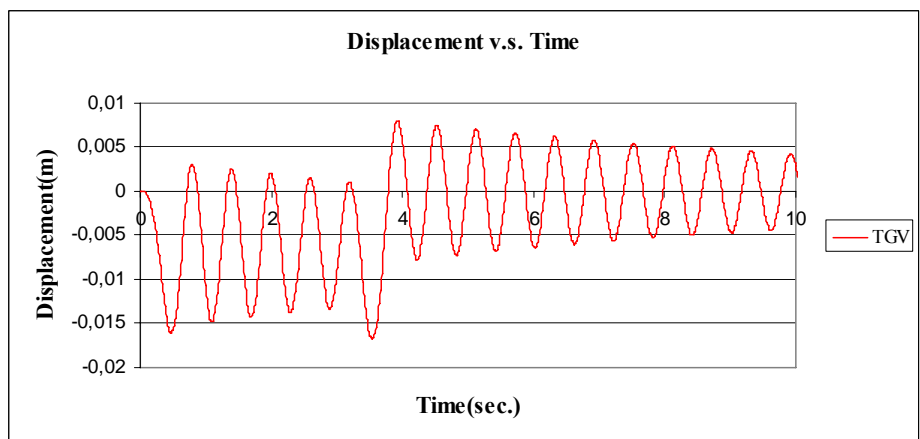


Figure C.136 Displacement v.s. Time graph, (Analysis 8, V =93.54 m/s, TGV)

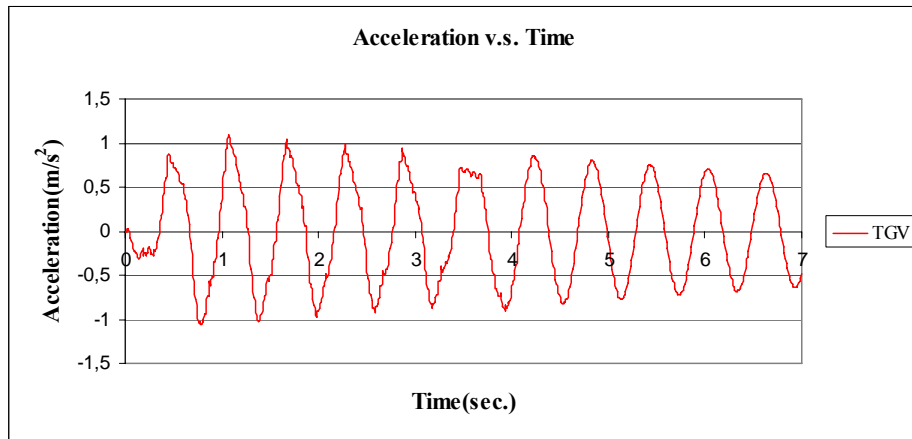


Figure C.137 Acceleration v.s. Time graph, (Analysis 8, $V = 93.54$ m/s, TGV)

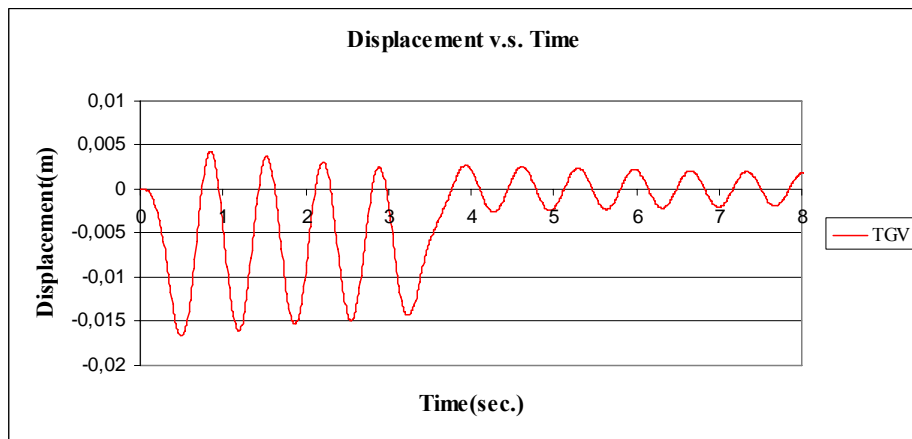


Figure C.138 Displacement v.s. Time graph, (Analysis 9, $V = 97.22$ m/s, TGV)

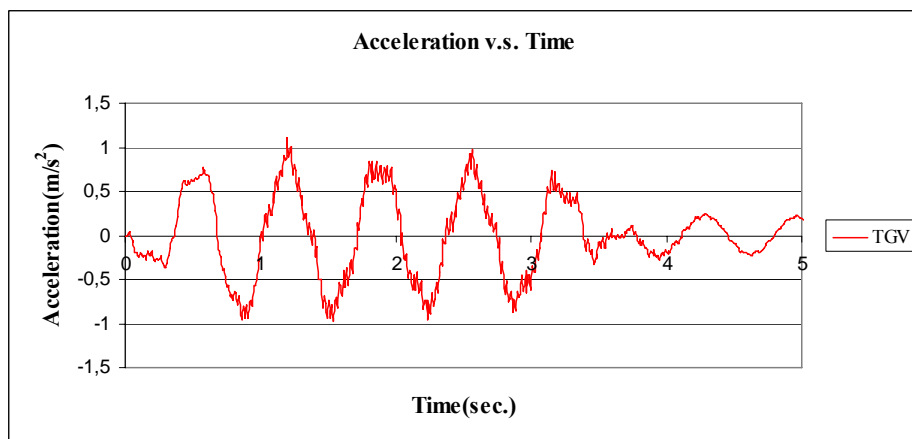


Figure C.139 Acceleration v.s. Time graph, (Analysis 9, $V = 97.22$ m/s, TGV)

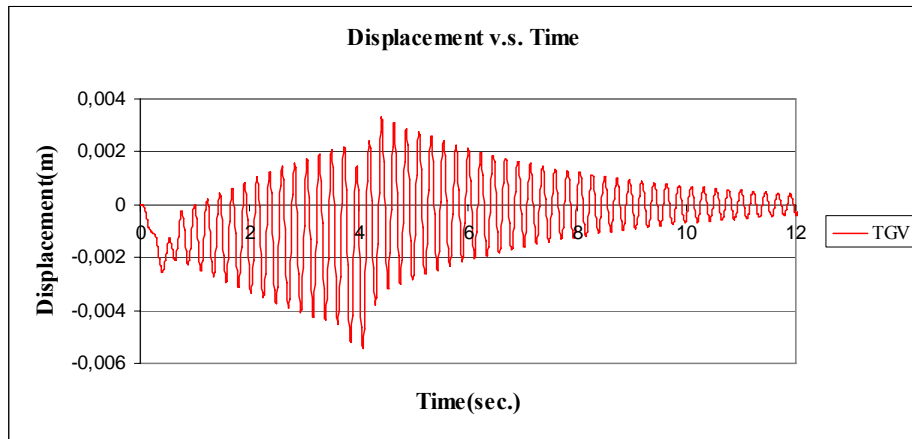


Figure C.140 Displacement v.s. Time graph, (Analysis 10, $V = 82.49$ m/s, TGV)

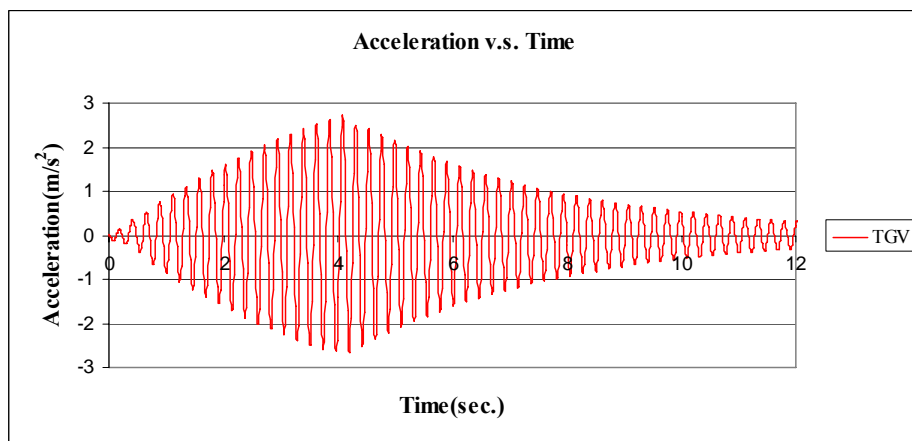


Figure C.141 Acceleration v.s. Time graph, (Analysis 10, $V = 82.49$ m/s, TGV)

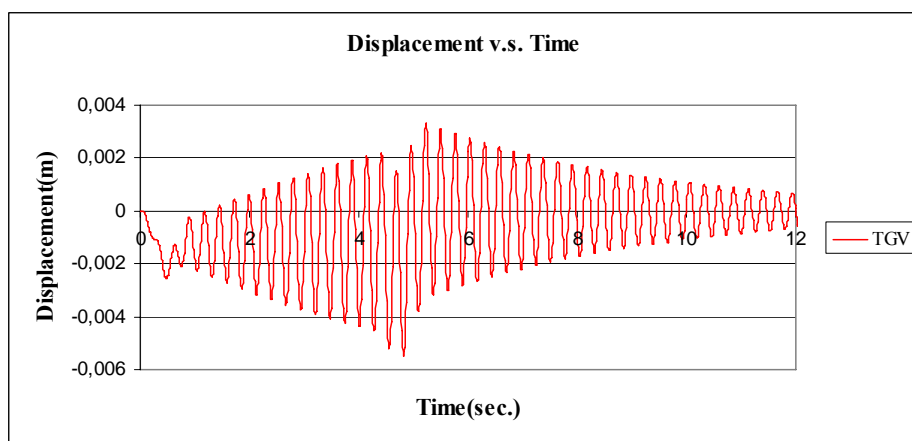


Figure C.142 Displacement v.s. Time graph, (Analysis 11, $V = 69.72$ m/s, TGV)

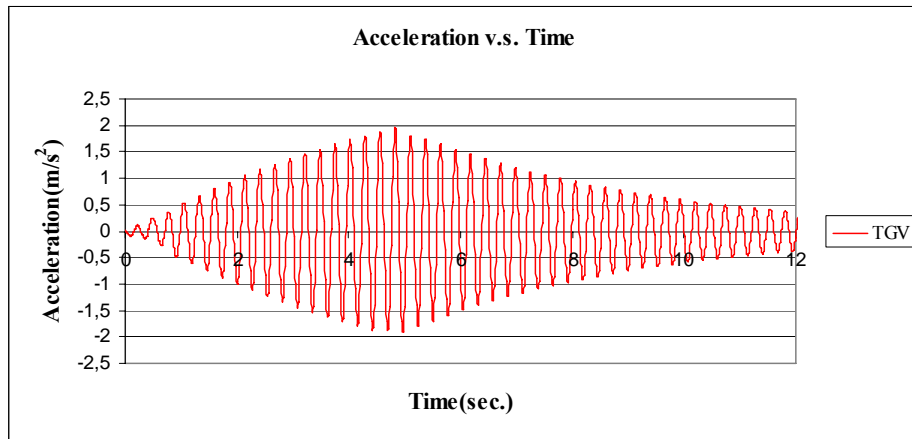


Figure C.143 Acceleration v.s. Time graph, (Analysis 11, $V = 69.72$ m/s, TGV)

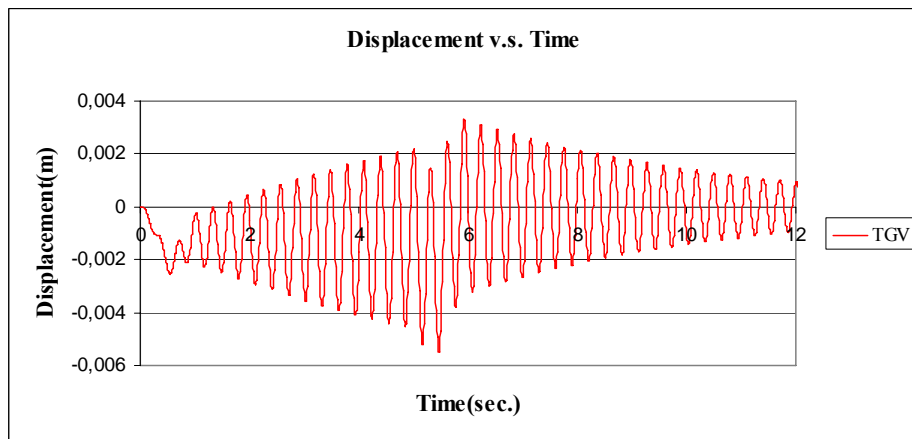


Figure C.144 Displacement v.s. Time graph, (Analysis 12, $V = 61.50$ m/s, TGV)

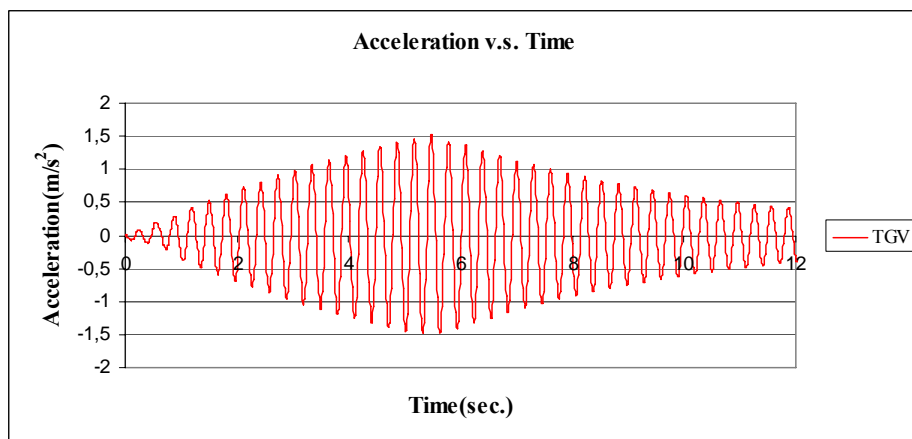


Figure C.145 Acceleration v.s. Time graph, (Analysis 12, $V = 61.50$ m/s, TGV)

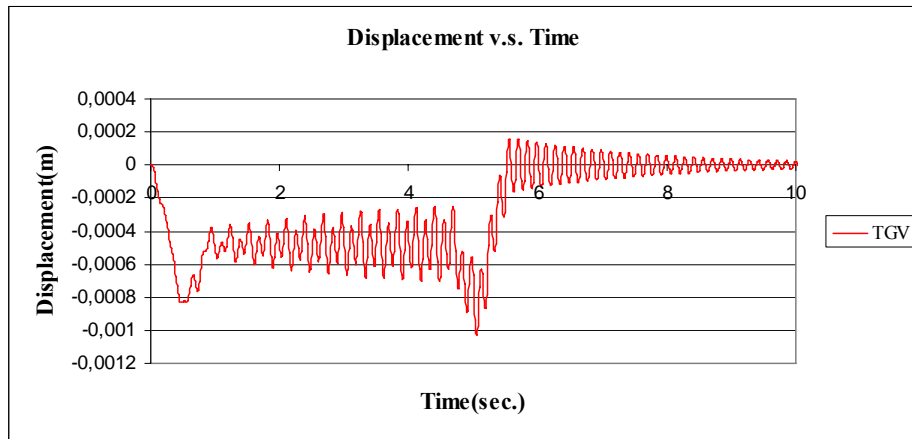


Figure C.146 Displacement v.s. Time graph, (Analysis 13, V =65.22 m/s, TGV)

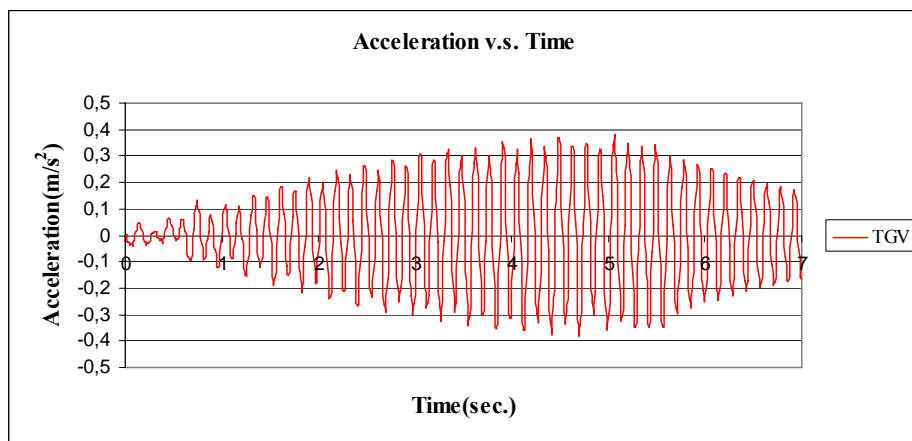


Figure C.147 Acceleration v.s. Time graph, (Analysis 13, V = 65.22 m/s, TGV)

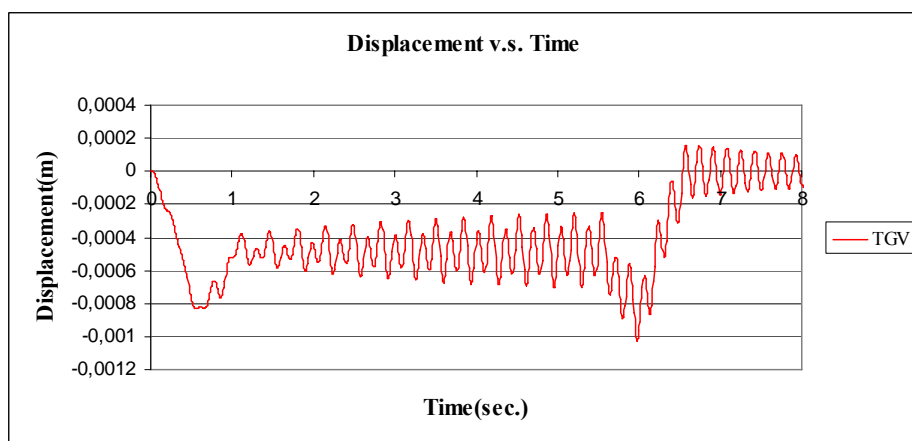


Figure C.148 Displacement v.s. Time graph, (Analysis 14, V =55.12 m/s, TGV)

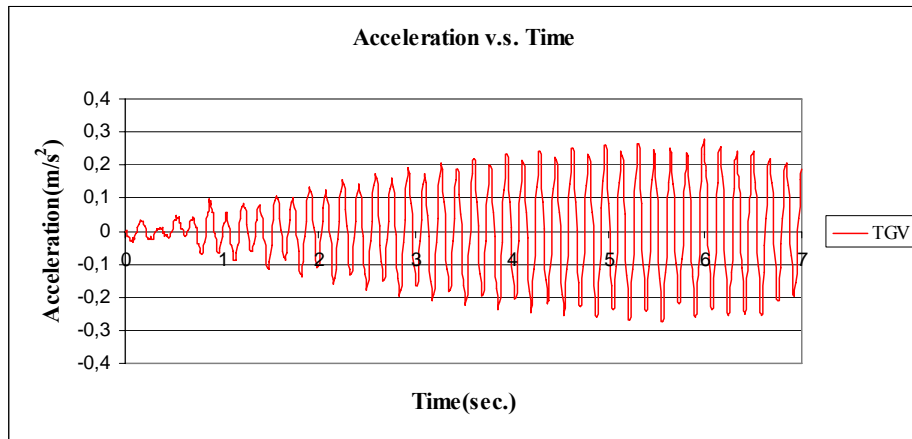


Figure C.149 Acceleration v.s. Time graph, (Analysis 14, $V = 55.12$ m/s, TGV)

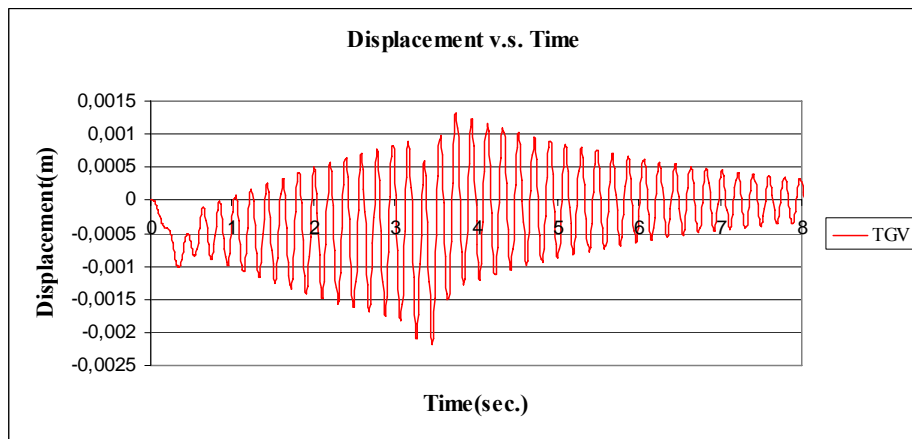


Figure C.150 Displacement v.s. Time graph, (Analysis 15, $V = 97.22$ m/s, TGV)

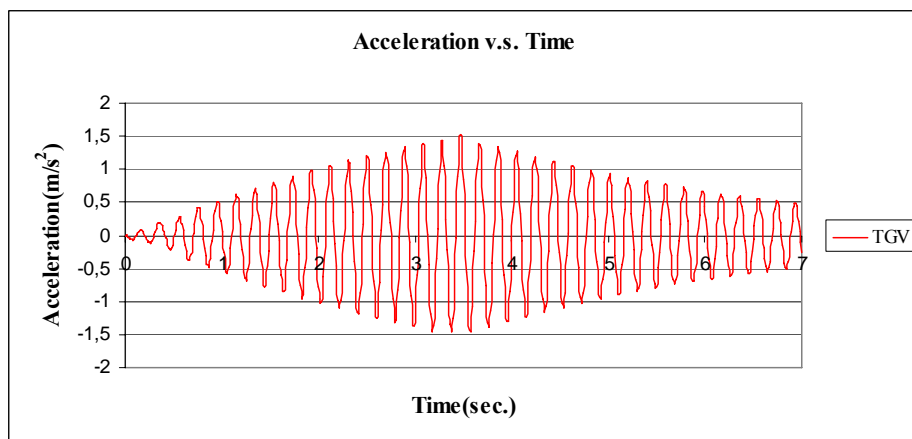


Figure C.151 Acceleration v.s. Time graph, (Analysis 15, $V = 97.22$ m/s, TGV)

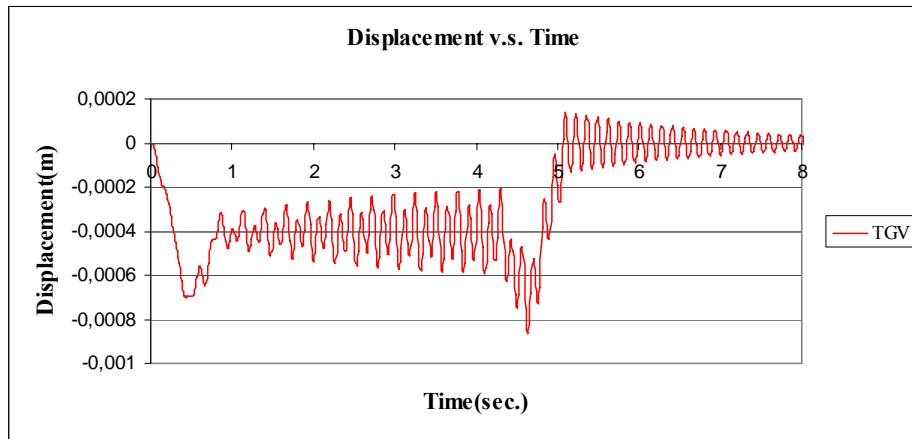


Figure C.152 Displacement v.s. Time graph, (Analysis 16, V =71.10 m/s, TGV)

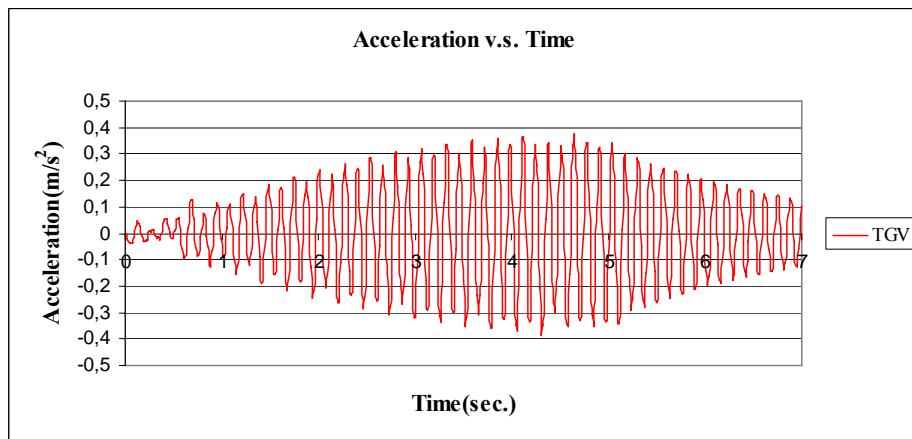


Figure C.153 Acceleration v.s. Time graph, (Analysis 16, V = 71.10 m/s, TGV)

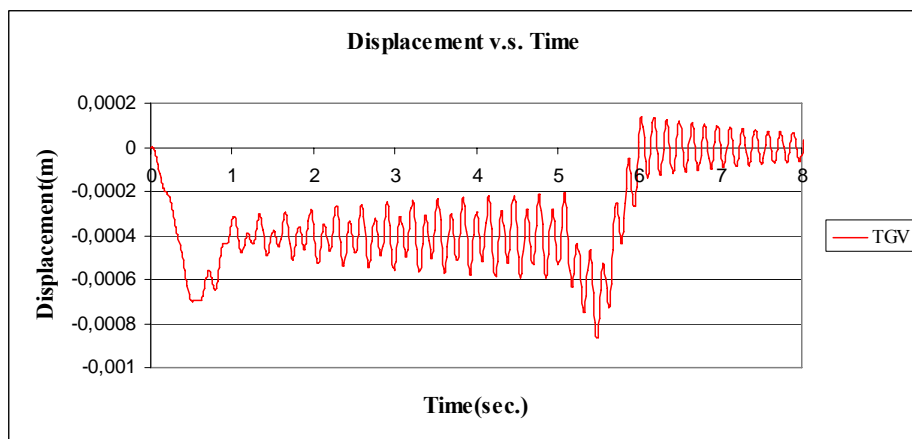


Figure C.154 Displacement v.s. Time graph, (Analysis 17, V =60.10 m/s, TGV)

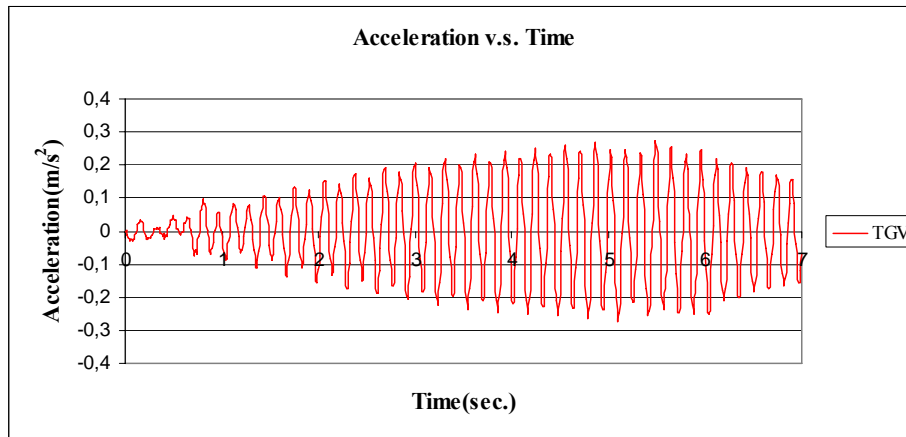


Figure C.155 Acceleration v.s. Time graph, (Analysis 17, $V = 60.10$ m/s, TGV)

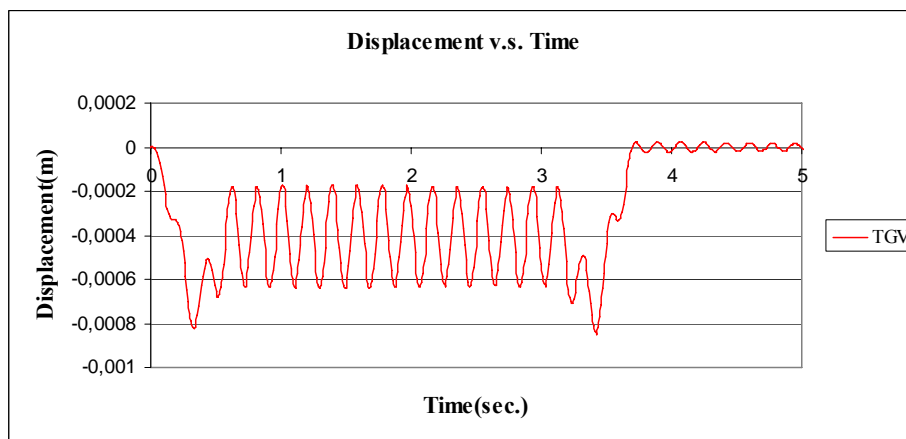


Figure C.156 Displacement v.s. Time graph, (Analysis 18, $V = 97.22$ m/s, TGV)

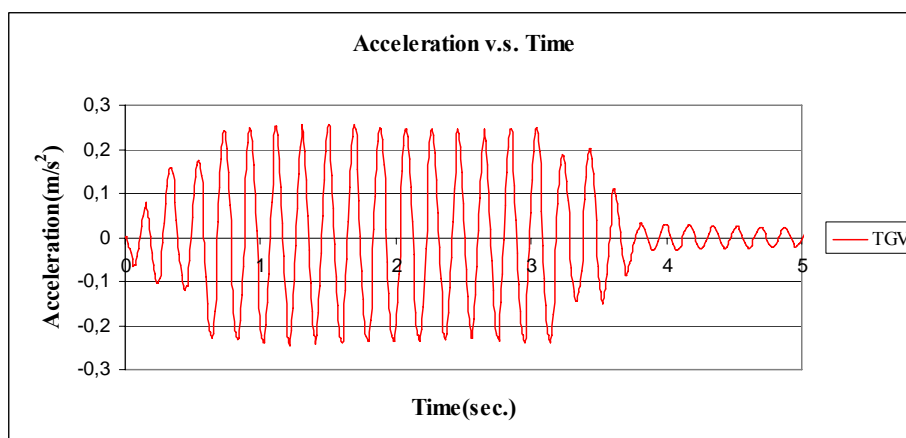


Figure C.157 Acceleration v.s. Time graph, (Analysis 18, $V = 97.22$ m/s, TGV)

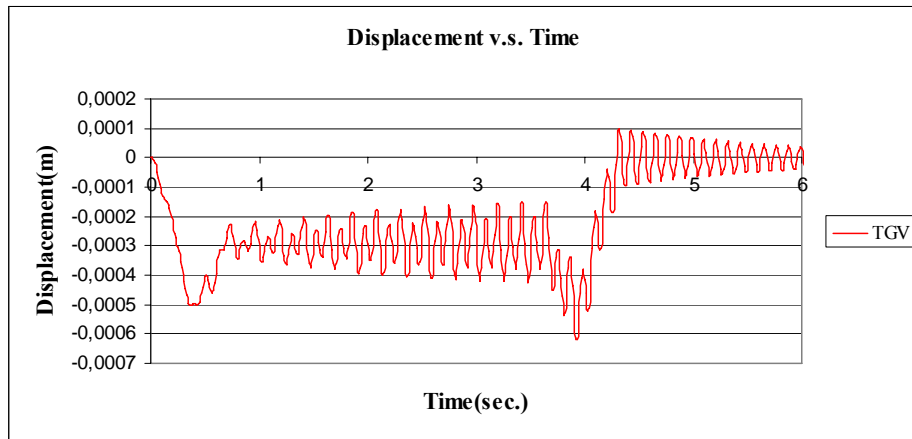


Figure C.158 Displacement v.s. Time graph, (Analysis 19, $V = 83.93$ m/s, TGV)

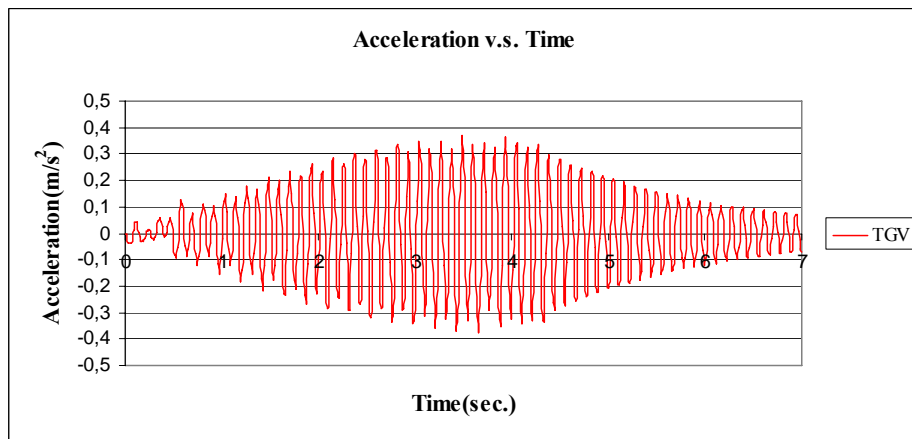


Figure C.159 Acceleration v.s. Time graph, (Analysis 19, $V = 83.93$ m/s, TGV)

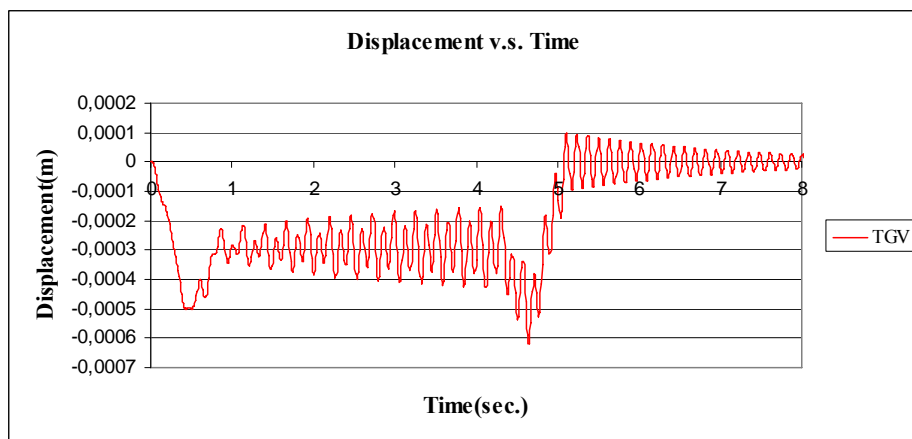


Figure C.160 Displacement v.s. Time graph, (Analysis 20, $V = 70.93$ m/s, TGV)

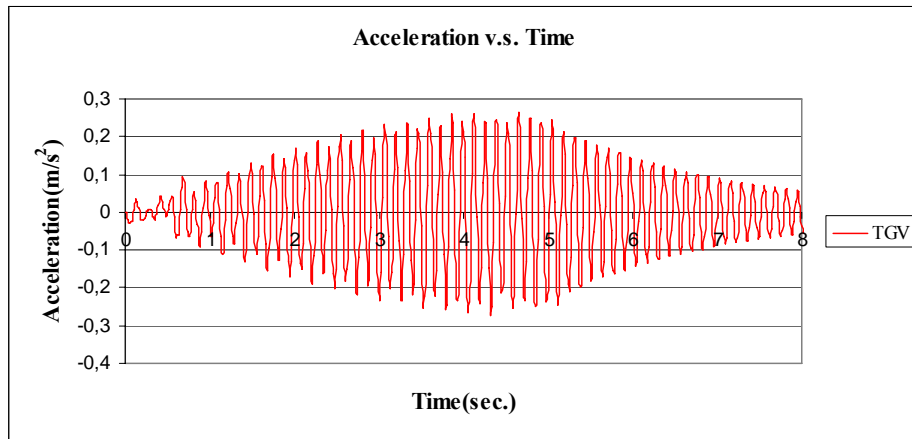


Figure C.161 Acceleration v.s. Time graph, (Analysis 20, $V = 70.93$ m/s, TGV)

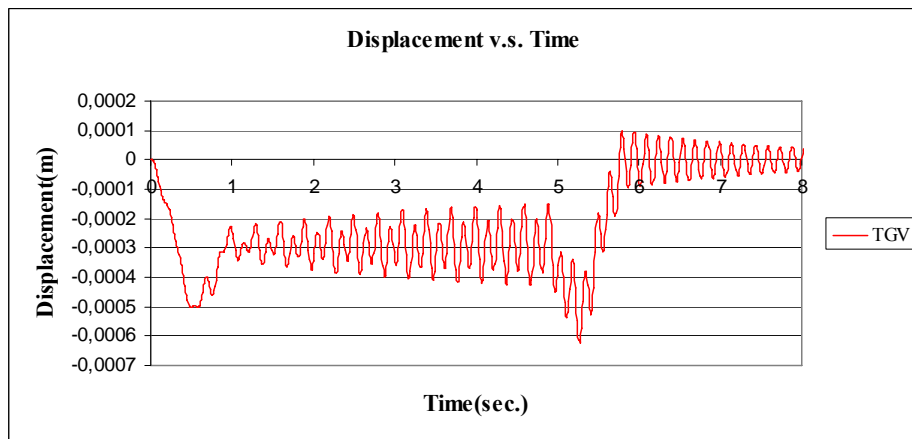


Figure C.162 Displacement v.s. Time graph, (Analysis 21, $V = 62.55$ m/s, TGV)

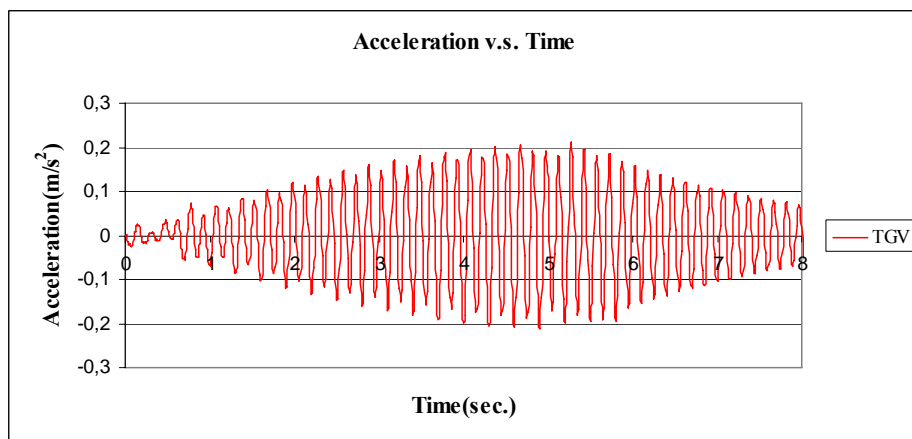


Figure C.163 Acceleration v.s. Time graph, (Analysis 21, $V = 62.55$ m/s, TGV)

APPENDIX D

FREQUENCY V.S. MODE SHAPE GRAPHS FOR PARAMETRIC STUDY

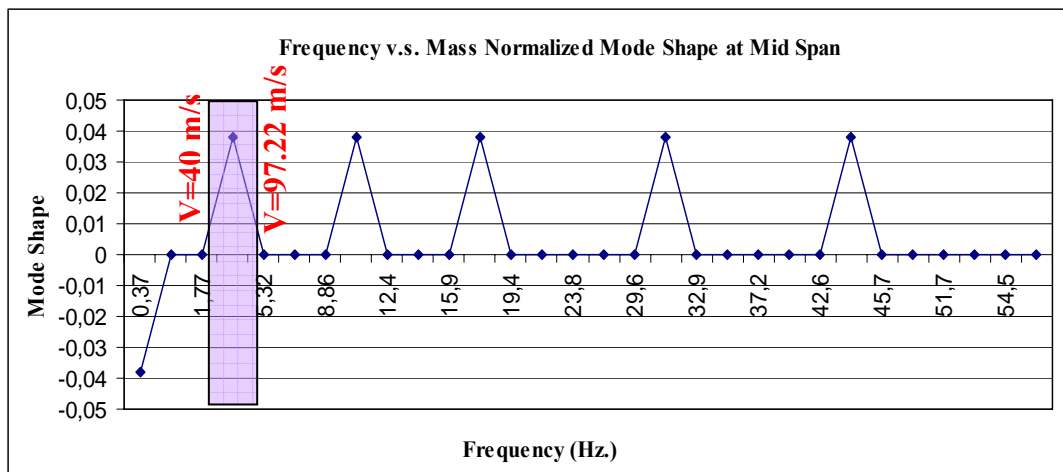


Figure D.1 Frequency v.s. Mode Shape, (Analysis 2)

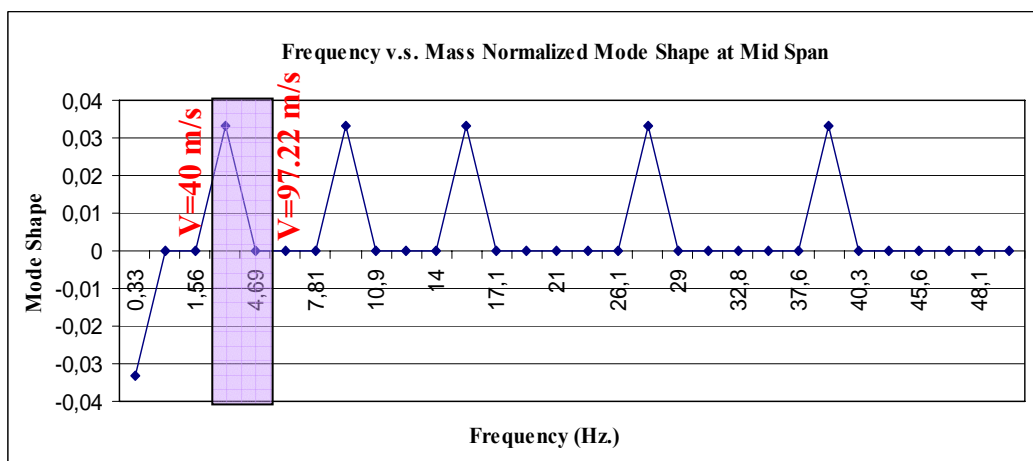


Figure D.2 Frequency v.s. Mode Shape, (Analysis 3)

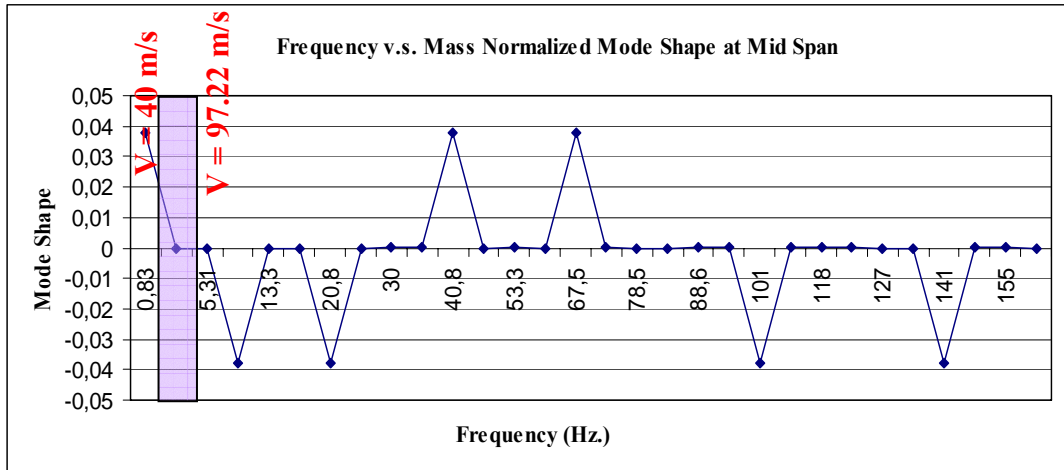


Figure D.3 Frequency v.s. Mode Shape, (Analysis 5)

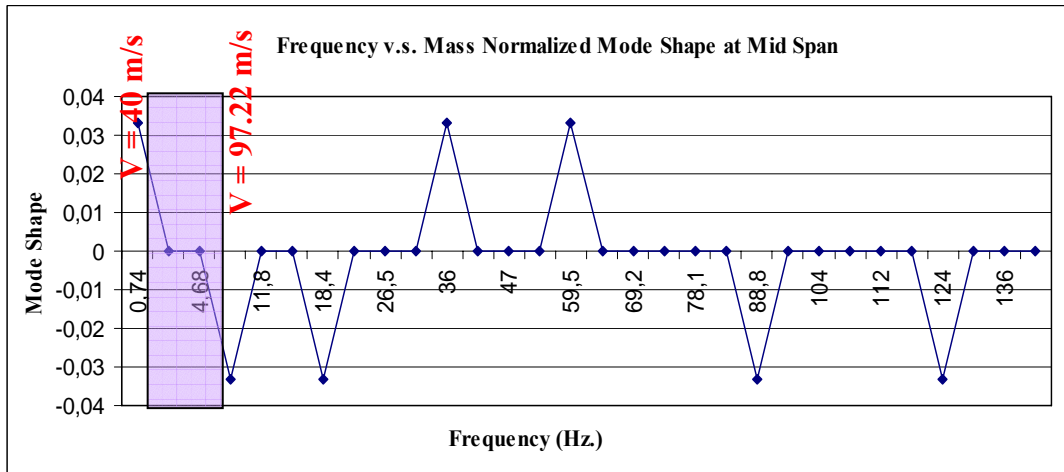


Figure D.4 Frequency v.s. Mode Shape, (Analysis 6)

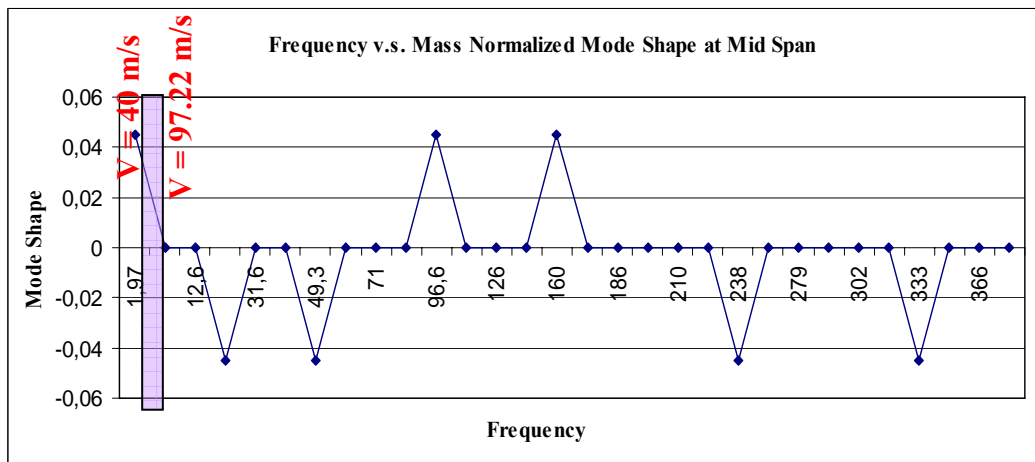


Figure D.5 Frequency v.s. Mode Shape, (Analysis 7)

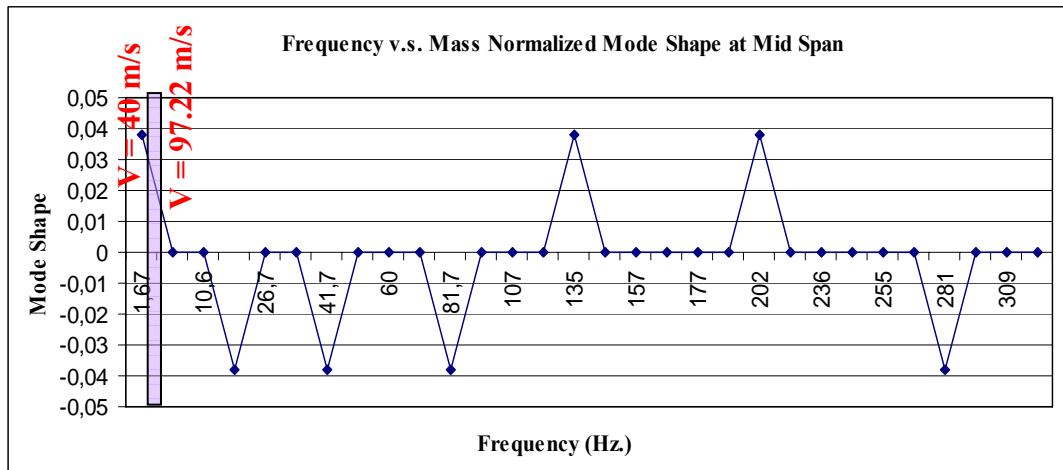


Figure D.6 Frequency v.s. Mode Shape, (Analysis 8)

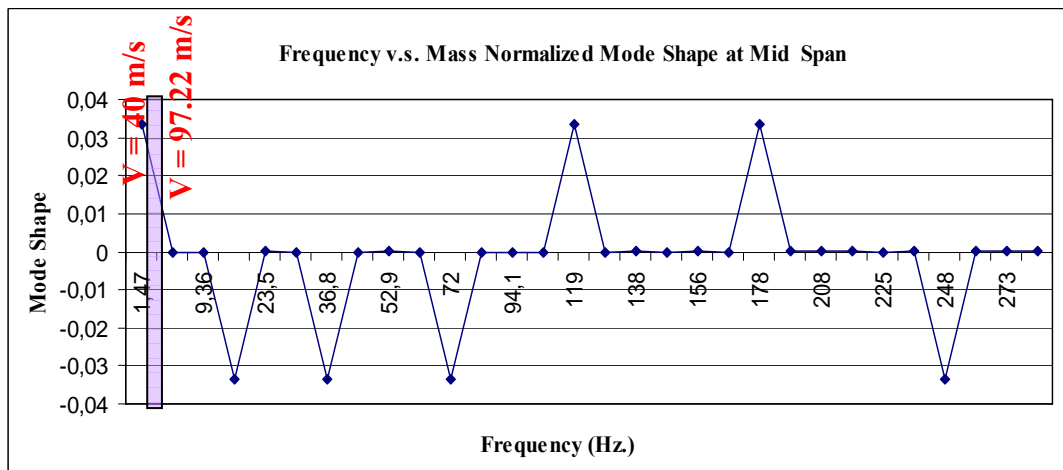


Figure D.7 Frequency v.s. Mode Shape, (Analysis 9)

APPENDIX E

MATLAB CODE FOR ANALYTICAL APPROACH

```
function [y,T]=EUROCODEHSLM()
%input parameters
L = 40; % span length of bridge(m)
naxle = 30; % number of axles in EN + 14
nmode = 10; % number of modes
xcheck = (5)*L/10; % point of beam where response is analysed(m)
dninitial = 20; % spacing of vehicles
dc=18; % axle distance between adjacent axles (m)
v =97.22; % velocity of train(m/s)
P = -180; % axle loading(kN)
m = 35; % (t/m) Linear density
E = 100955600; % Young modulus(kN/m2)
I = 1; % Moment of Inertia(m4)
damping=0.01; % damping ratio
timestep = 0.001; % timestep

%formulas
arm1=dninitial-dc;
aramesafe=dninitial-3.525*0.5-(arm1)*1.5;
T = [0:timestep:(L+dninitial*(naxle))*5/v]';
[nrow_T,nclmn_T]=size(T);
y = zeros(size(T));
y1 = zeros(size(T));
for j = 1:nmode
    for n = 1
        wj=((j^2).*(pi^2)/(L^2)).*((E.*I)/m)^0.5;
        Sj=(j.*pi.*v)./(wj.*L);
        omegaj=(j.*pi.*v)/L;
        tn= (n-1).*dninitial./v;
        Tn= tn+(L./v);
        tc=0./v;
```


wdj=wj.*(1-damping^2)^0.5;

A1=(1-Sj.^2).*sin(omegaj.*(T-tn))-2.*damping.*Sj.*cos(omegaj.*(T-tn))+exp(-damping.*wj.*(T-tn)).*((2.*damping.*Sj.*cos(wdj.*(T-tn)))+(((Sj)./(1-damping^2)^0.5)).*(2.*(damping^2)+(Sj^2)-1).*sin(wdj.*(T-tn))));

B1=(1-Sj.^2).*sin(omegaj.*(T-Tn))-2.*damping.*Sj.*cos(omegaj.*(T-Tn))+exp(-damping.*wj.*(T-Tn)).*((2.*damping.*Sj.*cos(wdj.*(T-Tn)))+(((Sj)./(1-damping^2)^0.5)).*(2.*damping^2+(Sj^2)-1).*sin(wdj.*(T-Tn))));

A2=(1-Sj.^2).*sin(omegaj.*(T-tc-tn))-2.*damping.*Sj.*cos(omegaj.*(T-tc-tn))+exp(-damping.*wj.*(T-tc-tn)).*((2.*damping.*Sj.*cos(wdj.*(T-tc-tn)))+(((Sj)./(1-damping^2)^0.5)).*(2.*(damping^2)+(Sj^2)-1).*sin(wdj.*(T-tc-tn))));

B2=(1-Sj.^2).*sin(omegaj.*(T-tc-Tn))-2.*damping.*Sj.*cos(omegaj.*(T-tc-Tn))+exp(-damping.*wj.*(T-tc-Tn)).*((2.*damping.*Sj.*cos(wdj.*(T-tc-Tn)))+(((Sj)./(1-damping^2)^0.5)).*(2.*damping^2+(Sj^2)-1).*sin(wdj.*(T-tc-Tn))));

t1 = T-tn;
t2 = T-Tn;
t3 = T-tc-tn;
t4 = T-tc-Tn;
h1=[];
h2=[];
h3=[];
h4=[];

```
for s=1:nrow_T
    t1_s=t1(s,1);
    t2_s=t2(s,1);
    t3_s=t3(s,1);
    t4_s=t4(s,1);
    if t1_s<0
        h1_s=0;
    else
        h1_s=1;
    end
    if t2_s<0
        h2_s=0;
    else
        h2_s=1;
    end
    if t3_s<0
```

```

        h3_s=0;
    else
        h3_s=1;
    end
    if t4_s<0
        h4_s=0;
    else
        h4_s=1;
    end
    h1=[h1;h1_s];
    h2=[h2;h2_s];
    h3=[h3;h3_s];
    h4=[h4;h4_s];
end

    pt1=(1/(j^4)).*(1./(((1-Sj^2)^2)+4.*(damping.*Sj)^2)).*(A1.*h1+((-1)^(j+1)).*B1.*h2);

    pt2=(1/(j^4)).*(1./(((1-Sj^2)^2)+4.*(damping.*Sj)^2)).*(A2.*h3+((-1)^(j+1)).*B2.*h4);

    %deltay1=((2.*P.*(L^3))./(E.*I.*(pi^4))).*(pt1+pt2)
    deltax1=((2.*P.*(L^3))./(E.*I.*(pi^4))).*(pt1);
    y1=y1+deltay1;
end
%%%%%%%%%%%%%%%%%%%%%%%%%%%%%%%%%%%%%%%%%%%%%%%%%%%%%%%%%%%%%%%%%%%%%%%%
for n = 2
    wj=((j^2).*(pi^2)/(L^2)).*((E.*I)/m)^0.5;
    Sj=(j.*pi.*v)/(wj.*L);
    omegaj=(j.*pi.*v)/L;
    tn= (n-1).*3./v
    Tn= tn+(L./v);
    tc=0./v;
    wdj=wj.*(1-damping^2)^0.5;

    A1=(1-Sj.^2).*sin(omegaj.*(T-tn))-2.*damping.*Sj.*cos(omegaj.*(T-tn))+exp(-damping.*wj.*(T-tn)).*((2.*damping.*Sj.*cos(wdj.*(T-tn)))+(((Sj)/((1-damping^2)^0.5)).*(2.*(damping^2)+(Sj^2)-1).*sin(wdj.*(T-tn))));

    B1=(1-Sj.^2).*sin(omegaj.*(T-Tn))-2.*damping.*Sj.*cos(omegaj.*(T-Tn))+exp(-damping.*wj.*(T-Tn)).*((2.*damping.*Sj.*cos(wdj.*(T-Tn)))+(((Sj)/((1-damping^2)^0.5)).*(2.*damping^2+(Sj^2)-1).*sin(wdj.*(T-Tn))));

```

```

A2=(1-Sj.^2).*sin(omegaj.*(T-tc-tn))-2.*damping.*Sj.*cos(omegaj.*(T-tc-
tn))+exp(-damping.*wj.*(T-tc-tn)).*((2.*damping.*Sj.*cos(wdj.*(T-tc-
tn)))+((Sj)/((1-damping^2)^0.5)).*(2.*(damping^2)+(Sj^2)-1).*sin(wdj.*(T-tc-
tn))));

```

```

B2=(1-Sj.^2).*sin(omegaj.*(T-tc-Tn))-2.*damping.*Sj.*cos(omegaj.*(T-tc-
Tn))+exp(-damping.*wj.*(T-tc-Tn)).*((2.*damping.*Sj.*cos(wdj.*(T-tc-
Tn)))+((Sj)/((1-damping^2)^0.5)).*(2.*(damping^2)+(Sj^2)-1).*sin(wdj.*(T-tc-
Tn))));

```

```

t1 = T-tn;
t2 = T-Tn;
t3 = T-tc-tn;
t4 = T-tc-Tn;
h1=[];
h2=[];
h3=[];
h4=[];
for s=1:nrow_T
    t1_s=t1(s,1);
    t2_s=t2(s,1);
    t3_s=t3(s,1);
    t4_s=t4(s,1);
    if t1_s<0
        h1_s=0;
    else
        h1_s=1;
    end
    if t2_s<0
        h2_s=0;
    else
        h2_s=1;
    end
    if t3_s<0
        h3_s=0;
    else
        h3_s=1;
    end
    if t4_s<0
        h4_s=0;
    else
        h4_s=1;
    end
    h1=[h1;h1_s];
    h2=[h2;h2_s];
    h3=[h3;h3_s];

```

```

        h4=[h4;h4_s];
    end

    pt1=(1/(j^4)).*(1./(((1-Sj^2)^2)+4.*(damping.*Sj)^2)).*(A1.*h1+((-1)^(j+1)).*B1.*h2);

    pt2=(1/(j^4)).*(1./(((1-Sj^2)^2)+4.*(damping.*Sj)^2)).*(A2.*h3+((-1)^(j+1)).*B2.*h4);

    %deltay1=((2.*P.*(L^3))./(E.*I.*(pi^4))).*(pt1+pt2)
    deltax1=((2.*P.*(L^3))./(E.*I.*(pi^4))).*(pt1);
    y1=y1+deltay1;
end
%%%%%%%%%%%%%%%%%%%%%%%%%%%%%%%%%%%%%%%%%%%%%%%%%%%%%%%%%%%%%%%%%%%%%%%%
for n = 3
    wj=(j.^2).*(pi^2)/(L^2)).*((E.*I)/m)^0.5;
    Sj=(j.*pi.*v)./(wj.*L);
    omegaj=(j.*pi.*v)/L;
    tn= 14./v;
    Tn= tn+(L./v);
    tc=0./v;
    wdj=wj.*(1-damping^2)^0.5;

    A1=(1-Sj.^2).*sin(omegaj.*(T-tn))-2.*damping.*Sj.*cos(omegaj.*(T-tn))+exp(-damping.*wj.*(T-tn)).*((2.*damping.*Sj.*cos(wdj.*(T-tn)))+(((Sj)./((1-damping^2)^0.5)).*(2.*(damping^2)+(Sj^2)-1).*sin(wdj.*(T-tn))));

    B1=(1-Sj.^2).*sin(omegaj.*(T-Tn))-2.*damping.*Sj.*cos(omegaj.*(T-Tn))+exp(-damping.*wj.*(T-Tn)).*((2.*damping.*Sj.*cos(wdj.*(T-Tn)))+(((Sj)./((1-damping^2)^0.5)).*(2.*(damping^2)+(Sj^2)-1).*sin(wdj.*(T-Tn))));

    A2=(1-Sj.^2).*sin(omegaj.*(T-tc-tn))-2.*damping.*Sj.*cos(omegaj.*(T-tc-tn))+exp(-damping.*wj.*(T-tc-tn)).*((2.*damping.*Sj.*cos(wdj.*(T-tc-tn)))+(((Sj)./((1-damping^2)^0.5)).*(2.*(damping^2)+(Sj^2)-1).*sin(wdj.*(T-tc-tn))));

    B2=(1-Sj.^2).*sin(omegaj.*(T-tc-Tn))-2.*damping.*Sj.*cos(omegaj.*(T-tc-Tn))+exp(-damping.*wj.*(T-tc-Tn)).*((2.*damping.*Sj.*cos(wdj.*(T-tc-Tn)))+(((Sj)./((1-damping^2)^0.5)).*(2.*(damping^2)+(Sj^2)-1).*sin(wdj.*(T-tc-Tn))));

    t1 = T-tn;
    t2 = T-Tn;
    t3 = T-tc-tn;
    t4 = T-tc-Tn;

```

```

h1=[];
h2=[];
h3=[];
h4=[];
for s=1:nrow_T
    t1_s=t1(s,1);
    t2_s=t2(s,1);
    t3_s=t3(s,1);
    t4_s=t4(s,1);
    if t1_s<0
        h1_s=0;
    else
        h1_s=1;
    end
    if t2_s<0
        h2_s=0;
    else
        h2_s=1;
    end
    if t3_s<0
        h3_s=0;
    else
        h3_s=1;
    end
    if t4_s<0
        h4_s=0;
    else
        h4_s=1;
    end
    h1=[h1;h1_s];
    h2=[h2;h2_s];
    h3=[h3;h3_s];
    h4=[h4;h4_s];
end

pt1=(1/(j^4)).*(1./(((1-Sj^2)^2)+4.*(damping.*Sj)^2)).*(A1.*h1+((-1)^(j+1)).*B1.*h2);

pt2=(1/(j^4)).*(1./(((1-Sj^2)^2)+4.*(damping.*Sj)^2)).*(A2.*h3+((-1)^(j+1)).*B2.*h4);

%delatay1=((2.*P.*(L^3))./(E.*I.*(pi^4))).*(pt1+pt2)
deltay1=((2.*P.*(L^3))./(E.*I.*(pi^4))).*(pt1);
y1=y1+deltay1;
end
%%%%%%%%%%%%%%%%%%%%%%%%%%%%%%%%%%%%%%%%%%%%%%%%%%%%%%%%%%%%%%%%%%%%%%%%

```

```

for n = 4
wj=(j^2).*(pi^2)/(L^2)).*((E.*I)/m)^0.5;
Sj=(j.*pi.*v)/(wj.*L);
omegaj=(j.*pi.*v)/L;
tn= 17./v;
Tn= tn+(L./v);
tc=0./v;
wdj=wj.*(1-damping^2)^0.5;

A1=(1-Sj.^2).*sin(omegaj.*(T-tn))-2.*damping.*Sj.*cos(omegaj.*(T-
tn))+exp(-damping.*wj.*(T-tn)).*((2.*damping.*Sj.*cos(wdj.*(T-tn)))+((Sj)/((1-
damping^2)^0.5)).*(2.*(damping^2)+(Sj^2)-1).*sin(wdj.*(T-tn))));

B1=(1-Sj.^2).*sin(omegaj.*(T-Tn))-2.*damping.*Sj.*cos(omegaj.*(T-
Tn))+exp(-damping.*wj.*(T-Tn)).*((2.*damping.*Sj.*cos(wdj.*(T-
Tn)))+((Sj)/((1-damping^2)^0.5)).*(2.*damping^2+(Sj^2)-1).*sin(wdj.*(T-
Tn))));

A2=(1-Sj.^2).*sin(omegaj.*(T-tc-tn))-2.*damping.*Sj.*cos(omegaj.*(T-tc-
tn))+exp(-damping.*wj.*(T-tc-tn)).*((2.*damping.*Sj.*cos(wdj.*(T-tc-
tn)))+((Sj)/((1-damping^2)^0.5)).*(2.*(damping^2)+(Sj^2)-1).*sin(wdj.*(T-tc-
tn))));

B2=(1-Sj.^2).*sin(omegaj.*(T-tc-Tn))-2.*damping.*Sj.*cos(omegaj.*(T-tc-
Tn))+exp(-damping.*wj.*(T-tc-Tn)).*((2.*damping.*Sj.*cos(wdj.*(T-tc-
Tn)))+((Sj)/((1-damping^2)^0.5)).*(2.*damping^2+(Sj^2)-1).*sin(wdj.*(T-tc-
Tn))));

t1 = T-tn;
t2 = T-Tn;
t3 = T-tc-tn;
t4 = T-tc-Tn;
h1=[];
h2=[];
h3=[];
h4=[];
for s=1:nrow_T
t1_s=t1(s,1);
t2_s=t2(s,1);
t3_s=t3(s,1);
t4_s=t4(s,1);
if t1_s<0
h1_s=0;
else
h1_s=1;
end

```

```

if t2_s<0
    h2_s=0;
else
    h2_s=1;
end
if t3_s<0
    h3_s=0;
else
    h3_s=1;
end
if t4_s<0
    h4_s=0;
else
    h4_s=1;
end
h1=[h1;h1_s];
h2=[h2;h2_s];
h3=[h3;h3_s];
h4=[h4;h4_s];
end

pt1=(1/(j^4)).*(1./(((1-Sj^2)^2)+4.*(damping.*Sj)^2)).*(A1.*h1+((-1)^(j+1)).*B1.*h2);

pt2=(1/(j^4)).*(1./(((1-Sj^2)^2)+4.*(damping.*Sj)^2)).*(A2.*h3+((-1)^(j+1)).*B2.*h4);

%delatay1=((2.*P.*(L^3))./(E.*I.*(pi^4))).*(pt1+pt2)
deltay1=((2.*P.*(L^3))./(E.*I.*(pi^4))).*(pt1);
y1=y1+deltay1;
end
%%%%%%%%%%%%%%%%%%%%%%%%%%%%%%%%%%%%%%%%%%%%%%%%%%%%%%%%%%%%%%%%%%%%%%%%
for n = 5
    wj=((j^2).*(pi^2)/(L^2)).*((E.*I)/m)^0.5;
    Sj=(j.*pi.*v)/(wj.*L);
    omegaj=(j.*pi.*v)/L;
    tn= (20.525)/v;
    Tn= tn+(L./v);
    tc=0./v;
    wdj=wj.*(1-damping^2)^0.5;

    A1=(1-Sj.^2).*sin(omegaj.*(T-tn))-2.*damping.*Sj.*cos(omegaj.*(T-tn))+exp(-damping.*wj.*(T-tn)).*((2.*damping.*Sj.*cos(wdj.*(T-tn)))+(((Sj)/((1-damping^2)^0.5)).*(2.*(damping^2)+(Sj^2)-1).*sin(wdj.*(T-tn))));

```

```

B1=(1-Sj.^2).*sin(omegaj.*(T-Tn))-2.*damping.*Sj.*cos(omegaj.*(T-
Tn))+exp(-damping.*wj.*(T-Tn)).*((2.*damping.*Sj.*cos(wdj.*(T-
Tn)))+(((Sj)./((1-damping^2)^0.5)).*(2.*damping^2+(Sj^2)-1).*sin(wdj.*(T-
Tn))));

```

```

A2=(1-Sj.^2).*sin(omegaj.*(T-tc-tn))-2.*damping.*Sj.*cos(omegaj.*(T-tc-
tn))+exp(-damping.*wj.*(T-tc-tn)).*((2.*damping.*Sj.*cos(wdj.*(T-tc-
tn)))+(((Sj)./((1-damping^2)^0.5)).*(2.*(damping^2)+(Sj^2)-1).*sin(wdj.*(T-tc-
tn))));

```

```

B2=(1-Sj.^2).*sin(omegaj.*(T-tc-Tn))-2.*damping.*Sj.*cos(omegaj.*(T-tc-
Tn))+exp(-damping.*wj.*(T-tc-Tn)).*((2.*damping.*Sj.*cos(wdj.*(T-tc-
Tn)))+(((Sj)./((1-damping^2)^0.5)).*(2.*damping^2+(Sj^2)-1).*sin(wdj.*(T-tc-
Tn))));

```

```

t1 = T-tn;
t2 = T-Tn;
t3 = T-tc-tn;
t4 = T-tc-Tn;
h1=[];
h2=[];
h3=[];
h4=[];
for s=1:nrow_T
    t1_s=t1(s,1);
    t2_s=t2(s,1);
    t3_s=t3(s,1);
    t4_s=t4(s,1);
    if t1_s<0
        h1_s=0;
    else
        h1_s=1;
    end
    if t2_s<0
        h2_s=0;
    else
        h2_s=1;
    end
    if t3_s<0
        h3_s=0;
    else
        h3_s=1;
    end
    if t4_s<0
        h4_s=0;
    else

```



```

        h4_s=1;
    end
    h1=[h1;h1_s];
    h2=[h2;h2_s];
    h3=[h3;h3_s];
    h4=[h4;h4_s];
end

    pt1=(1/(j^4)).*(1./(((1-Sj^2)^2)+4.*(damping.*Sj)^2)).*(A1.*h1+((-1)^(j+1)).*B1.*h2);

    pt2=(1/(j^4)).*(1./(((1-Sj^2)^2)+4.*(damping.*Sj)^2)).*(A2.*h3+((-1)^(j+1)).*B2.*h4);

    %deltay1=((2.*P.*(L^3))./(E.*I.*(pi^4))).*(pt1+pt2)
    deltay1=((2.*P.*(L^3))./(E.*I.*(pi^4))).*(pt1);
    y1=y1+deltay1;
end
%%%%%%%%%%%%%%%%%%%%%%%%%%%%%%%%%%%%%%%%%%%%%%%%%%%%%%%%%%%%%%%%%%%%%%%%
for n = 6
    wj=((j^2).*(pi^2)/(L^2)).*((E.*I)/m)^0.5;
    Sj=(j.*pi.*v)/(wj.*L);
    omegaj=(j.*pi.*v)/L;
    tn= (20.525 + arm1)/v;
    Tn= tn+(L./v);
    tc=0./v;
    wdj=wj.*(1-damping^2)^0.5;

    A1=(1-Sj.^2).*sin(omegaj.*(T-tn))-2.*damping.*Sj.*cos(omegaj.*(T-tn))+exp(-damping.*wj.*(T-tn)).*((2.*damping.*Sj.*cos(wdj.*(T-tn)))+(((Sj)/((1-damping^2)^0.5)).*(2.*(damping^2)+(Sj^2)-1).*sin(wdj.*(T-tn))));

    B1=(1-Sj.^2).*sin(omegaj.*(T-Tn))-2.*damping.*Sj.*cos(omegaj.*(T-Tn))+exp(-damping.*wj.*(T-Tn)).*((2.*damping.*Sj.*cos(wdj.*(T-Tn)))+(((Sj)/((1-damping^2)^0.5)).*(2.*damping^2+(Sj^2)-1).*sin(wdj.*(T-Tn))));

    A2=(1-Sj.^2).*sin(omegaj.*(T-tc-tn))-2.*damping.*Sj.*cos(omegaj.*(T-tc-tn))+exp(-damping.*wj.*(T-tc-tn)).*((2.*damping.*Sj.*cos(wdj.*(T-tc-tn)))+(((Sj)/((1-damping^2)^0.5)).*(2.*(damping^2)+(Sj^2)-1).*sin(wdj.*(T-tc-tn))));

    B2=(1-Sj.^2).*sin(omegaj.*(T-tc-Tn))-2.*damping.*Sj.*cos(omegaj.*(T-tc-Tn))+exp(-damping.*wj.*(T-tc-Tn)).*((2.*damping.*Sj.*cos(wdj.*(T-tc-Tn)))+(((Sj)/((1-damping^2)^0.5)).*(2.*damping^2+(Sj^2)-1).*sin(wdj.*(T-tc-Tn))));

```

```

t1 = T-tn;
t2 = T-Tn;
t3 = T-tc-tn;
t4 = T-tc-Tn;
h1=[];
h2=[];
h3=[];
h4=[];
for s=1:nrow_T
    t1_s=t1(s,1);
    t2_s=t2(s,1);
    t3_s=t3(s,1);
    t4_s=t4(s,1);
    if t1_s<0
        h1_s=0;
    else
        h1_s=1;
    end
    if t2_s<0
        h2_s=0;
    else
        h2_s=1;
    end
    if t3_s<0
        h3_s=0;
    else
        h3_s=1;
    end
    if t4_s<0
        h4_s=0;
    else
        h4_s=1;
    end
    h1=[h1;h1_s];
    h2=[h2;h2_s];
    h3=[h3;h3_s];
    h4=[h4;h4_s];
end

```

```

pt1=(1/(j^4)).*(1./(((1-Sj^2)^2)+4.*(damping.*Sj)^2)).*(A1.*h1+((-1)^(j+1)).*B1.*h2);

```

```

pt2=(1/(j^4)).*(1./(((1-Sj^2)^2)+4.*(damping.*Sj)^2)).*(A2.*h3+((-1)^(j+1)).*B2.*h4);

```

```

%delta1=((2.*P.*(L^3))./(E.*I.*(pi^4))).*(pt1+pt2)

```

```

deltay1=((2.*P.*(L^3))./(E.*I.*(pi^4))).*(pt1);
y1=y1+deltay1;
end
%%%%%%%%%%%%%%%%%%%%%%%%%%%%%%%%%%%%%%%%%%%%%%%%%%%%%%%%%%%%%%%%%%%%%%%%
for n = 7
    wj=(j^2).*(pi^2)/(L^2).*((E.*I)/m)^0.5;
    Sj=(j.*pi.*v)./(wj.*L);
    omegaj=(j.*pi.*v)/L;
    tn= (20.525 + arm1 + aramesafe)./v;
    Tn= tn+(L./v);
    tc=0./v;
    wdj=wj.*(1-damping^2)^0.5;

    A1=(1-Sj.^2).*sin(omegaj.*(T-tn))-2.*damping.*Sj.*cos(omegaj.*(T-
tn))+exp(-damping.*wj.*(T-tn)).*((2.*damping.*Sj.*cos(wdj.*(T-tn)))+((Sj)/((1-
damping^2)^0.5))).*(2.*(damping^2)+(Sj^2)-1).*sin(wdj.*(T-tn)));

    B1=(1-Sj.^2).*sin(omegaj.*(T-Tn))-2.*damping.*Sj.*cos(omegaj.*(T-
Tn))+exp(-damping.*wj.*(T-Tn)).*((2.*damping.*Sj.*cos(wdj.*(T-
Tn)))+((Sj)/((1-damping^2)^0.5))).*(2.*damping^2+(Sj^2)-1).*sin(wdj.*(T-
Tn)));

    A2=(1-Sj.^2).*sin(omegaj.*(T-tc-tn))-2.*damping.*Sj.*cos(omegaj.*(T-tc-
tn))+exp(-damping.*wj.*(T-tc-tn)).*((2.*damping.*Sj.*cos(wdj.*(T-tc-
tn)))+((Sj)/((1-damping^2)^0.5))).*(2.*(damping^2)+(Sj^2)-1).*sin(wdj.*(T-tc-
tn)));

    B2=(1-Sj.^2).*sin(omegaj.*(T-tc-Tn))-2.*damping.*Sj.*cos(omegaj.*(T-tc-
Tn))+exp(-damping.*wj.*(T-tc-Tn)).*((2.*damping.*Sj.*cos(wdj.*(T-tc-
Tn)))+((Sj)/((1-damping^2)^0.5))).*(2.*damping^2+(Sj^2)-1).*sin(wdj.*(T-tc-
Tn)));

    t1 = T-tn;
    t2 = T-Tn;
    t3 = T-tc-tn;
    t4 = T-tc-Tn;
    h1=[];
    h2=[];
    h3=[];
    h4=[];
    for s=1:nrow_T
        t1_s=t1(s,1);
        t2_s=t2(s,1);
        t3_s=t3(s,1);
        t4_s=t4(s,1);
        if t1_s<0

```

```

        h1_s=0;
    else
        h1_s=1;
    end
    if t2_s<0
        h2_s=0;
    else
        h2_s=1;
    end
    if t3_s<0
        h3_s=0;
    else
        h3_s=1;
    end
    if t4_s<0
        h4_s=0;
    else
        h4_s=1;
    end
    h1=[h1;h1_s];
    h2=[h2;h2_s];
    h3=[h3;h3_s];
    h4=[h4;h4_s];
end

pt1=(1/(j^4)).*(1./(((1-Sj^2)^2)+4.*(damping.*Sj)^2)).*(A1.*h1+((-
1)^(j+1)).*B1.*h2);

pt2=(1/(j^4)).*(1./(((1-Sj^2)^2)+4.*(damping.*Sj)^2)).*(A2.*h3+((-
1)^(j+1)).*B2.*h4);

%deltay1=((2.*P.*(L^3))./(E.*I.*(pi^4))).*(pt1+pt2)
deltay1=((2.*P.*(L^3))./(E.*I.*(pi^4))).*(pt1);
y1=y1+deltay1;
end
%%%%%%%%%%%%%%%%%%%%%%%%%%%%%%%%%%%%%%%%%%%%%%%%%%%%%%%%%%%%%%%%%%%%%%%%
for n = 8:naxle-7
    wj=((j^2).*(pi^2)/(L^2)).*((E.*I)/m)^0.5;
    Sj=(j.*pi.*v)/(wj.*L);
    omegaj=(j.*pi.*v)/L;
    tn= ((n-8).*dninitial+(20.525 + arm1 + aramesafe + arm1))./v;
    Tn= tn+(L./v);
    tc=dc./v;
    wdj=wj.*(1-damping^2)^0.5;

```

$$A1=(1-Sj.^2).*sin(omegaj.*(T-tn))-2.*damping.*Sj.*cos(omegaj.*(T-tn))+exp(-damping.*wj.*(T-tn)).*((2.*damping.*Sj.*cos(wdj.*(T-tn)))+(((Sj)./(1-damping^2)^0.5)).*(2.*(damping^2)+(Sj^2)-1).*sin(wdj.*(T-tn))));$$

$$B1=(1-Sj.^2).*sin(omegaj.*(T-Tn))-2.*damping.*Sj.*cos(omegaj.*(T-Tn))+exp(-damping.*wj.*(T-Tn)).*((2.*damping.*Sj.*cos(wdj.*(T-Tn)))+(((Sj)./(1-damping^2)^0.5)).*(2.*damping^2+(Sj^2)-1).*sin(wdj.*(T-Tn))));$$

$$A2=(1-Sj.^2).*sin(omegaj.*(T-tc-tn))-2.*damping.*Sj.*cos(omegaj.*(T-tc-tn))+exp(-damping.*wj.*(T-tc-tn)).*((2.*damping.*Sj.*cos(wdj.*(T-tc-tn)))+(((Sj)./(1-damping^2)^0.5)).*(2.*(damping^2)+(Sj^2)-1).*sin(wdj.*(T-tc-tn))));$$

$$B2=(1-Sj.^2).*sin(omegaj.*(T-tc-Tn))-2.*damping.*Sj.*cos(omegaj.*(T-tc-Tn))+exp(-damping.*wj.*(T-tc-Tn)).*((2.*damping.*Sj.*cos(wdj.*(T-tc-Tn)))+(((Sj)./(1-damping^2)^0.5)).*(2.*damping^2+(Sj^2)-1).*sin(wdj.*(T-tc-Tn))));$$

```

t1 = T-tn;
t2 = T-Tn;
t3 = T-tc-tn;
t4 = T-tc-Tn;
h1=[];
h2=[];
h3=[];
h4=[];
for s=1:nrow_T
    t1_s=t1(s,1);
    t2_s=t2(s,1);
    t3_s=t3(s,1);
    t4_s=t4(s,1);
    if t1_s<0
        h1_s=0;
    else
        h1_s=1;
    end
    if t2_s<0
        h2_s=0;
    else
        h2_s=1;
    end
    if t3_s<0
        h3_s=0;
    else
        h3_s=1;
    end
end

```

```

end
if t4_s<0
    h4_s=0;
else
    h4_s=1;
end
h1=[h1;h1_s];
h2=[h2;h2_s];
h3=[h3;h3_s];
h4=[h4;h4_s];
end

pt1=(1/(j^4)).*(1./(((1-Sj^2)^2)+4.*(damping.*Sj)^2)).*(A1.*h1+((-
1)^(j+1)).*B1.*h2);

pt2=(1/(j^4)).*(1./(((1-Sj^2)^2)+4.*(damping.*Sj)^2)).*(A2.*h3+((-
1)^(j+1)).*B2.*h4);

deltay1=((2.*P.*(L^3))./(E.*I.*(pi^4))).*(pt1+pt2);
%deltay1=((2.*P.*(L^3))./(E.*I.*(pi^4))).*(pt1)
y1=y1+deltay1;
end
%%%%%%%%%%%%%%%%%%%%%%%%%%%%%%%%%%%%%%%%%%%%%%%%%%%%%%%%%%%%%%%%%%%%%%%%
for n = naxle-6
    wj=((j^2).*(pi^2)/(L^2)).*((E.*I)/m)^0.5;
    Sj=(j.*pi.*v)/(wj.*L);
    omegaj=(j.*pi.*v)/L;
    tn= ((naxle-14).*dninitial+(20.525 + arm1 + aramesafe+arm1))./v;
    Tn= tn+(L./v);
    tc=0./v;
    wdj=wj.*(1-damping^2)^0.5;

    A1=(1-Sj.^2).*sin(omegaj.*(T-tn))-2.*damping.*Sj.*cos(omegaj.*(T-
tn))+exp(-damping.*wj.*(T-tn)).*((2.*damping.*Sj.*cos(wdj.*(T-tn)))+(((Sj)/((1-
damping^2)^0.5)).*(2.*(damping^2)+(Sj^2)-1).*sin(wdj.*(T-tn))));

    B1=(1-Sj.^2).*sin(omegaj.*(T-Tn))-2.*damping.*Sj.*cos(omegaj.*(T-
Tn))+exp(-damping.*wj.*(T-Tn)).*((2.*damping.*Sj.*cos(wdj.*(T-
Tn)))+(((Sj)/((1-damping^2)^0.5)).*(2.*damping^2+(Sj^2)-1).*sin(wdj.*(T-
Tn))));

    A2=(1-Sj.^2).*sin(omegaj.*(T-tc-tn))-2.*damping.*Sj.*cos(omegaj.*(T-tc-
tn))+exp(-damping.*wj.*(T-tc-tn)).*((2.*damping.*Sj.*cos(wdj.*(T-tc-
tn)))+(((Sj)/((1-damping^2)^0.5)).*(2.*(damping^2)+(Sj^2)-1).*sin(wdj.*(T-tc-
tn))));

```

```

B2=(1-Sj.^2).*sin(omegaj.*(T-tc-Tn))-2.*damping.*Sj.*cos(omegaj.*(T-tc-
Tn))+exp(-damping.*wj.*(T-tc-Tn)).*((2.*damping.*Sj.*cos(wdj.*(T-tc-
Tn)))+(((Sj)./((1-damping^2)^0.5)).*(2.*damping^2+(Sj^2)-1).*sin(wdj.*(T-tc-
Tn))));

```

```

t1 = T-tn;
t2 = T-Tn;
t3 = T-tc-tn;
t4 = T-tc-Tn;
h1=[];
h2=[];
h3=[];
h4=[];
for s=1:nrow_T
    t1_s=t1(s,1);
    t2_s=t2(s,1);
    t3_s=t3(s,1);
    t4_s=t4(s,1);
    if t1_s<0
        h1_s=0;
    else
        h1_s=1;
    end
    if t2_s<0
        h2_s=0;
    else
        h2_s=1;
    end
    if t3_s<0
        h3_s=0;
    else
        h3_s=1;
    end
    if t4_s<0
        h4_s=0;
    else
        h4_s=1;
    end
    h1=[h1;h1_s];
    h2=[h2;h2_s];
    h3=[h3;h3_s];
    h4=[h4;h4_s];
end

```

```

pt1=(1/(j^4)).*(1./(((1-Sj^2)^2)+4.*(damping.*Sj)^2)).*(A1.*h1+((-
1)^(j+1)).*B1.*h2);

```

```

    pt2=(1/(j^4)).*(1./(((1-Sj^2)^2)+4.*(damping.*Sj)^2)).*(A2.*h3+((-
1)^(j+1)).*B2.*h4);

    %deltay1=((2.*P.*(L^3))./(E.*I.*(pi^4))).*(pt1+pt2)
    deltay1=((2.*P.*(L^3))./(E.*I.*(pi^4))).*(pt1);
    y1=y1+deltay1;
end
%%%%%%%%%%%%%%%%%%%%%%%%%%%%%%%%%%%%%%%%%%%%%%%%%%%%%%%%%%%%%%%%%%%%%%%%
for n = naxle-5
    wj=(j^2).*(pi^2)/(L^2).*((E.*I)/m)^0.5;
    Sj=(j.*pi.*v)/(wj.*L);
    omegaj=(j.*pi.*v)/L;
    tn= ((naxle-14).*dninitial+(20.525 + arm1 + aramesafe+arm1)+aramesafe)/v;
    Tn= tn+(L./v);
    tc=0./v;
    wdj=wj.*(1-damping^2)^0.5;

    A1=(1-Sj.^2).*sin(omegaj.*(T-tn))-2.*damping.*Sj.*cos(omegaj.*(T-tn))+exp(-
damping.*wj.*(T-tn)).*((2.*damping.*Sj.*cos(wdj.*(T-tn)))+(((Sj)/((1-
damping^2)^0.5))).*(2.*(damping^2)+(Sj^2)-1).*sin(wdj.*(T-tn)));

    B1=(1-Sj.^2).*sin(omegaj.*(T-Tn))-2.*damping.*Sj.*cos(omegaj.*(T-
Tn))+exp(-damping.*wj.*(T-Tn)).*((2.*damping.*Sj.*cos(wdj.*(T-
Tn)))+(((Sj)/((1-damping^2)^0.5))).*(2.*(damping^2)+(Sj^2)-1).*sin(wdj.*(T-
Tn)));

    A2=(1-Sj.^2).*sin(omegaj.*(T-tc-tn))-2.*damping.*Sj.*cos(omegaj.*(T-tc-
tn))+exp(-damping.*wj.*(T-tc-tn)).*((2.*damping.*Sj.*cos(wdj.*(T-tc-
tn)))+(((Sj)/((1-damping^2)^0.5))).*(2.*(damping^2)+(Sj^2)-1).*sin(wdj.*(T-tc-
tn)));

    B2=(1-Sj.^2).*sin(omegaj.*(T-tc-Tn))-2.*damping.*Sj.*cos(omegaj.*(T-tc-
Tn))+exp(-damping.*wj.*(T-tc-Tn)).*((2.*damping.*Sj.*cos(wdj.*(T-tc-
Tn)))+(((Sj)/((1-damping^2)^0.5))).*(2.*(damping^2)+(Sj^2)-1).*sin(wdj.*(T-tc-
Tn)));

    t1 = T-tn;
    t2 = T-Tn;
    t3 = T-tc-tn;
    t4 = T-tc-Tn;
    h1=[];
    h2=[];
    h3=[];
    h4=[];
    for s=1:nrow_T
        t1_s=t1(s,1);

```



```

t2_s=t2(s,1);
t3_s=t3(s,1);
t4_s=t4(s,1);
if t1_s<0
    h1_s=0;
else
    h1_s=1;
end
if t2_s<0
    h2_s=0;
else
    h2_s=1;
end
if t3_s<0
    h3_s=0;
else
    h3_s=1;
end
if t4_s<0
    h4_s=0;
else
    h4_s=1;
end
h1=[h1;h1_s];
h2=[h2;h2_s];
h3=[h3;h3_s];
h4=[h4;h4_s];
end

pt1=(1/(j^4)).*(1./(((1-Sj^2)^2)+4.*(damping.*Sj)^2)).*(A1.*h1+((-1)^(j+1)).*B1.*h2);

pt2=(1/(j^4)).*(1./(((1-Sj^2)^2)+4.*(damping.*Sj)^2)).*(A2.*h3+((-1)^(j+1)).*B2.*h4);

%deltay1=((2.*P.*(L^3))./(E.*I.*(pi^4))).*(pt1+pt2)
deltay1=((2.*P.*(L^3))./(E.*I.*(pi^4))).*(pt1);
y1=y1+deltay1;
end
%%%%%%%%%%%%%%%%%%%%%%%%%%%%%%%%%%%%%%%%%%%%%%%%%%%%%%%%%%%%%%%%%%%%%%%%
for n = naxle-4
    wj=(j^2).*(pi^2)/(L^2)).*((E.*I)/m)^0.5;
    Sj=(j.*pi.*v)/(wj.*L);
    omegaj=(j.*pi.*v)/L;
    tn= ((naxle-14).*dninitial+(20.525 + arm1 +
aramesafe+arm1)+aramesafe+arm1)./v;

```

```

Tn= tn+(L./v);
tc=0./v;
wdj=wj.*(1-damping^2)^0.5;

```

```

A1=(1-Sj.^2).*sin(omegaj.*(T-tn))-2.*damping.*Sj.*cos(omegaj.*(T-
tn))+exp(-damping.*wj.*(T-tn)).*((2.*damping.*Sj.*cos(wdj.*(T-tn)))+((Sj)/((1-
damping^2)^0.5)).*(2.*(damping^2)+(Sj^2)-1).*sin(wdj.*(T-tn))));

```

```

B1=(1-Sj.^2).*sin(omegaj.*(T-Tn))-2.*damping.*Sj.*cos(omegaj.*(T-
Tn))+exp(-damping.*wj.*(T-Tn)).*((2.*damping.*Sj.*cos(wdj.*(T-
Tn)))+((Sj)/((1-damping^2)^0.5)).*(2.*damping^2+(Sj^2)-1).*sin(wdj.*(T-
Tn))));

```

```

A2=(1-Sj.^2).*sin(omegaj.*(T-tc-tn))-2.*damping.*Sj.*cos(omegaj.*(T-tc-
tn))+exp(-damping.*wj.*(T-tc-tn)).*((2.*damping.*Sj.*cos(wdj.*(T-tc-
tn)))+((Sj)/((1-damping^2)^0.5)).*(2.*(damping^2)+(Sj^2)-1).*sin(wdj.*(T-tc-
tn))));

```

```

B2=(1-Sj.^2).*sin(omegaj.*(T-tc-Tn))-2.*damping.*Sj.*cos(omegaj.*(T-tc-
Tn))+exp(-damping.*wj.*(T-tc-Tn)).*((2.*damping.*Sj.*cos(wdj.*(T-tc-
Tn)))+((Sj)/((1-damping^2)^0.5)).*(2.*damping^2+(Sj^2)-1).*sin(wdj.*(T-tc-
Tn))));

```

```

t1 = T-tn;
t2 = T-Tn;
t3 = T-tc-tn;
t4 = T-tc-Tn;
h1=[];
h2=[];
h3=[];
h4=[];
for s=1:nrow_T
    t1_s=t1(s,1);
    t2_s=t2(s,1);
    t3_s=t3(s,1);
    t4_s=t4(s,1);
    if t1_s<0
        h1_s=0;
    else
        h1_s=1;
    end
    if t2_s<0
        h2_s=0;
    else
        h2_s=1;
    end
end

```

```

if t3_s<0
    h3_s=0;
else
    h3_s=1;
end
if t4_s<0
    h4_s=0;
else
    h4_s=1;
end
h1=[h1;h1_s];
h2=[h2;h2_s];
h3=[h3;h3_s];
h4=[h4;h4_s];
end

pt1=(1/(j^4)).*(1./(((1-Sj^2)^2)+4.*(damping.*Sj)^2)).*(A1.*h1+((-1)^(j+1)).*B1.*h2);

pt2=(1/(j^4)).*(1./(((1-Sj^2)^2)+4.*(damping.*Sj)^2)).*(A2.*h3+((-1)^(j+1)).*B2.*h4);

%deltay1=((2.*P.*(L^3))./(E.*I.*(pi^4))).*(pt1+pt2)
deltay1=((2.*P.*(L^3))./(E.*I.*(pi^4))).*(pt1);
y1=y1+deltay1;
end
%%%%%%%%%%%%%%%%%%%%%%%%%%%%%%%%%%%%%%%%%%%%%%%%%%%%%%%%%%%%%%%%%%%%%%%%
for n = naxle-3
    wj=((j^2).*(pi^2)/(L^2)).*((E.*I)/m)^0.5;
    Sj=(j.*pi.*v)/(wj.*L);
    omegaj=(j.*pi.*v)/L;
    tn= ((naxle-14).*dninitial+(20.525 + arm1 +
aramesafe+arm1)+aramesafe+arm1+3.525)./v;
    Tn= tn+(L./v);
    tc=0./v;
    wdj=wj.*(1-damping^2)^0.5;

    A1=(1-Sj.^2).*sin(omegaj.*(T-tn))-2.*damping.*Sj.*cos(omegaj.*(T-tn))+exp(-damping.*wj.*(T-tn)).*((2.*damping.*Sj.*cos(wdj.*(T-tn)))+(((Sj)/((1-damping^2)^0.5)).*(2.*(damping^2)+(Sj^2)-1).*sin(wdj.*(T-tn))));

    B1=(1-Sj.^2).*sin(omegaj.*(T-Tn))-2.*damping.*Sj.*cos(omegaj.*(T-Tn))+exp(-damping.*wj.*(T-Tn)).*((2.*damping.*Sj.*cos(wdj.*(T-Tn)))+(((Sj)/((1-damping^2)^0.5)).*(2.*(damping^2)+(Sj^2)-1).*sin(wdj.*(T-Tn))));

```

```

A2=(1-Sj.^2).*sin(omegaj.*(T-tc-tn))-2.*damping.*Sj.*cos(omegaj.*(T-tc-
tn))+exp(-damping.*wj.*(T-tc-tn)).*((2.*damping.*Sj.*cos(wdj.*(T-tc-
tn)))+((Sj)/((1-damping^2)^0.5)).*(2.*(damping^2)+(Sj^2)-1).*sin(wdj.*(T-tc-
tn))));

```

```

B2=(1-Sj.^2).*sin(omegaj.*(T-tc-Tn))-2.*damping.*Sj.*cos(omegaj.*(T-tc-
Tn))+exp(-damping.*wj.*(T-tc-Tn)).*((2.*damping.*Sj.*cos(wdj.*(T-tc-
Tn)))+((Sj)/((1-damping^2)^0.5)).*(2.*(damping^2)+(Sj^2)-1).*sin(wdj.*(T-tc-
Tn))));

```

```

t1 = T-tn;
t2 = T-Tn;
t3 = T-tc-tn;
t4 = T-tc-Tn;
h1=[];
h2=[];
h3=[];
h4=[];
for s=1:nrow_T
    t1_s=t1(s,1);
    t2_s=t2(s,1);
    t3_s=t3(s,1);
    t4_s=t4(s,1);
    if t1_s<0
        h1_s=0;
    else
        h1_s=1;
    end
    if t2_s<0
        h2_s=0;
    else
        h2_s=1;
    end
    if t3_s<0
        h3_s=0;
    else
        h3_s=1;
    end
    if t4_s<0
        h4_s=0;
    else
        h4_s=1;
    end
    h1=[h1;h1_s];
    h2=[h2;h2_s];
    h3=[h3;h3_s];

```

```

        h4=[h4;h4_s];
    end

    pt1=(1/(j^4)).*(1./(((1-Sj^2)^2)+4.*(damping.*Sj)^2)).*(A1.*h1+((-
1)^(j+1)).*B1.*h2);

    pt2=(1/(j^4)).*(1./(((1-Sj^2)^2)+4.*(damping.*Sj)^2)).*(A2.*h3+((-
1)^(j+1)).*B2.*h4);
    %deltay1=((2.*P.*(L^3))./(E.*I.*(pi^4))).*(pt1+pt2)
    deltay1=((2.*P.*(L^3))./(E.*I.*(pi^4))).*(pt1);
    y1=y1+deltay1;
    end
%%%%%%%%%%%%%%%%%%%%%%%%%%%%%%%%%%%%%%%%%%%%%%%%%%%%%%%%%%%%%%%%%%%%%%%%
    for n = naxle-2
        wj=(j^2).*(pi^2)/(L^2)).*((E.*I)/m)^0.5;
        Sj=(j.*pi.*v)/(wj.*L);
        omegaj=(j.*pi.*v)/L;
        tn= ((naxle-14).*dninitial+(20.525 + arm1 +
aramesafe+arm1)+aramesafe+arm1+3.525+3)./v;
        Tn= tn+(L./v);
        tc=0./v;
        wdj=wj.*(1-damping^2)^0.5;

        A1=(1-Sj.^2).*sin(omegaj.*(T-tn))-2.*damping.*Sj.*cos(omegaj.*(T-
tn))+exp(-damping.*wj.*(T-tn)).*((2.*damping.*Sj.*cos(wdj.*(T-tn)))/((1-
damping^2)^0.5)).*(2.*(damping^2)+(Sj^2)-1).*sin(wdj.*(T-tn)));

        B1=(1-Sj.^2).*sin(omegaj.*(T-Tn))-2.*damping.*Sj.*cos(omegaj.*(T-
Tn))+exp(-damping.*wj.*(T-Tn)).*((2.*damping.*Sj.*cos(wdj.*(T-
Tn)))/((1-damping^2)^0.5)).*(2.*damping^2+(Sj^2)-1).*sin(wdj.*(T-
Tn)));

        A2=(1-Sj.^2).*sin(omegaj.*(T-tc-tn))-2.*damping.*Sj.*cos(omegaj.*(T-tc-
tn))+exp(-damping.*wj.*(T-tc-tn)).*((2.*damping.*Sj.*cos(wdj.*(T-tc-
tn)))/((1-damping^2)^0.5)).*(2.*(damping^2)+(Sj^2)-1).*sin(wdj.*(T-tc-
tn)));

        B2=(1-Sj.^2).*sin(omegaj.*(T-tc-Tn))-2.*damping.*Sj.*cos(omegaj.*(T-tc-
Tn))+exp(-damping.*wj.*(T-tc-Tn)).*((2.*damping.*Sj.*cos(wdj.*(T-tc-
Tn)))/((1-damping^2)^0.5)).*(2.*damping^2+(Sj^2)-1).*sin(wdj.*(T-tc-
Tn)));

        t1 = T-tn;
        t2 = T-Tn;
        t3 = T-tc-tn;
        t4 = T-tc-Tn;

```

```

h1=[];
h2=[];
h3=[];
h4=[];
for s=1:nrow_T
    t1_s=t1(s,1);
    t2_s=t2(s,1);
    t3_s=t3(s,1);
    t4_s=t4(s,1);
    if t1_s<0
        h1_s=0;
    else
        h1_s=1;
    end
    if t2_s<0
        h2_s=0;
    else
        h2_s=1;
    end
    if t3_s<0
        h3_s=0;
    else
        h3_s=1;
    end
    if t4_s<0
        h4_s=0;
    else
        h4_s=1;
    end
    h1=[h1;h1_s];
    h2=[h2;h2_s];
    h3=[h3;h3_s];
    h4=[h4;h4_s];
end

```

```

pt1=(1/(j^4)).*(1./(((1-Sj^2)^2)+4.*(damping.*Sj)^2)).*(A1.*h1+((-1)^(j+1)).*B1.*h2);

```

```

pt2=(1/(j^4)).*(1./(((1-Sj^2)^2)+4.*(damping.*Sj)^2)).*(A2.*h3+((-1)^(j+1)).*B2.*h4);

```

```

% $\delta y_1 = ((2 \cdot P \cdot (L^3)) / (E \cdot I \cdot (\pi^4))) \cdot (pt_1 + pt_2)$ 

```

```

deltay1=((2.*P.*(L^3))./(E.*I.*(pi^4))).*(pt1);

```

```

y1=y1+deltay1;

```

```

end

```

```

%%%%%%%%%%%%%%%%%%%%%%%%%%%%%%%%%%%%%%%%%%%%%%%%%%%%%%%%%%%%%%%%%%%%%%%%

```

```

for n = naxle-1
    wj=(j^2)*(pi^2)/(L^2).*((E.*I)/m)^0.5;
    Sj=(j.*pi.*v)/(wj.*L);
    omegaj=(j.*pi.*v)/L;
    tn= ((naxle-14).*dninitial+(20.525 + arm1 +
    aramesafe+arm1)+aramesafe+arm1+3.525+3+11)./v;
    Tn= tn+(L./v);
    tc=0./v;
    wdj=wj.*(1-damping^2)^0.5;

    A1=(1-Sj.^2).*sin(omegaj.*(T-tn))-2.*damping.*Sj.*cos(omegaj.*(T-
    tn))+exp(-damping.*wj.*(T-tn)).*((2.*damping.*Sj.*cos(wdj.*(T-tn)))+((Sj)/((1-
    damping^2)^0.5)).*(2.*(damping^2)+(Sj^2)-1).*sin(wdj.*(T-tn))));

    B1=(1-Sj.^2).*sin(omegaj.*(T-Tn))-2.*damping.*Sj.*cos(omegaj.*(T-
    Tn))+exp(-damping.*wj.*(T-Tn)).*((2.*damping.*Sj.*cos(wdj.*(T-
    Tn)))+((Sj)/((1-damping^2)^0.5)).*(2.*damping^2+(Sj^2)-1).*sin(wdj.*(T-
    Tn))));

    A2=(1-Sj.^2).*sin(omegaj.*(T-tc-tn))-2.*damping.*Sj.*cos(omegaj.*(T-tc-
    tn))+exp(-damping.*wj.*(T-tc-tn)).*((2.*damping.*Sj.*cos(wdj.*(T-tc-
    tn)))+((Sj)/((1-damping^2)^0.5)).*(2.*(damping^2)+(Sj^2)-1).*sin(wdj.*(T-tc-
    tn))));

    B2=(1-Sj.^2).*sin(omegaj.*(T-tc-Tn))-2.*damping.*Sj.*cos(omegaj.*(T-tc-
    Tn))+exp(-damping.*wj.*(T-tc-Tn)).*((2.*damping.*Sj.*cos(wdj.*(T-tc-
    Tn)))+((Sj)/((1-damping^2)^0.5)).*(2.*damping^2+(Sj^2)-1).*sin(wdj.*(T-tc-
    Tn))));

    t1 = T-tn;
    t2 = T-Tn;
    t3 = T-tc-tn;
    t4 = T-tc-Tn;
    h1=[];
    h2=[];
    h3=[];
    h4=[];
    for s=1:nrow_T
        t1_s=t1(s,1);
        t2_s=t2(s,1);
        t3_s=t3(s,1);
        t4_s=t4(s,1);
        if t1_s<0
            h1_s=0;
        else
            h1_s=1;
        end
    end

```

```

end
if t2_s<0
    h2_s=0;
else
    h2_s=1;
end
if t3_s<0
    h3_s=0;
else
    h3_s=1;
end
if t4_s<0
    h4_s=0;
else
    h4_s=1;
end
h1=[h1;h1_s];
h2=[h2;h2_s];
h3=[h3;h3_s];
h4=[h4;h4_s];
end

pt1=(1/(j^4)).*(1./(((1-Sj^2)^2)+4.*(damping.*Sj)^2)).*(A1.*h1+((-1)^(j+1)).*B1.*h2);

pt2=(1/(j^4)).*(1./(((1-Sj^2)^2)+4.*(damping.*Sj)^2)).*(A2.*h3+((-1)^(j+1)).*B2.*h4);

%delatay1=((2.*P.*(L^3))./(E.*I.*(pi^4))).*(pt1+pt2)
deltay1=((2.*P.*(L^3))./(E.*I.*(pi^4))).*(pt1);
y1=y1+deltay1;
end
%%%%%%%%%%%%%%%%%%%%%%%%%%%%%%%%%%%%%%%%%%%%%%%%%%%%%%%%%%%%%%%%%%%%%%%%
for n = naxle
    wj=(j^2).*(pi^2)/(L^2)).*((E.*I)/m)^0.5;
    Sj=(j.*pi.*v)/(wj.*L);
    omegaj=(j.*pi.*v)/L;
    tn= ((naxle-14).*dninitial+(20.525 + arm1 +
aramesafe+arm1)+aramesafe+arm1+3.525+3+11+3)./v;
    Tn= tn+(L./v);
    tc=0./v;
    wdj=wj.*(1-damping^2)^0.5;

    A1=(1-Sj.^2).*sin(omegaj.*(T-tn))-2.*damping.*Sj.*cos(omegaj.*(T-tn))+exp(-damping.*wj.*(T-tn)).*((2.*damping.*Sj.*cos(wdj.*(T-tn)))+(((Sj)/((1-damping^2)^0.5)).*(2.*(damping^2)+(Sj^2)-1).*sin(wdj.*(T-tn))));

```



```

B1=(1-Sj.^2).*sin(omegaj.*(T-Tn))-2.*damping.*Sj.*cos(omegaj.*(T-
Tn))+exp(-damping.*wj.*(T-Tn)).*((2.*damping.*Sj.*cos(wdj.*(T-
Tn)))+(((Sj)./((1-damping^2)^0.5)).*(2.*damping^2+(Sj^2)-1).*sin(wdj.*(T-
Tn))));

```

```

A2=(1-Sj.^2).*sin(omegaj.*(T-tc-tn))-2.*damping.*Sj.*cos(omegaj.*(T-tc-
tn))+exp(-damping.*wj.*(T-tc-tn)).*((2.*damping.*Sj.*cos(wdj.*(T-tc-
tn)))+(((Sj)./((1-damping^2)^0.5)).*(2.*(damping^2)+(Sj^2)-1).*sin(wdj.*(T-tc-
tn))));

```

```

B2=(1-Sj.^2).*sin(omegaj.*(T-tc-Tn))-2.*damping.*Sj.*cos(omegaj.*(T-tc-
Tn))+exp(-damping.*wj.*(T-tc-Tn)).*((2.*damping.*Sj.*cos(wdj.*(T-tc-
Tn)))+(((Sj)./((1-damping^2)^0.5)).*(2.*damping^2+(Sj^2)-1).*sin(wdj.*(T-tc-
Tn))));

```

```

t1 = T-tn;
t2 = T-Tn;
t3 = T-tc-tn;
t4 = T-tc-Tn;
h1=[];
h2=[];
h3=[];
h4=[];
for s=1:nrow_T
    t1_s=t1(s,1);
    t2_s=t2(s,1);
    t3_s=t3(s,1);
    t4_s=t4(s,1);
    if t1_s<0
        h1_s=0;
    else
        h1_s=1;
    end
    if t2_s<0
        h2_s=0;
    else
        h2_s=1;
    end
    if t3_s<0
        h3_s=0;
    else
        h3_s=1;
    end
    if t4_s<0
        h4_s=0;
    else

```

```

        h4_s=1;
    end
    h1=[h1;h1_s];
    h2=[h2;h2_s];
    h3=[h3;h3_s];
    h4=[h4;h4_s];
end
    pt1=(1/(j^4)).*(1./(((1-Sj^2)^2)+4.*(damping.*Sj)^2)).*(A1.*h1+((-
1)^(j+1)).*B1.*h2);

    pt2=(1/(j^4)).*(1./(((1-Sj^2)^2)+4.*(damping.*Sj)^2)).*(A2.*h3+((-
1)^(j+1)).*B2.*h4);

    %deltay1=((2.*P.*(L^3))./(E.*I.*(pi^4))).*(pt1+pt2)
    deltax1=((2.*P.*(L^3))./(E.*I.*(pi^4))).*(pt1);
    y1=y1+deltax1;
end
%%%%
y1=y1.*sin(j.*pi.*xcheck./L);
y = y + y1;
end
plot(T,y,'r-')
hold on
end

```